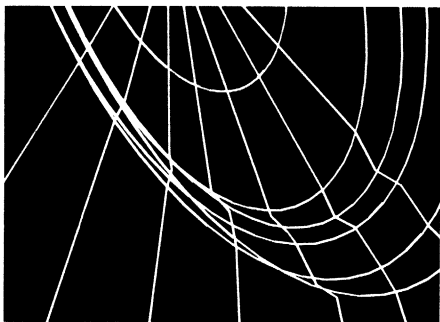


**MARC**



**Volume E**

**Demonstration Problems**

Version K7



Copyright © 1997 MARC Analysis Research Corporation

Printed in U. S. A.

This notice shall be marked on any reproduction of this data, in whole or in part.

MARC Analysis Research Corporation

260 Sheridan Avenue, Suite 309

Palo Alto, CA 94306 USA

Phone: (650) 329-6800

FAX: (650) 323-5892

Document Title: **MARC Volume E: Demonstration Problems, Part III, Version K7**

Part Number: RF-3018-07.III

Revision Date: June, 1998

## Proprietary Notice

MARC Analysis Research Corporation reserves the right to make changes in specifications and other information contained in this document without prior notice.

ALTHOUGH DUE CARE HAS BEEN TAKEN TO PRESENT ACCURATE INFORMATION, MARC ANALYSIS RESEARCH CORPORATION DISCLAIMS ALL WARRANTIES WITH RESPECT TO THE CONTENTS OF THIS DOCUMENT (INCLUDING, WITHOUT LIMITATION, WARRANTIES OR MERCHANTABILITY AND FITNESS FOR A PARTICULAR PURPOSE) EITHER EXPRESSED OR IMPLIED. MARC ANALYSIS RESEARCH CORPORATION SHALL NOT BE LIABLE FOR DAMAGES RESULTING FROM ANY ERROR CONTAINED HEREIN, INCLUDING, BUT NOT LIMITED TO, FOR ANY SPECIAL, INCIDENTAL OR CONSEQUENTIAL DAMAGES ARISING OUT OF, OR IN CONNECTION WITH, THE USE OF THIS DOCUMENT.

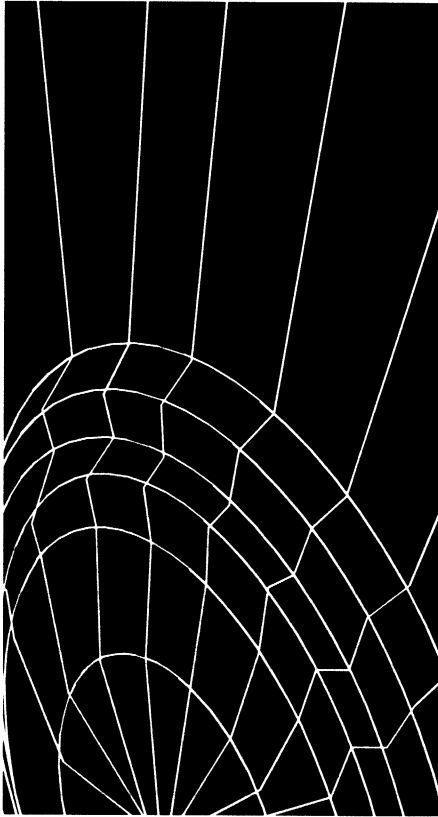
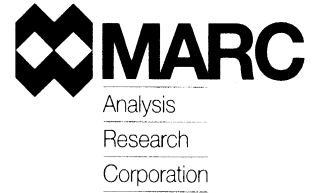
This software product and its documentation set are copyrighted and all rights are reserved by MARC Analysis Research Corporation. Usage of this product is only allowed under the terms set forth in the MARC Analysis Research Corporation License Agreement. Any reproduction or distribution of this document, in whole or in part, without the prior written consent of MARC Analysis Research Corporation is prohibited.

## Restricted Rights Notice

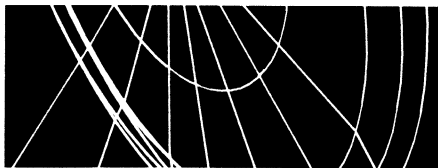
This computer software is commercial computer software submitted with "restricted rights." Use, duplication, or disclosure by the government is subject to restrictions as set forth in subparagraph (c)(i)(ii) or the Rights in technical Data and Computer Software clause at DFARS 252.227-7013, NASA FAR Supp. Clause 1852.227-86, or FAR 52.227-19. Unpublished rights reserved under the Copyright Laws of the United States.

## Trademarks

All products mentioned are the trademarks, service marks, or registered trademarks of their respective holders.



**MARC**



# **Volume E**

## **Demonstration Problems**

Version K7

Part III

- Heat Transfer
- Dynamics





# Part III

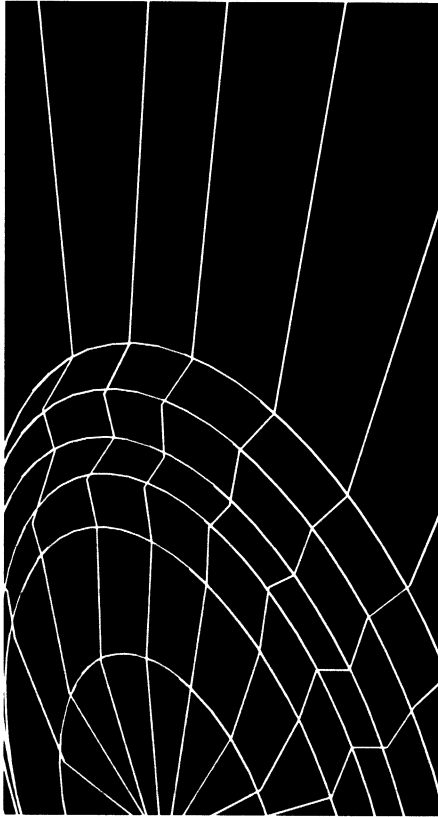
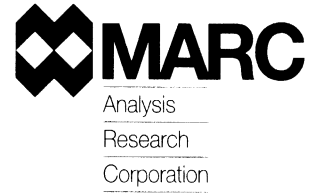
## *Volume E: Demonstration Problems*



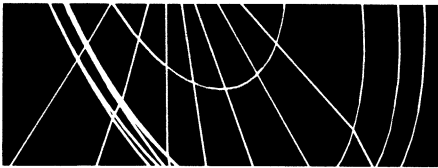
**Chapter 5**      **Heat Transfer**

**Chapter 6**      **Dynamics**





**MARC**



# **Volume E**

**Demonstration Problems**

Version K7

**Chapter 5**  
**Heat Transfer**





---

5

## *Heat Transfer Contents*



<b>Description</b>	<b>Problem</b>
One-Dimensional Steady State Heat Conduction . . . . .	5.1
One-Dimensional Transient Heat Conduction . . . . .	5.2
Plate with a Fluid Passing through a Circular Hole . . . . .	5.3
Three-Dimensional Transient Heat Conduction . . . . .	5.4
Pressure Vessel Subjected to Thermal Downshock . . . . .	5.5
Axisymmetric Transient Heat Conduction Simulated by Planar Elements . . . . .	5.6
Steady State Analysis of an Anisotropic Plate . . . . .	5.7
Nonlinear Heat Conduction of a Channel . . . . .	5.8
Latent Heat Effect . . . . .	5.9
Centerline Temperature of a Bare Steel Wire . . . . .	5.10
Heat Transfer and Stress Analysis of a Jominy End Quench Test Specimen . . . . .	5.11
Cylinder-plane Electrode . . . . .	5.12
Axisymmetric Transient Heat Conduction Simulated by Heat Transfer Shell Elements	5.13
Steady-state Temperature Distribution of a Generic Fuel Nozzle . . . . .	5.14
Radiation Between Concentric Spheres . . . . .	5.15
Three-Dimensional Thermal Shock . . . . .	5.16
Cooling of Electronic Chips . . . . .	5.17
Square Plate Heated at a Center Portion . . . . .	5.18



## **5** *Heat Transfer Contents*

---

---



## *Heat Transfer List of Figures*



<b>Figure</b>	<b>Page</b>
5.1-1 One-Dimensional Link and Mesh. . . . .	5.1-3
5.2-1 One-Dimensional Link and Mesh. . . . .	5.2-3
5.2-2 Temperature Distributions, $t = 4$ seconds . . . . .	5.2-4
5.2-3 Temperature Distributions, $t = 10$ seconds . . . . .	5.2-5
5.2-4 Temperature Distribution, $t = 20$ seconds. . . . .	5.2-6
5.3-1 Mesh for Element Type 41 . . . . .	5.3-6
5.3-2 Mesh for Element Type 69 . . . . .	5.3-7
5.3-3 Mesh for Element Type 39 . . . . .	5.3-8
5.3-4 Mesh for Element Type 37 . . . . .	5.3-9
5.3-5 Mesh for Element Type 121 . . . . .	5.3-10
5.3-6 Mesh for Element Type 131 . . . . .	5.3-11
5.3-7 Temperature History for Elements Types: 37, 39, 41, 69, 121, and 131 . . . . .	5.3-12
5.4-1 Mesh for the Unit Cube Linear Elements . . . . .	5.4-4
5.4-2 Mesh for the Unit Cube Parabolic Elements . . . . .	5.4-5
5.4-3 Cube Center Temperature History for Element Types: 43, 44, 71, and 123 . . . . .	5.4-6
5.5-1 Temperature Time History . . . . .	5.5-4
5.5-2 Geometry and Mesh . . . . .	5.5-4
5.5-3 Transient Temperature Time History (Auto Time Step) . . . . .	5.5-5
5.5-4 Temperature Distribution in Cylinder Wall . . . . .	5.5-6
5.6-1 Cylinder and Mesh . . . . .	5.6-4
5.7-1 Plate and Mesh . . . . .	5.7-3
5.8-1 Geometry for Nonlinear Heat Conduction . . . . .	5.8-7
5.8-2 Heat Transfer Example Mesh. . . . .	5.8-8
5.8-3 Isotherms at 100 Seconds . . . . .	5.8-9



<b>Figure</b>	<b>Page</b>
5.8-4 Isotherms at 400 Seconds . . . . .	5.8-10
5.8-5 Isotherms at 1000 Seconds . . . . .	5.8-11
5.8-6 Temperature History . . . . .	5.8-12
5.9-1 Cylinder Meshes . . . . .	5.9-5
5.9-2 Temperature Dependent Thermal Properties . . . . .	5.9-6
5.9-3 Temperature History for Center and Outer Surface of Cylinder . . . . .	5.9-7
5.10-1 Mesh of Steel Wire . . . . .	5.10-3
5.11-1 Thermal Conductivity vs. Temperature . . . . .	5.11-7
5.11-2 Specific Heat vs. Temperature . . . . .	5.11-8
5.11-3 Jominy Bar – Axisymmetric Finite Element Model (Elements) . . . . .	5.11-9
5.11-4 Jominy Bar – Axisymmetric Finite Element Model (Nodes) . . . . .	5.11-10
5.11-5 Material Properties vs. Temperature . . . . .	5.11-11
5.11-6 Yield Stress vs. Temperature . . . . .	5.11-12
5.11-7 Workhardening vs. Temperature . . . . .	5.11-13
5.11-8 Jominy End Quench Test – Temperature vs. Time . . . . .	5.11-14
5.11-9 Jominy End Quench Test – Temperature vs. Increment . . . . .	5.11-15
5.11-10 Jominy End Quench Test – Equivalent Stress vs. Increment . . . . .	5.11-16
5.11-11 Jominy End Quench Test – Axial Stress vs. Increment . . . . .	5.11-17
5.11-12 Jominy End Quench Test – Radial Stress vs. Increment . . . . .	5.11-18
5.11-13 Jominy End Quench Text – Hoop Stress vs. Increment . . . . .	5.11-19
5.12-1 Geometry of the Problem . . . . .	5.12-2
5.12-2 Temperature Dependent Properties . . . . .	5.12-2
5.12-3 Mesh . . . . .	5.12-3
5.12-4 Temperature Distribution . . . . .	5.12-4
5.12-5 Voltage Distribution . . . . .	5.12-5
5.12-6 Current Distribution . . . . .	5.12-6
5.13-1 Cylinder Model and Fluid Temperature History . . . . .	5.13-6
5.13-2 Finite Element Model (Model A - Element 85) . . . . .	5.13-7
5.13-3 Finite Element Model (Model B - Element 86) . . . . .	5.13-8
5.13-4 Finite Element Model (Model C - Element 87) . . . . .	5.13-9
5.13-5 Finite Element Model (Model D - Element 88) . . . . .	5.13-9

<b>Figure</b>	<b>Page</b>
5.14-1 Simplified Nozzle . . . . .	5.14-5
5.14-2 Simplified Nozzle (Finite Element Mesh) . . . . .	5.14-6
5.14-3 Simplified Nozzle Solid and Fluid Temperatures) . . . . .	5.14-7
5.15-1 Radiating Concentric Spheres. . . . .	5.15-4
5.15-2 Mesh with Element Numbers . . . . .	5.15-5
5.15-3 Mesh with Node Numbers . . . . .	5.15-6
5.16-1 Temperature History for Free End Node 136 Element Type 44. . . . .	5.16-4
5.16-2 Temperature History for Free End Node 126 (Element Type 123) . . . . .	5.16-5
5.16-3 Iso-thermal Surfaces at $t = 0.0196$ seconds (Element Type 123) . . . . .	5.16-6
5.16-4 Temperature History for Free End Node 26 (Element Type 133) . . . . .	5.16-7
5.16-5 Iso-thermal Surfaces at $t = 0.0193$ seconds (Element Type 133) . . . . .	5.16-8
5.17-1 Complete Finite Element Mesh . . . . .	5.17-3
5.17-2 Finite Element Mesh of Chips and Board. . . . .	5.17-4
5.17-3 Temperature Distribution Excluding Heat Convection . . . . .	5.17-5
5.17-4 Temperature Distribution Including Heat Convection . . . . .	5.17-6
5.18-1 Heated Square Plate, Geometry, and Finite Element Mesh . . . . .	5.18-4
5.18-2 Temperature Distribution Steady-state Analysis . . . . .	5.18-5
5.18-3 Path Plots for Upper and Lower Temperature at $x = 0$ (inc = 1) . . . . .	5.18-6
5.18-4 Path Plots for Upper and Lower Temperature at $x = 0$ (inc = 15) . . . . .	5.18-7



## **5** *Heat Transfer List of Figures*

---

---

 **5**

## *Heat Transfer List of Tables*



<b>Table</b>	<b>Page</b>
5.1 Heat Transfer Analysis Demonstration Problems . . . . .	5-2
5.2-1 Nodal Temperatures. . . . .	5.2-2
5.6-1 Comparison of Nodal Temperatures . . . . .	5.6-2
5.10-1 Nodal Voltages and Temperatures . . . . .	5.10-2
5.11-1 Thermal Conductivity vs. Temperature (AISI 4140 Steel) . . . . .	5.11-2
5.11-2 Specific Heat vs. Temperature (AISI 4140) . . . . .	5.11-3
5.11-3 Coefficient of Thermal Expansion (AISI 4140) . . . . .	5.11-4
5.13-1 Comparison of Nodal Temperatures . . . . .	5.13-3



## **5** *Heat Transfer List of Tables*

---



---

 **5**

## ***Heat Transfer***



MARC contains a solid body heat transfer capability for one-, two- and three-dimensional, steady-state and transient analyses. A discussion of the use of this capability can be found in *MARC Volume A: Theory and User Information* and a summary of the features is given below.

Selection of elements:

- 1-D: Three-dimensional links (2-, 3-node)
- 2-D: Planar and axisymmetric elements (3-, 4-, 6-, and 8-node)
- 3-D: Brick elements (8- and 20-node)
- Reduced integration elements with hourglass control

Time integration operator:

- Backward difference –unconditionally stable for linear problems; automatic time-step choice; in-core and out-of-core solutions.

Temperature dependent materials (including latent heat effects); anisotropic thermal conductivity.

Extrapolated averaging for the evaluation of temperature-dependent properties.

Nonuniform initial conditions.

Temperature, time-dependent boundary conditions: prescribed temperature history, volumetric flux, surface flux, film coefficients, radiation; change of prescribed temperature boundary conditions during analysis.

Tying constraints on nodal temperatures.

Two- and three-dimensional mesh generation; bandwidth optimization.

Contour or temperature time history plots; mesh plots.

Ability to restart the analysis.

Selective print of nodal and/or element temperatures; consistent nodal fluxes.

Direct interface with stress analysis.

User subroutines.

A number of solved problems are compiled in this chapter. These problems illustrate the use of various MARC heat transfer elements and demonstrate the selection of different options. Table 5.1 shows MARC elements and options used in these demonstration problems.

**Table 5.1** Heat Transfer Analysis Demonstration Problems

Problem Number (E)	Element Type	Parameters	Model Definition	History Definition	User Subroutines	Problem Description
5.1	36	HEAT	—	TRANSIENT NON AUTO	—	One-dimensional steady-state heat conduction, constant properties, prescribed temperature boundary conditions, 2-node link element.
5.2	65	HEAT FORCDT	FORCDT INITIAL TEMP	TRANSIENT NON AUTO	FORCDT	One-dimensional transient heat conduction, constant properties, prescribed temperature boundary conditions, 3-node link element.
5.3	41 69 39 37 121 131	HEAT FILMS ALIAS	INITIAL TEMP FILMS CONTROL OPTIMIZE	TRANSIENT NON AUTO	—	Two-dimensional transient heat conduction, constant properties, prescribed temperature and convective boundary conditions, 3-, 4-, and 8-node reduced integration planar elements.
5.4	43 44 71 123	HEAT	INITIAL TEMP CONTROL PRINT CHOICE UDUMP	TRANSIENT NON AUTO	—	Three-dimensional transient heat conduction, constant properties, prescribed temperature and insulated boundary conditions, 8-, 20-node and reduced integration elements.
5.5	42 70	HEAT FILMS ALIAS	INITIAL TEMP CONTROL FILMS	TRANSIENT	FILM	Axisymmetric transient heat conduction, constant properties, convective boundary conditions, 8-node axisymmetric and reduced integration elements.



## 5 Heat Transfer

**Table 5.1** Heat Transfer Analysis Demonstration Problems (Continued)

Problem Number (E)	Element Type	Parameters	Model Definition	History Definition	User Subroutines	Problem Description
5.6	41	HEAT FILMS	INITIAL TEMP CONTROL FILMS	TRANSIENT	FILM	Same as problem 5.5, except using 8-node planar element.
5.7	39	HEAT	ANISOTROPIC	TRANSIENT NON AUTO	ANKOND	Two-dimensional heat conduction, constant properties, anisotropic conductivity, prescribed conditions, 4-node planar element.
5.8	41	HEAT MESH PLOT	FILMS FLUXES INITIAL TEMP CONTROL TEMP EFFECTS RESTART OPTIMIZE	TRANSIENT	FILM FLUX	Nonlinear heat conduction, temperature dependent properties, prescribed temperature, convective, and radiative boundary conditions, 8-node planar element.
5.9	40 122 132	HEAT	TEMP EFFECTS INITIAL TEMP CONTROL FILMS PRINT CHOICE UDUMP	TRANSIENT NON AUTO	—	Latent heat effect, temperature dependent properties, convective boundary condition 4-node axisymmetric element.
5.10	40	HEAT JOULE	JOULE DIST CURRENT VOLTAGE FILMS	TRANSIENT NON AUTO	—	Evaluate temperatures in a wire due to current.
5.11	42 28	HEAT MARC.PLOT THERMAL T-T-T	TEMP EFFECTS FILMS TIME-TEMP CHANGE STATE INITIAL TEMP	TRANSIENT AUTO THERM CHANGE STATE	—	Evaluate transient temperature response due quenching process. Evaluate thermally-induced stresses.
5.12	39	ALIAS JOULE HEAT	VOLTAGE POST JOULE	TRANSIENT	—	Electro static planar analysis.



**Table 5.1** Heat Transfer Analysis Demonstration Problems (Continued)

Problem Number (E)	Element Type	Parameters	Model Definition	History Definition	User Subroutines	Problem Description
5.13	85 86 87 88	HEAT SHELL SECT	INITIAL TEMP FILMS POST	TRANSIENT	FILM	Thermal ratcheting using shell elements.
5.14	39	HEAT PRINT, 7	DEFINE TEMP EFFECTS CONRAD GAP CHANNEL FILMS	TRANSIENT	FILM FLOW	Steady state temperature distribution of a fuel nozzle.
5.15	42	HEAT RADIATION	RADIATING CAVITY TEMP EFFECTS FIXED TEMP	STEADY STATE	—	Radiating concentric spherical bodies.
5.16	123 133 135	HEAT LUMP	INITIAL TEMP	TRANSIENT	—	Thermal shock.
5.17	39	HEAT	FIXED TEMP INITIAL TEMP VELOCITY	TRANSIENT NONAUTO	—	Cooling of electronic chips.
5.18	50	HEAT LUMP SHELL SECT	ORTHOTROPIC ORIENTATION INITIAL TEMP DIST FLUXES	STEADY STATE TRANSIENT	—	Thermal behavior in orthotropic shell.



## 5.1 One-Dimensional Steady State Heat Conduction

A bar has an initial temperature of 0°F. One end is subsequently subjected to 100°F; the other to 200°F. The temperature distribution along the bar is calculated for subsequent times.

### Model/Element

This one-dimensional steady-state heat conduction problem is analyzed by using element type 36 (three-dimensional link). The model consists of six nodes and five elements, which allows a linear variation of temperature along its length. The dimensions of the model and a finite element mesh are shown in Figure 5.1-1.

### Material Properties

The conductivity is 0.000213 Btu/sec-in.-°F. The specific heat is 0.105 BTU/lb-°F. The mass density is 0.283 lb/cu/inch.

### Geometry

The default value of 1.0 square inch is used for the cross-sectional area of the link. No geometry input data is required.

### Boundary Conditions

Constant nodal temperatures of 100°F and 200°F are prescribed at nodes 1 and 6, respectively.

### Transient

A very large time step ( $\Delta t = 100,000$  sec) is chosen for obtaining the steady-state solution and the total transient time is also assumed to be 100,000 seconds. Consequently, the steady state solution is reached in one time step. The nonautomatic TIME STEP option in MARC is invoked in the analysis. As an alternative, the STEADY STATE option could be used.

### Results

A linear distribution of steady state temperatures is obtained, as expected. The nodal temperatures are:

Node Number	Temperature °F
1	100
2	120
3	140
4	160
5	180
6	200



**Parameters, Options, and Subroutines Summary**

Example e5x1.dat:

<b>Parameters</b>	<b>Model Definition Options</b>	<b>History Definition Options</b>
ELEMENT	CONNECTIVITY	CONTINUE
END	COORDINATE	TRANSIENT
HEAT	END OPTION	
SIZING	FIXED TEMPERATURE	
TITLE	ISOTROPIC	

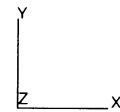
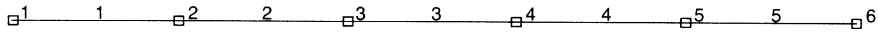
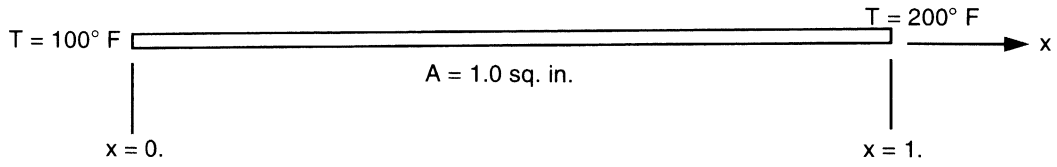


Figure 5.1-1 One-Dimensional Link and Mesh



## **5 Heat Transfer**

*One-Dimensional Steady State Heat Conduction*

---





## 5.2 One-Dimensional Transient Heat Conduction

A bar has an initial temperature of 0°F. One end is subsequently subjected to 100°F, the other to 200°F. The temperature distribution along the bar is calculated for subsequent times.

This problem is modeled using the two techniques summarized below.

Data Set	Element Type(s)	Number of Elements	Number of Nodes	Differentiating Features
e5x2a	65	5	11	
e5x2b	65	5	11	FORCDT

### Model

This one-dimensional transient heat conduction problem is analyzed by using element type 65 (3-node truss). The model consists of eleven nodes and five elements. The element type 65 allows a quadratic variation of temperature along its length. The dimension of the model and a finite element mesh are shown in Figure 5.2-1.

### Material Properties

Material properties of the model are:

Conductivity is 0.000213 Btu/sec-in.-°F

Specific heat is 0.105 Btu/lb-°F

Mass density is 0.283 lb/cubic inch

### Geometry

The default value of 1.0 square inch is used for the cross-section area of the link. No geometry input data is required.

### Boundary Conditions

Constant nodal temperatures of 100°F and 200°F are prescribed at nodes 1 and 11, respectively. This problem is evaluated twice: In the first input, the boundary temperature is specified using the FIXED TEMP option; in the second case, subroutine FORCDT is used to specify the temperatures.

### Initial Condition

Initial nodal temperatures are assumed to be 0°F.

### Transient

The transient time is assumed to be 20 seconds and a constant time step of 1.0 seconds selected for the analysis. The total number of time steps in the analysis is 20. The time step is kept constant by using the nonautomatic TIME STEP option in the program.

**Results**

Temperature distributions are tabulated in Table 5.2-1 and plotted in Figure 5.2-2, Figure 5.2-3 and Figure 5.2-4. At the end of 20 seconds, the steady-state conditions have not yet been achieved.

Because there are no temperature-dependent material properties and the time increment is fixed, the analysis is performed through a series of back substitutions. In increment 3, the total temperature change was greater than that given in the CONTROL option. In increment 4, MARC resassembled. This was not necessary for the accuracy of this particular problem.

**Table 5.2-1** Nodal Temperatures

Time Sec.	Node 1	Node 2	Node 3	Node 4	Node 5	Node 6	Node 7	Node 8	Node 9	Node 10	Node 11
2.	100	49.0	20.3	8.3	3.9	3.3	6.5	16.2	40.4	98.0	200
4.	100	64.9	37.8	21.0	13.2	13.0	20.7	39.5	74.5	129.5	200
6.	100	72.4	49.3	33.2	25.4	26.5	37.3	59.8	95.5	143.7	200
8.	100	77.4	58.0	44.3	38.1	40.6	53.0	76.1	109.7	152.3	200
10.	100	81.4	65.4	54.3	50.1	54.0	67.0	89.4	120.4	158.3	200
S.S	100	110	120	130	140	150	160	170	180	190	200

**Parameters, Options, and Subroutines Summary**

Example e5x2a.dat:

Parameters	Model Definition Options	History Definition Options
ELEMENT	CONNECTIVITY	CONTINUE
END	CONTROL	TRANSIENT
HEAT	COORDINATE	
SIZING	END OPTION	
TITLE	FIXED TEMP	
	INITIAL TEMP	
	ISOTROPIC	

User subroutine in u5x2.f:

FORCDT

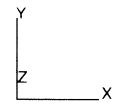
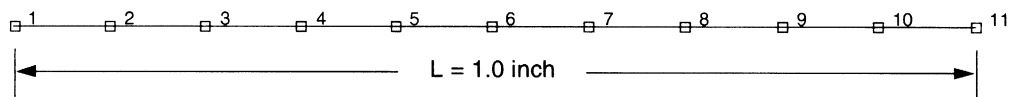


**Figure 5.2-1** One-Dimensional Link and Mesh

INC : 4  
SUB : 0  
TIME : 4.000e+00  
FREQ : 0.000e+00

prob 5.2 heat - elmt 65



Temperatures (x100)

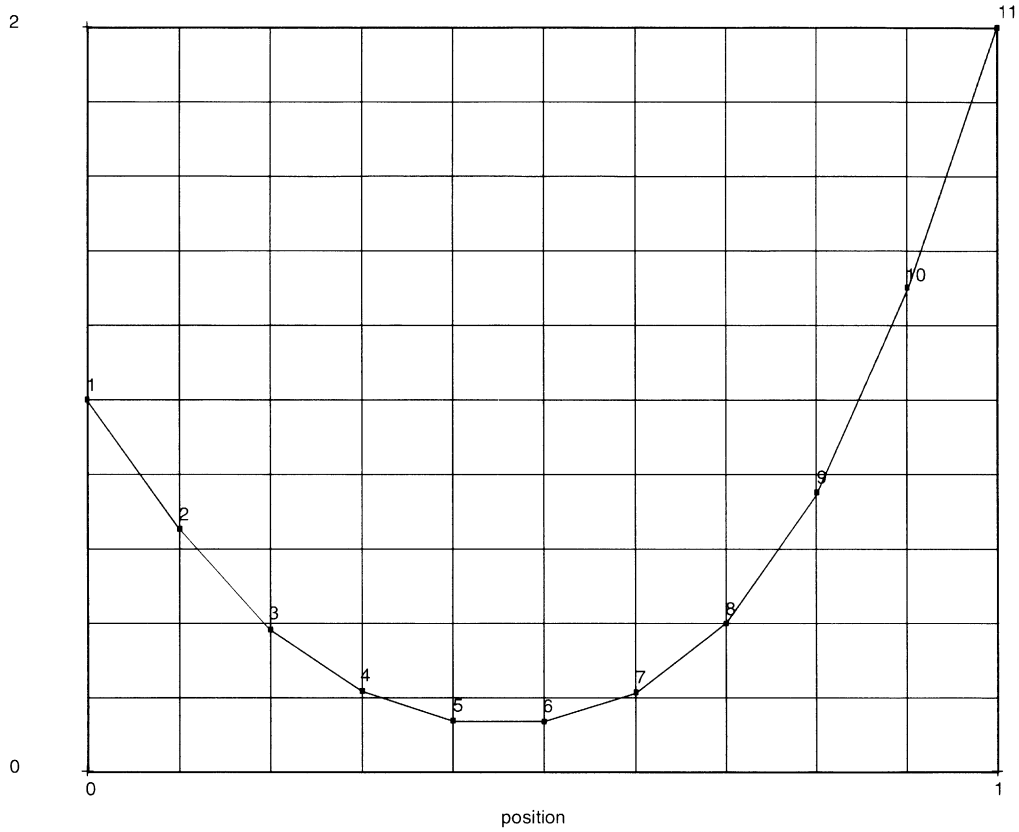


**Figure 5.2-2** Temperature Distributions, t = 4 seconds

INC : 10  
SUB : 0  
TIME : 1.000e+01  
FREQ : 0.000e+00

prob 5.2 heat - elmt 65



Temperatures (x100)

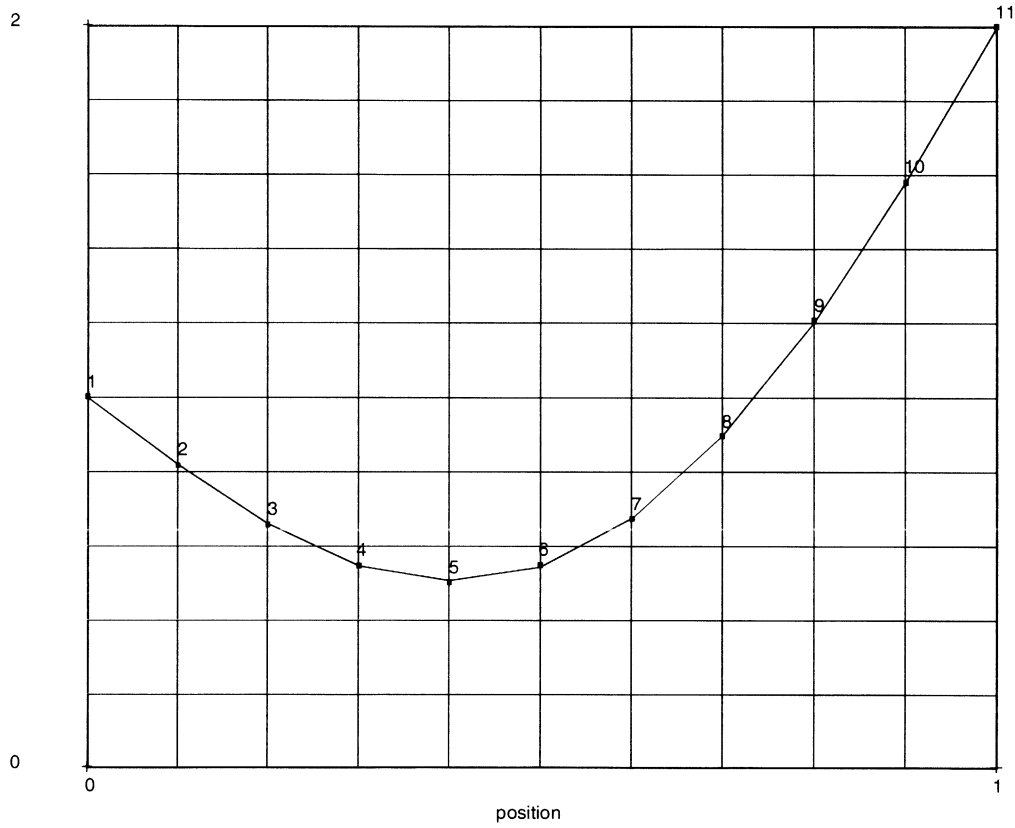


**Figure 5.2-3** Temperature Distributions,  $t = 10$  seconds

INC : 20  
SUB : 0  
TIME : 2.000e+01  
FREQ : 0.000e+00

prob 5.2 heat - elmt 65



Temperatures (x100)

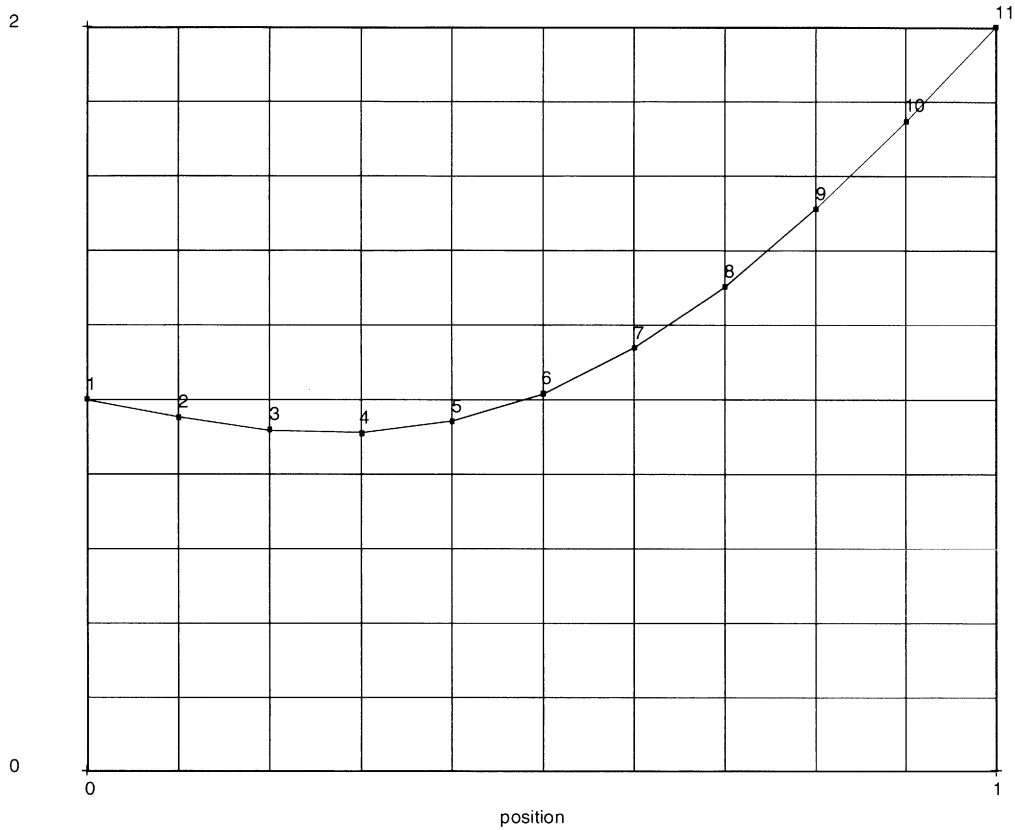


**Figure 5.2-4** Temperature Distribution,  $t = 20$  seconds

### 5.3 Plate with a Fluid Passing through a Circular Hole

A two-dimensional transient heat conduction problem of a plate with a circular hole is analyzed by using several MARC elements. The hole is filled with a fluid at a temperature 1000°F with the exterior square edges at a fixed temperature of 500°F. The plate is initially at 500°F and is allowed to heat up for 5 seconds.

This problem is modeled using the six techniques summarized below.

Data Set	Element Type(s)	Number of Elements	Number of Nodes
e5x3a	41	8	37
e5x3b	69	8	37
e5x3c	39	32	45
e5x3d	37	64	65
e5x3e	121	32	45
e5x3f	131	16	45

#### Elements

Element types 37, 39, 41, 69, 121, and 131 (3-, 4-, 8-, 8-, 4-, and 6-node planar elements). Type 69 is an 8-node quadrilateral element with reduced integration. Type 121 is a 4-node quadrilateral element with reduced integration with hourglass control. Type 131 is a 6-node triangular element.

#### Model

This problem demonstrates the use of a variety of elements and the FILM option for prescribing convective boundary conditions. A rectangular plate 20 inches by 29 inches with a hole of radius 5 inches placed in the center is modeled.

Due to symmetry only a quarter of the plate is modeled for the analysis as shown in Figure 5.3-1 through Figure 5.3-4.

#### Thermal Property

One set of thermal properties is specified in the PROPERTY block: the isotropic thermal conductivity value of 0.42117 E5 Btu/sec-in.-°F; the specific heat is 0.3523 E-3 Btu/lb-°F; and the mass density is 0.7254 E-3 lb/cubic inch.

#### Geometry

The thickness of the plate is 0.1 inches.

**Thermal Boundary Conditions**

The initial temperature distribution is that all nodes have a temperature of 500.0°F. The lines of symmetry ( $x = 0$  and  $y = 0$ ) are adiabatic and require no data input. At time,  $t = 0$ , the fluid is exposed to the circular hole with a sink temperature of 1000°F, and a film coefficient of  $0.4678E-5$  Btu/sec-sq.in.-°F. The outer edges ( $x = y = 12$  inches) are held at a fixed temperature of 500°F.

**Load History**

The maximum number of time points are fixed at 10 with a final time of 5 seconds. Nonautomatic time stepping is used with a constant time step of 0.5 seconds/increment.

**Results**

The temperature history at the center point between the radius of the hole and the corner of the plate (nodes 11, 23, 9, 9, 23, 9 for mesh composed of element type 37, 39, 41, 69, 121 and 131) is shown in Figure 5.3-4.

**Parameters, Options, and Subroutines Summary**

Example e5x3a.dat:

<b>Parameters</b>	<b>Model Definition Options</b>	<b>History Definition Options</b>
ELEMENT	CONNECTIVITY	CONTINUE
END	CONTROL	STEADY STATE
HEAT	COORDINATE	TRANSIENT
SIZING	END OPTION	
TITLE	FILMS	
	FIXED TEMP	
	GEOMETRY	
	INITIAL TEMP	
	ISOTROPIC	
	POST	
	UDUMP	





Example e5x3b.dat:

<b>Parameters</b>	<b>Model Definition Options</b>	<b>History Definition Options</b>
ELEMENT	CONNECTIVITY	CONTINUE
END	CONTROL	TRANSIENT
HEAT	COORDINATE	
SIZING	END OPTION	
TITLE	FILMS	
	FIXED TEMP	
	GEOMETRY	
	INITIAL TEMP	
	ISOTROPIC	
	POST	

Example e5x3c.dat:

<b>Parameters</b>	<b>Model Definition Options</b>	<b>History Definition Options</b>
ELEMENT	CONNECTIVITY	CONTINUE
END	CONTROL	TRANSIENT
HEAT	COORDINATE	
SIZING	END OPTION	
TITLE	EXIT	
	FILMS	
	FIXED TEMP	
	GEOMETRY	
	INITIAL TEMP	
	ISOTROPIC	
	POST	



Example e5x3d.dat:

<b>Parameters</b>	<b>Model Definition Options</b>	<b>History Definition Options</b>
ELEMENT	CONNECTIVITY	CONTINUE
END	CONTROL	TRANSIENT
HEAT	COORDINATE	
SIZING	END OPTION	
TITLE	EXIT	
	FILMS	
	FIXED TEMP	
	GEOMETRY	
	INITIAL TEMP	
	ISOTROPIC	
	POST	

Example e5x3e.dat:

<b>Parameters</b>	<b>Model Definition Options</b>	<b>History Definition Options</b>
ALIAS	CONNECTIVITY	CONTINUE
ELEMENT	CONTROL	TRANSIENT
END	COORDINATE	
HEAT	END OPTION	
SIZING	FILMS	
TITLE	FIXED TEMP	
	GEOMETRY	
	INITIAL TEMP	
	ISOTROPIC	
	POST	



Example e5x3f.dat:

**Parameters**

ALL POINTS  
ELEMENT  
END  
HEAT  
SIZING  
TITLE

**Model Definition Options**

CONNECTIVITY  
CONTROL  
COORDINATE  
END OPTION  
FILMS  
FIXED TEMP  
GEOMETRY  
INITIAL TEMP  
ISOTROPIC  
POST

**History Definition Options**

CONTINUE  
TRANSIENT

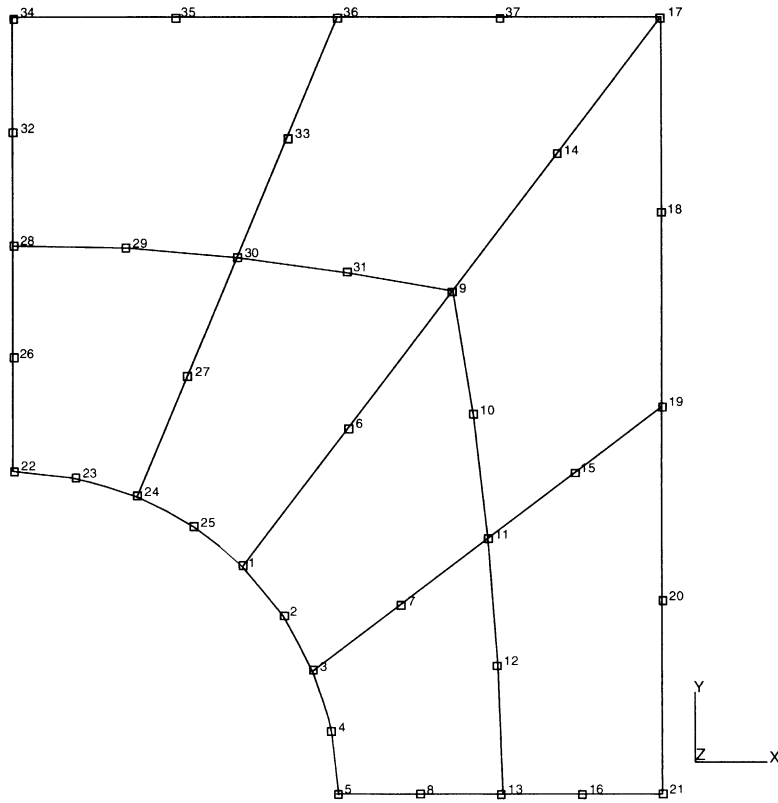
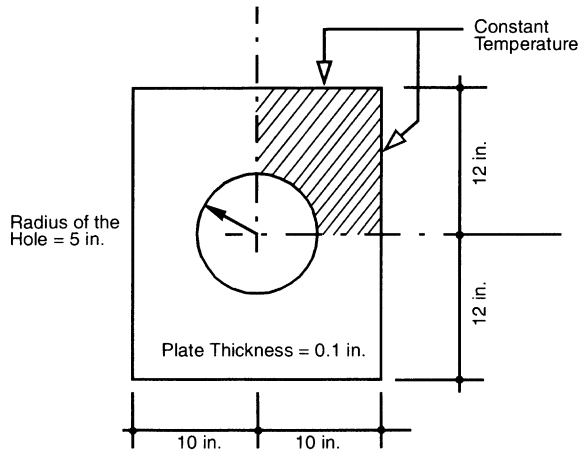


**Figure 5.3-1** Mesh for Element Type 41

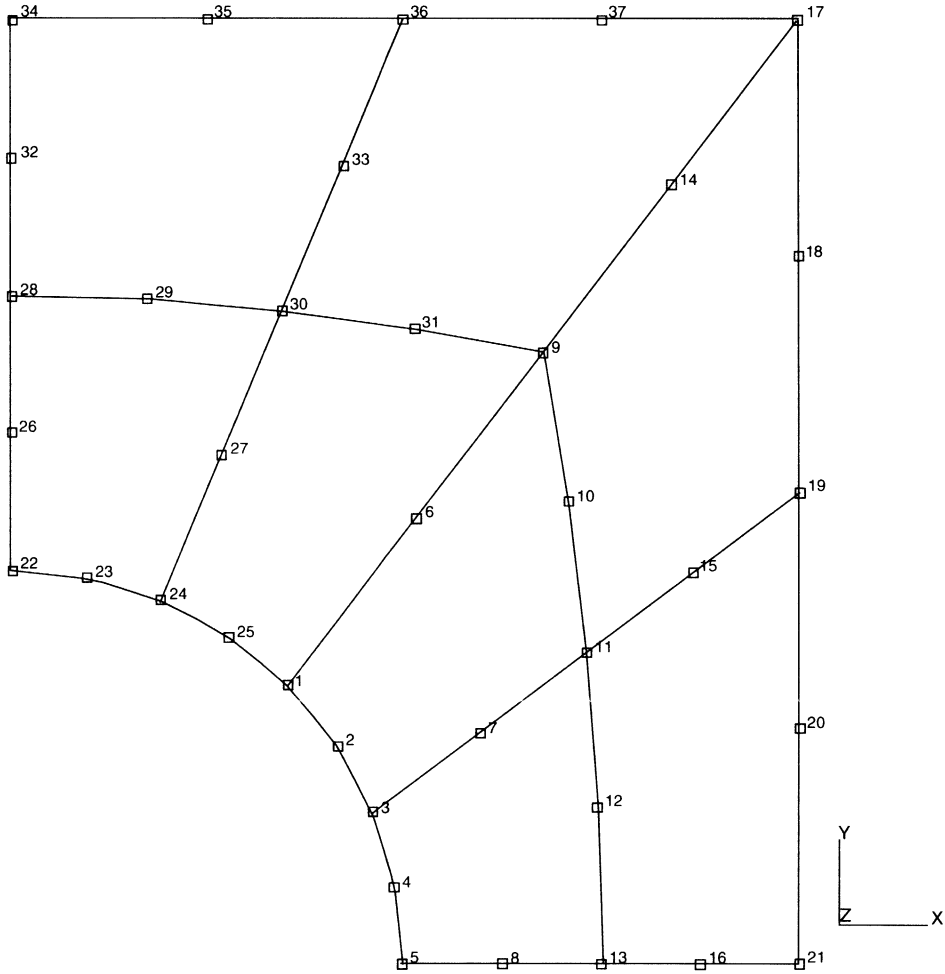
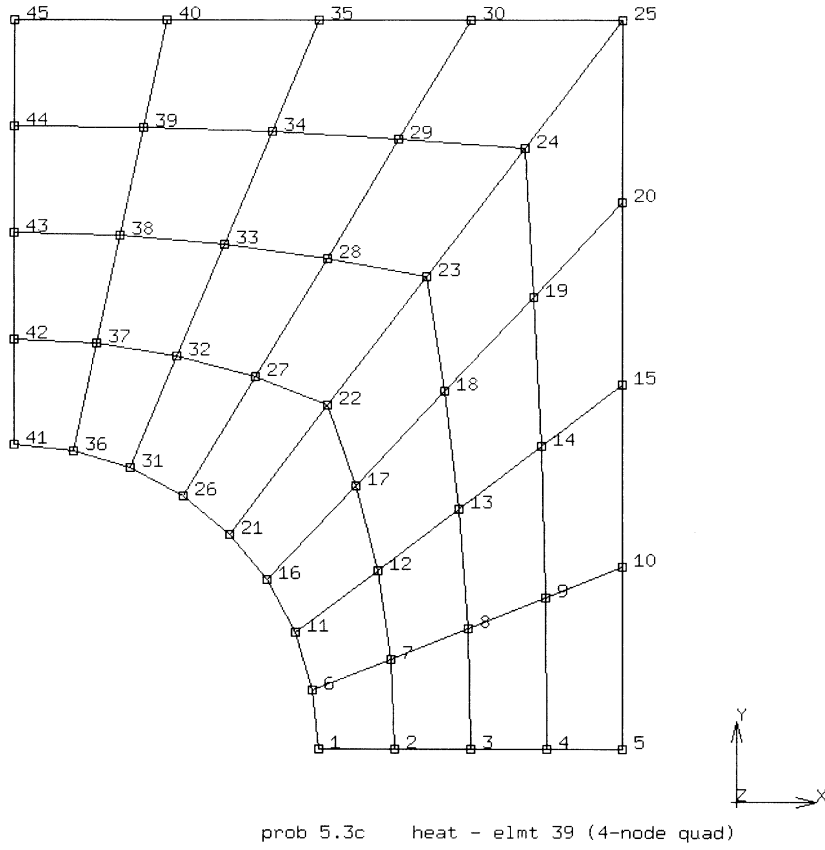
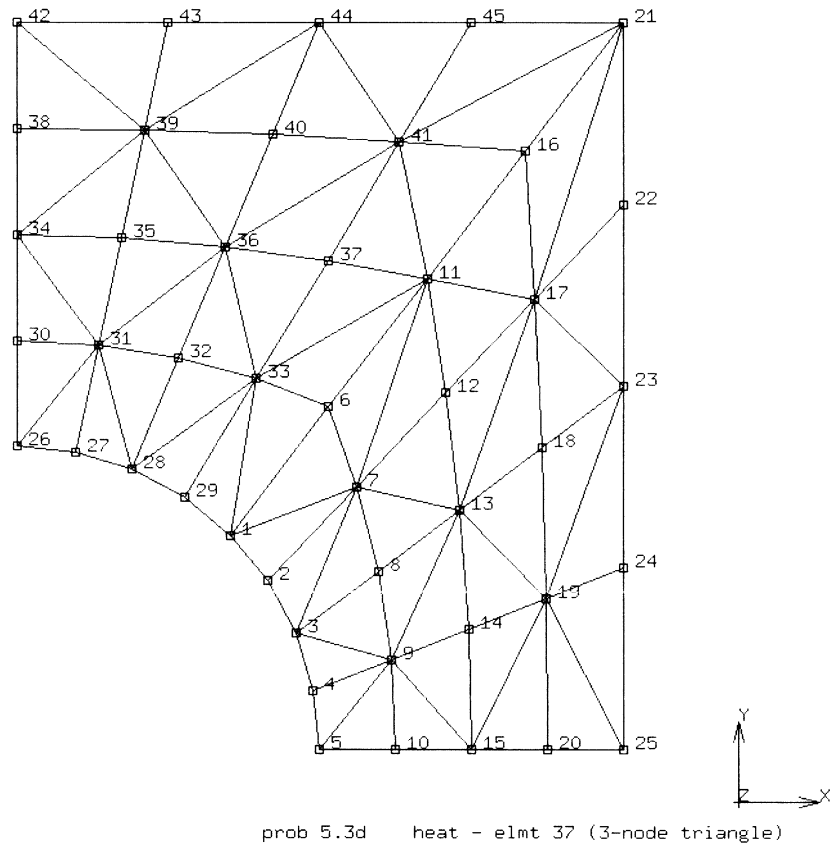


Figure 5.3-2 Mesh for Element Type 69



**Figure 5.3-3** Mesh for Element Type 39



**Figure 5.3-4** Mesh for Element Type 37

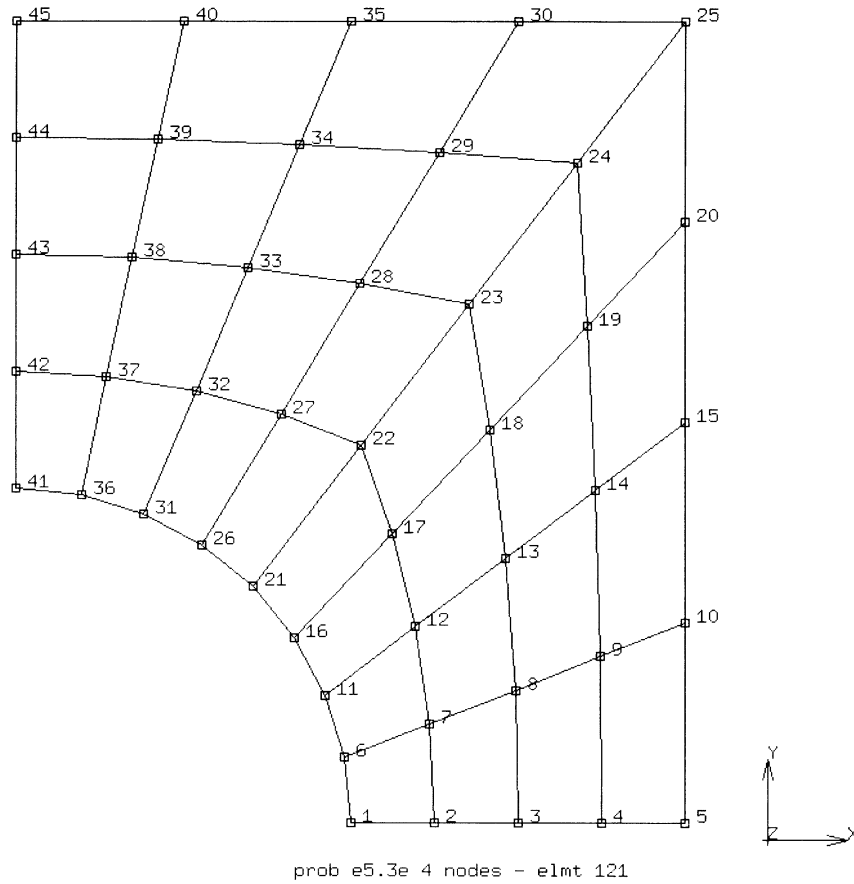


**Figure 5.3-5** Mesh for Element Type 121



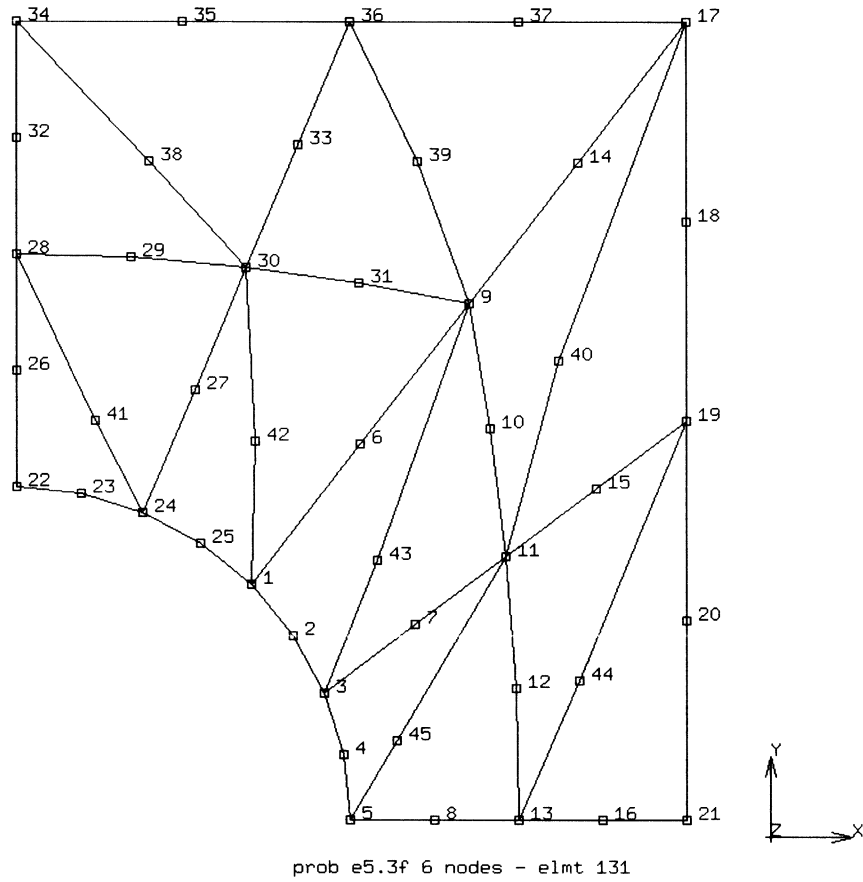
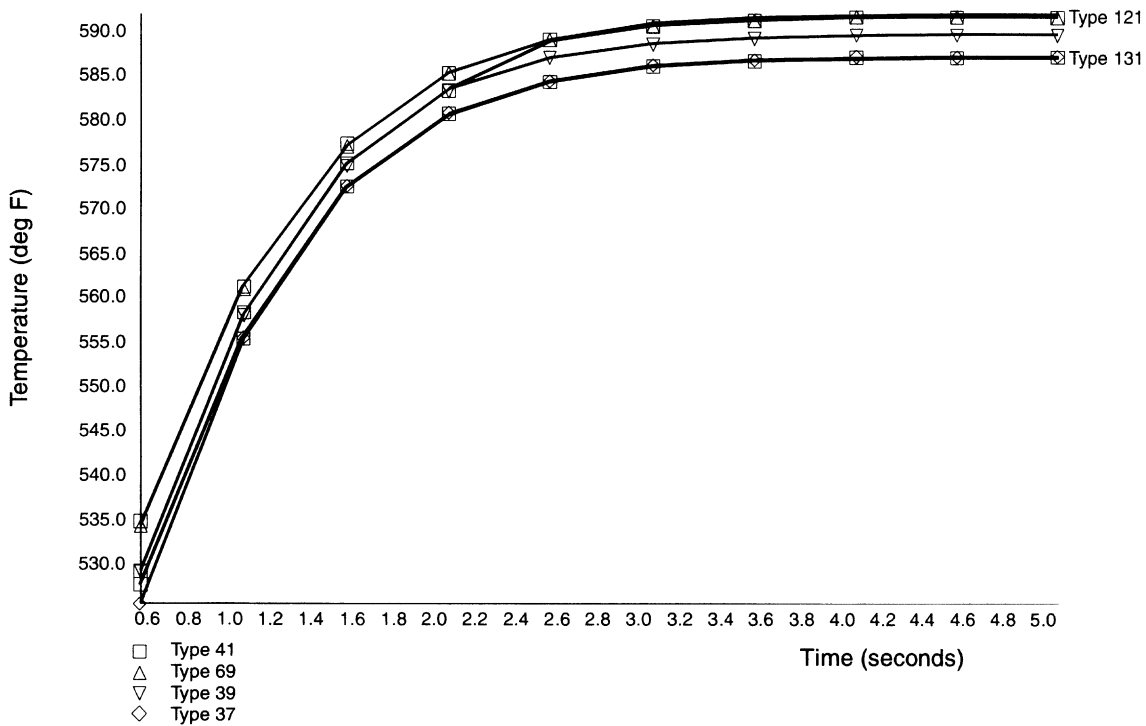


Figure 5.3-6 Mesh for Element Type 131

Time Sec	Temperatures (element type, node number)					
	41, n9	69, n9	39, n23	37, n11	121, n23	131, n9
.50	535.403	534.993	529.728	526.038	529.731	528.283
1.0	561.951	561.689	558.964	555.728	558.690	556.195
1.5	577.971	577.786	575.893	573.122	575.814	573.194
2.0	585.914	585.783	584.044	581.475	584.040	581.393
2.5	589.609	589.509	587.735	585.241	589.839	585.109
3.0	591.287	591.206	589.369	586.900	591.577	586.756
3.5	592.042	591.970	590.086	587.624	592.278	587.481
4.0	592.381	592.314	590.400	587.939	592.577	587.799
4.5	592.533	592.468	590.537	588.076	592.707	587.938
5.0	592.601	592.538	590.597	588.136	592.763	587.999



**Figure 5.3-7** Temperature History for Elements Types: 37, 39, 41, 69, 121, and 131



## 5.4 Three-Dimensional Transient Heat Conduction

A unit cube is initially at a temperature of 100°F throughout. Two faces of the cube have a temperature of 0°F. The other faces are insulated. The temperature at the center of the cube is calculated for subsequent times (0 to 10 seconds).

This problem is modeled using the three techniques summarized below.

Data Set	Element Type(s)	Number of Elements	Number of Nodes
e5x4a	43	8	27
e5x4c	71	8	81
e5x4d	123	8	27

### Elements

Element types 43 and 123 are 8-node linear brick elements where type 123 has reduced integration with hourglass control. Types 44 and 71 are 20-node parabolic brick elements where type 71 uses reduced integration. The cube has equal dimensions of 1 inch where  $x$ ,  $y$ , and  $z$  range from 0 to 1 inch. The cube is modeled with 8 brick elements as shown in Figure 5.4-1 and Figure 5.4-3 for the linear and parabolic meshes.

### Thermal Properties

One set of thermal properties is specified in the ISOTROPIC block: the isotropic thermal conductivity value is 1.0 Btu/sec-in-°F; the specific heat is 1.0 Btu/lb-°F; and the mass density is 1.0 lb/cubic inch.

### Thermal Boundary Conditions

The initial temperature distribution is that all nodes have a temperature of 100.0°F. At time  $t = 0$ ,  $x = 0$  and  $z = 1$  surfaces have a prescribed temperature of 0°F; all other surfaces are adiabatic and require no data input. A transient solution is performed with 10 uniform time steps of 0.1 seconds each for a total time of 1 second.

### Results

The temperature at the center of the unit cube is plotted versus time for the various element types and is shown in Figure 5.4-3. The cube has almost cooled down completely after 1 second. The linear elements (types 43 and 123) initially cool down slower than the parabolic elements (types 44 and 71).



**Parameters, Options, and Subroutines Summary**

Example e5x4a.dat:

<b>Parameters</b>	<b>Model Definition Options</b>	<b>History Definition Options</b>
ELEMENT	CONNECTIVITY	CONTINUE
END	CONTROL	TRANSIENT
HEAT	COORDINATE	
SIZING	END OPTION	
TITLE	FIXED TEMP	
	INITIAL TEMP	
	ISOTROPIC	
	POST	
	PRINT CHOICE	
	UDUMP	

Example e5x4b.dat:

<b>Parameters</b>	<b>Model Definition Options</b>	<b>History Definition Options</b>
ELEMENT	CONNECTIVITY	
END	CONTROL	CONTINUE
HEAT	COORDINATE	TRANSIENT
SIZING	END OPTION	
TITLE	FIXED TEMP	
	INITIAL TEMP	
	ISOTROPIC	
	POST	
	PRINT CHOICE	



Example e5x4c.dat:

<b>Parameters</b>	<b>Model Definition Options</b>	<b>History Definition Options</b>
ELEMENT	CONNECTIVITY	CONTINUE
END	CONTROL	TRANSIENT
HEAT	COORDINATE	
SIZING	END OPTION	
TITLE	FIXED TEMP	
	INITIAL TEMP	
	ISOTROPIC	
	POST	
	PRINT CHOICE	

Example e5x4d.dat:

<b>Parameters</b>	<b>Model Definition Options</b>	<b>History Definition Options</b>
ALIAS	CONNECTIVITY	CONTINUE
ELEMENT	CONTROL	TRANSIENT
END	COORDINATE	
HEAT	END OPTION	
SIZING	FIXED TEMP	
TITLE	INITIAL TEMP	
	ISOTROPIC	
	POST	
	PRINT CHOICE	

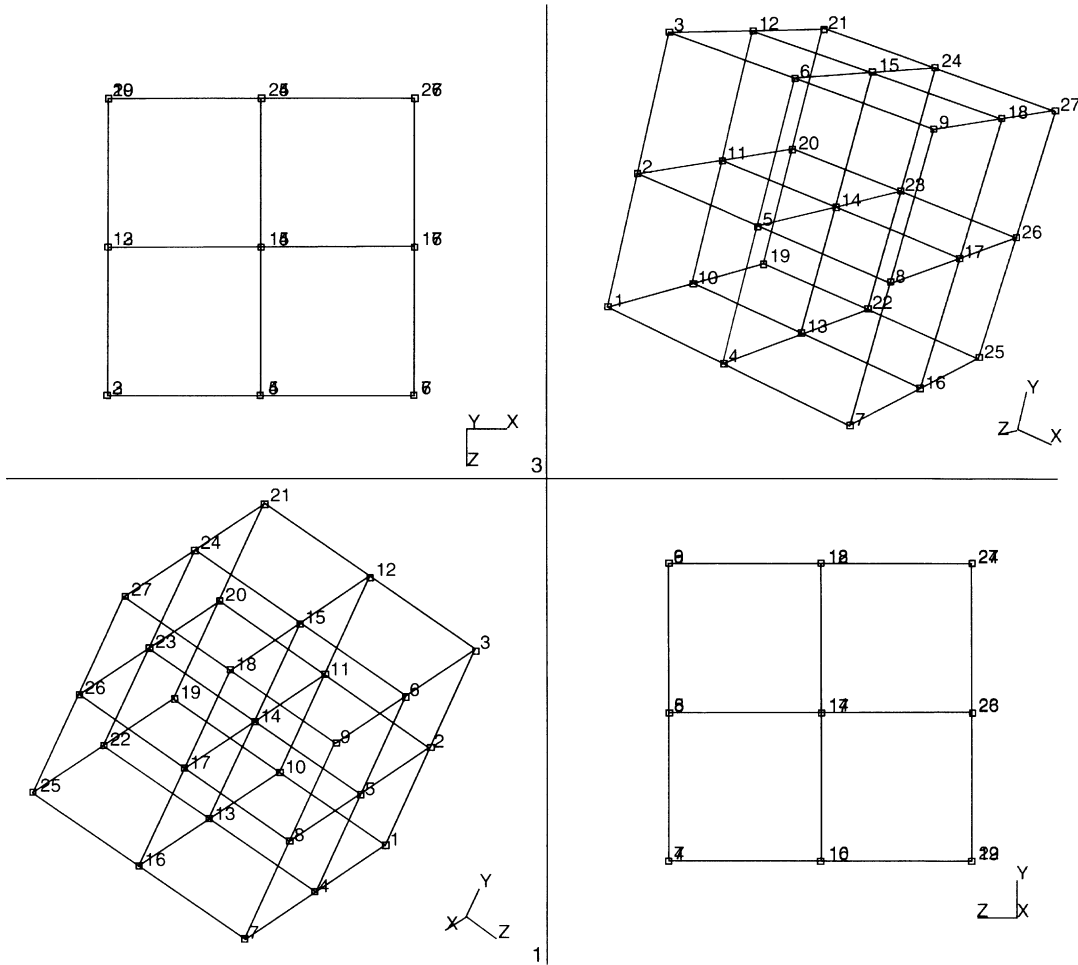


**Figure 5.4-1** Mesh for the Unit Cube Linear Elements

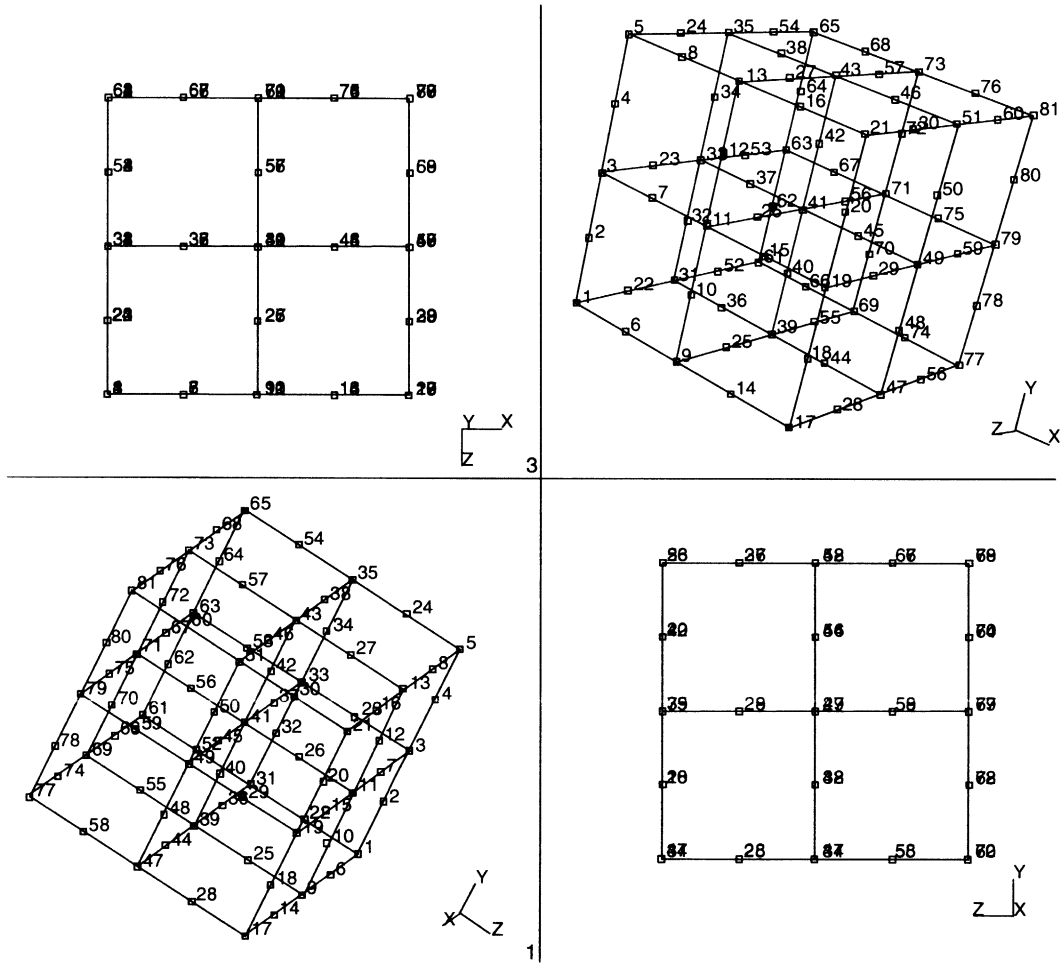


**Figure 5.4-2** Mesh for the Unit Cube Parabolic Elements

Time (Seconds)	Temperatures (element type, node number)			
	Type 43, n14	Type 44, n41	Type 71, n41	Type 123, n41
0.0	1.00000E+02	1.00000E+02	1.00000E+02	1.00000E+02
1.00000E-01	7.49796E+01	6.36616E+01	6.33202E+01	7.49796E+01
2.00000E-01	4.22526E+01	4.03147E+01	4.02325E+01	4.22526E+01
3.00000E-01	2.62808E+01	2.55396E+01	2.55179E+01	2.62808E+01
4.00000E-01	1.69623E+01	1.66272E+01	1.66202E+01	1.69623E+01
5.00000E-01	1.10900E+01	1.09937E+01	1.09915E+01	1.10900E+01
6.00000E-01	7.28266E+00	7.32065E+00	7.32054E+00	7.28266E+00
7.00000E-01	4.78960E+00	4.88981E+00	4.89058E+00	4.78960E+00
8.00000E-01	3.15160E+00	3.27040E+00	3.27148E+00	3.15160E+00
9.00000E-01	2.07415E+00	2.18852E+00	2.18962E+00	2.07415E+00
1.00001E+00	1.36513E+00	1.46487E+00	1.46587E+00	1.36513E+00

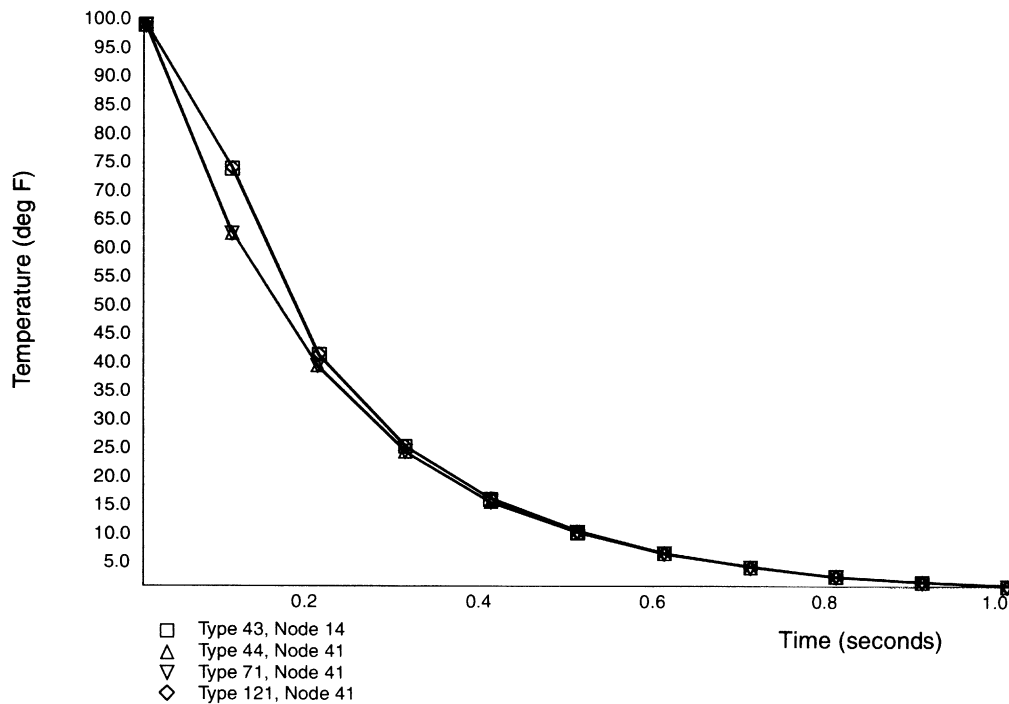


**Figure 5.4-3** Cube Center Temperature History for Element Types: 43, 44, 71, and 123



## 5.5 Pressure Vessel Subjected to Thermal Downshock

A realistic design problem, such as thermal ratcheting analysis, involves a working knowledge of a significant number of MARC features. This example illustrates how these features are used to analyze a simplified form of a pressure vessel component which is subjected to a thermal downshock. This problem is typical of reactor component analysis. The general temperature-time history which is used is shown in Figure 5.5-1.

An analysis of this type requires heat transfer analysis to determine the transient temperature distribution. This distribution is calculated for the wall of a cylindrical pressure vessel under cool-down conditions. The resulting data must be saved for use in the stress analysis.

This problem is modeled using the two techniques summarized below.

Data Set	Element Type(s)	Number of Elements	Number of Nodes
e5x5a	42	6	33
e5x5b	70	6	33

### Elements

The 8-node axisymmetric, quadrilateral elements are used in this example. The heat transfer elements 42 and 70, are used in the determination of the transient temperature distributions.

### Model

The geometry and mesh for this example are shown in Figure 5.5-2. A cylindrical wall segment is evenly divided in six axisymmetric quadrilateral elements with a total of 33 nodes. The mesh data is entered as element type 28. The ALIAS parameter allows you to generate your connectivity data with the stress analysis element and then to replace this element with the corresponding heat transfer element type.

### Heat Transfer Properties

It is assumed here that the material properties do not depend on temperature; no slope-breakpoint data is input. The uniform properties used here are:

- specific heat ( $c$ ) = 0.116 Btu/lb-°F
- thermal conductivity ( $k$ ) =  $4.85 (10^{-4})$  Btu/in-sec-°F
- density ( $\rho$ ) = 0.283 lb/cubic inch

### Heat Transfer Boundary Conditions

The initial temperature across the wall and ambient temperature are 1100°F as specified in the initial conditions block. The outer ambient temperature is held constant at 1100°F while the inner ambient temperature decreases from 1100°F to 800°F in 10 secs and remains constant thereafter.



The FILMS option is used to input the film coefficients and associated sink temperatures for the inner and outer surface. A uniform film coefficient for the outside surface is specified for element 6 as  $1.93 \times 10^{-6}$  Btu/sq.in-sec-°F in order to provide a nearly insulated wall condition. The inner surface has a film coefficient of  $38.56 \times 10^{-5}$  Btu/sq.in-sec-°F to simulate forced convection. The temperature down-ramp of 300°F for this inner wall is specified here as a nonuniform sink temperature and is applied using user subroutine FILM.

Subroutine FILM linearly interpolates the 300°F decrease in ambient temperature over 10 secs and holds the inner wall temperature constant at 800°F. It is called at each time step for each integration point on each element surface given in the FILMS option. Thus, this subroutine does nothing if it is called for element 6 to keep the outer surface at 1100°F. It applies the necessary ratio to reduce the inner wall temperature.

The TRANSIENT option controls the heat transfer analysis. MARC automatically calculates the time steps to be used based on the maximum nodal temperature change allowed as input in the CONTROL option. The solution begins with the suggested initial time step of one-half second input and ends according to the time period of 250 secs specified. It will not exceed the maximum number of steps input as 120 in this option.

The CONTROL option requires that the maximum temperature change per increment is 15°F. If this is exceeded, MARC automatically scales down the time step. The second tolerance on the CONTROL option requires that the program reassembles the operator matrix if the temperature has changed by 1000°F since the last reassembly.

Finally, note in the heat transfer run the use of the POST option. This allows the creation of a postprocessor file containing element temperatures at each integration point and nodal point temperatures. The file is used later as input to the stress analysis run.

### **Heat Transfer Results**

The transient thermal analysis is linear in that material properties do not depend on temperature and the boundary conditions depend on the surface temperature linearly. The analysis has been completed using the automatic time step feature in the TRANSIENT option.

The transient run reached completion in 33 increments with a specified starting time step of 0.5 seconds. A 15°F temperature change tolerance was input in the CONTROL option and controlled the auto time stepping scheme. The reduction to approximately 800°F throughout the wall was reached in increment 33 at a total time of 250 seconds.

The temperature-time histories of elements 1 (inner wall) and 6 (outer wall) for auto time stepping is shown in Figure 5.5-3.

The temperature distribution across the wall at various solution times is shown in Figure 5.5-4. Convergence to steady state is apparent here as is the thermal gradient characteristic of the downshock.

**Parameters, Options, and Subroutines Summary**

Example e5x5a.dat:

<b>Parameters</b>	<b>Model Definition Options</b>	<b>History Definition Options</b>
ALIAS	CONNECTIVITY	CONTINUE
ELEMENT	CONTROL	TRANSIENT
END	COORDINATE	
HEAT	END OPTION	
SIZING	FILMS	
TITLE	INITIAL TEMP	
	ISOTROPIC	
	POST	

User subroutine in u5x5.f:

FILM

Example e5x5b.dat:

<b>Parameters</b>	<b>Model Definition Options</b>	<b>History Definition Options</b>
ELEMENT	CONNECTIVITY	CONTINUE
END	CONTROL	TRANSIENT
HEAT	COORDINATE	
SIZING	END OPTION	
TITLE	FILMS	
	INITIAL TEMPERATURE	
	ISOTROPIC	
	POST	

User subroutine in u5x5.f:

FILM

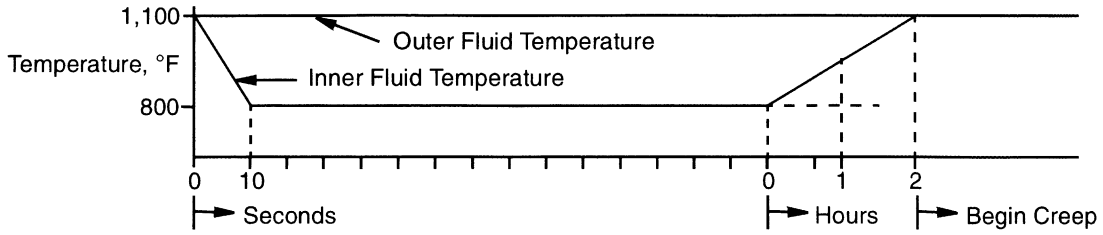


**Figure 5.5-1** Temperature Time History

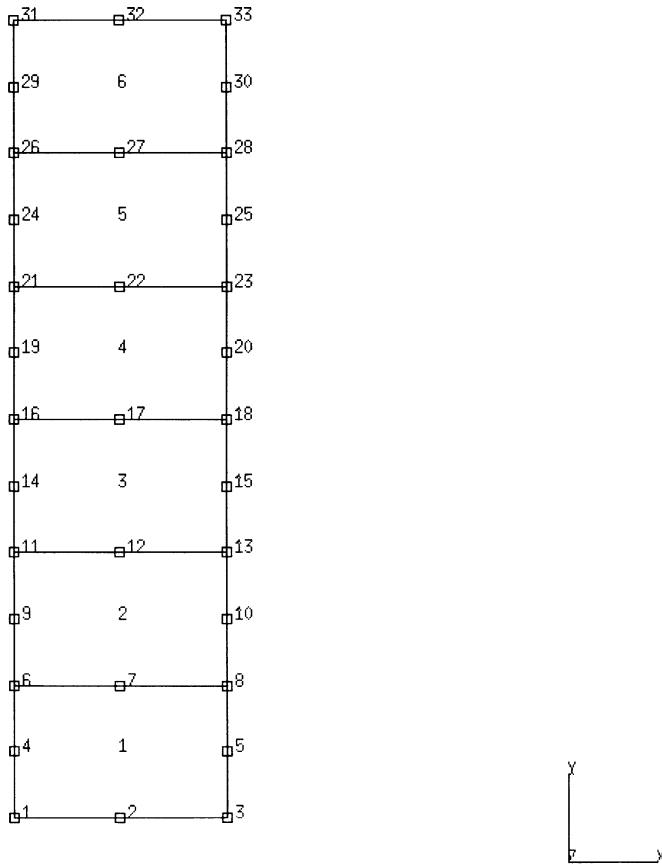


**Figure 5.5-2** Geometry and Mesh

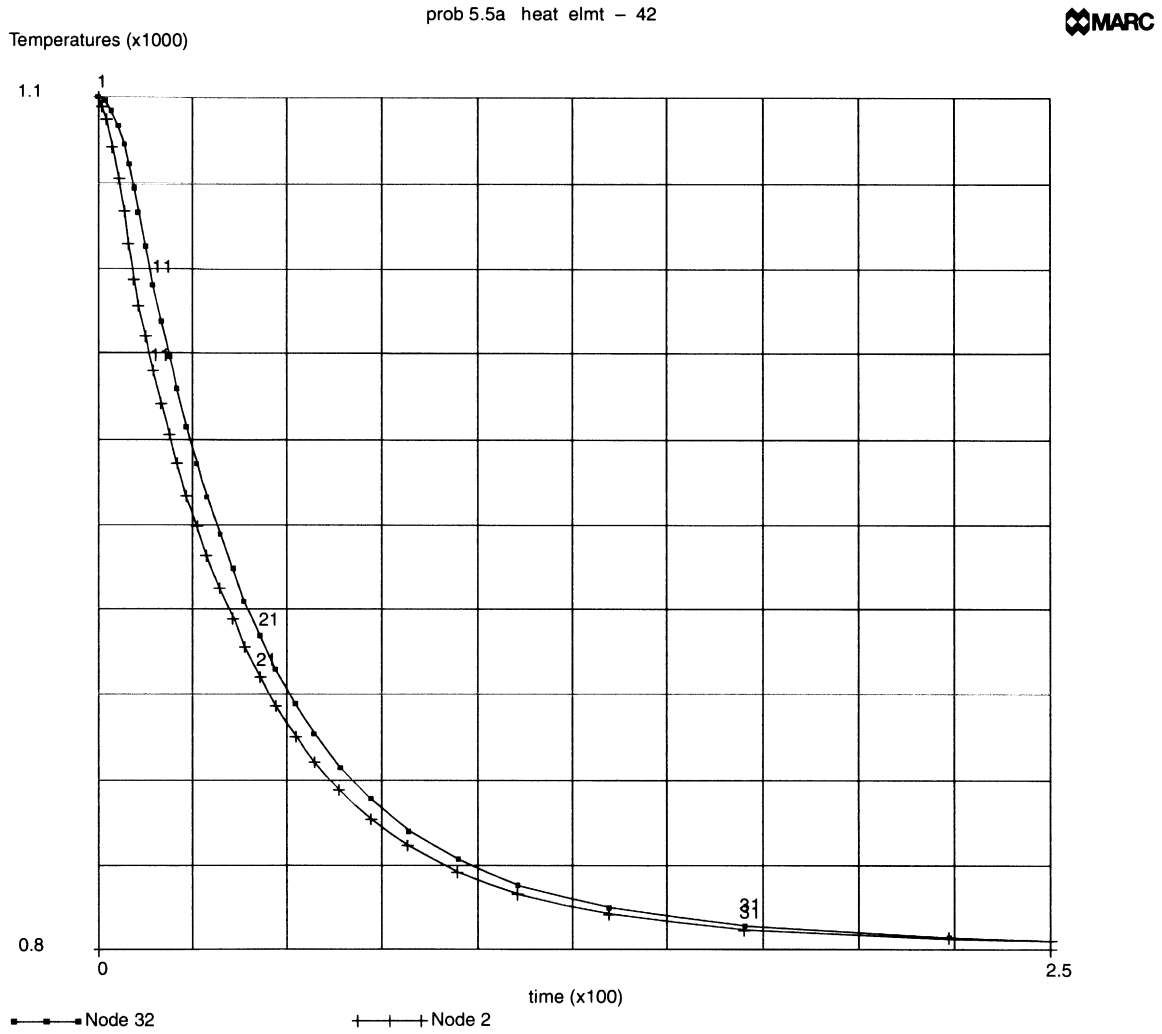


**Figure 5.5-3** Transient Temperature Time History (Auto Time Step)

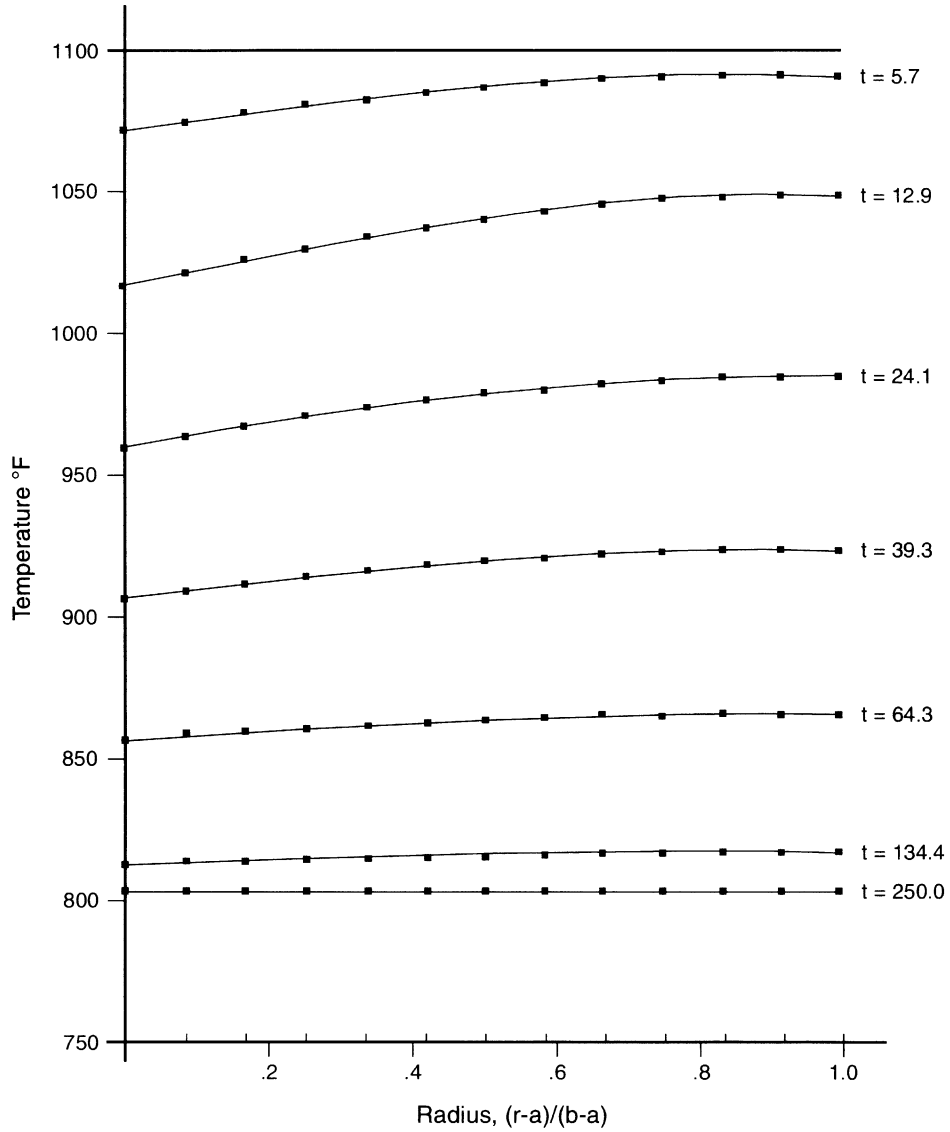


**Figure 5.5-4** Temperature Distribution in Cylinder Wall



## 5.6 Axisymmetric Transient Heat Conduction Simulated by Planar Elements

The transient heat conduction of a thick cylinder, subjected to a thermal downshock, is analyzed by using MARC planar heat transfer element. This is the same as problem 5.5.

### Model/Element

A 45-degree sector of the cylinder is modeled in the x-y plane as shown in Figure 5.6-1. The MARC heat transfer element type 41 (8-node planar quadrilateral) is selected for the analysis.

### Material Properties

The conductivity is  $4.85 \times 10^{-4}$  Btu/sec-in-°F. The specific heat is 0.116 Btu/lb-°F. The mass density is 0.283 lb/cu.inch.

### Initial Condition

Initial nodal temperatures are assumed to be homogeneous at 1100°F.

### Boundary Conditions

No input data is required for insulated boundary conditions along symmetry lines at  $y = 0$  and  $y = x$ . Fluid temperatures and film coefficients for both inner and outer surfaces of the cylinder are:

$$\begin{aligned} \text{Inner surface: } H_i &= 38.56 \times 10^{-5} \text{ Btu/sec-sq.in-}^\circ\text{F} \\ T_i &= 1100^\circ\text{F at } t = 0. \text{ second} \\ &800^\circ\text{F at } t = 10. \text{ second} \end{aligned}$$

$$\begin{aligned} \text{Outer surface: } H_0 &= 1.93 \times 10^6 \text{ Btu/sec-sq.in-}^\circ\text{F} \\ &(\text{low value to simulate insulated boundary condition}). \\ T_0 &= 1100^\circ\text{F} \end{aligned}$$

The FILMS option is used to input the film coefficients and associated fluid temperatures for the inner and outer surfaces. Subroutine FILM linearly interpolates the 300°F decrease in ambient temperature over 10 seconds and holds the inner wall temperature constant at 800°F. It is called at each time step for each integration point on each element surface given in the FILMS option.

### POST

In the heat transfer run, the use of the POST option allows the creation of a postprocessor file containing element temperatures at each integration point and nodal point temperatures. The file can be used later as input to the stress analysis run.

**TRANSIENT**

The TRANSIENT option controls the heat transfer analysis. MARC automatically calculates the time steps to be used based on the maximum nodal temperature change allowed as input in the CONTROL option. The solution begins with the suggested initial time step input of 0.5 seconds and ends according to the time period specified of 250 seconds. It does not exceed the maximum number of steps input in this option.

**Results**

A comparison of nodal temperatures with the results of an axisymmetric model (problem 5.5) are shown in Table 5.6-1.

**Table 5.6-1** Comparison of Nodal Temperatures

Increment No.	Time (Seconds)	Nodal Temperature (°F)	
		Problem 5.5	Problem 5.6
2	1.25	1099.3	1099.3
4	4.06	1092.6	1092.6
6	7.22	1078.1	1078.1
8	9.94	1068.4	1060.4
10	12.96	1039.8	1039.8
12	17.21	1014.0	1014.0
14	21.44	990.8	990.8
16	26.72	965.7	965.7
18	32.65	941.7	941.5
20	39.2	919.0	918.8





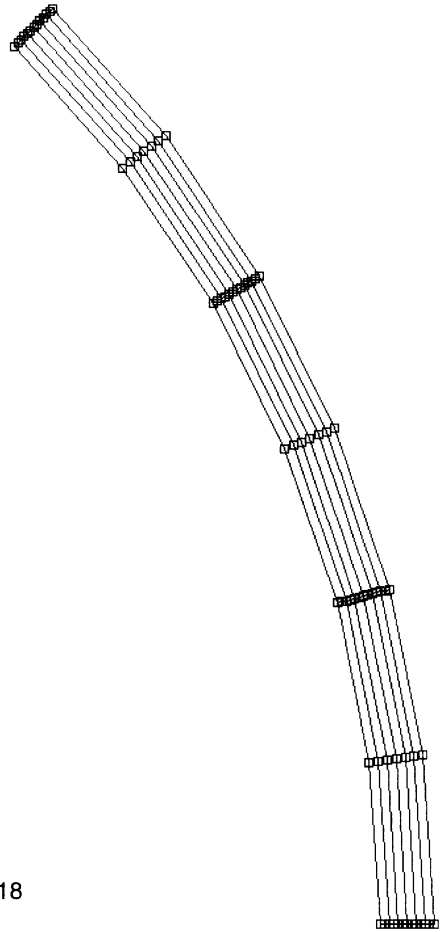
### Parameters, Options, and Subroutines Summary

Example e5x6.dat:

<b>Parameters</b>	<b>Model Definition Options</b>	<b>History Definition Options</b>
ELEMENT	CONNECTIVITY	CONTINUE
END	CONTROL	TRANSIENT
HEAT	COORDINATE	
SIZING	END OPTION	
TITLE	FILMS	
	INITIAL TEMP	
	ISOTROPIC	
	POST	

User subroutine in u5x6.f:

FILM



Element type = 41  
Number of elements = 18  
Number of nodes = 73

**Figure 5.6-1** Cylinder and Mesh



## 5.7 Steady State Analysis of an Anisotropic Plate

Two plates are subjected to similar temperature conditions. One plate has thermally isotropic properties; the other is anisotropic. The temperatures of the plate centers are calculated. In this problem, the thermal conductivity of the material is assumed to be anisotropic.

This problem is modeled using the two techniques summarized below.

Data Set	Element Type(s)	Number of Elements	Number of Nodes	Differentiating Features
e5x7a	39	4	9	ANISOTROPIC
e5x7b	39	4	9	ISOTROPIC

### Model/Element

This two-dimensional steady state heat conduction problem is analyzed using MARC heat transfer element type 39 (4-node planar quadrilateral). A plate is modeled by using four MARC planar heat transfer elements; the number of nodes in the mesh is nine. The size of the plate is 2.0 x 2.0 sq.in. for the anisotropic material and 0.2 x 2.0 sq.in. for the isotropic material. The plate and meshes are shown in Figure 5.7-1.

### Material Properties

The conductivity is 1.0 Btu/sec-in-°F for the isotropic material.  $k_x$  is 100.0 and  $k_y$  is 1.0 for the anisotropic material. The specific heat is 1.0 Btu/lb.-°F for both plates. The mass density of 1.0 lb/cu.in. is the same for both cases.

### Boundary Conditions

A constant temperature of 100°F is prescribed at nodes 1, 2, 3, 4, 6 and of 0°F at nodes 7, 8, and 9.

### Transient

A transient time of 1000 seconds is assumed for the analysis and the selected time step is 250 seconds. Nonautomatic TIME STEP option is also invoked.

### User Subroutine ANKOND

The COND array in the subroutine ANKOND is used for the modification of conductivity due to anisotropic behavior of the material.

### Results

Node temperatures at node 5 are identical (25.743°F) for both plates. This is to be expected as the length of the anisotropic plate was adjusted so that the same behavior would be obtained.



**Parameters, Options, and Subroutines Summary**

Example e5x7a.dat:

<b>Parameters</b>	<b>Model Definition Options</b>	<b>History Definition Options</b>
ELEMENT	ANISOTROPIC	CONTINUE
END	CONNECTIVITY	TRANSIENT
HEAT	COORDINATE	
SIZING	END OPTION	
TITLE	FIXED TEMP	

User subroutine in u5x7a.f:

ANKOND

Example e5x7b.dat:

<b>Parameters</b>	<b>Model Definition Options</b>	<b>History Definition Options</b>
ELEMENT	CONNECTIVITY	CONTINUE
END	COORDINATE	TRANSIENT
HEAT	END OPTION	
SIZING	FIXED TEMP	
TITLE	ISOTROPIC	

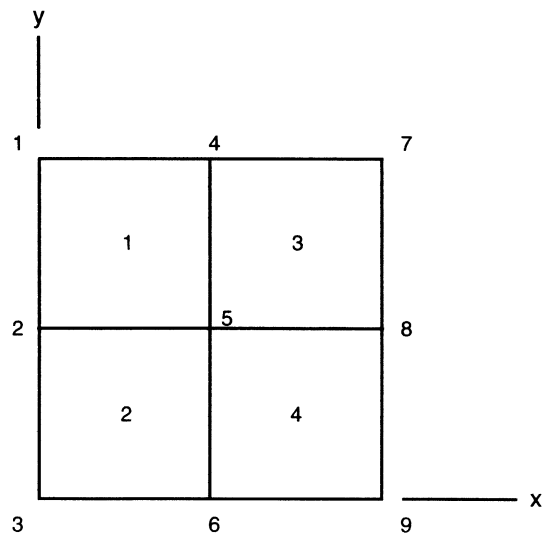
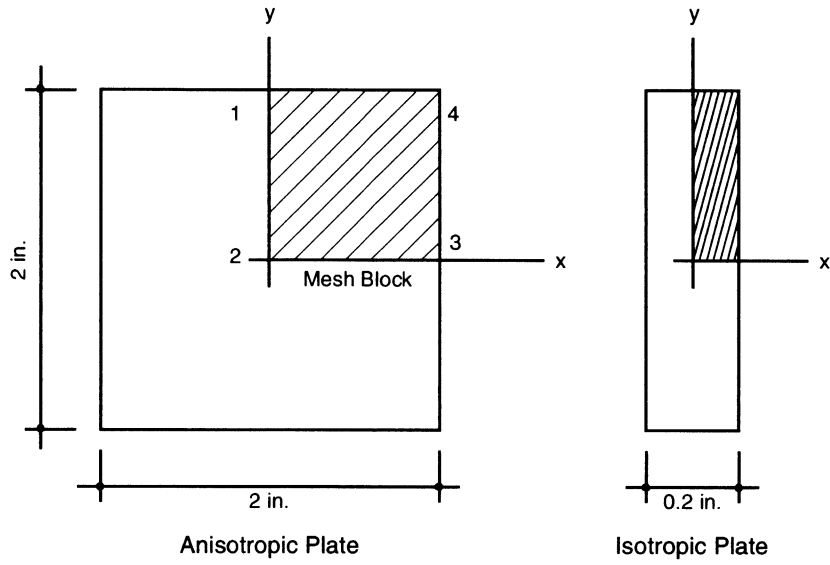


**Figure 5.7-1** Plate and Mesh





## 5.8 Nonlinear Heat Conduction of a Channel

Many important problems in heat transfer involve the interaction between transient heat conduction in a solid body and convection and radiative heat transfer in surrounding media. These problems are inherently nonlinear (although a linearized model is often sufficient) due to the complex nature of this interaction. For instance, radiative heat transfer rates depend on the surface temperature raised to the fourth power, and the emissivity  $\epsilon$  of a gray body can be a strong function of surface temperature, as well. Convective heat transfer rates depend linearly on the surface temperature explicitly, but the convective coefficients themselves may depend on the surface temperature (for example, in evaluating mean film properties), giving rise to an implicit nonlinear dependence.

This example illustrates the ability of MARC to treat this class of nonlinear problems, provided that some care is taken in modeling. A user-supplied subroutine is exhibited which computes the radiation and convection effects for the surface of the solid by using estimates of the surface temperatures, iterating if necessary.

The mesh used and tolerances set in this example are intended for demonstration purposes only – an accurate solution would require a more detailed mesh as well as tighter tolerances.

This problem is modeled using the four techniques summarized below.

Data Set	Element Type(s)	Number of Elements	Number of Nodes	Differentiating Features
e5x8a	41	40	149	TRANSIENT
e5x8b	41	40	149	TRANSIENT (RESTART)
e5x8c	41	40	149	TRANSIENT NONAUTO
e5x8d	41	40	149	TRANSIENT NONAUTO
e5x8e	41	40	149	AUTO STEP

### Element

The element used here is the 8-node planar heat transfer element, element type 41. (See *MARC Volume B: Element Library* for details of this element.)

### Model

The geometry for the heat transfer problem is shown in Figure 5.8-1. A liquid flows down a U-shaped channel at 10 in/second. The liquid temperature increases steadily from 70°F to 400°F and remains at 400°F for the rest of the analysis. A uniform heat flux of  $10^{-4}$  Btu/sq.in-sec is being steadily applied along the extremities of the channel legs; free convective transfer and radiative transfer are specified on the inside and outside faces of the channel legs, respectively; and a

uniform temperature of 70°F is maintained on the base of the channel. The problem is not intended to represent any physical situation – it simply serves as an illustration of the modeling techniques used with heat transfer analysis.

The mesh is shown in Figure 5.8-2. For a more accurate geometric modeling, more blocks should be used at the corner.

### Boundary Conditions

The boundary conditions for the analysis are shown in Figure 5.8-1. The simpler conditions (fixed temperature, flux) are input directly. The more complex radiation and convection conditions are input through subroutine FILM.

The FILMS model definition option causes the routine to be called at each surface integration point of each element listed in that model definition set. Then, based on the element number (which is passed in to the routine) the following sections are provided:

- A. Forced, liquid metal convection on all elements adjacent to the metal stream. Here the routine calculates a film coefficient as follows:

The liquid metal properties – conductivity, Prandtl number, and kinematic viscosity – are assumed to be functions of the average boundary layer temperature (the average temperature is based on the mean of the free stream temperature and the estimated surface temperature). Then, the hydraulic diameter is computed from the formula:

$$D_H = \frac{4 \text{ (flow cross-sectional area)}}{\text{(wetted perimeter)}}$$

For this example,  $D_H = 10$  inches approximately. The Reynolds number is given by the relation:

$$Re_D = \frac{D_H V}{\nu}$$

where:

- V is the velocity of the flow
- $\nu$  is the kinematic viscosity

The Peclet number, Pe, is given by the product of the Reynolds and Prandtl (Pr) numbers. Then the average Nusselt number, Nu, is found from the experimentally verified formula for fully developed turbulent flow of liquid metals (see Lubarsky, B, and Kaufman, S. J., “Review of Experimental Investigations of Liquid-Metal Heat Transfer”, NACA TN 3336, 1955.):





$$\bar{Nu} = 0.625 (Pe)^{0.4}$$

The final step is to find the average heat transfer coefficient from:

$$\bar{h}_e = \frac{k Nu}{D_H}$$

where  $k$  is the thermal conductivity of the liquid metal. The bulk fluid temperature increases linearly with time from 70°F to 400°F, then remains constant at 400°F for the rest of the analysis. These values of  $\bar{h}_e$  and the bulk fluid temperature are passed back from FILM in H and TINF, respectively. Note that the film coefficient is so high that the surface nodes effectively take on the bulk fluid temperature directly as a prescribed surface temperature boundary condition.

**B. Free Convection:**

Here the constant film coefficient and bulk temperature are entered directly in H and TINF.

**C. Radiation:**

The radiation law is:  $q = \epsilon\sigma(T^4 - T_\infty^4)$

where  $\epsilon$  is the emissivity of the surface (here assumed to be 0.6),  $\sigma$  is the Stefan-Boltzmann constant, and temperatures are in absolute units. In this case,  $T_\infty$  is  $460 + 70 = 530^\circ R$ . In order to perform a linear time stepping scheme, the above equation is rewritten as:

$$q = \epsilon\sigma(T^3 + T^2T_\infty + T T_\infty^2)(T - T_\infty)$$

and a temperature dependent film coefficient:

$$h = \epsilon\sigma(T^3 + T^2T_\infty + T T_\infty^2 + T_\infty^3)$$

is calculated in the subroutine.

Subroutine FILM defines relative values; that is, multipliers of the data values for H and TINF entered on the FILMS model definition set. In this case, it is more convenient to program absolute values in FILM; therefore, values of 1. are entered in the model definition set.

**Time Stepping**

In this case, the automatic time stepping scheme is chosen based on a maximum temperature change per increment of 50°F. MARC adjusts time steps to conform to this criterion according to the scheme defined in *MARC Volume F: Background Information*. Tolerances are also placed



on the maximum temperature change before the program recalculates nonlinear effects; that is, temperature-dependent material properties and temperature-dependent boundary conditions, both of which are present in this example, and on the maximum temperature variation between the temperature used to evaluate properties and the resulting solution to allow iteration as necessary. It should be emphasized that for an accurate solution as well as a finer mesh, a tighter tolerance on temperature change per step should be provided.

**Results**

Isotherm plots are shown in Figure 5.8-3, Figure 5.8-4 and Figure 5.8-5 showing the temperature field after 100, 400 and 10,000 seconds. They illustrate the progress toward steady state conditions. At 10,000 seconds, the solution is not yet at steady state. The last step of about 1000 seconds shows a maximum nodal temperature change of 11°F. Therefore, steady state would be reached in a smaller number of additional steps. The program used 18 steps to produce this solution (based on the 50°F per step maximum temperature change tolerance) with an initial step of 100 seconds and a final step size of about 2000 seconds. This is a typical illustration of the effectiveness of the automatic stepping scheme. The transient temperature for selected nodes is shown in Figure 5.8-6.

**Parameters, Options, and Subroutines Summary**

Example e5x8a.dat:

<b>Parameters</b>	<b>Model Definition Options</b>	<b>History Definition Options</b>
ELEMENT	CONNECTIVITY	CONTINUE
END	CONTROL	TRANSIENT
HEAT	COORDINATE	
MESH PLOT	DIST FLUXES	
SIZING	END OPTION	
TITLE	FILMS	
	FIXED TEMP	
	INITIAL TEMP	
	ISOTROPIC	
	OPTIMIZE	
	POST	
	RESTART	
	TEMPERATURE EFFECTS	



User subroutine found in u5x8.f:

FILM  
FLUX

Example e5x8b.dat:

<b>Parameters</b>	<b>Model Definition Options</b>	<b>History Definition Options</b>
ELEMENT	END OPTION	CONTINUE
END	RESTART	
HEAT		
MESH PLOT		
SIZING		
TITLE		

Example e5x8c.dat:

<b>Parameters</b>	<b>Model Definition Options</b>	<b>History Definition Options</b>
ELEMENT	CONTROL	CONTINUE
END	COORDINATE	TRANSIENT
HEAT	DIST FLUXES	
SIZING	END OPTION	
TITLE	FILMS	
	FIXED TEMP	
	INITIAL TEMP	
	ISOTROPIC	
	OPTIMIZE	
	POST	
	RESTART	
	TEMPERATURE EFFECTS	



Example e5x8d.dat:

<b>Parameters</b>	<b>Model Definition Options</b>	<b>History Definition Options</b>
ELEMENT	CONNECTIVITY	CONTINUE
END	CONTROL	TRANSIENT
HEAT	COORDINATE	
SIZING	DIST FLUXES	
TITLE	END OPTION	
	FILMS	
	FIXED TEMP	
	INITIAL TEMP	
	ISOTROPIC	
	OPTIMIZE	
	POST	
	RESTART	
	TEMPERATURE EFFECTS	

Example e5x8e.dat:

<b>Parameters</b>	<b>Model Definition Options</b>	<b>History Definition Options</b>
ELEMENT	CONNECTIVITY	CONTINUE
END	CONTROL	AUTO STEP
HEAT	COORDINATE	
SIZING	DIST FLUXES	
TITLE	END OPTION	
	FILMS	
	FIXED TEMP	
	INITIAL TEMP	
	ISOTROPIC	
	OPTIMIZE	
	POST	
	RESTART	
	TEMPERATURE EFFECTS	

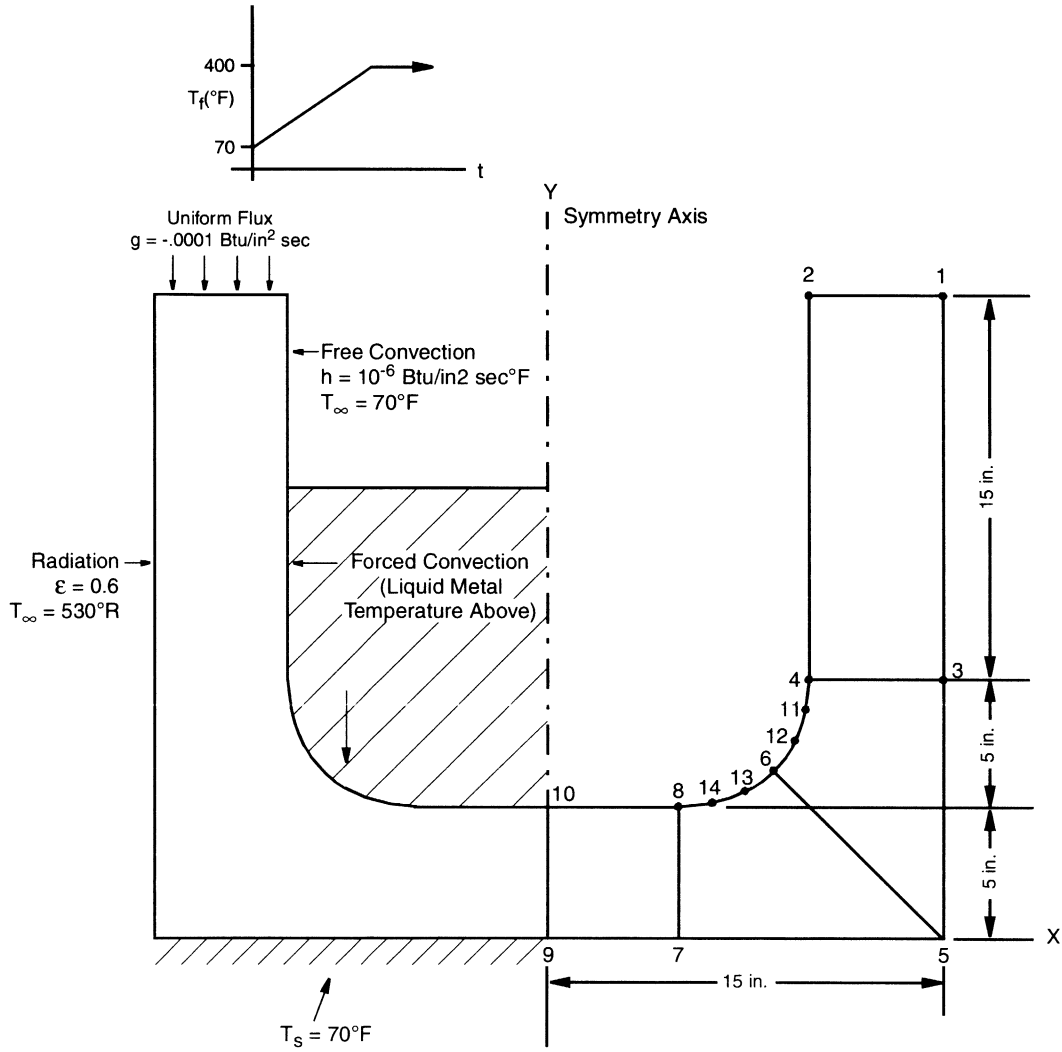
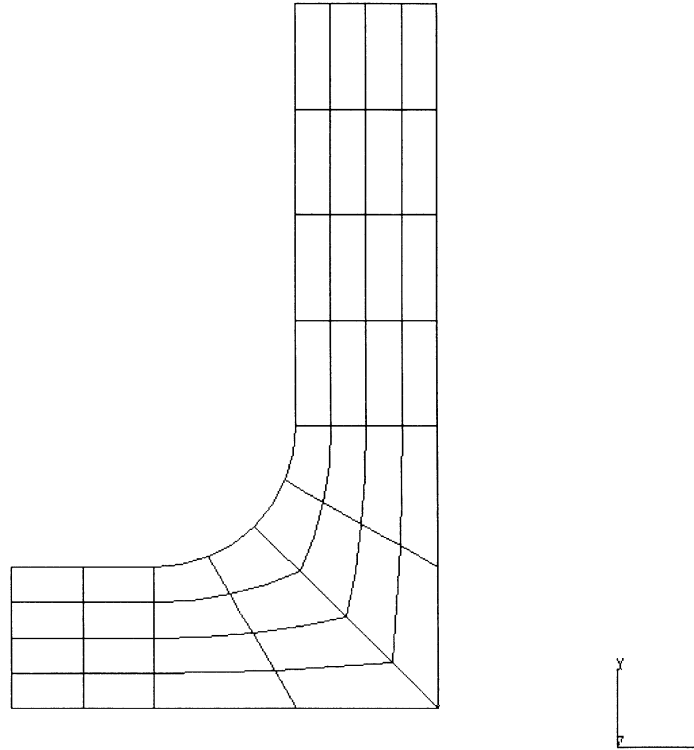
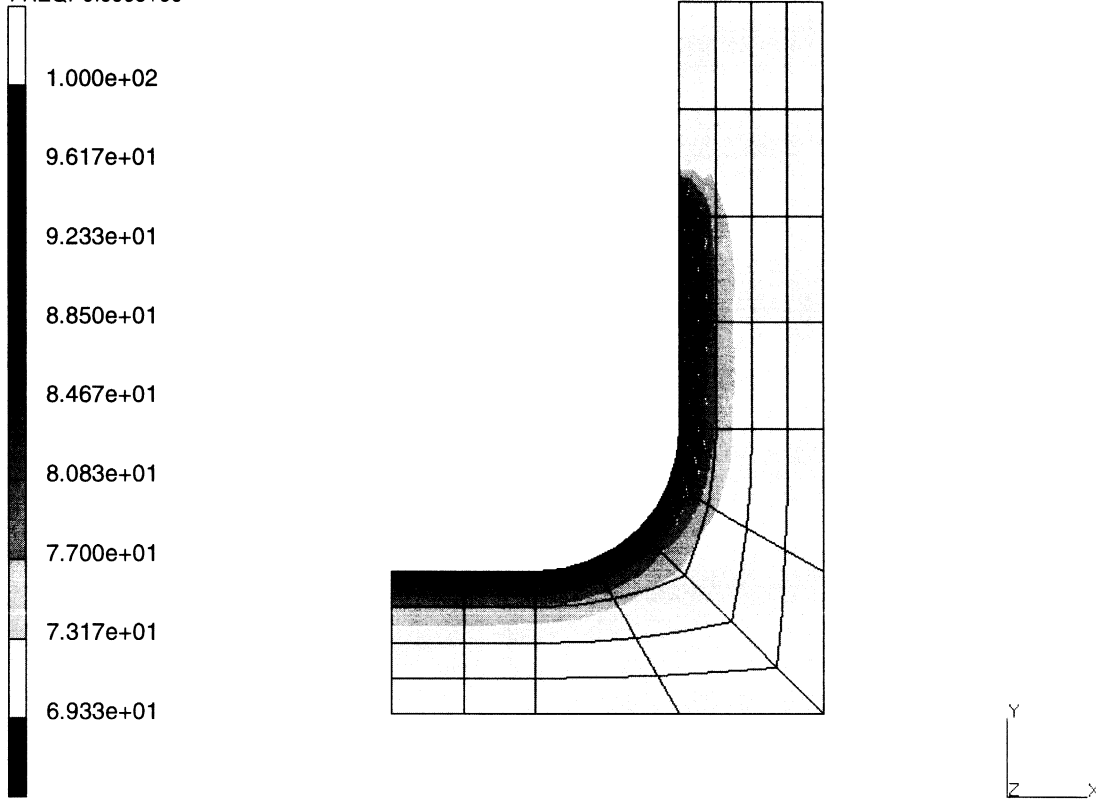


Figure 5.8-1 Geometry for Nonlinear Heat Conduction



**Figure 5.8-2** Heat Transfer Example Mesh

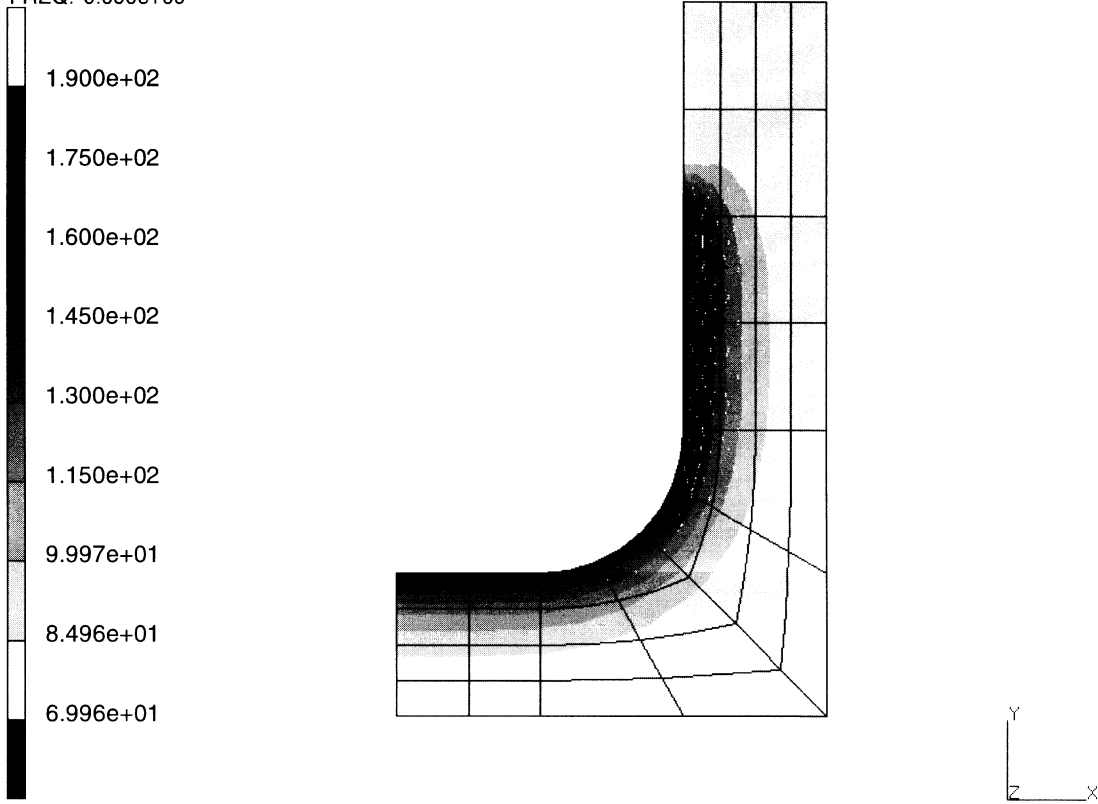
INC : 1  
SUB : 0  
TIME : 1.000e+02  
FREQ: 0.000e+00



prob 5.8 heat - elmt 41  
Temperatures

**Figure 5.8-3** Isotherms at 100 Seconds

INC : 3  
SUB : 0  
TIME : 4.000e+02  
FREQ: 0.000e+00

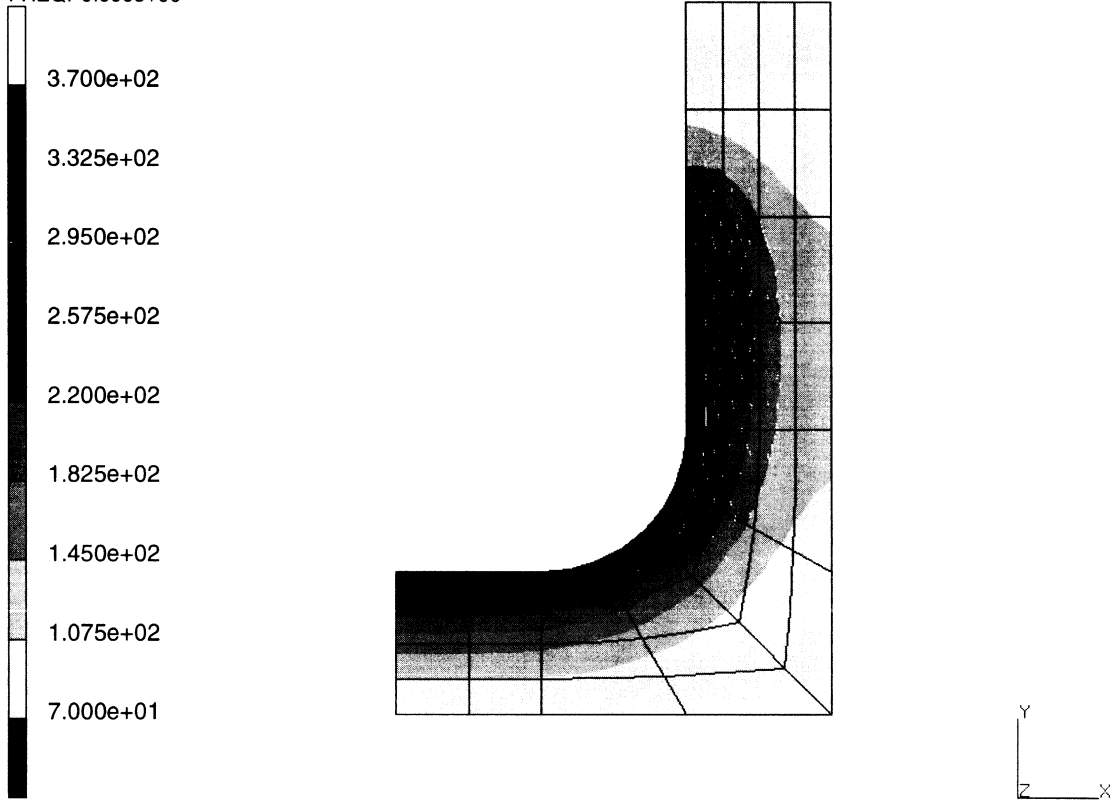


prob 5.8 heat - elmt 41  
Temperatures

**Figure 5.8-4** Isotherms at 400 Seconds



INC : 7  
SUB : 0  
TIME : 1.000e+03  
FREQ: 0.000e+00



prob 5.8 heat - elmt 41  
Temperatures

**Figure 5.8-5** Isotherms at 1000 Seconds

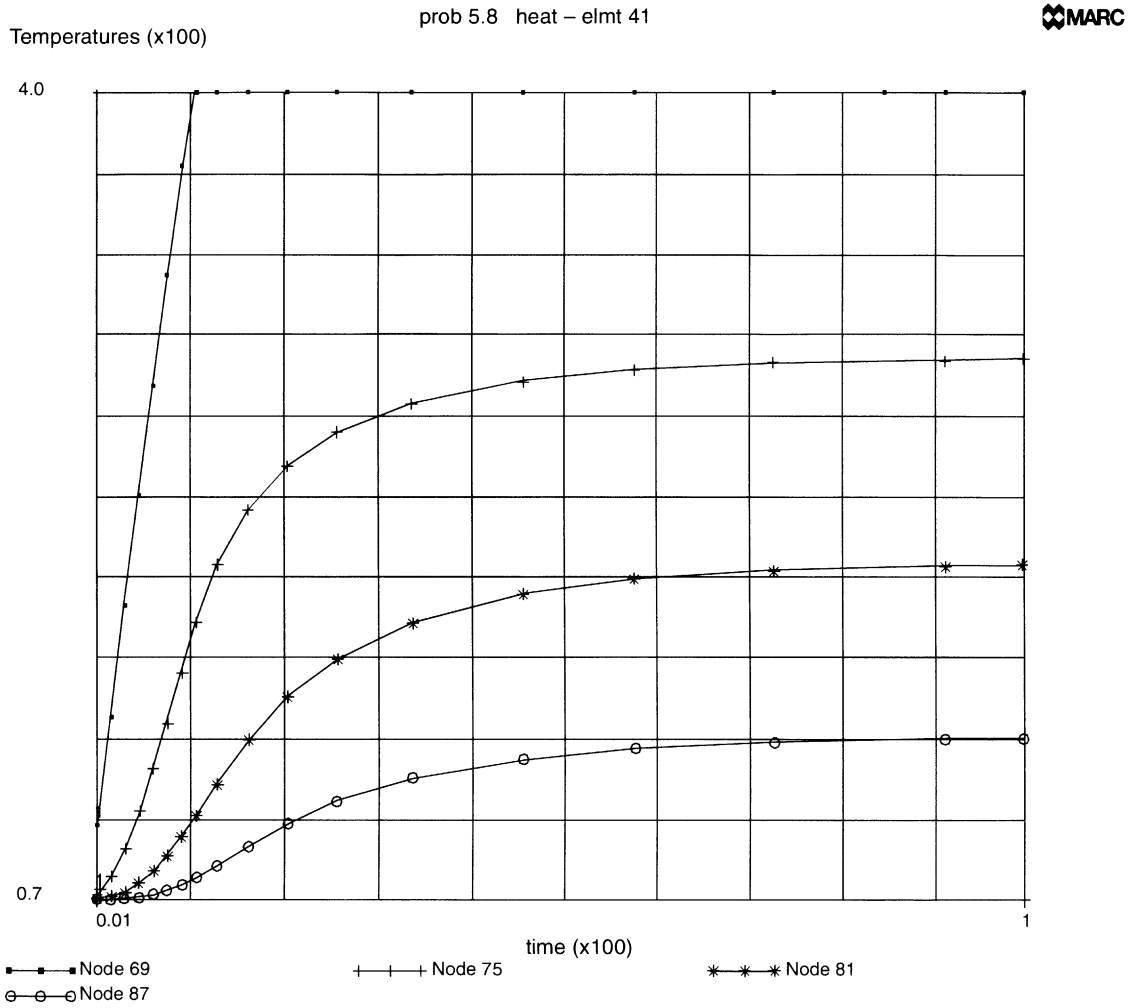


**Figure 5.8-6** Temperature History

## 5.9 Latent Heat Effect

In heat conduction analysis, the material may exhibit phase change at certain temperature levels. This change of phase can be characterized by a sharp change in temperature dependent specific heat of the material or a latent heat associated with a given temperature range. A solid cylinder subjected to convective boundary condition and the effect of latent heat on the thermal response is studied.

This problem is modeled using the four techniques summarized below.

Data Set	Element Type(s)	Number of Elements	Number of Nodes	Differentiating Features
e5x9a	40	10	22	Include latent heat
e5x9b	40	10	22	ELEM SORT, NODE SORT
e5x9d	122	10	22	Include latent heat
e5x9e	132	20	63	Triangular 6-noded element 132 used

### Model

The cylinder is of radius 0.594 inches and length 0.1 inches. For data sets e5x9a and e5x9b, the 4-noded axisymmetric quadrilateral element number 40 is used. For data set e5x9d, the 4-noded reduced integration element number 122 is used. For data set e5x9e, the 6-noded axisymmetric triangular element number 132 is used. The initial model is shown in Figure 5.9-1.

### Thermal Properties

Material properties are as follows: isotropic thermal conductivity is 0.5712E-04 Btu/sec-in°F; specific heat is 0.11199 Btu/lb-°F; mass density is 0.281 lb/cu.in.; latent heat is 76.51 Btu/lb with a solidus temperature of 423°F and a liquidus temperature of 757°F.

The properties as a function of temperature are shown in Figure 5.9-2. A second temperature dependent specific heat curve with a latent heat is also shown in the same figure. The TEMPERATURE EFFECTS option is used to input these functions.

**Thermal Boundary Conditions**

The initial temperature distribution is that all nodes have a temperature of 1550.0°F. At time  $t = 0$ , the outer surface begins to convect to the surroundings with a sink temperature of 100°F and a film coefficient of 0.009412 Btu/sec.-sq.-in.-°F. Nonautomatic time-stepping is invoked where the total transient time is 100 seconds using eight different time steps. The time steps are:

<b>Time Step (seconds)</b>	<b>Number of Steps</b>	<b>Transient Time (seconds)</b>
0.001	10	0.01
0.005	8	0.04
0.01	15	0.15
0.05	16	0.80
0.1	20	2.00
0.5	44	22.00
1.0	15	15.00
5.0	12	60.00
Total =	140	100.00

**Results**

The thermal response is summarized by plotting the temperature history of the center and outer surface of the cylinder shown in Figure 5.9-3. Notice how the temperature at the center of the cylinder drops as the material solidifies.

**Parameters, Options, and Subroutines Summary**

Example e5x9a.dat:

<b>Parameters</b>	<b>Model Definition Options</b>	<b>History Definition Options</b>
ELEMENT	CONNECTIVITY	CONTINUE
END	CONTROL	CONTINUE
HEAT	COORDINATE	
SIZING	END OPTION	
TITLE	FILMS	
	INITIAL TEMP	
	ISOTROPIC	
	POST	
	TEMPERATURE EFFECTS	
	UDUMP	

Example e5x9b.dat:

<b>Parameters</b>	<b>Model Definition Options</b>	<b>History Definition Options</b>
END	CONNECTIVITY	CONTINUE
SIZING	CONTROL	TRANSIENT
TITLE	COORDINATE	
	END OPTION	
	FILMS	
	INITIAL TEMP	
	ISOTROPIC	
	POST	
	PRINT CHOICE	
	TEMPERATURE EFFECTS	

MARC-PLOT is used in example e5.9c.

Example e5x9d.dat:

<b>Parameters</b>	<b>Model Definition Options</b>	<b>History Definition Options</b>
ELEMENT	CONNECTIVITY	CONTINUE
END	CONTROL	TRANSIENT
HEAT	COORDINATE	
SIZING	END OPTION	
TITLE	FILMS	
	INITIAL TEMP	
	ISOTROPIC	
	POST	
	TEMPERATURE EFFECTS	



Example e5x9e.dat:

**Parameters**

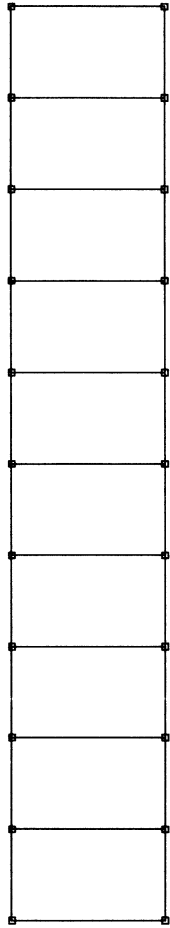
ELEMENT  
END  
HEAT  
SIZING  
TITLE

**Model Definition Options**

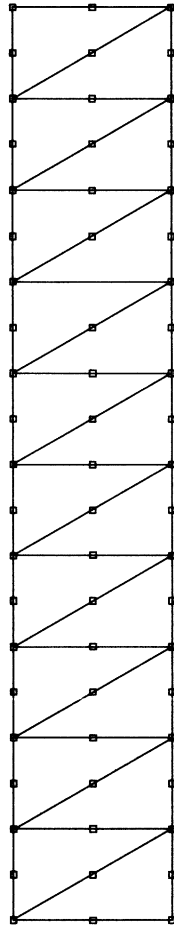
CONNECTIVITY  
CONTROL  
COORDINATE  
DEFINE  
END OPTION  
FILMS  
INITIAL TEMP  
ISOTROPIC  
POST  
TEMPERATURE EFFECTS

**History Definition Options**

CONTINUE  
TRANSIENT



Mesh used for element types 40 and 122



Mesh used for element type 132

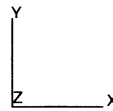
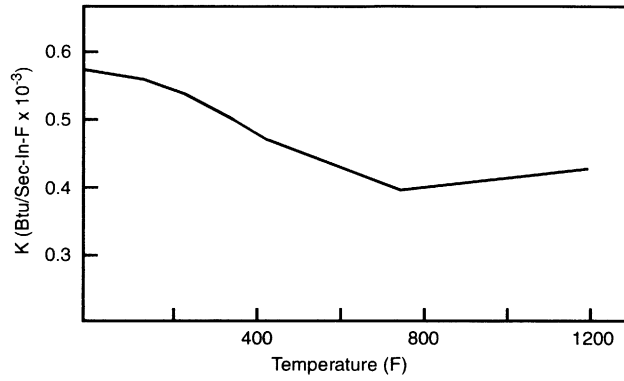
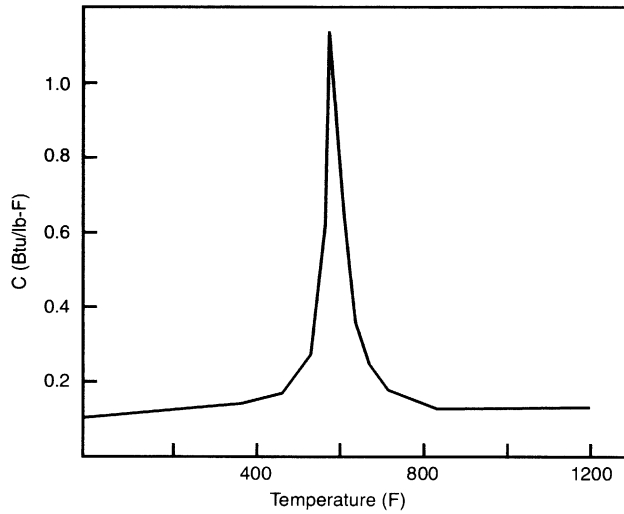


**Figure 5.9-1** Cylinder Meshes



Specific heat as a function of temperature used in problem 5.9A



Specific heat as a function of temperature used in problem 5.9B

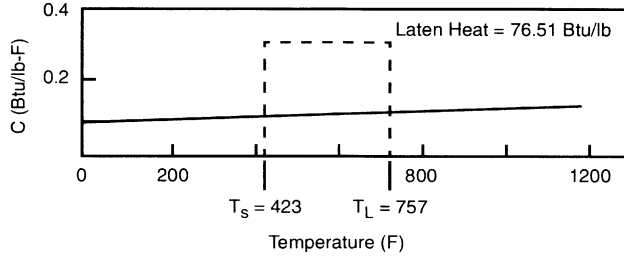


Figure 5.9-2 Temperature Dependent Thermal Properties



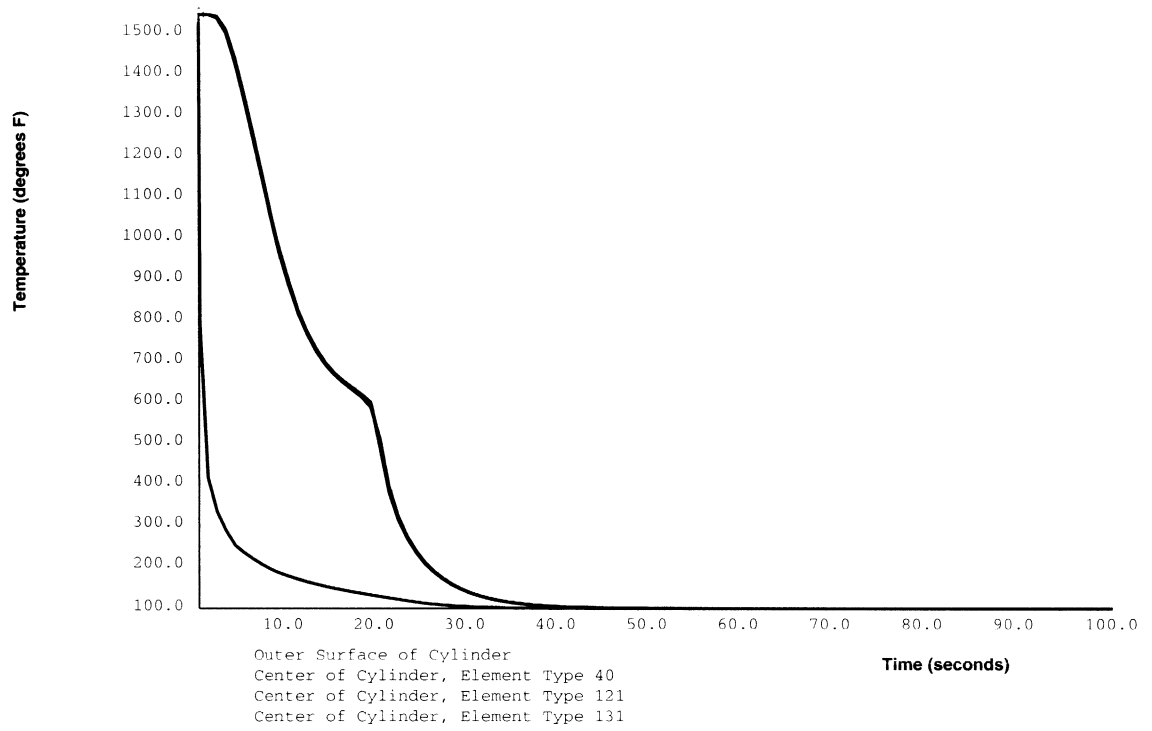


Figure 5.9-3 Temperature History for Center and Outer Surface of Cylinder

**Table 5.10-1** Nodal Voltages and Temperatures

Node Number	Voltages	Temperatures
1	0.1	417.63
2	0.1	418.39
3	0.1	418.98
4	0.1	419.40
5	0.1	419.66
6	0.1	419.77
7	0.0	417.63
8	0.0	418.39
9	0.0	418.98
10	0.0	419.40
11	0.0	419.66
12	0.0	419.77

**Reference**

Rohsenow, W. M. and Choi, H. Y., *Heat, Mass and Momentum Transfer*, Prentice-Hall, Inc., 1961, p. 106.

**Parameters, Options, and Subroutines Summary**

Example e5x10.dat:

Parameters	Model Definition Options	History Definition Options
END	CONNECTIVITY	CONTINUE
HEAT	COORDINATE	TRANSIENT
JOULE	DIST CURRENT	
SIZING	END OPTION	
TITLE	FILMS	
	ISOTROPIC	
	JOULE	
	VOLTAGE	

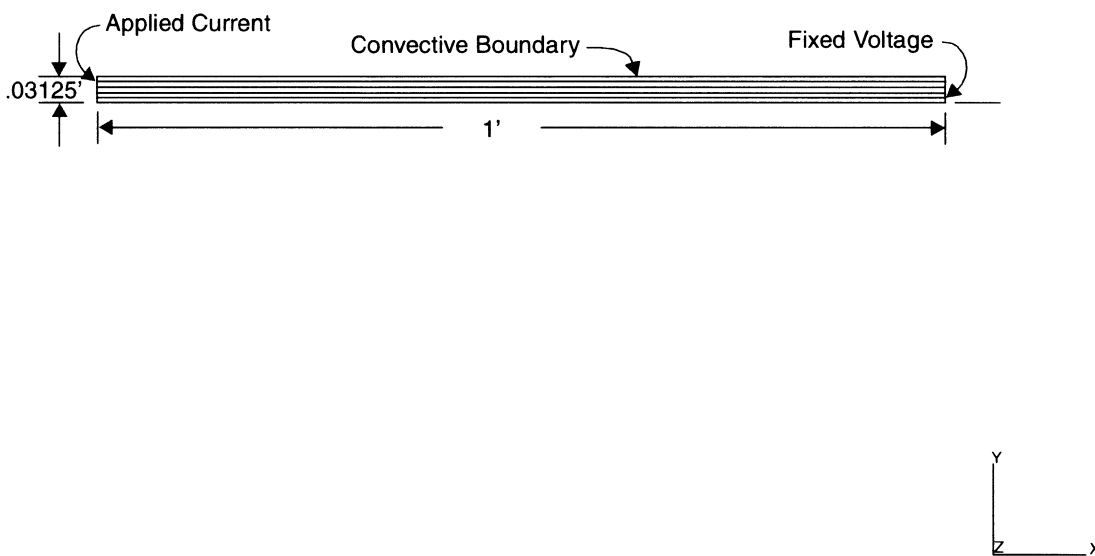


**Figure 5.10-1** Mesh of Steel Wire



## **5 Heat Transfer**

*Centerline Temperature of a Bare Steel Wire*

---



## 5.11 Heat Transfer and Stress Analysis of a Jominy End Quench Test Specimen

This example considers the transient heat transfer and thermal stress analyses of the Jominy End Quench Test. A right circular cylindrical bar of 1-inch diameter and 3-inch length, initially at a uniform temperature of 1550°F, is quenched to steady-state temperature. The quenching process consists of water impinging on one of the circular faces of the cylinder. The quench water temperature is 71°F. The bar is made from AISI 4140 steel. Its thermal (that is, heat transfer) properties are a function of temperature only. The thermal conductivity data is listed in Table 5.11-1 and plotted in Figure 5.11-1. The specific heat data is listed in Table 5.11-2 and plotted in Figure 5.11-2.

Cooling occurs by forced convection along the quench end and by free convection along the cylindrical surface. It is assumed that the cylindrical face opposite the quench end is fully insulated. The “forced” heat transfer coefficient for cooling of the material in water is  $9.412 \times 10^{-3}$  Btu/sec-°F-sq.in. The “free” heat transfer coefficient for cooling in air is  $5.5941 \times 10^{-6}$  Btu/sec-°F-sq.in.

### Element

Element type 42 is used for the heat-transfer analysis of the specimen. This is an axisymmetric 8-node biquadratic element, with one degree of freedom (temperature). Element type 28 is used for the stress analysis portion of this example. This element is an 8-node distorted quadrilateral, with two degrees of freedom at each node.

### Model

The nonuniform transient temperature field was computed in a preliminary heat transfer analysis. The finite element model is illustrated in Figure 5.11-3 and Figure 5.11-4. Due to symmetry, only one-half of the bar is modeled. This same model is used in the subsequent transient thermal stress analysis.

### Geometry

No values need be given in this option.

### Material Properties

The mechanical properties of AISI 4140 are a function of both time and temperature. The data pertaining to Young’s modulus, Poisson’s ratio, yield stress, and the workhardening rate are given in Figure 5.11-5, Figure 5.11-6, and Figure 5.11-7. The data is presented in the form of property values as a function of both temperature and the previously described fixed cooling rates. Data is provided for two rates. The durations of these two “Newton Cooling” processes (see Figure 5.11-3) are 6 and 20 seconds. The mass density of the material is 0.281 lb/cu.in.

**Table 5.11-1** Thermal Conductivity vs. Temperature (AISI 4140 Steel)

<b>Temperature (°C)</b>	<b>Conductivity (cal/cm-sec)</b>	<b>Temperature (°C)</b>	<b>Conductivity (cal/cm-sec)</b>
0	.102	500	.052
19	.102	550	.054
39	.101	600	.055
58	.099	650	.056
78	.098	700	.058
97	.095	750	.059
116	.093	800	.060
136	.092	850	.062
155	.088	900	.063
174	.084	950	.064
193	.080	1000	.065
213	.073	1050	.067
233	.068	1100	.068
252	.063	1150	.069
271	.057	1200	.071
291	.051	1250	.072
310	.047	1300	.074
350	.048	1350	.075
400	.050	1400	.076

**Table 5.11-2** Specific Heat vs. Temperature (AISI 4140)

<b>Temperature (°C)</b>	<b>Specific Heat (cal/cm-sec)</b>
50	.112
110	.117
120	.118
130	.121
140	.126
150	.132
160	.141
170	.153
180	.167
190	.184
200	.205
210	.238
220	.289
230	.615
240	1.482
250	.824
260	.530
270	.357
280	.290
290	.247
300	.214
310	.189
320	.168
330	.150
340	.136
350	.121
450	.122
550	.126
650	.131

The thermal conductivity vs. temperature curve (Figure 5.11-7) was approximated by three straight-line segments. The corresponding slope-breakpoint data was entered in the TEMPERATURE EFFECTS block. The data for the specific heat (Figure 5.11-2) was re-expressed in slope-breakpoint form and also entered in this block.

The thermal coefficient of expansion is also a function of time and temperature. In this instance, this property is derived from thermal strain data which is described in terms of fourth order polynomial expansions about different temperature levels. This is done for the above two mentioned cooling rates. The coefficients for each of the polynomials are listed in Table 5.11-3 along with the corresponding temperature levels.

**Table 5.11-3** Coefficient of Thermal Expansion (AISI 4140)

A <sub>1</sub>	A <sub>2</sub>	A <sub>3</sub>	A <sub>4</sub>	A <sub>5</sub>	T	Cooling Rate (seconds)
0.3439E-02	0.1063E-04	0.2847E-07	0.4245E-10	-0.2345E-13	32	6
0.1603E-01	0.3600E-04	0.2147E-07	0.0	0.0	753	
0.5852E-02	0.2047E-05	0.5401E-09	0.0	0.0	1148	
0.2204E-01	0.5857E-04	-0.5401E-09	0.4211E-09	-0.2792E-12	32	20
0.7145E-01	0.7366E-04	-0.5966E-07	-0.3517E-10	0.3747E-13	545	
0.2193-01	-0.7130E-06	0.5190E-08	-0.1872E-11	0.2479E-15	896	

**Results**

**Thermal Analysis**

A variable time step is used in the analysis and that 61 increments are required. MARC automatically recomputes the time step at each increment such that the maximum incremental change in temperature never exceeds 100°F. Also, the temperature-dependent heat transfer properties were recomputed whenever a maximum change of 100°F occurred anywhere within the model.

The quenching process was found to take approximately 1600 seconds. The temperatures at selective points along the axis are plotted as a function of time in Figure 5.11-8. Stress contours and deformed structure plots will be presented for the same four stages of the thermal stress analysis. The temperature history for each integration point in the model was stored on a post file for subsequent use in the stress run.



**Stress Analysis**

The time-temperature dependent material property data is described in the TIME-TEMP model definition option. The thermal loading is read from the heat transfer post file via the CHANGE STATE option. MARC controls are such that the maximum allowable temperature change in any increment did not exceed 100°F. In view of the controls which were set for the heat transfer analysis, this causes two or more heat increments to be merged into a single stress increment at occasional stages in the analysis. Eighty increments are required for this analysis. The resultant temperature, as a function of increment, is given in Figure 5.11-9.

It is interesting to note that in the early stages of cooling (that is, within approximately the first 50 seconds), the Jominy bar actually increases in volume. As the nominal steady-state room temperature is approached, the bar then shrinks to less than its initial dimensions. The initial increase in volume can be attributed to phase changes which occur at the higher temperatures. These are accounted for via the piecewise polynomial description of the thermal coefficient of expansion. (See Table 5.11-3.)

The effective, or von Mises, equivalent stress, the axial, radial and hoop components of stress are plotted against the increment number in Figure 5.11-10 to Figure 5.11-13. The most severely stressed region occurs at the intersection between the quench end face and the center cylindrical surface. It is interesting to note from the equivalent stress plots that the stress intensity in this region grows from a level of 32,930 psi at stage 1 to a final level of 130,400 psi. Nevertheless, throughout the cooling process the maximum intensity never exceeded the corresponding instantaneous yield stress level; that is, no plastic deformation was found to occur.

Despite this fact, as observed from the stress contour plots there is still a significant nonuniform and appreciable distribution of stress in the bar. However, it should be noted that the analysis was terminated before a uniform steady-state temperature was reached. At the final increment of the analysis, a temperature gradient still exists which ranges from 73°F at the quench end to approximately 90°F at the opposite end. It is believed that a portion of the essentially residual stress state is not due simply to thermal gradients, but rather to nonuniform volumetric changes which occurred in the early stages of cooling. The temperature at elements 1, 10, 13, and 16 are plotted against increment and temperature, respectively, in Figure 5.11-12 and Figure 5.11-13. Coefficients for a polynomial fit of thermal strain,  $\epsilon(T)$ , where:

$$\epsilon(T) = A_1 + A_2T + A_3T^2 + A_4T^3 + A_5T^4$$



**Parameters, Options, and Subroutines Summary**

Example e5x11a.dat:

<b>Parameters</b>	<b>Model Definition Options</b>	<b>History Definition Options</b>
END	CONNECTIVITY	CONTINUE
HEAT	CONTROL	TRANSIENT
MATERIAL	COORDINATE	
SIZING	END OPTION	
THERMAL	FILMS	
TITLE	INITIAL TEMP	
	ISOTROPIC	
	POST	
	PRINT CHOICE	
	TEMPERATURE EFFECTS	

Example e5x11b.dat:

**Parameters**  
ELEMENT  
END  
TITLE

Example e5x11c.dat:

<b>Parameters</b>	<b>Model Definition Options</b>	<b>History Definition Options</b>
END	CHANGE STATE	AUTO THERM
SIZING	CONNECTIVITY	CHANGE STATE
T-T-T	CONTROL	CONTINUE
THERMAL	COORDINATE	
TITLE	END OPTION	
	FIXED DISP	
	POST	
	PRINT CHOICE	
	RESTART	
	TIME-TEMP	



Example e5x11d.dat:

**Parameters**

ELEMENT

END

TITLE

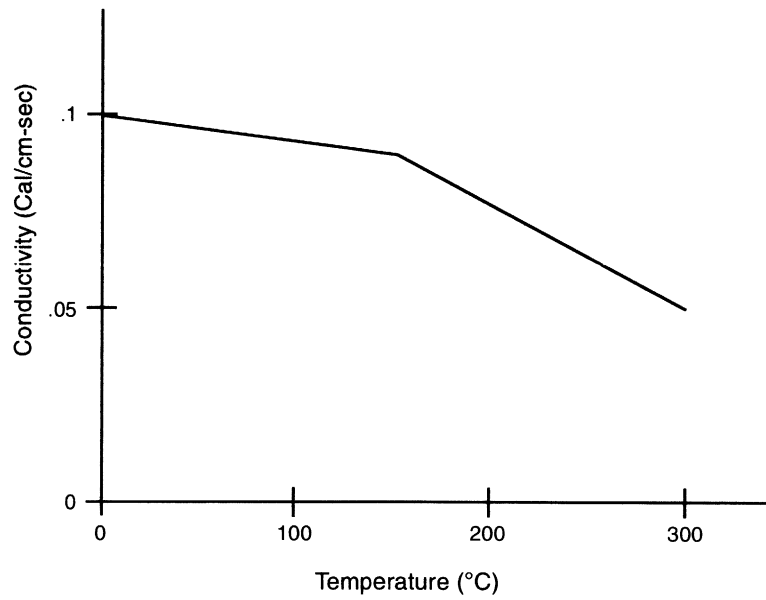


**Figure 5.11-1** Thermal Conductivity vs. Temperature

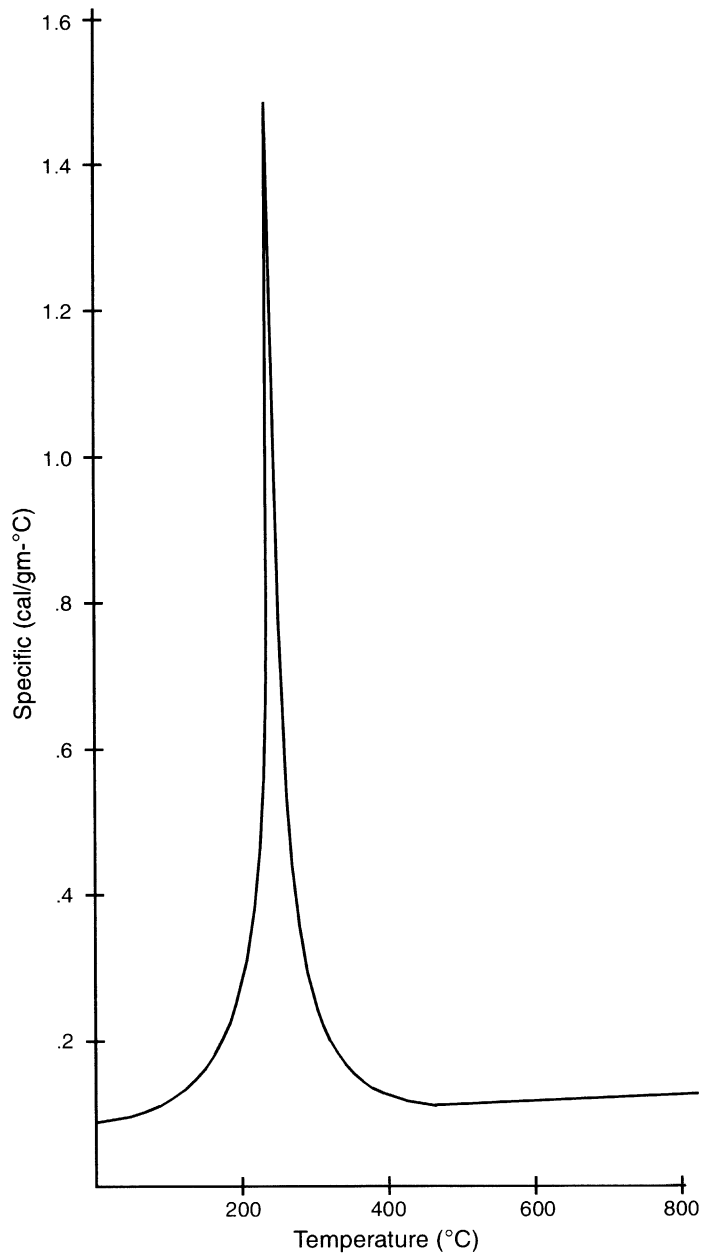


**Figure 5.11-2** Specific Heat vs. Temperature



1	2	3	10	11	12	13	14	15	16
4	6	8	17	19	21	23	25	27	29
5	7	9	18	20	22	24	26	28	30

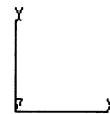


**Figure 5.11-3** Jominy Bar – Axisymmetric Finite Element Model (Elements)

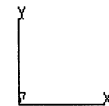
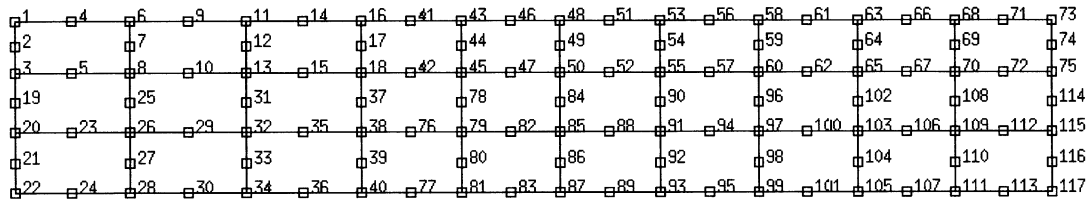


**Figure 5.11-4** Jominy Bar – Axisymmetric Finite Element Model (Nodes)

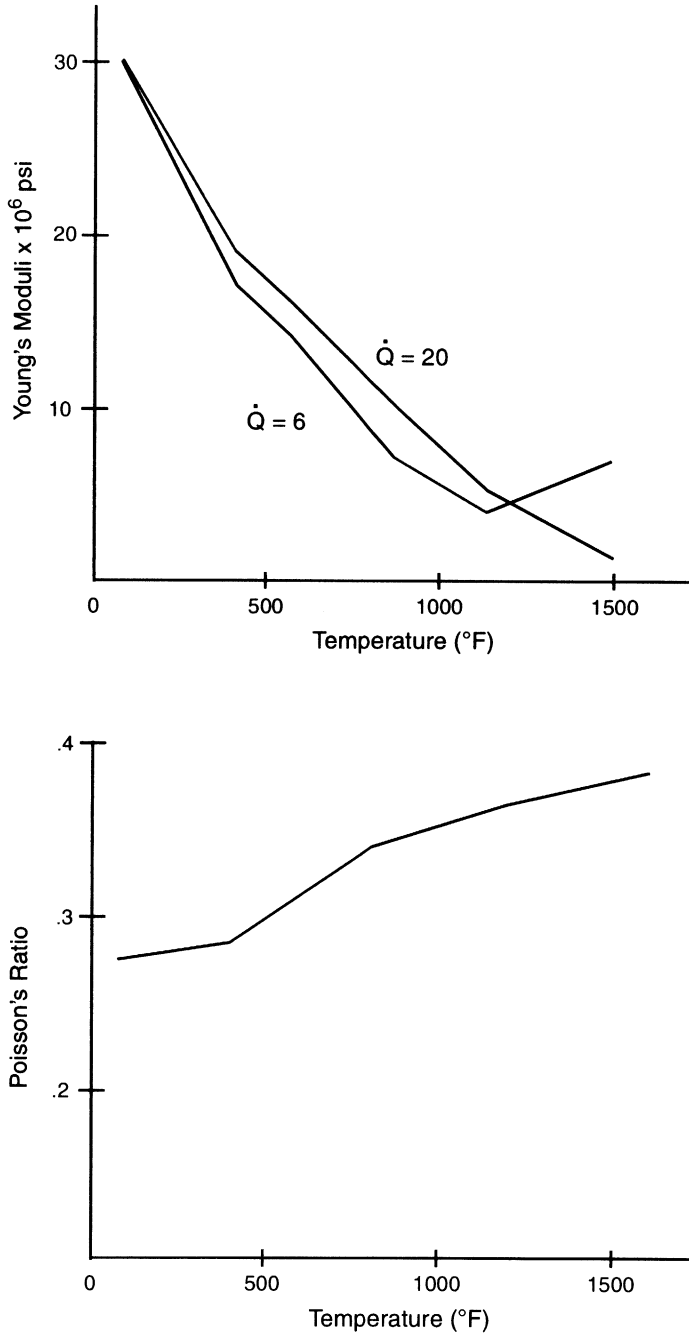


Figure 5.11-5 Material Properties vs. Temperature

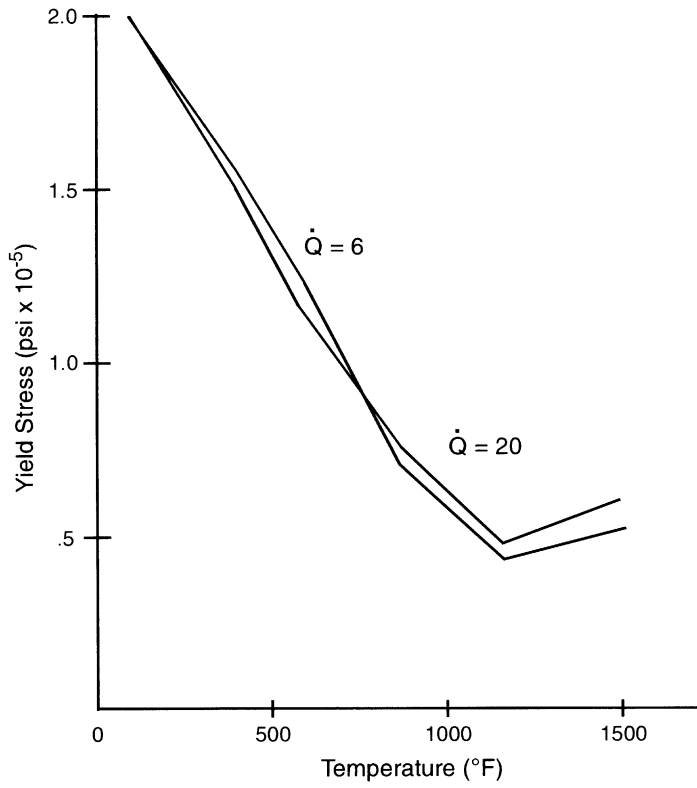
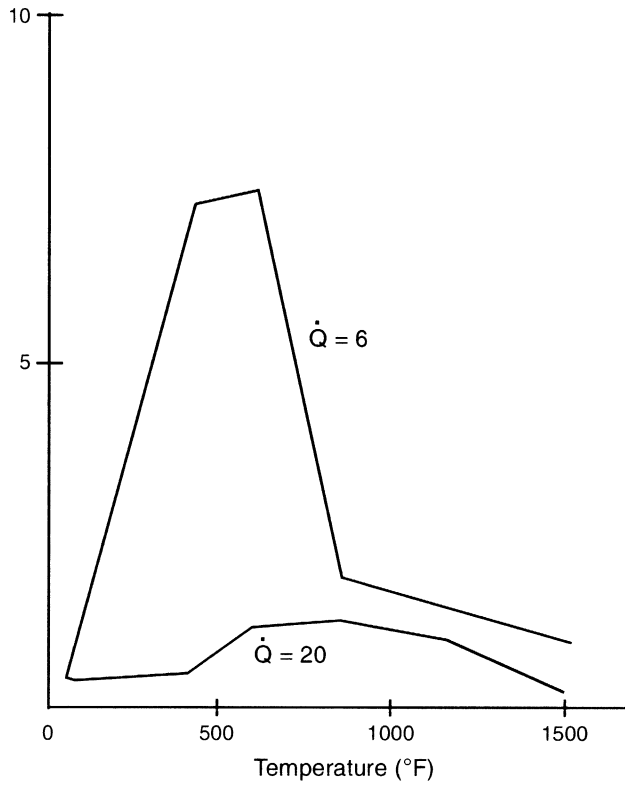
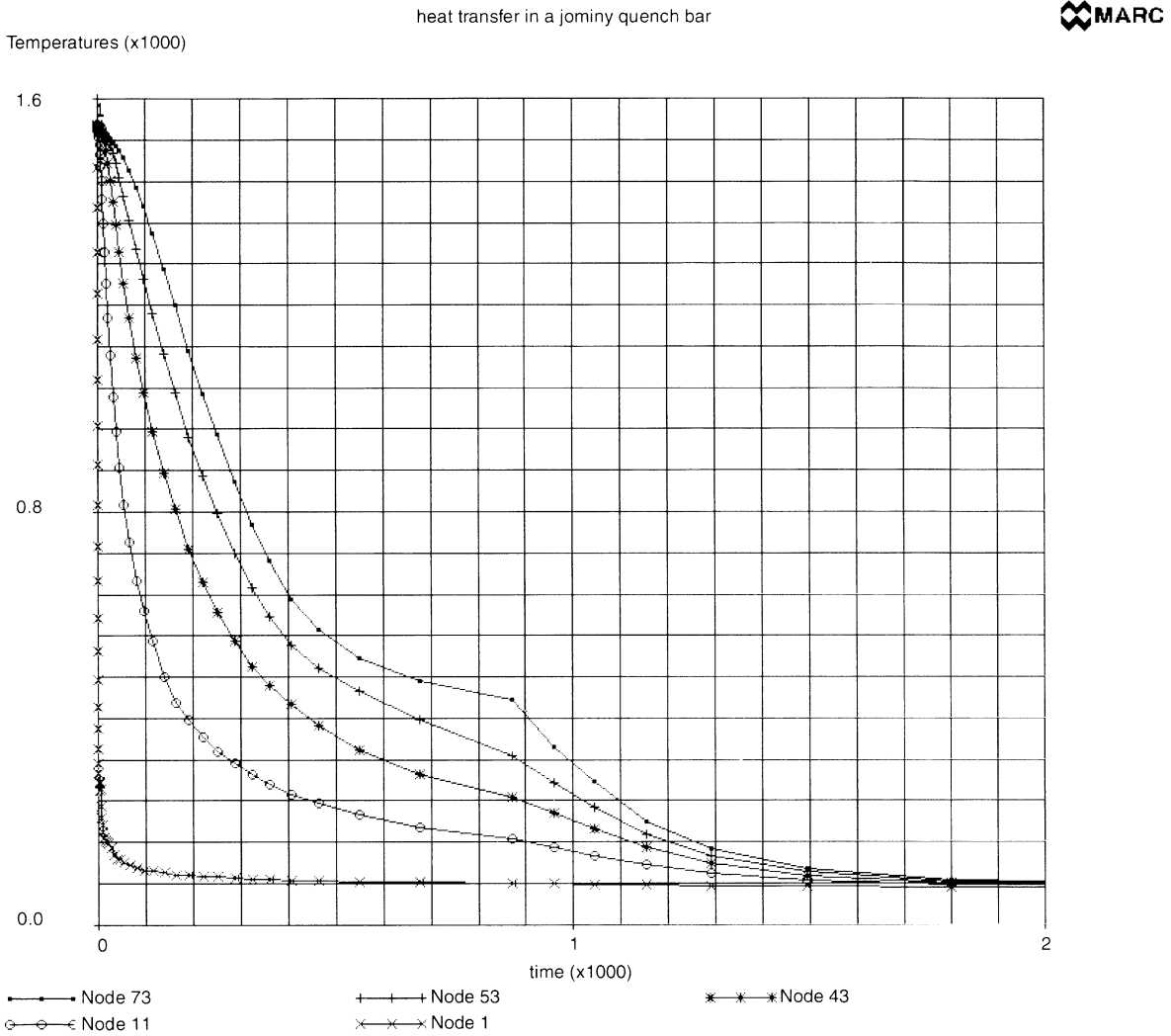


Figure 5.11-6 Yield Stress vs. Temperature





**Figure 5.11-7** Workhardening vs. Temperature



**Figure 5.11-8** Jominy End Quench Test – Temperature vs. Time

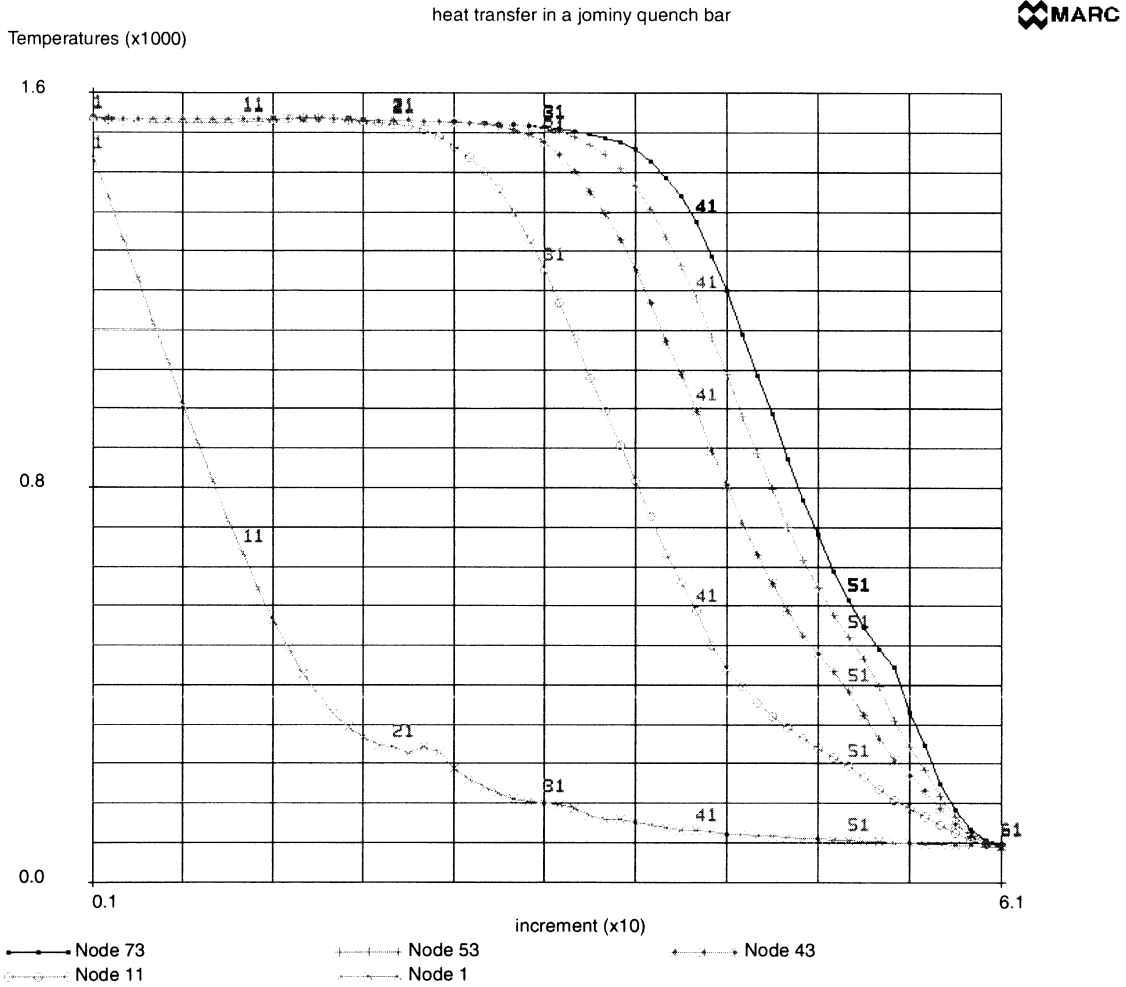


**Figure 5.11-9** Jominy End Quench Test – Temperature vs. Increment

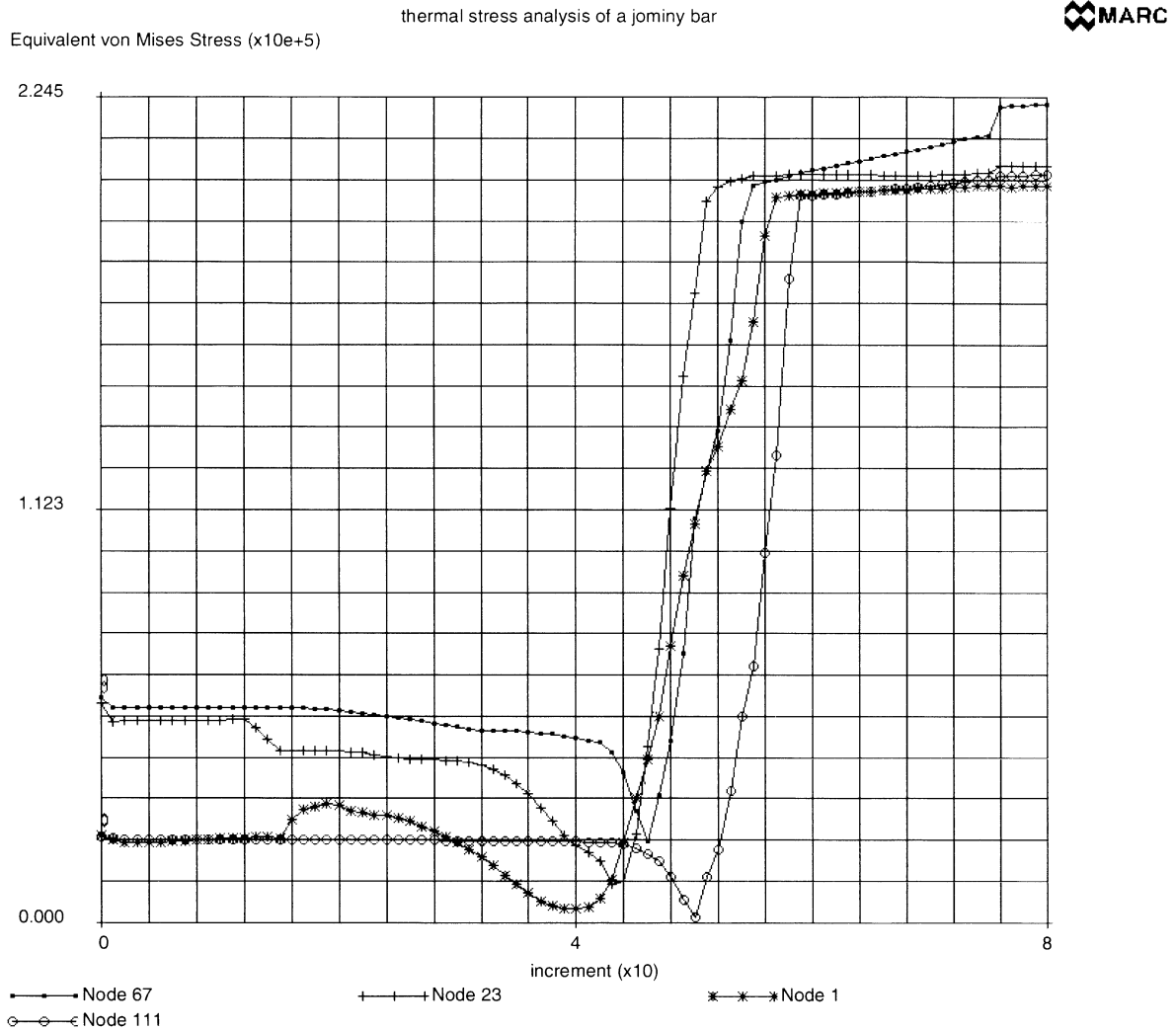


Figure 5.11-10 Jominy End Quench Test – Equivalent Stress vs. Increment

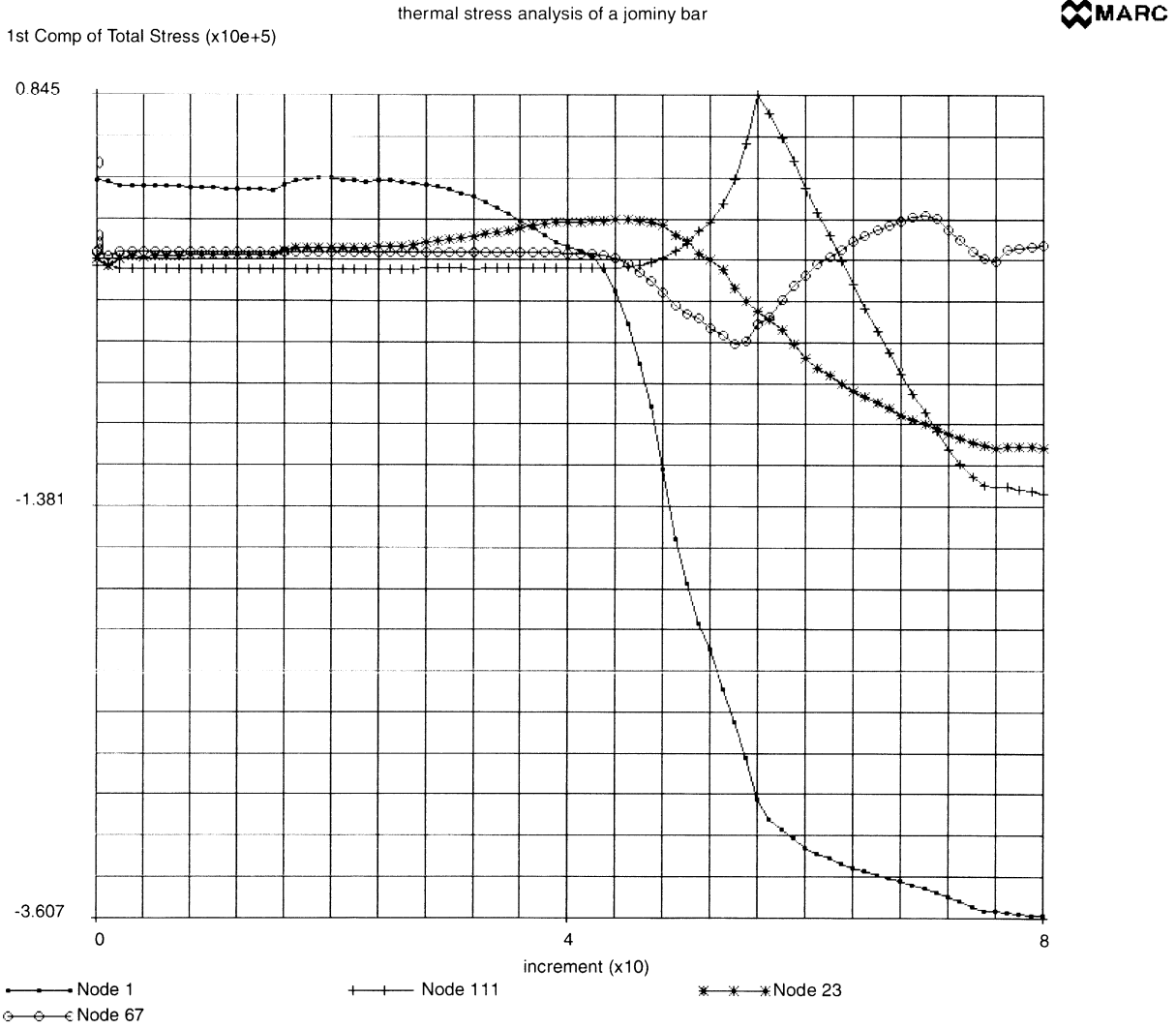
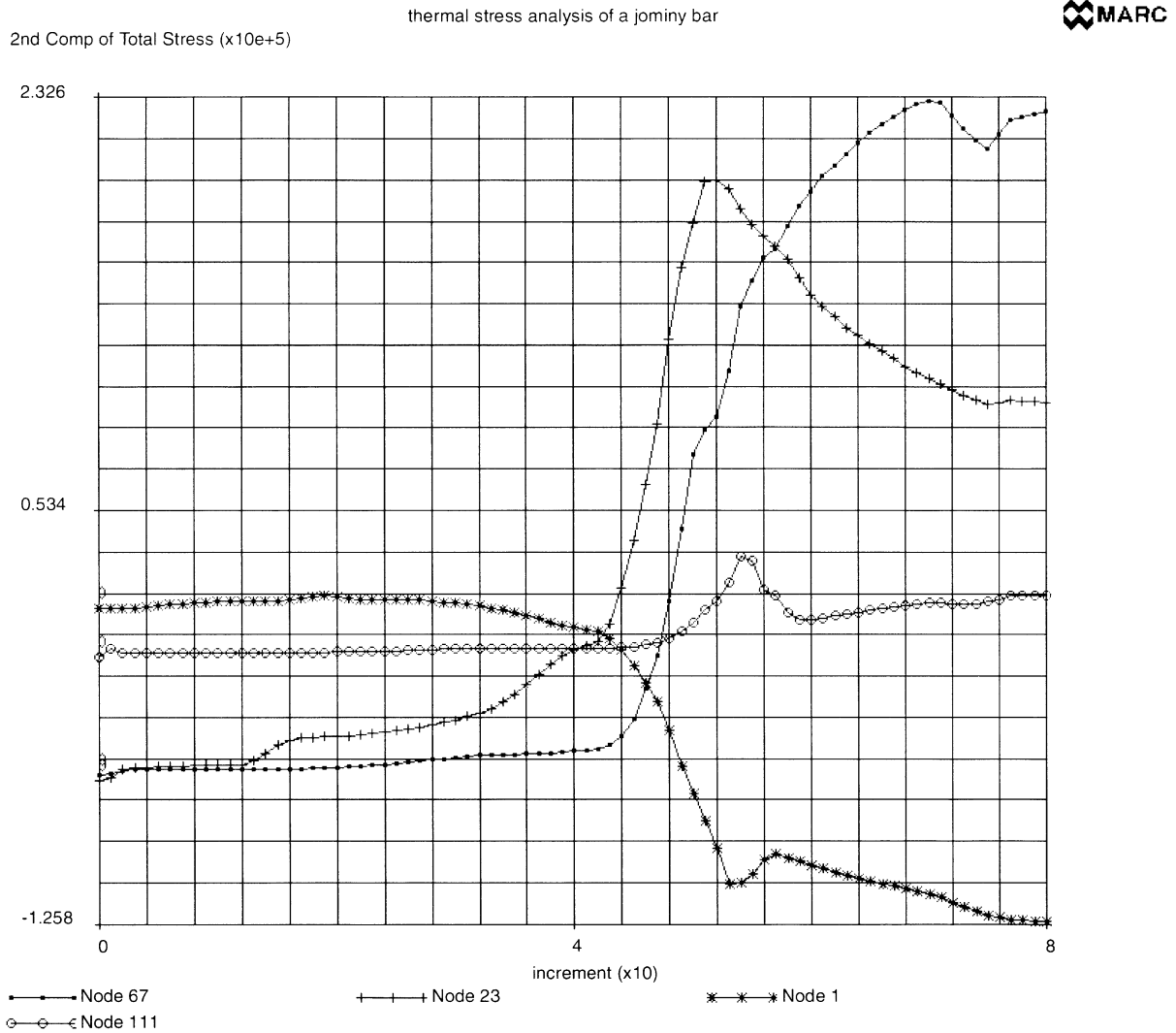
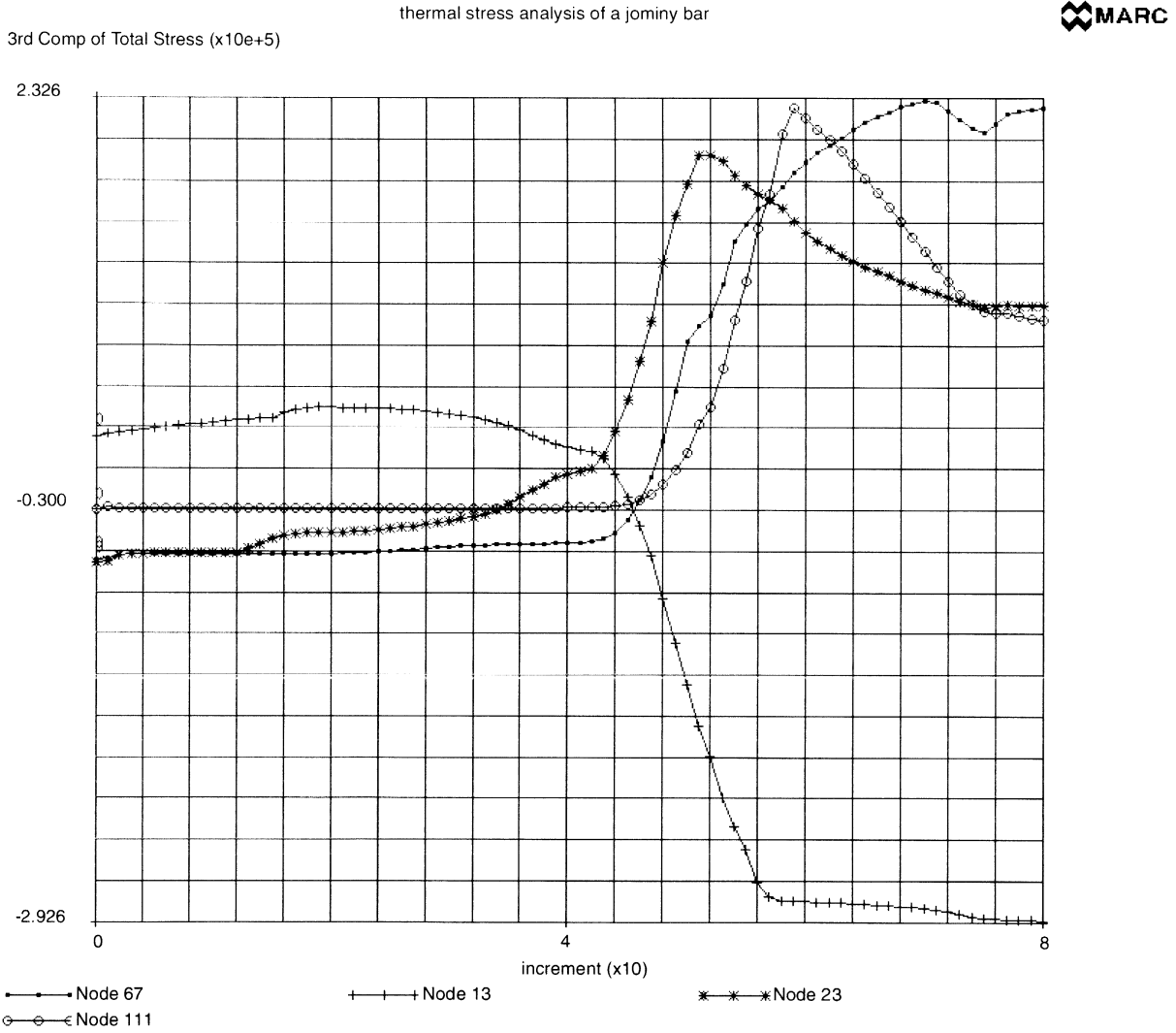


Figure 5.11-11 Jominy End Quench Test – Axial Stress vs. Increment



**Figure 5.11-12** Jominy End Quench Test – Radial Stress vs. Increment



**Figure 5.11-13** Jominy End Quench Text – Hoop Stress vs. Increment



## **5 Heat Transfer**

*Heat Transfer and Stress Analysis of a Jominy End Quench Test Specimen*

---





## 5.12 Cylinder-plane Electrode

A cylinder-plane electrode has been analyzed using a coupled thermo-electric model. MARC element type 39 (4-node isoparametric quadrilateral element) has been used. Two electrodes are applied to the two faces shown in Figure 5.12-1, producing a uniform difference of electric potential between the upper and the lower face.

### Model

This problem demonstrates the use of the JOULE option for Joule heating problems. (See *MARC Volume A: Theory and User Information* for a general discussion of the problem).

### Material Properties

The specific heat and density of the material are 0.26 cal/gm-°C and 3.4 gm/cm<sup>3</sup>, respectively. The surface film coefficient is 0.677-3 cal/sec-cm<sup>2</sup>-°C. The temperature dependent thermal conductivity and resistivity are shown in Figure 5.12-2.

### Initial Conditions

The initial nodal temperatures are 20°C throughout.

### Boundary Conditions

The upper face has 1 V;  $V = 0$  at the lower face. Convective boundary conditions are assumed to exist at the lower face.

### Transient

Nonautomatic time stepping is used setting the initial step at 100 seconds. The transient solution lasts for 100 seconds.

### Results

Voltage, current and temperature distributions are shown in Figure 5.12-4 through Figure 5.12-6.

### Parameters, Options, and Subroutines Summary

Example e5x12.dat:

Parameters	Model Definition Options	History Definition Options
ALIAS	CONNECTIVITY	CONTINUE
END	COORDINATE	TRANSIENT
HEAT	END OPTION	
JOULE	FIXED TEMP	
SIZING	ISOTROPIC	
TITLE	JOULE	
	POST	
	VOLTAGE	

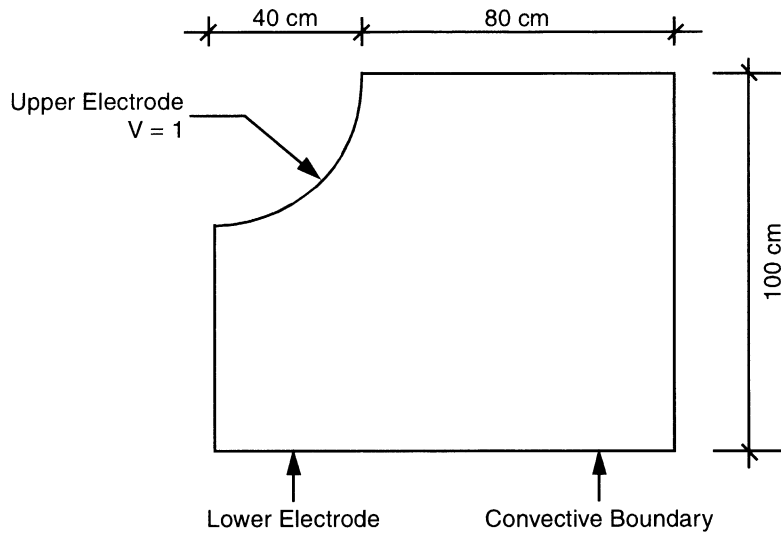


**Figure 5.12-1** Geometry of the Problem

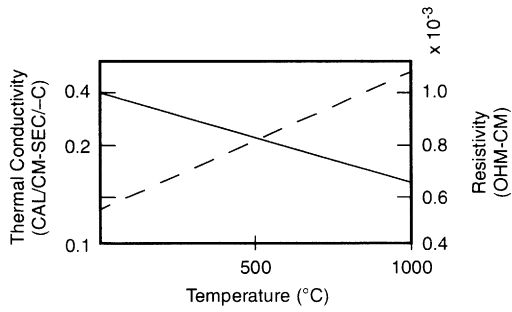


**Figure 5.12-2** Temperature Dependent Properties

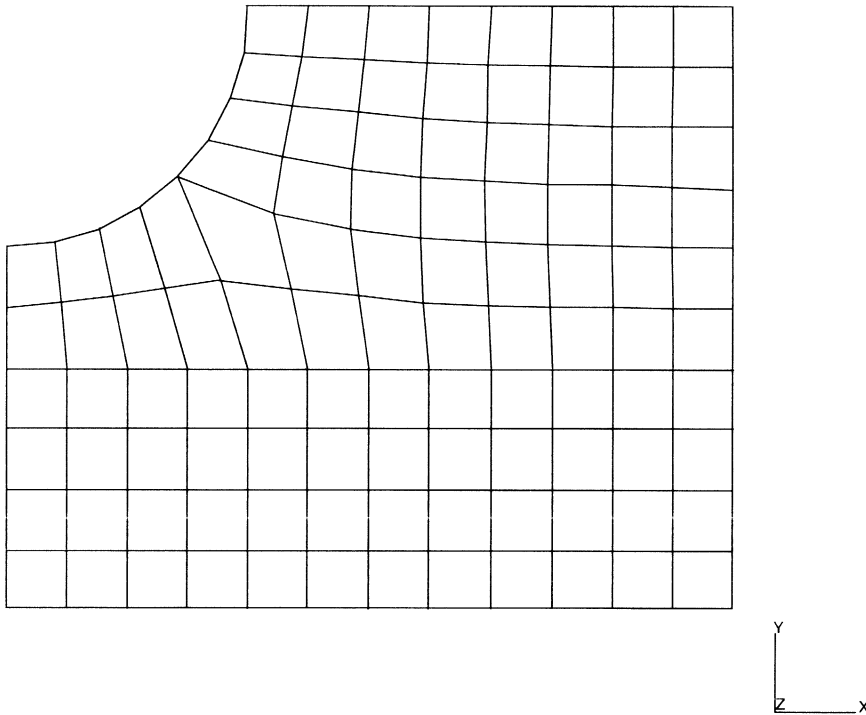
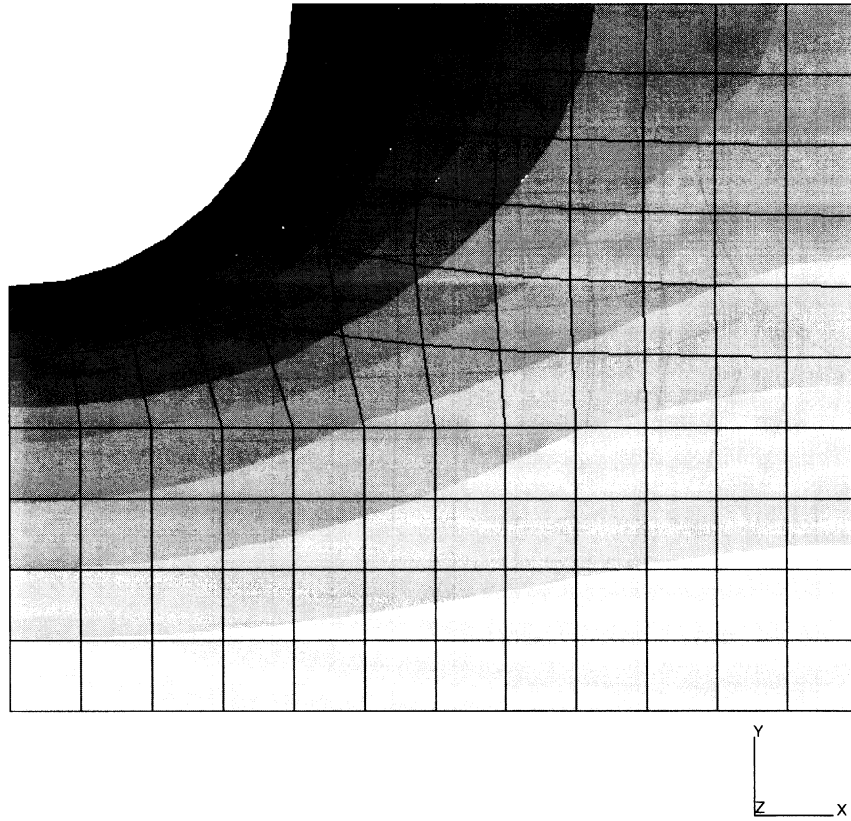
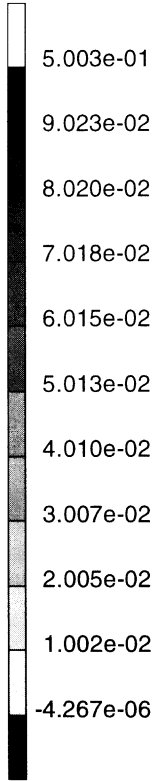


Figure 5.12-3 Mesh

INC : 1  
SUB : 0  
TIME : 1.000e+04  
FREQ: 0.000e+00

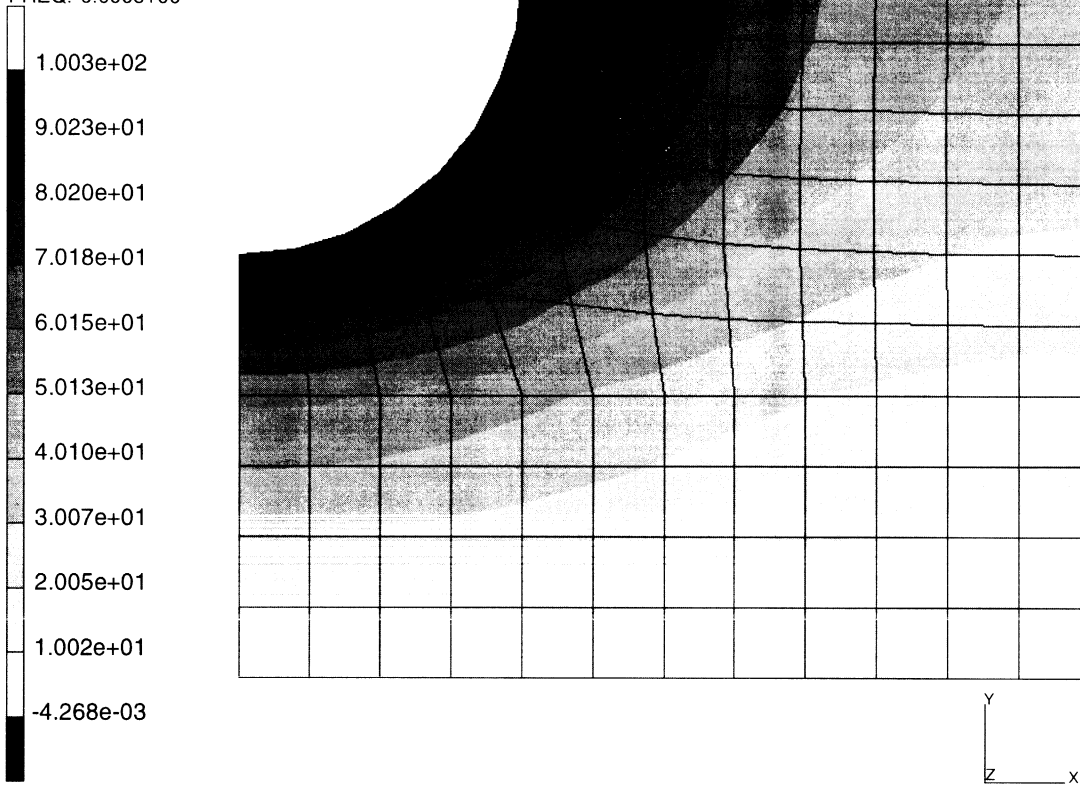


electrostatic demo  
Temperature

Figure 5.12-4 Temperature Distribution



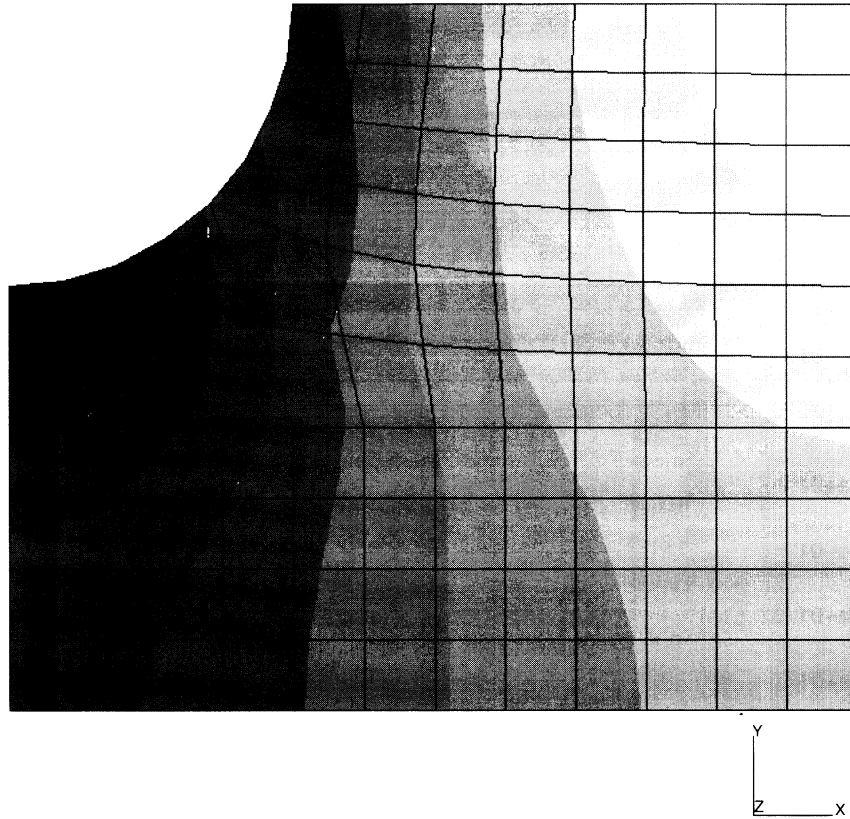
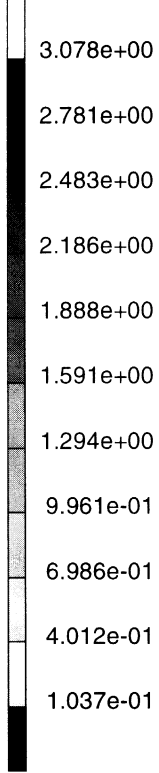
INC : 1  
SUB : 0  
TIME : 1.000e+04  
FREQ: 0.000e+00



electrostatic demo  
Voltage

Figure 5.12-5 Voltage Distribution

INC : 1  
SUB : 0  
TIME : 1.000e+04  
FREQ: 0.000e+00



electrostatic demo  
Current

**Figure 5.12-6** Current Distribution



## 5.13 Axisymmetric Transient Heat Conduction Simulated by Heat Transfer Shell Elements

The transient heat conduction of a cylinder, subjected to a thermal downshock, is analyzed by using MARC heat transfer shell elements. This is the same as problem 5.5. The model and input data of the problem are:

This problem is modeled using the four techniques summarized below.

Data Set	Element Type(s)	Number of Elements	Number of Nodes
e5x13a	85	6	12
e5x13b	86	6	29
e5x13c	87	2	5
e5x13d	88	2	3

### Model/Elements

The MARC heat transfer shell elements consist of elements 85 (4-node), 86 (8-node), 87 (3-node axisymmetric) and 88 (2-node axisymmetric). Element temperatures are either linearly (elements 85 and 88) or quadratically interpolated in the plane of the shell and assumed to have a linear/quadratic distribution in the thickness direction of the shell. The nodal degrees of freedom is two if a linear distribution of temperatures is assumed in the shell thickness direction, and three if a quadratic distribution of temperatures is assumed in the thickness direction of the shell. This is set by you on the HEAT parameter. These heat transfer shell elements are compatible with stress shell elements (see below) for thermal stress analysis.

Heat Transfer Shell Elements	Stress Shell Elements
85	72, 75
86	22
87	89
88	1

### Models

As shown in Figure 5.13-1, the cylinder has an inner radius of 8.625 inches and a wall thickness of 0.375 inches. It is subjected to a constant initial condition and different convective boundary conditions on the inner and outer surfaces of the cylinder. Finite meshes for heat transfer shell elements 85, 86, 87, and 88 and shown in Figure 5.13-2 through Figure 5.13-5, respectively. The number of elements and number of nodes in each mesh are:



Mesh	Element	Number of Elements	Number of Nodes
A	85	6	12
B	86	6	29
C	87	2	5
D	88	2	3

**SHELL SECT**

The SHELL SECT option allows you to specify the number of points to be used for numerical integration in the thickness direction of the shell. The number of integration points in the thickness direction of the shell is chosen to be seven in this example.

**Geometry**

The shell thickness of 0.375 inches is entered as EGEOM1 in the GEOMETRY block and a positive (nonzero) number is entered as EGEOM2 for the selection of a quadratic distribution of temperatures in the thickness direction.

**Material Properties**

The conductivity is  $4.85E-4$  BTU/sec-in-°F. The specific heat is 0.116 BTU/lb-°F. The mass density is 0.283 lb/cubic inch.

**Initial Condition**

Initial nodal temperatures are assumed to be homogeneous at 1100°F.

**Boundary Conditions**

No input data is required for insulated boundary conditions at  $z = 0$  and  $z = 2.0$ . Fluid temperatures and film coefficients for both inner and outer surfaces of the cylinder are:

Inner surface:

$$H_i = 38.56E-5 \text{ BTU/second-square inch-}^\circ\text{F}$$

$$T_i = 1100^\circ\text{F at } t = 0. \text{ second}$$

$$800^\circ\text{F at } t = 10. \text{ seconds}$$

Outer surface:

$$H_0 = 1.93E-6 \text{ BTU/second-square inch-}^\circ\text{F} \text{ (low value to simulate insulated boundary condition).}$$

$$T_0 = 1100^\circ\text{F}$$

The low value of  $H_0$  simulates an insulated boundary.



The FILMS option is used to input the film coefficients and associated fluid temperatures for the inner and outer surfaces. Subroutine FILM linearly interpolates the 300°F decrease in ambient temperature over 10 seconds and then holds the inner wall temperature constant at 800°F. It is called at each time step for each integration point on each element surface given in the FILMS option.

### Post

In a heat transfer run, the use of the POST option allows the creation of a post file containing element temperatures at each integration point and nodal point temperatures. The file can be used later as input to the stress analysis run. The code number for element temperatures of heat transfer elements is 9 followed by a layer number (that is, 9,1, and 9,2, etc.). These code numbers must be entered sequentially.

### Transient

The TRANSIENT option controls time steps in a transient heat transfer analysis. MARC automatically calculates the time steps to be used based on the maximum nodal temperature change allowed as input in the CONTROL option. The solution begins with the suggested initial time step input and ends according to the time period specified. It does not exceed the maximum number of steps input in this option.

### Results

A comparison of nodal temperatures with the results of an axisymmetric model (problem 5.5) is shown in Table 5.13-1.

**Table 5.13-1** Comparison of Nodal Temperatures

Time (Sec.)	Nodal Temperature (°F) (Node 17)  5.5	Element Temperatures (°F) – 4th Layer			
		Element 85	Element 86	Element 87	Element 88
		(Model A)	(Model B)	(Model C)	(Model D)
1.25	1099.3	1099.3	1099.3	1099.3	1099.3
4.06	1092.6	1092.4	1092.4	1092.4	1092.4
7.18	1078.3	1077.9	1077.9	1077.9	1077.9
9.84	1061.2	1060.3	1060.3	1060.3	1060.3
12.79	1041.1	1039.7	1039.7	1039.7	1039.7
16.90	1015.7	1013.8	1013.8	1013.8	1013.8
21.00	993.1	990.7	990.7	990.7	990.7
26.13	968.3	965.5	965.5	965.5	965.5
31.90	944.3	941.3	941.3	941.3	941.3
38.31	921.8	918.5	918.5	918.5	918.5



**Parameters, Options, and Subroutines Summary**

Example e5x13a.dat:

<b>Parameters</b>	<b>Model Definition Options</b>	<b>History Definition Options</b>
ELEMENT	CONNECTIVITY	CONTINUE
END	CONTROL	TRANSIENT
SHELL SECT	COORDINATE	
SIZING	END OPTION	
TITLE	FILMS	
	GEOMETRY	
	INITIAL TEMP	
	ISOTROPIC	
	POST	
	PRINT CHOICE	

User subroutine in u5x13.f:

FILM

Example e5x13b.dat:

<b>Parameters</b>	<b>Model Definition Options</b>	<b>History Definition Options</b>
ELEMENT	CONNECTIVITY	CONTINUE
END	CONTROL	TRANSIENT
SHELL SECT	COORDINATE	
SIZING	END OPTION	
TITLE	FILMS	
	GEOMETRY	
	INITIAL TEMP	
	ISOTROPIC	
	POST	
	PRINT CHOICE	

User subroutine found in u5x13.f:

FILM



Example e5x13c.dat:

<b>Parameters</b>	<b>Model Definition Options</b>	<b>History Definition Options</b>
ELEMENT	CONNECTIVITY	CONTINUE
END	CONTROL	TRANSIENT
SHELL SECT	COORDINATE	
SIZING	END OPTION	
TITLE	FILMS	
	GEOMETRY	
	INITIAL TEMP	
	ISOTROPIC	
	POST	
	PRINT CHOICE	

User subroutine found in u5x13.f:

FILM

Example e5x13d.dat:

<b>Parameters</b>	<b>Model Definition Options</b>	<b>History Definition Options</b>
ELEMENT	CONNECTIVITY	CONTINUE
END	CONTROL	TRANSIENT
SHELL SECT	COORDINATE	
SIZING	END OPTION	
TITLE	FILMS	
	GEOMETRY	
	INITIAL TEMP	
	ISOTROPIC	
	POST	
	PRINT CHOICE	

User subroutine in u5x13.f:

FILM

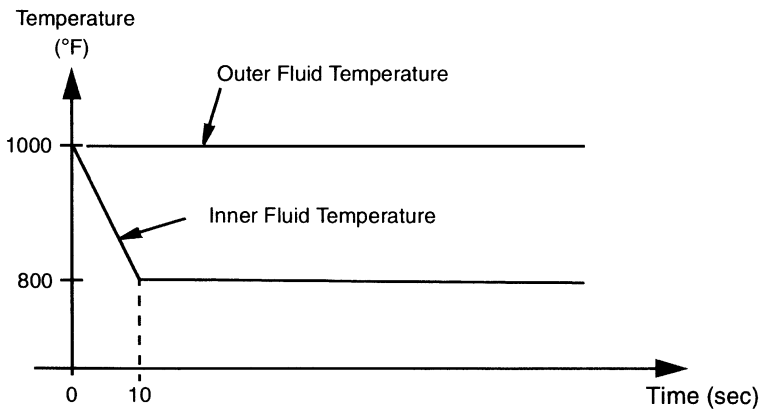
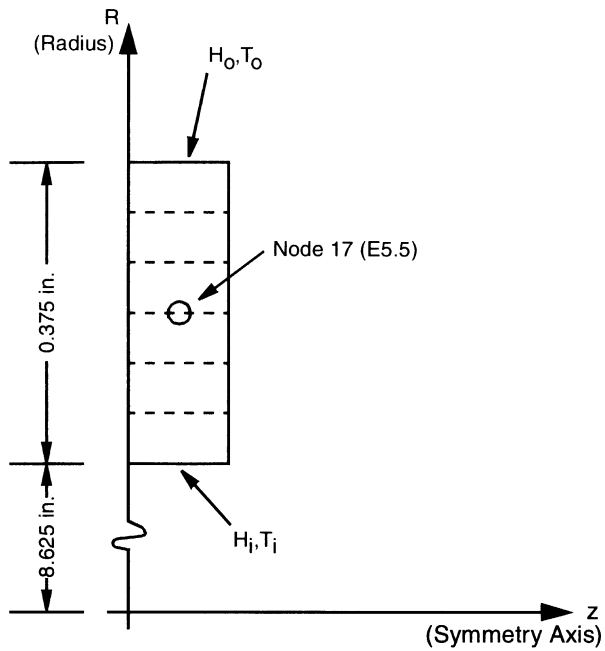


**Figure 5.13-1** Cylinder Model and Fluid Temperature History

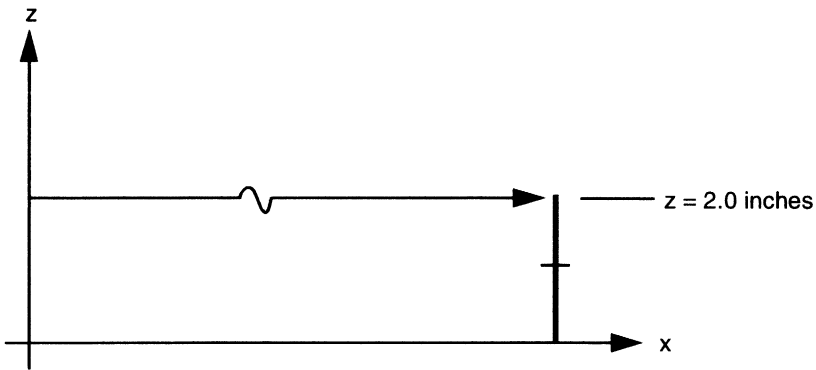
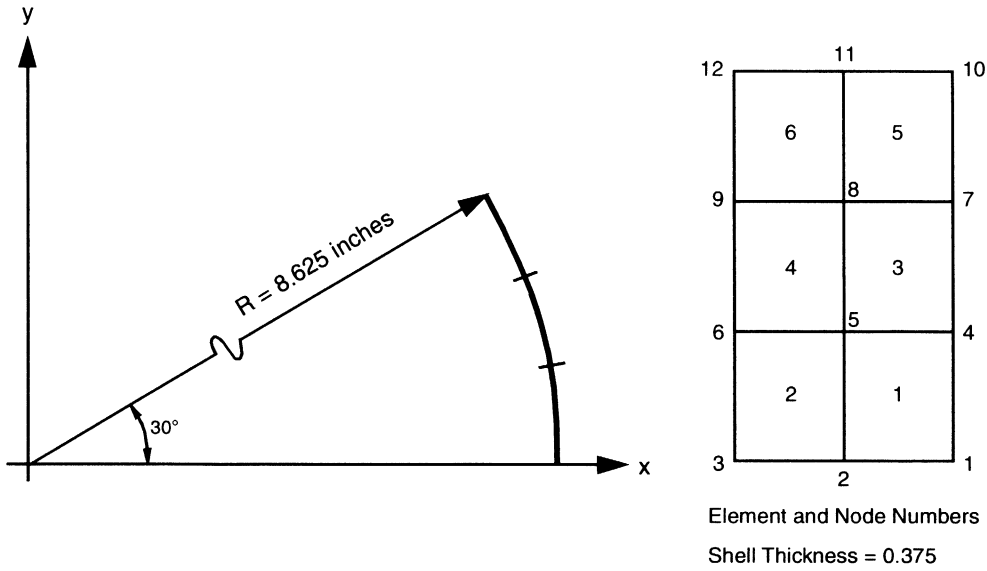
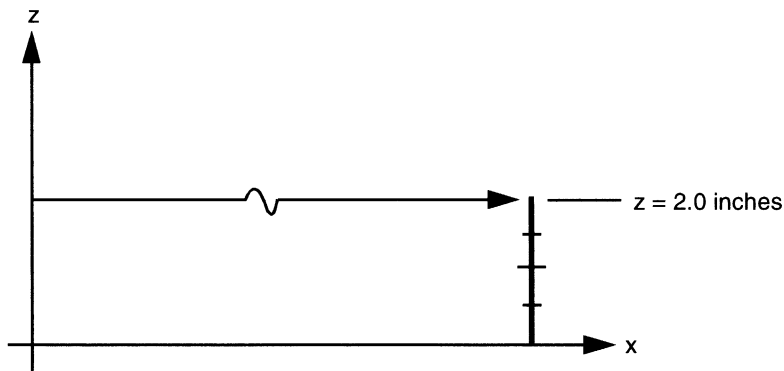
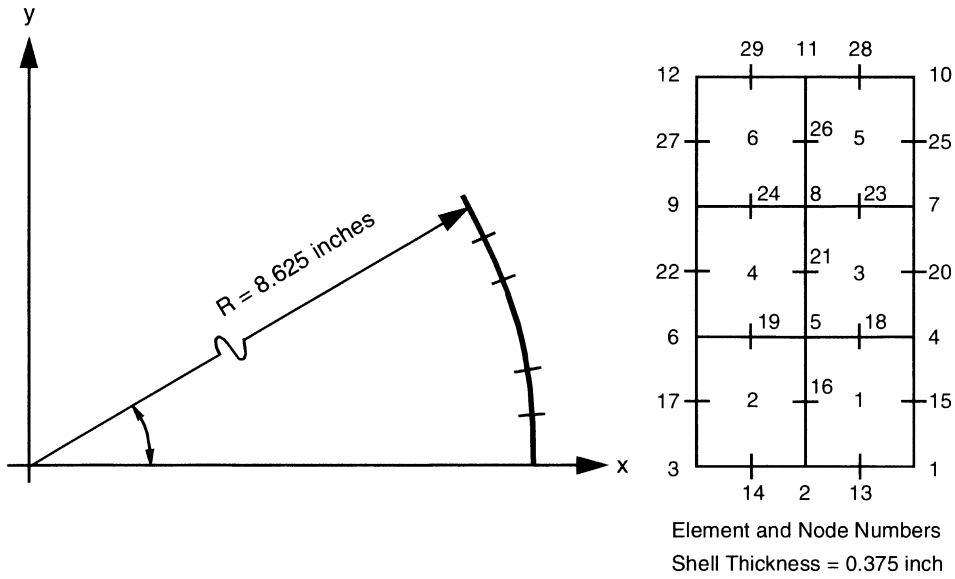
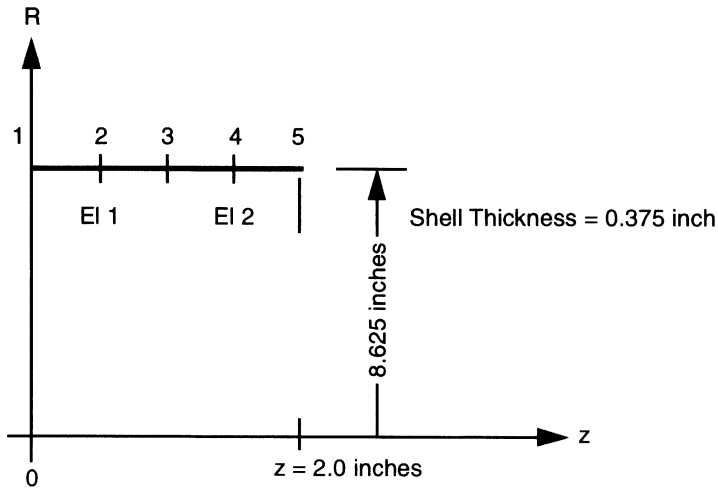


Figure 5.13-2 Finite Element Model (Model A - Element 85)



**Figure 5.13-3** Finite Element Model (Model B - Element 86)



**Figure 5.13-4** Finite Element Model (Model C - Element 87)

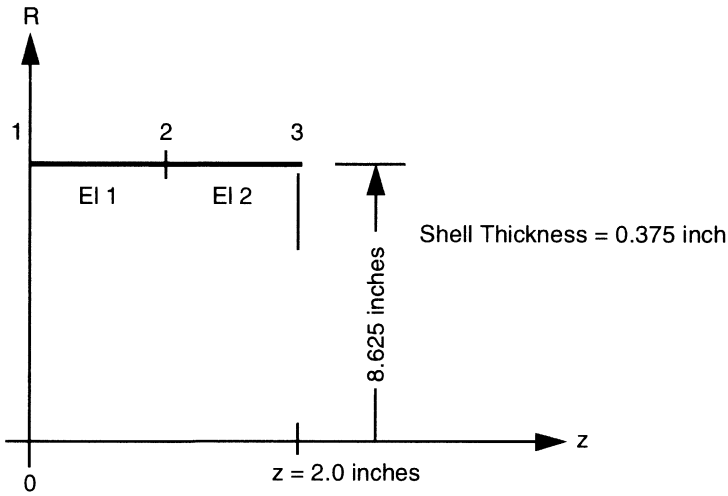


**Figure 5.13-5** Finite Element Model (Model D - Element 88)



## **5 Heat Transfer**

*Axisymmetric Transient Heat Conduction Simulated by Heat Transfer Shell Elements*

---





## 5.14 Steady-state Temperature Distribution of a Generic Fuel Nozzle

A steady-state heat transfer analysis is performed on a simplified two-dimensional model of a generic fuel nozzle for a turbine engine. The nozzle has both fluid heat-up and radiation across gaps which are simulated by fluid channel and thermal contact gap elements in the program. Model definition options CHANNEL and CONRAD GAP are used for fluid channel and radiation gaps, respectively. A 4-node-planar quad is chosen for modeling the entire nozzle.

### Element

Library element type 39 is a 4-node planar isoparametric quadrilateral heat transfer element. Each nodal point is defined by two global coordinates (x,y) and has temperature as the nodal degrees of freedom. See *MARC Volume B: Element Library* for further details.

### Model

As shown in Figure 5.14-1, the simplified nozzle model is a two-dimensional structure, made of steel, containing two radiational gaps and a fluid channel. The nozzle is heated up from room temperature by a 200°F fluid flow in the channel as well as convective heat transfers from the external boundaries with ambient temperatures at 400°F and 1600°F, respectively. Thermal properties of steel and fluid are assumed to be dependent on temperatures.

Figure 5.14-2 shows a finite element mesh for the MARC heat transfer analysis. The mesh contains 103 4-node quad elements and 142 nodes. A fluid channel consisting of elements 1, 30 through 37, 24 through 29, and two thermal contact gaps (GAP1: elements 38 through 45; GAP2: elements 82 through 89), are also depicted in Figure 5.14-2.

### Define (Element Set)

In the MARC input, set names are used to represent various regions in the model. The set WHOLE contains all the elements in the model. The fluid channel and two thermal gaps are represented by set names CHANL, GAP1, and GAP2, respectively. A set operation, WHOLE EXCEPT GAP1 EXCEPT GAP2 EXCEPT CHANL, defines the steel elements.

### Material Properties

Thermal properties for steel are:  $K = 1.85 \times 10^{-4}$  BTU/sec-in-°F,  $C = 0.1$  BTU/lb-°F, and  $\rho = 0.285$  lb/in<sup>3</sup>. The specific heat of the fluid is assumed to be 0.4625 BTU/lb-°F. Both the thermal conductivity (k) and the specific heat (C) are dependent on temperature. Slopes and break point data are entered through the TEMPERATURE EFFECTS model definition option. Material identifications 1, 2 and 3 are assigned to STEEL, CHANL (fluid), GAP1 and GAP2 (thermal gaps), respectively. Both the thermal conductivity and mass density of fluid, as well as the thermal properties of thermal gap elements, are set to zero.

**Initial Temp**

A constant initial temperature of 70°F is assumed for the entire model.

**Geometry**

The model thickness of 1.0 inch is entered through the GEOMETRY block.

**Input for Thermal Contact Gap**

In problems involving thermal contact gaps, the model definition option CONRAD GAP is used for the input of all gap properties. The data needed for each gap are: face identification, emissivity, Stefan-Boltzmann constant, absolute temperature conversion factor, film coefficient, gap closure temperature and a list of elements in the gap. Discussions on the gap face identification can be found in *MARC Volume B: Element Library*.

Since the thermal gap element serves as a radiation/convection link or, as tying constraints, thermal properties are not required for the element. Consequently, all the entries (conductivity, specific heat, density) in the ISOTROPIC option must be set to zero for all thermal contact elements.

In addition, because thermal contact and solid elements have same topology, the connectivity data format of thermal contact element is same as that of a solid element. As a result, mesh generators such as MESH2D or Mentat can be used for the generation of thermal contact gaps. All the thermal contact elements in one gap must be numbered in the same order.

**Conrad Gap**

The CONRAD GAP model definition option is used for entering thermal contact gap information. In the model, the number of thermal gaps is 2; and in each gap: the Stefan-Boltzmann constant is  $0.3306E-14$  BTU/sec - in<sup>2</sup> - °R<sup>4</sup>; the absolute temperature conversion factor from Fahrenheit to Rankine is 459.7; and the gap-closure temperature is assumed to be 2000°F (thermal gaps remain open throughout the analysis). The thermal gap elements are defined in sets GAP1 and GAP2, respectively.

**Input for Fluid Channel**

The data associated with fluids channels can be entered using the model definition option CHANNEL. The data needed for each channel are: channel face identification, lead element number, inlet temperature, mass flow rate, film coefficient and a list of fluid elements in the channel. Discussions on the channel face identification can be found in *MARC Volume B: Element Library*.

The topology of the fluid channel element is the same as that of solid element. Additional input is not needed for the mesh definition of fluid channels. All the fluid channel elements in one channel must be numbered in the same order.



Since the fluid flow in the channel is assumed to be convective, and based on the mass flow rate, in the ISOTROPIC block only the specific heat of the fluid is required. Both the conductivity and density of the fluid must be set to zero. The model definition option TEMPERATURE EFFECTS can be used for temperature dependent specific heat of the fluid.

For planar elements, the GEOMETRY block is needed for the input of channel thickness.

**Channel**

The CHANNEL model definition option is used for the input of fluid channel data. In the current model, the number of channels is 1; the channel face identification is 2; the lead element number is 1; the inlet temperature is 200°F; the mass flow rate is 0.02778 lb/sec (or 100 lb/hr); and the film coefficients in the channel are entered using user subroutine FLOW (set to 0. in the input deck). A list of the subroutine FLOW is shown on a latter page. Finally, the fluid elements is contained in the set CHANL.

**Films**

Finally, 16 sets of film data are used for the input of convective thermal boundary conditions in the model. The user subroutine FILM is used for entering film coefficient and sink temperature of each film boundary ( $H = 1.0$ ,  $T_{inf} = 1.0$  in the input). Both the film index and the fluid temp index are used for film boundary condition input.

**Transient**

Steady state temperatures in the generic fuel nozzle with temperature dependent thermal properties can be obtained from a MARC heat transfer analysis using: (1) several transient time-steps with large time increments or, (2) one time-step with a number of iterations within the time-step. Both approaches converge to the same steady-state solution.

**Results**

Both the channel and solid temperatures are depicted in Figure 5.14-3. Comparisons between finite element and finite difference results are favorable.



## **5 Heat Transfer**

*Steady-state Temperature Distribution of a Generic Fuel Nozzle*

---



## 5.15 Radiation Between Concentric Spheres

A typical radiation heat-exchange problem between gray bodies is solved here in order to show the capabilities of MARC in dealing with the radiations boundary conditions in heat conduction problems. The radiation heat exchange is based on the computation of the “view factors” depending purely upon the geometrical shape of the radiating boundaries. The computed steady-state temperature distribution is shown and is compared with an analytical solution.

The geometry of the model is shown in Figure 5.15-1; two concentric spherical bodies and four spherical surfaces can be identified: surfaces 1 and 2 define the first body and surfaces 3 and 4 define the second spherical gray body. Surface 1 has a radius of  $r_1$ , surface 2 – radius of  $r_2$ , surface 3 – radius of  $r_3$ , and surface 4 – radius of  $r_4$  (Figure 5.15-1). Temperatures on surfaces 1 and 4 are known; radiative heat transfer takes place between surfaces 2 and 3.

This example uses two data sets. Data set e5x15 involves radiation view factor calculation by MARC. Data set e5x15b uses the view factors generated by Mentat. the view factor file e5x15b.vfs stores the Mentat generated view factors.

### Element

Element type 42, a second order distorted axisymmetric quadrilateral element for heat-transfer analysis, is used. There are eight nodes per element and one degree of freedom (temperature) per node. (See *MARC Volume B: Element Library* for further details.)

### Model

The axisymmetric section and the finite element model shown in Figure 5.15-2; 24 elements, with two elements in the radial direction, describe each body for a total of 48 elements and 202 nodes.

### Radiation

The RADIATION parameter is used to activate the heat transfer analysis with radiative heat exchange and to specify the view factors calculation (or for reading them from a file). In addition, the units are specified for length and for temperature. In problem e5x15, the view factors during analysis are calculated using RADIATING CAVITY input. Problem e5x15b uses MENTAT to calculate the view factors. They are read in from e5x15b.vfs.

### Radiating Cavity

One radiating cavity is defined in this option: the cavity is bounded by the spherical surfaces nos. 2 and 3 in Figure 5.15-1. The anti-clockwise list of nodes defining the outline of the cavity is assigned.

**Thermal Properties**

One set of thermal properties is specified in the ISOTROPIC block; the isotropic thermal conductivity value of 1.E-4 W/mm °C is assigned in the first field and the temperature-dependent value of the emissivity is specified in the fourth field. (Special input for radiation problems.)

**Thermal Boundary Conditions**

The temperature value of the internal and external spherical surfaces is imposed in the FIXED TEMP option as follows:

Surface no. 1  $T_1 = 332.561$  °C                      Surface no. 4  $T_4 = 532.114$  °C

See Figure 5.15-1 for cross reference.

**Control for Thermal Analysis**

The maximum error in temperature estimate used for property evaluation is set to 0.1 °C. This control provides a recycling capability to improve accuracy in this highly non-linear heat transfer problem. See *MARC Volume C: User Input* model definition option CONTROL for further details.

**Thermal History**

A steady-state thermal analysis is specified via STEADY STATE history definition option.

**Results**

The computed distribution of the temperature at the steady-state condition is compared with the analytical solution and it is summarized below.

Surface Temperature	Analytic (°C)	e5x15.dat	e5x15b.dat
T1	332.561	332.561	332.561
T2	400.00	401.364	391.624
T3	500.00	500.475	504.185
T4	532.114	532.114	532.114

**Reference**

Frank Kreith, *Principles of Heat Transfer*, Donnelly Publishing Corp., N.Y.



**Parameters, Options, and Subroutines Summary**

Example e5x15.dat:

<b>Parameters</b>	<b>Model Definition Options</b>	<b>History Definition Options</b>
ELEMENT	BOUNDARY CONDITIONS	CONTINUE
END	CONNECTIVITY	STEADY STATE
HEAT	CONTROL	
RADIATION	COORDINATE	
SIZING	END OPTION	
TITLE	ISOTROPIC	
	RADIATING	
	TEMPERATURE EFFECTS	

**Parameters, Options, and Subroutines Summary**

Example e5x15b.dat:

<b>Parameters</b>	<b>Model Definition Options</b>	<b>History Definition Options</b>
ALL POINTS	CONNECTIVITY	CONTINUE
ELEMENT	COORDINATE	CONTROL
END	END OPTION	STEADY STATE
HEAT	FIXED TEMPERATURE	TEMP CHANGE
RADIATION	ISOTROPIC	
SET NAME	NON PRINT	
SIZING	OPTIMIZE	
TITLE	POST	
	SOLVER	
	VIEW FACTOR	

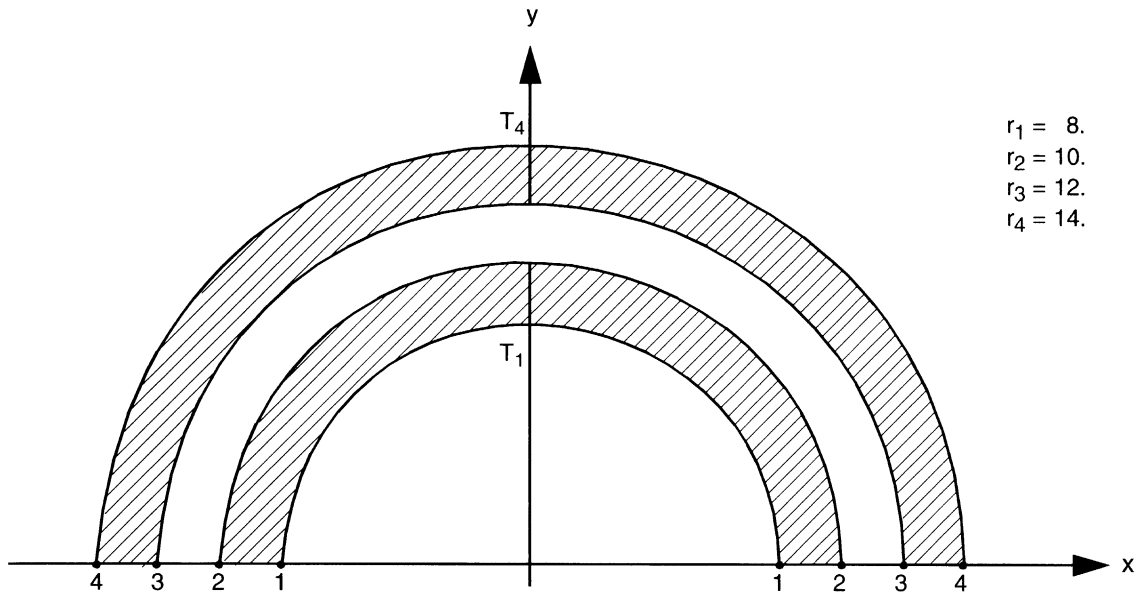


Figure 5.15-1 Radiating Concentric Spheres



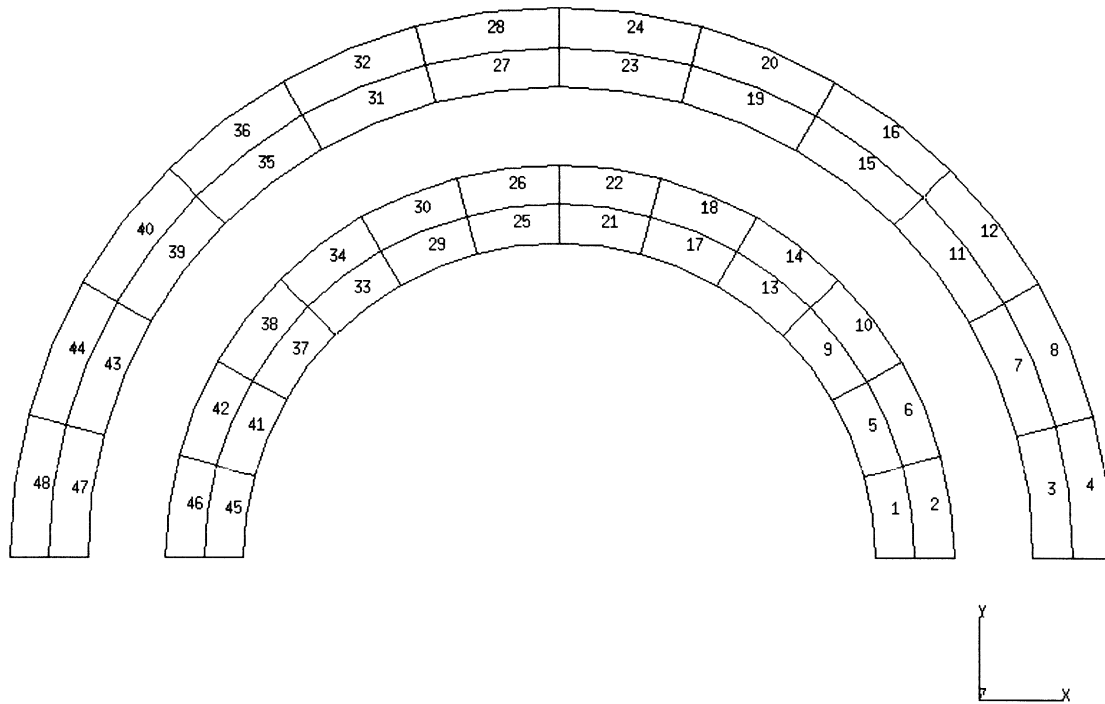
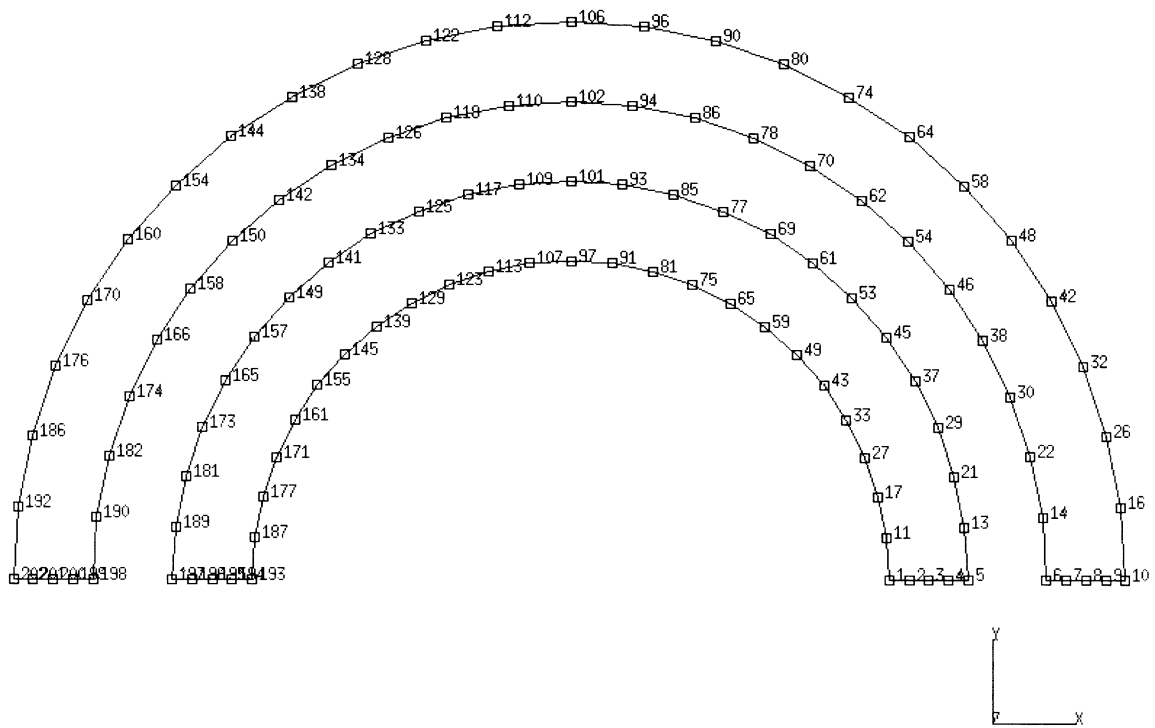


Figure 5.15-2 Mesh with Element Numbers



**Figure 5.15-3** Mesh with Node Numbers



## 5.16 Three-Dimensional Thermal Shock

The bar of a rectangular cross section is initially at rest. At time  $t = 0$ , one end of the bar is held at a fixed temperature of  $1000^{\circ}\text{F}$ , and a transient conduction problem is solved.

This problem is modeled using the three techniques summarized below.

Data Set	Element Type(s)	Number of Elements	Number of Nodes
e5x16a	123	16	45
e5x16b	133	43	120
e5x16c	135	43	27

### Element

Element types 44 and 133 are second-order isoparametric three-dimensional heat conduction elements. There are twenty nodes for brick element type 44 and 10 nodes for the tetrahedral element type 133. Element type 123 is an 8-node brick with reduced integration and hourglass control.

### Model

The bar cross section is square with a thickness of one inch and a length of two inches. This transient conduction problem is performed for three meshes comprised of element types 44, 123, and 133.

### Thermal Properties

The isotropic thermal conductivity value of  $0.42117\text{E-}5$  Btu/sec.-in.- $^{\circ}\text{F}$ . The specific heat is  $0.3523\text{E-}3$  Btu/lb $^{\circ}\text{F}$ . The mass density is  $0.7254\text{E-}3$  lb/cu.inch.

### Thermal Boundary Conditions

The initial temperature distribution is that all nodes have a temperature of  $0.0^{\circ}\text{F}$ . At time,  $t = 0$ , the nodal temperatures of one end of the bar are fixed at  $1000^{\circ}\text{F}$ , and a transient conduction problem is solved to its completion at steady state, where all nodes will have a final temperature of  $1000^{\circ}\text{F}$ .

### Control for Thermal Analysis

The maximum number of time points are fixed at 100. The maximum change in nodal temperature will be  $100^{\circ}\text{F}$ .

**Thermal History**

A transient thermal analysis is specified via the TRANSIENT option, with the automatic time stepping feature turned on. The initial time increment is 1.0E-2 seconds, with a final time period of 10 seconds.

**Results**

From the temperature history shown in Figure 5.16-1, Figure 5.16-2, and Figure 5.16-4 for element types 44, 123, and 133, respectively, the automatic time stepping feature shows ever increasing time steps as the solution approaches steady state. The temperature of the free end goes slightly negative by about a tenth of a degree for element types 123 and 133. This effect has been minimized by the inclusion of the LUMP parameter which instructs MARC to lump the capacitance matrix, instead of using the consistent capacitance matrix which is the default. There is virtually no difference in the thermal history of the free end between different element types. Figure 5.16-3, and Figure 5.16-5 are iso-thermal surfaces at a time when the free end starts to heat up significantly. These iso-thermal surfaces should be flat and perpendicular to the axis of the bar. The iso-thermal surfaces become flatter as the bar becomes hotter. Also, the iso-thermal surfaces are more irregular for the tetrahedron mesh than the brick mesh, because the brick element faces are either perpendicular or parallel to the head flow. This effect is minimized if more tetrahedron elements are used.

**Parameters, Options, and Subroutines Summary**

Example e5x16a.dat:

<b>Parameters</b>	<b>Model Definition Options</b>	<b>History Definition Options</b>
ELEMENT	CONNECTIVITY	CONTINUE
END	CONTROL	TRANSIENT
HEAT	COORDINATE	
LUMP	END OPTION	
SIZING	FIXED TEMP	
TITLE	INITIAL TEMP	
	ISOTROPIC	
	NO PRINT	
	POST	



Example e5x16b.dat:

**Parameters**

ALIAS  
ELEMENT  
END  
HEAT  
LUMP  
SIZING  
TITLE

**Model Definition Options**

CONNECTIVITY  
CONTROL  
COORDINATE  
END OPTION  
FIXED TEMP  
INITIAL TEMP  
ISOTROPIC  
POST

**History Definition Options**

CONTINUE  
TRANSIENT

Time	Temperature (°F)	Time	Temperature (°F)
0.0	0.0		
1.82307E-04	7.62101E-02	8.46059E-02	4.34587E+02
3.64615E-04	2.46594E-01	1.00722E-01	5.12089E+02
5.92499E-04	5.48778E-01	1.20868E-01	5.93519E+02
8.77355E-04	9.32763E-01	1.41014E-01	6.61590E+02
1.30464E-03	1.32789E+00	1.66196E-01	7.29694E+02
1.83874E-03	1.53547E+00	1.97673E-01	7.94479E+02
2.63990E-03	1.53524E+00	2.44890E-01	8.60475E+02
3.84163E-03	1.49460E+00	3.03910E-01	9.12322E+02
5.64423E-03	2.05263E+00	3.92441E-01	9.53537E+02
7.89748E-03	4.10911E+00	5.25236E-01	9.80063E+02
1.07140E-02	9.03647E+00	7.24430E-01	9.93345E+02
1.42348E-02	1.88757E+01	1.02322E+00	9.98334E+02
1.86356E-02	3.63171E+01	1.47141E+00	9.99697E+02
2.41367E-02	6.43750E+01	2.14369E+00	9.99961E+02
3.23884E-02	1.14785E+02	3.15211E+00	9.99996E+02
4.27029E-02	1.82812E+02	4.66473E+00	1.00000E+03
5.55962E-02	2.67022E+02	6.93368E+00	1.00000E+03
6.84894E-02	3.46206E+02	1.00003E+01	1.00000E+03

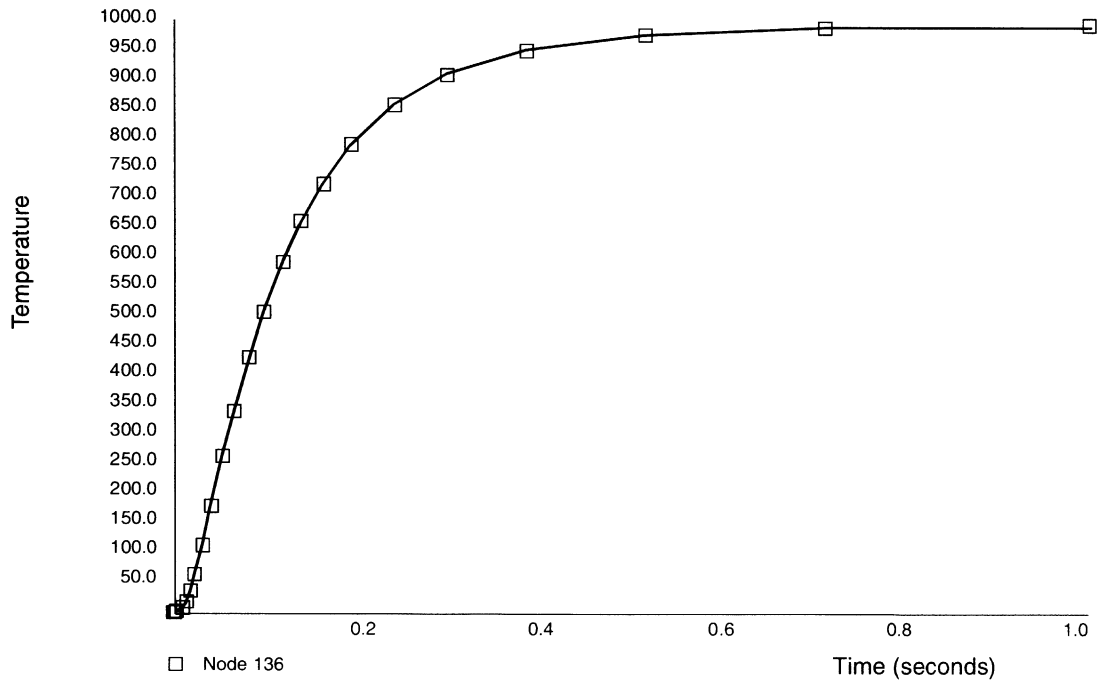


**Figure 5.16-1** Temperature History for Free End Node 136 Element Type 44

Time	Temperature (°F)	Time	Temperature (°F)
0.0	0.0		
1.99113E-04	-3.03712E-03	1.04521E-01	4.03045E+02
3.98226E-04	1.81682E-04	1.24798E-01	4.74083E+02
6.47118E-04	8.32631E-03	1.50145E-01	5.50460E+02
1.02045E-03	3.44541E-02	1.81829E-01	6.29444E+02
1.58046E-03	1.14610E-01	2.13513E-01	6.94672E+02
2.42047E-03	3.42895E-01	2.53118E-01	7.59006E+02
3.68048E-03	9.54424E-01	3.02624E-01	8.19336E+02
5.57050E-03	2.52048E+00	3.76883E-01	8.79604E+02
7.93302E-03	5.50497E+00	4.88272E-01	9.31265E+02
1.08862E-02	1.08245E+01	6.55355E-01	9.67696E+02
1.45776E-02	1.97886E+01	9.05980E-01	9.88009E+02
1.91919E-02	3.40969E+01	1.28192E+00	9.96615E+02
2.61134E-02	6.06809E+01	1.84582E+00	9.99298E+02
3.47652E-02	9.86775E+01	2.69168E+00	9.99896E+02
4.77429E-02	1.59734E+02	3.96047E+00	9.99989E+02
6.39651E-02	2.35397E+02	5.86365E+00	9.99999E+02
8.42428E-02	3.23410E+02	8.71842E+00	1.00000E+03
		1.00001E+01	1.00000E+03

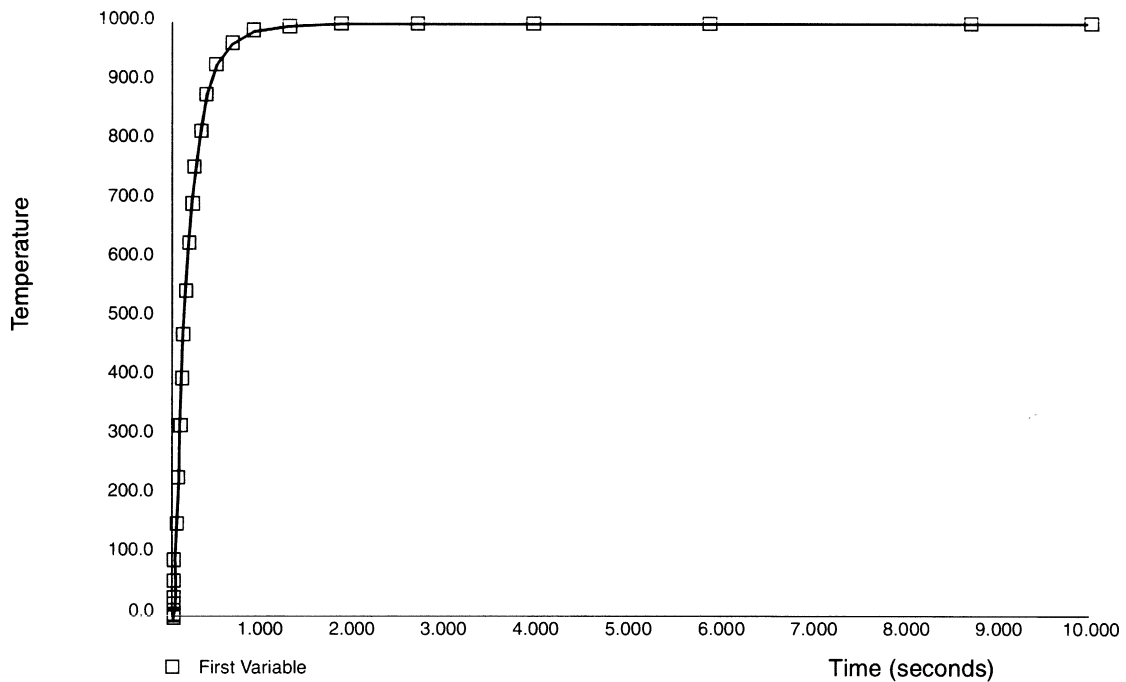


**Figure 5.16-2** Temperature History for Free End Node 126 (Element Type 123)

Inc : 7  
Time : 1.958e-02

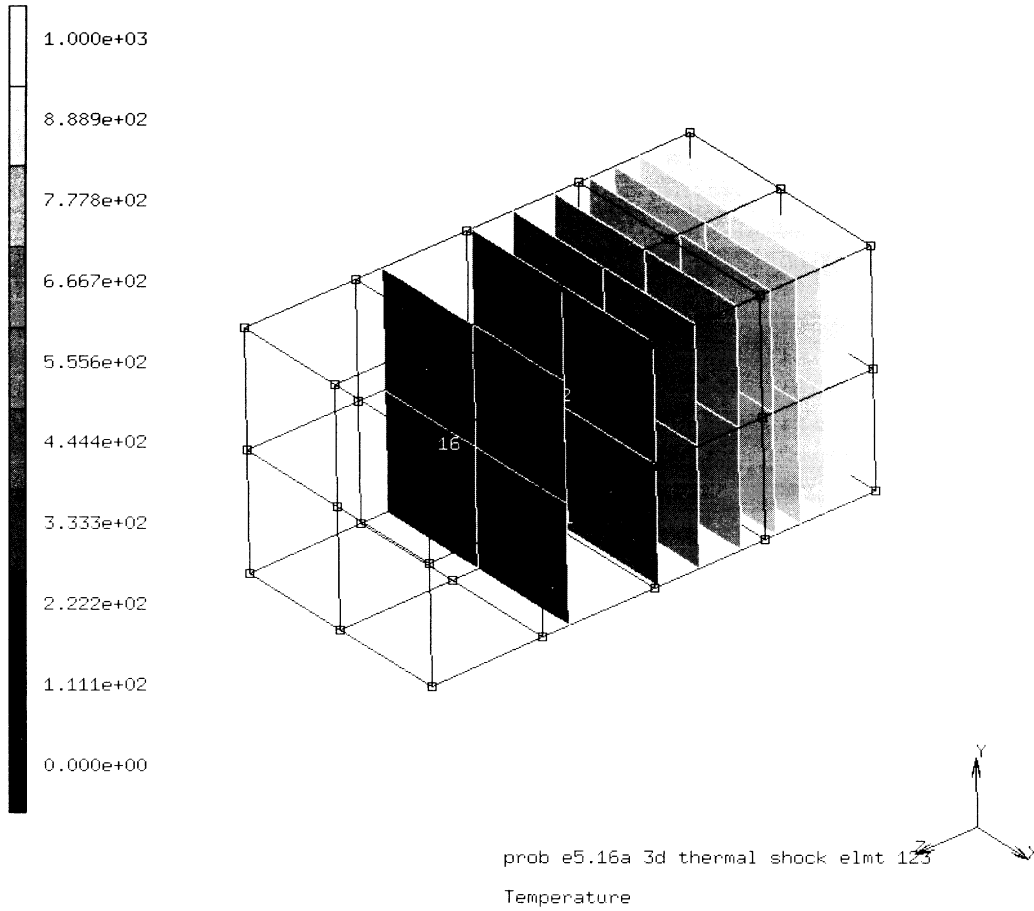


**Figure 5.16-3** Iso-thermal Surfaces at  $t = 0.0196$  seconds (Element Type 123)





Time	Temperature (°F)	Time	Temperature (°F)
0.0	0.0		
7.10402E-04	-1.63117E-01	1.14734E-01	5.64931E+02
1.42080E-03	-3.29948E-01	1.33342E-01	6.33486E+02
2.30881E-03	-4.95783E-01	1.56602E-01	7.03065E+02
3.64081E-03	-6.80945E-01	1.85677E-01	7.70386E+02
5.30582E-03	-7.92613E-01	2.22020E-01	8.31985E+02
7.38707E-03	-4.82283E-01	2.76536E-01	8.91606E+02
1.05090E-02	2.03853E+00	3.58309E-01	9.40608E+02
1.44113E-02	9.60317E+00	4.80968E-01	9.73458E+02
1.92893E-02	2.61956E+01	6.64957E-01	9.90708E+02
2.53867E-02	5.59788E+01	9.40940E-01	9.97545E+02
3.30085E-02	1.02089E+02	1.35492E+00	9.99526E+02
4.25357E-02	1.65698E+02	1.97588E+00	9.99935E+02
5.44447E-02	2.45701E+02	2.90732E+00	9.99994E+02
6.63538E-02	3.21802E+02	4.30449E+00	1.00000E+03
8.12401E-02	4.07738E+02	6.40024E+00	1.00000E+03
9.61264E-02	4.83906E+02	9.54387E+00	1.00000E+03
		1.0000E+01	1.00000E+03

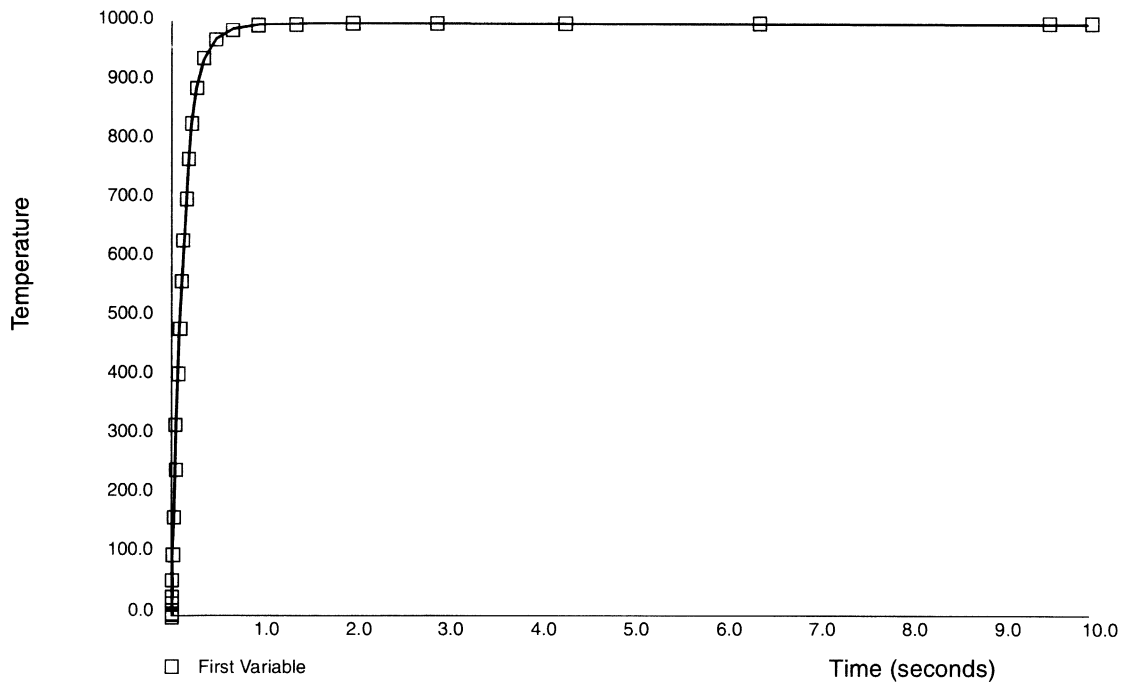
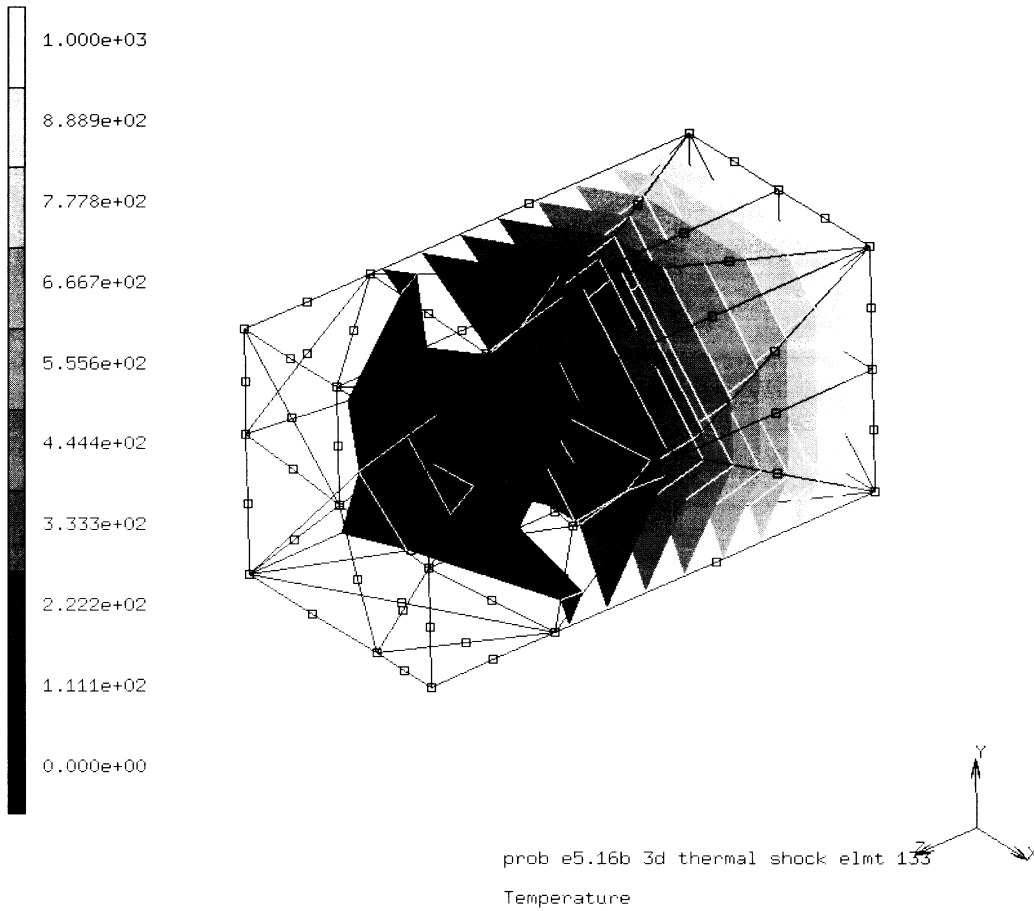


Figure 5.16-4 Temperature History for Free End Node 26 (Element Type 133)

Inc : 9  
Time : 1.929e-02



**Figure 5.16-5** Iso-thermal Surfaces at  $t = 0.0193$  seconds (Element Type 133)



## 5.17 Cooling of Electronic Chips

This problem demonstrates the air cooling of an electronic chip at room temperature. The comparison of the no-inclusion of heat convection, e5x17a.dat, and the inclusion of the contribution of heat convection, e5x17b.dat, by air is made. The nonsymmetric solver is turned on automatically when heat convection is included.

This problem is modeled using the two techniques summarized below.

Data Set	Element Type(s)	Number of Elements	Number of Nodes	Differentiating Features
e5x17a	39	360	399	Exclude convection
e5x17b	39	360	399	Include convection

### Element

Element type 39 is used for both the air region and the chip body. The model is shown in Figure 5.17-1 and Figure 5.17-3.

### Material properties

Room temperature thermal properties for air are used. The specific heat is  $5.8e-5$  kJ/kg. $^{\circ}$ C, the density is  $0.241$  kg/m $^3$ , and thermal conductivity is  $0.129e-2$  W/m. $^{\circ}$ C. Thermal properties for pure copper are used for the chip. The specific heat is  $0.93$  kJ/kg. $^{\circ}$ C, the density is  $0.0914$  kg/m $^3$ , and thermal conductivity is  $8.94$  W/m. $^{\circ}$ C. Assume the variation of properties with temperature is negligible.

### Initial Conditions

The initial nodal temperature for chips is  $40^{\circ}$ C and for air is  $10^{\circ}$ C throughout.

### Boundary Conditions

The temperature of the air far away from chips is fixed at  $10^{\circ}$ C and velocity of the air is kept at a constant  $100$  cm/second. The velocity of the chips is zero.

### Transient Nonauto

A fixed, large time step is used to simulate the cooling process near steady-state condition.

### Results

The temperature distributions shown in Figure 5.17-4 and Figure 5.17-2 indicate the effect of heat convection on the cooling of the chips. The chips have cooled down faster on the left side because, as heat convection of the air is included, more heat is carried away by the air. The



effect of the boundary layer between the air and the surface of the chips is neglected. Because the Courant number is too large, which indicates the time step is also too large, numerical dispersion occurs at the air region far away from the chips.

**Parameters, Options, and Subroutines Summary**

Example e5x17a.dat:

<b>Parameters</b>	<b>Model Definition Options</b>	<b>History Definition Options</b>
ALL POINTS	CONNECTIVITY	CONTINUE
COMMENT	CONTROL	TRANSIENT
DIST LOADS	COORDINATE	
END	DEFINE	
HEAT	END OPTION	
PRINT	FIXED TEMP	
SETNAME	INITIAL TEMP	
SIZING	ISOTROPIC	
TITLE	NO PRINT	
	POST	
	VELOCITY	

Example e5x17b.dat:

<b>Parameters</b>	<b>Model Definition Options</b>	<b>History Definition Options</b>
ALL POINTS	CONNECTIVITY	CONTINUE
COMMENT	CONTROL	
DIST LOADS	COORDINATE	
END	DEFINE	TRANSIENT
HEAT	END OPTION	
PRINT	FIXED TEMP	
SETNAME	INITIAL TEMP	
SIZING	ISOTROPIC	
TITLE	NO PRINT	
	POST	
	VELOCITY	

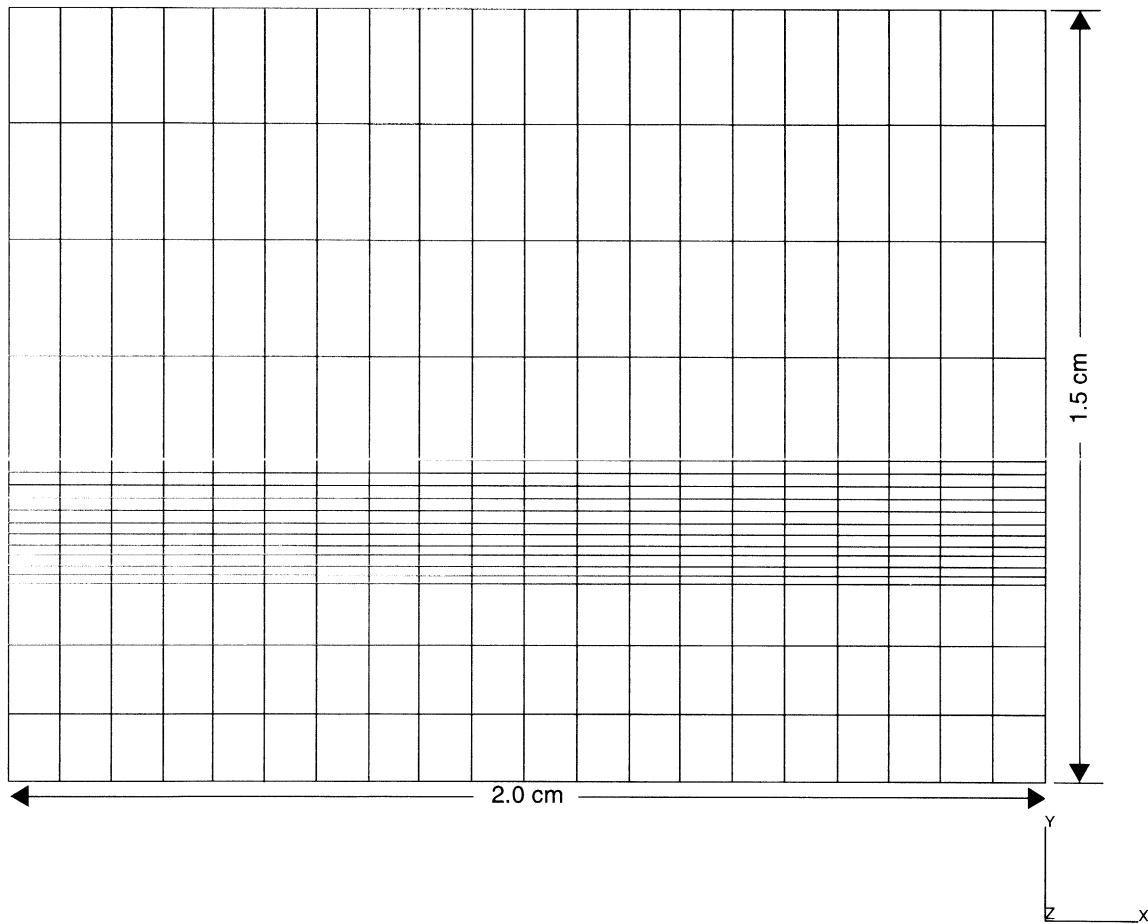


**Figure 5.17-1** Complete Finite Element Mesh

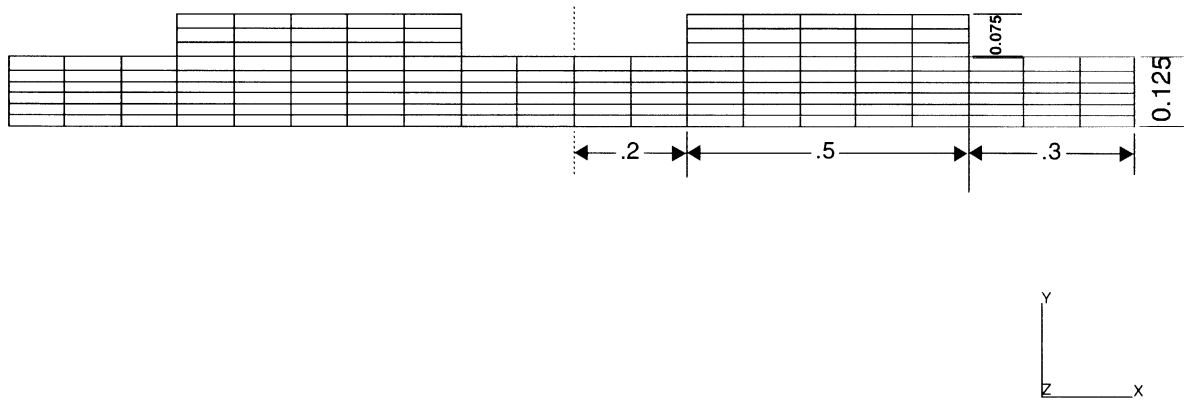
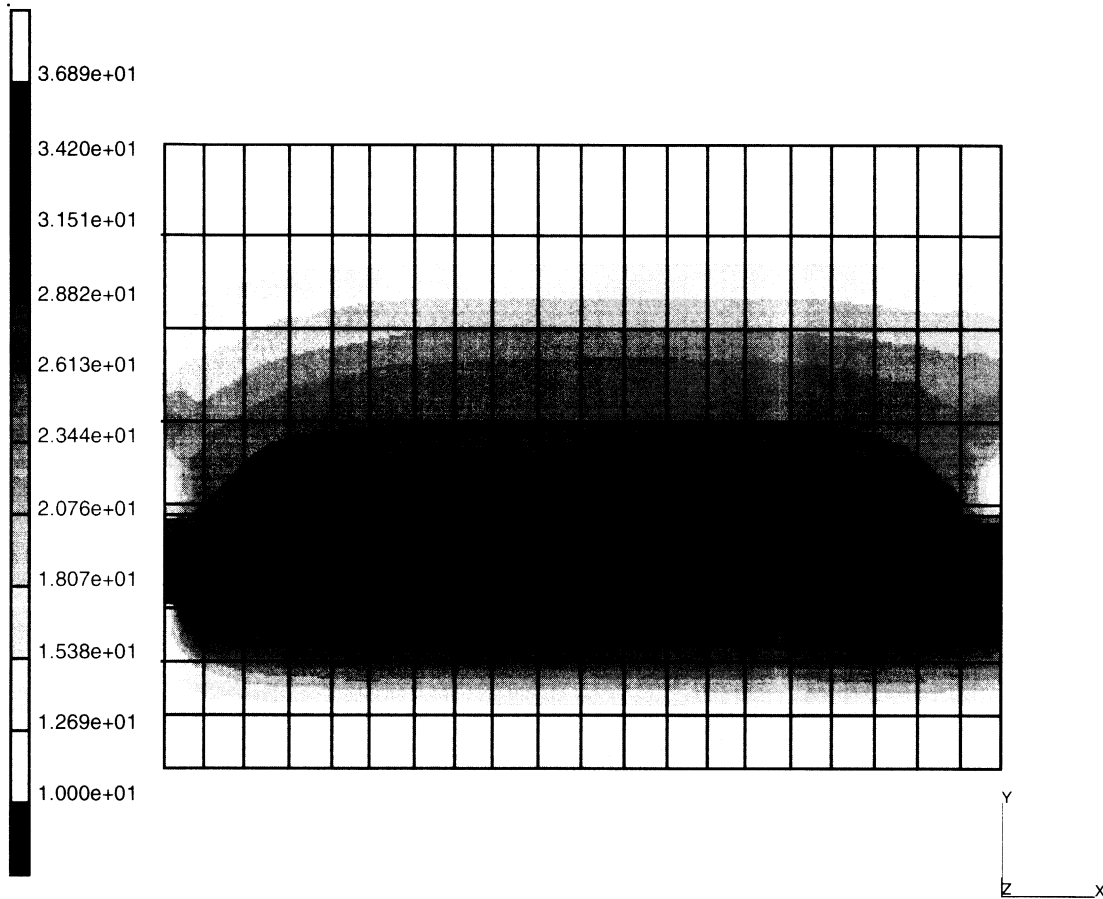


**Figure 5.17-2** Finite Element Mesh of Chips and Board

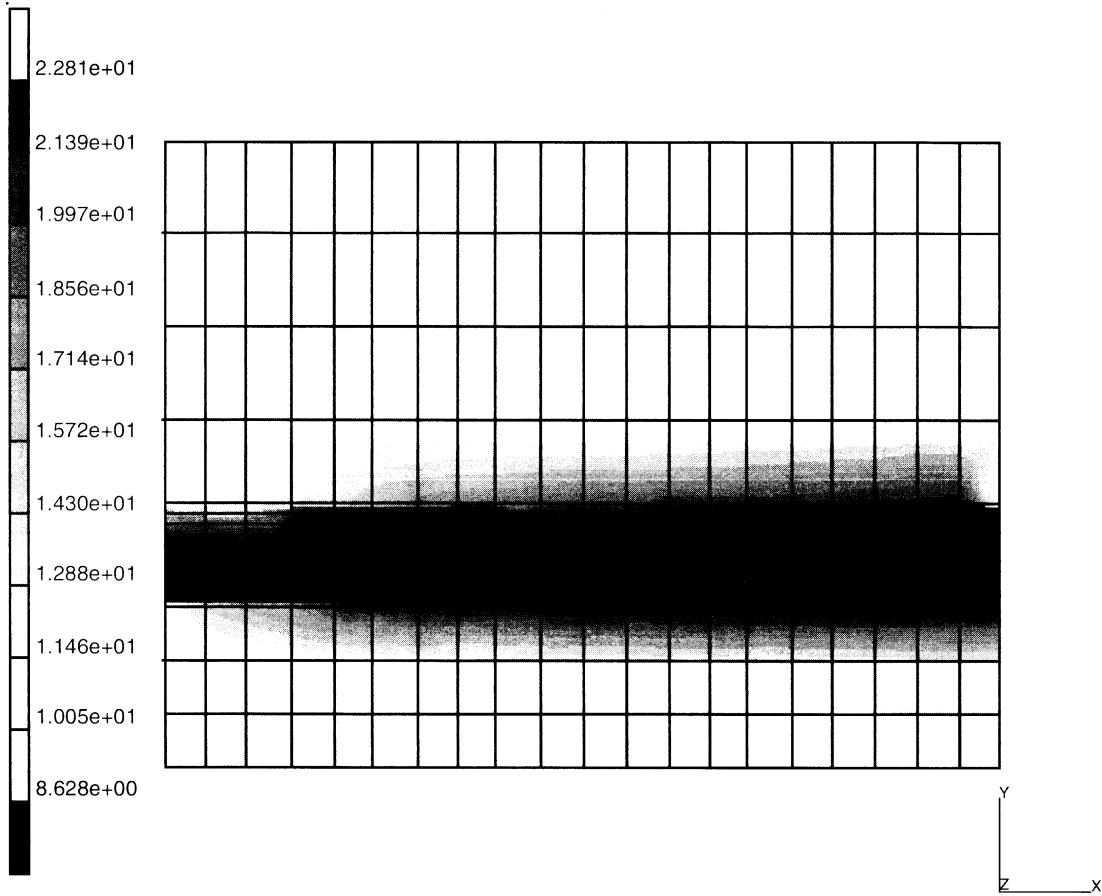
INC : 50  
SUB : 0  
TIME : 5.000e+01  
FREQ : 0.000e+00



prob e5.17a cooling of chips: heat convection  
Temperature

**Figure 5.17-3** Temperature Distribution Excluding Heat Convection

INC : 50  
SUB : 0  
TIME : 5.000e+01  
FREQ : 0.000e+00



prob e5.17b cooling of chips: heat convection  
Temperature

**Figure 5.17-4** Temperature Distribution Including Heat Convection



## 5.18 Square Plate Heated at a Center Portion

A square plate with an initial temperature of 20°C is heated at the upper side of a square center portion (see Figure 5.18-1). The temperature at the outer edges is kept constant.

This problem is modeled using the two techniques summarized below.

Data Set	Element Type(s)	Number of Elements	Number of Nodes	Differentiating Features
e5x18a	50	128	81	STEADY STATE
e5x18b	50	128	81	TRANSIENT

### Element

Library element type 50 is a 3-node triangular heat transfer shell element.

### Model

The dimensions of the plate and the finite element mesh are shown in Figure 5.18-1. Based on symmetry considerations, only one quarter of the plate is modeled. The mesh is composed of 128 elements and 81 nodes.

### Material Properties

The material is orthotropic with the following material constants:

Conductivity:  $\lambda_{11} = 50 \text{ W/m}^\circ\text{C}$ ,  $\lambda_{22} = 5000 \text{ W/m}^\circ\text{C}$ ,  $\lambda_{33} = 500 \text{ W/m}^\circ\text{C}$

Density:  $\rho = 7000 \text{ kg/m}^3$

Specific Heat:  $c = 450 \text{ J/kg}^\circ\text{C}$

Since, by default, the properties are applied with respect to element directions, the orientation option is used to specify an offset of 0 to the zx-plane (see Figure 5.18-1).

### Geometry

A uniform thickness of 0.5 m is assumed. In thickness direction, a parabolic temperature distribution is selected using the HEAT parameter. The number of layers is set equal to 3 using the SHELL SECT parameter.

### Loading

The loading consists of a distributed flux of 800 W/m<sup>2</sup> on the upper side of a square center portion. Two analyses are carried out. The first one (a) is a steady-state analysis; the second one (b) is a transient analysis.

**Boundary Conditions**

Symmetry conditions are imposed on the edges  $x = 0$  and  $y = 0$ . Fixed temperatures are applied on the outer edges. Notice that this involves three degrees of freedom since, in thickness direction, a parabolic temperature distribution has been chosen.

**Results**

The steady-state temperature distribution of the top layer is shown in Figure 5.18-2. Due to the orthotropic material properties, the temperature distribution is nonsymmetric with respect to a diagonal of the plate. As a result of the transient analysis, the temperature distribution of the top and bottom layer along the line  $x = 0$  are shown in Figure 5.18-3 and Figure 5.18-4, where Figure 5.18-3 refers to increment 1 and Figure 5.18-4 refers to increment 15. The situation of increment 15 corresponds to the steady-state solution.

**Parameters, Options, and Subroutines Summary**

Example e5x18a.dat:

<b>Parameters</b>	<b>Model Definition Options</b>	<b>History Definition Options</b>
ALL POINTS	CONNECTIVITY	ACTIVATE
DIST LOADS	COORDINATE	CONTINUE
ELEMENTS	DEFINE	CONTROL
END	DIST FLUXES	DIST FLUXES
HEAT	END OPTION	STEADY STATE
LUMP	FIXED TEMP	TEMP CHANGE
SETNAME	GEOMETRY	
SHELL SECT	INITIAL TEMP	
SIZING	NO PRINT	
TITLE	OPTIMIZE	
	ORIENTATION	
	ORTHOTROPIC	
	POST	
	SOLVER	



Example e5x18b.dat:

**Parameters**

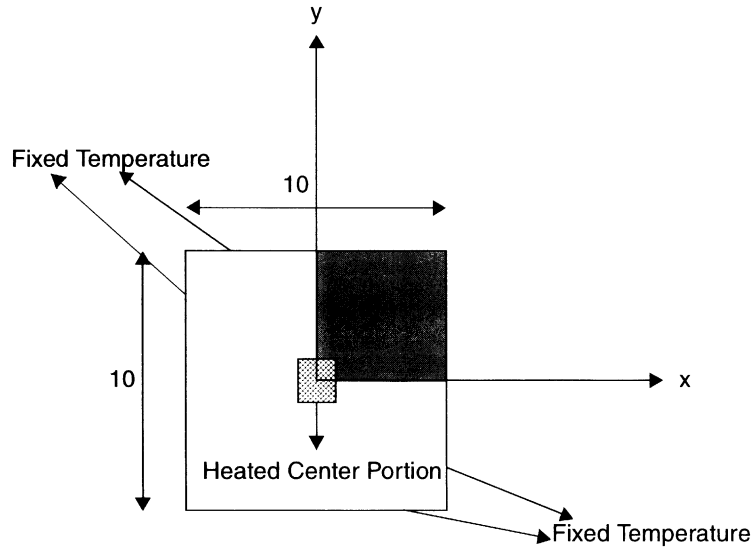
ALL POINTS  
DIST LOADS  
ELEMENTS  
END  
HEAT  
LUMP  
SETNAME  
SHELL SECT  
SIZING  
TITLE

**Model Definition Options**

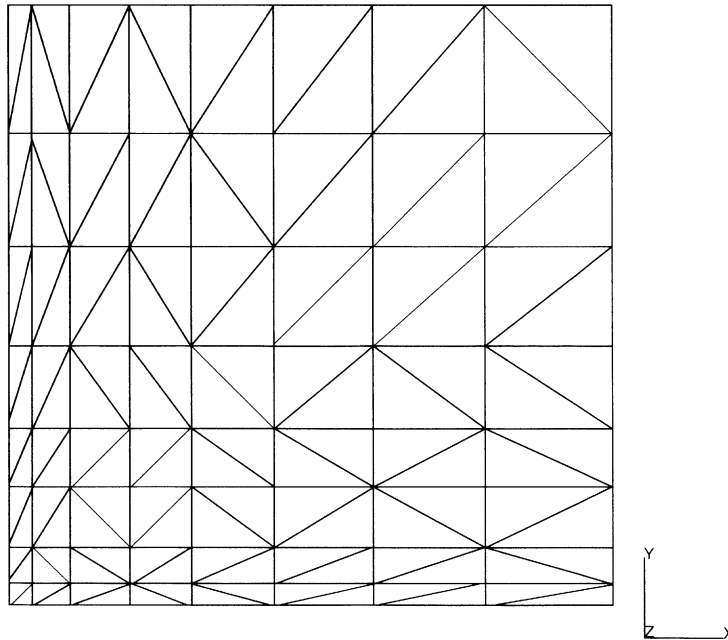
CONNECTIVITY  
COORDINATE  
DEFINE  
DIST FLUXES  
END OPTION  
FIXED TEMP  
GEOMETRY  
INITIAL TEMP  
NO PRINT  
OPTIMIZE  
ORIENTATION  
ORTHOTROPIC  
POST  
SOLVER

**History Definition Options**

ACTIVATE  
CONTINUE  
CONTROL  
DIST FLUXES  
STEADY STATE  
TEMP CHANGE



INC : 1  
 SUB : 0  
 TIME : 0.000e+00  
 FREQ : 0.000e+00

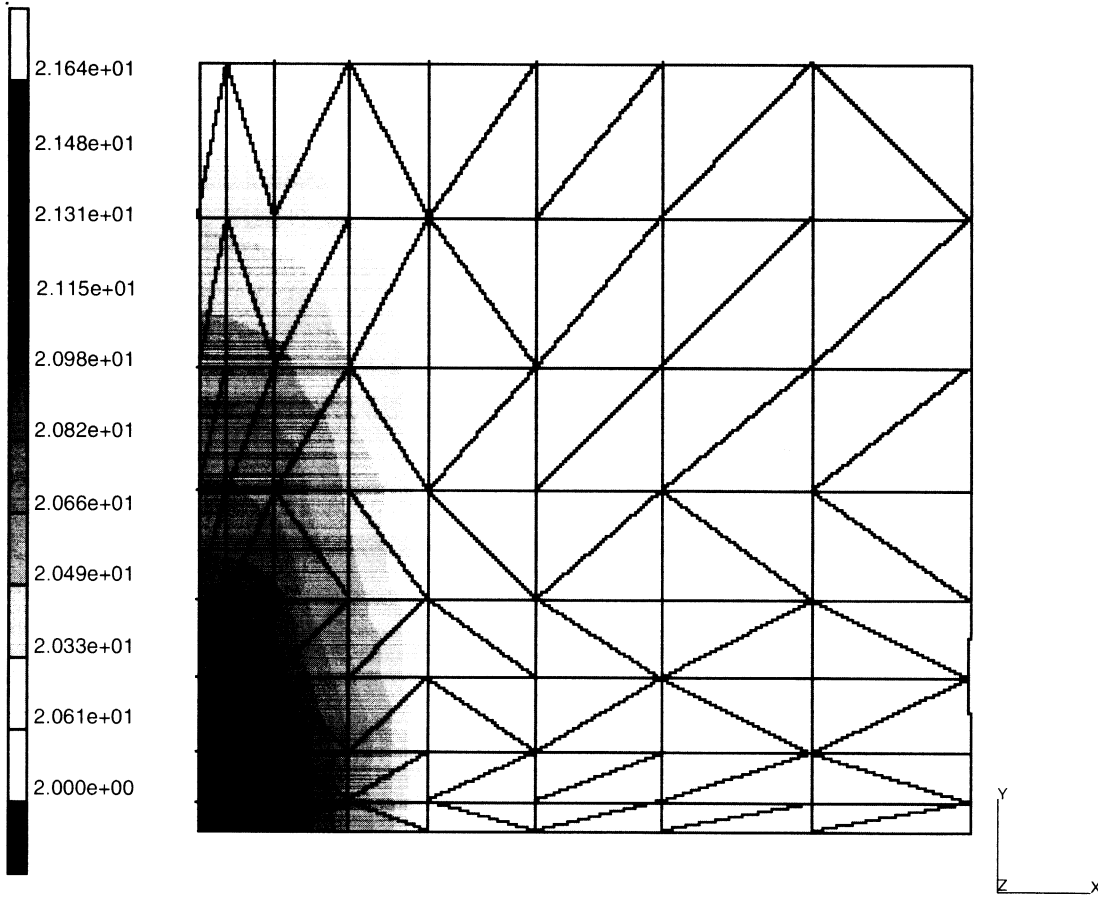


steady state analysis; orthotropic material

**Figure 5.18-1** Heated Square Plate, Geometry, and Finite Element Mesh



INC : 1  
SUB : 0  
TIME : 0.000e+01  
FREQ : 0.000e+00



steady state analysis: orthotropic material  
Temperature t

Figure 5.18-2 Temperature Distribution Steady-state Analysis

INC : 1  
 SUB : 0  
 TIME : 5.000e+02  
 FREQ : 0.000e+00

square\_plate\_transient\_elmt\_50



Y (x10)

2.165

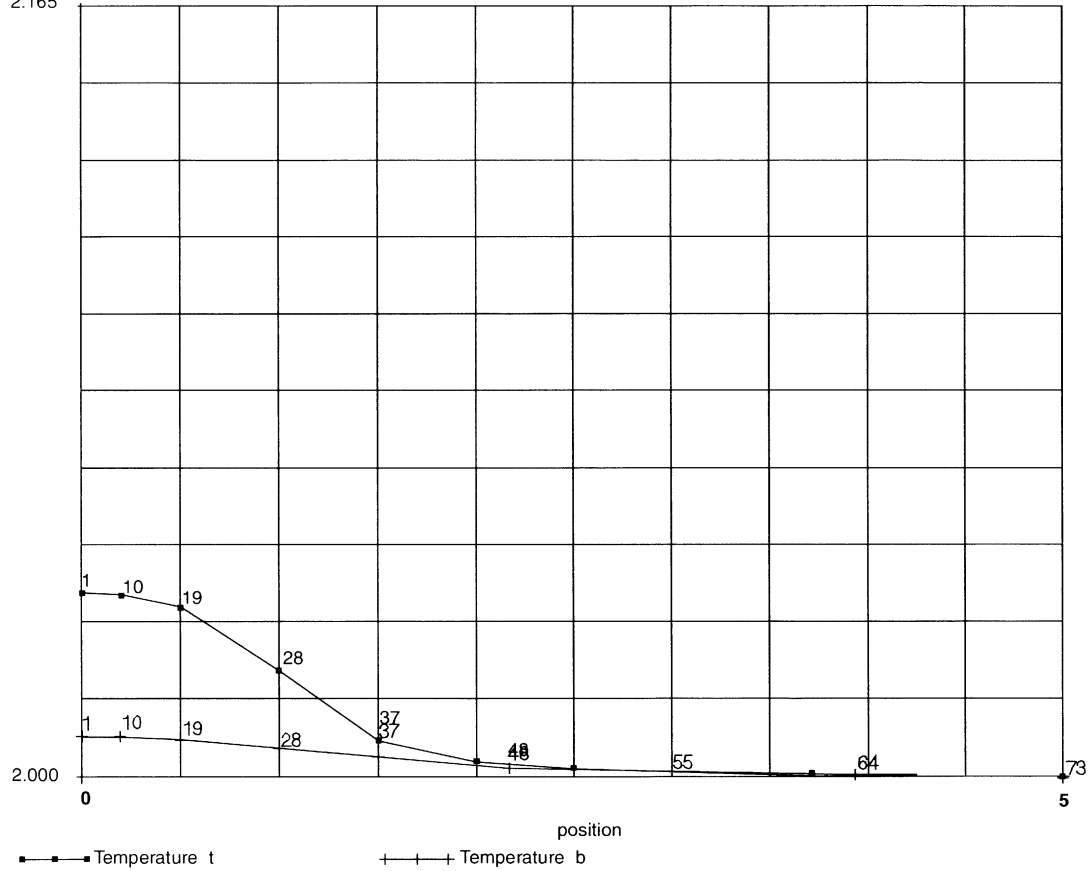


**Figure 5.18-3** Path Plots for Upper and Lower Temperature at x = 0 (inc = 1)

INC : 15  
 SUB : 0  
 TIME : 4.369e+05  
 FREQ : 0.000e+00

square\_plate\_transient\_elmt\_50

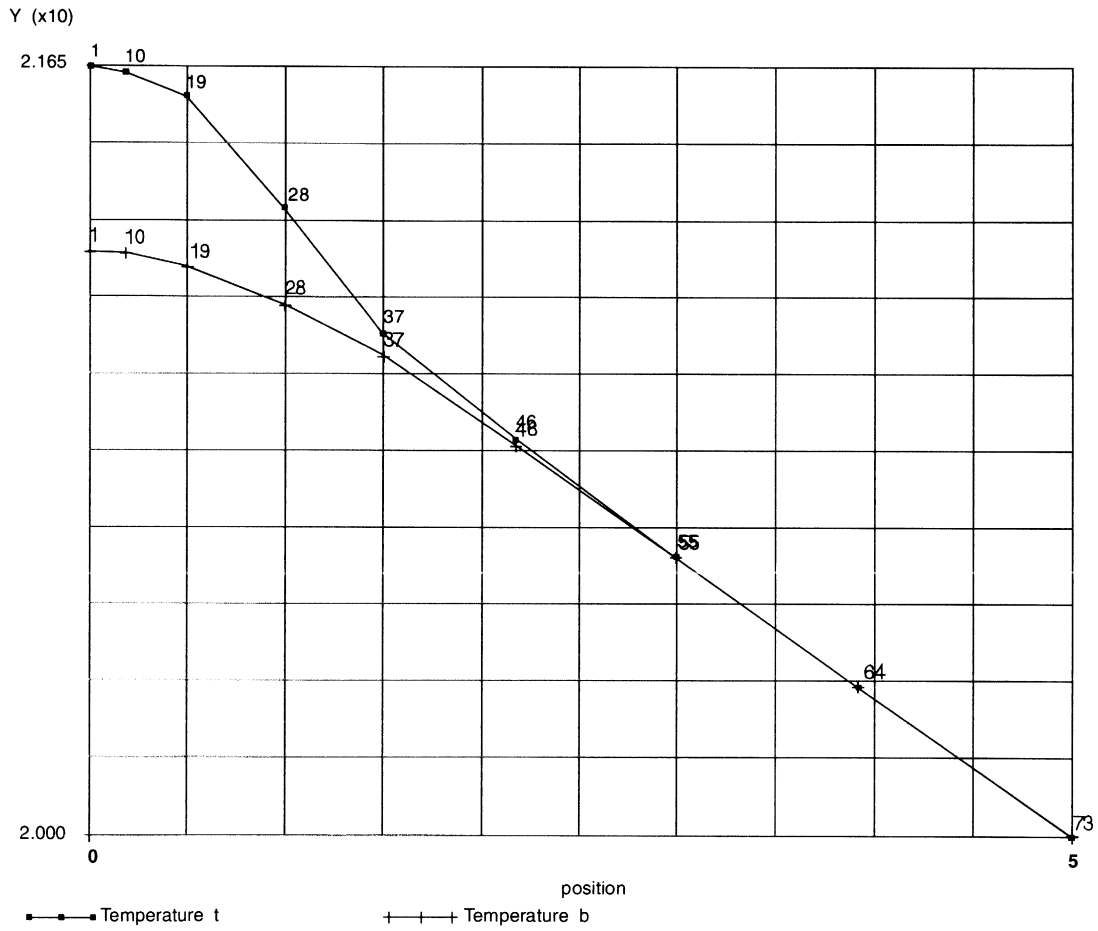


**Figure 5.18-4** Path Plots for Upper and Lower Temperature at x = 0 (inc = 15)

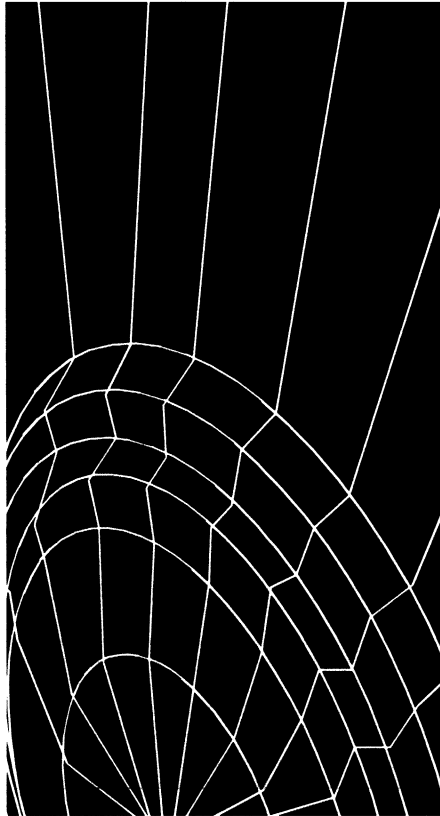


**5** *Heat Transfer*

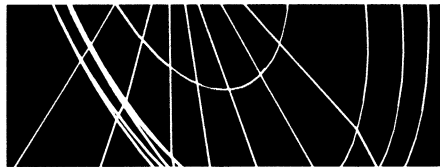
*Square Plate Heated at a Center Portion*

---





**MARC**



**Volume E**

**Demonstration Problems**

Version K7

**Chapter 6**  
**Dynamics**



---

 **6**

## *Dynamics Contents*



<b>Description</b>	<b>Problem</b>
Dynamic Analysis of a Beam with Small Displacement Response . . . . .	6.1
Beam Modes and Frequencies . . . . .	6.2
Dynamic Analysis of a Plate with the Modal Procedure . . . . .	6.3
Frequencies of a Rotating Disk . . . . .	6.4
Frequencies of Fluid-solid Coupled System. . . . .	6.5
Spectrum Response of a Space Frame. . . . .	6.6
Harmonic Analysis of a Capped Mount . . . . .	6.7
Harmonic Response of a Rubber Block . . . . .	6.8
Elastic Impact of a Bar. . . . .	6.9
Frequencies of an Alternator Mount. . . . .	6.10
Modal Analysis of a Wing Caisson . . . . .	6.11
Vibrations of a Cable . . . . .	6.12
Perfectly Plastic Beam Explosively Loaded. . . . .	6.13
Dynamic Fracture Mechanics . . . . .	6.14
Eigenmodes of a Plate . . . . .	6.15
Dynamic Contact Between a Projectile and a Rigid Barrier. . . . .	6.16
Dynamic Contact Between Two Deformable Bodies . . . . .	6.17
Spectral Response of a Pipe . . . . .	6.18
Dynamic Impact of Two Bars . . . . .	6.19
Elastic Beam Subjected to Fluid-Drag Loading . . . . .	6.20
Eigenvalue Analysis of a Box . . . . .	6.21



## **6** *Dynamics Contents*

---

---



## *Dynamics List of Figures*



<b>Figure</b>	<b>Page</b>
6.1-1 Element Type 5 Beam-Column Model . . . . .	6.1-5
6.1-2 Ramp Pressure Forcing Function . . . . .	6.1-6
6.1-3 Time Step = .001 Second . . . . .	6.1-7
6.1-4 Time Step = .00025 Second . . . . .	6.1-8
6.1-5 Timoshenko Beam, Time Step = .001 Second . . . . .	6.1-9
6.2-1 Timoshenko Beam . . . . .	6.2-3
6.2-2 Calculated Mode Shapes and Frequencies for a Timoshenko Cantilever Beam . . . . .	6.2-3
6.3-1 Element 4 Plate Model . . . . .	6.3-5
6.3-2 Element 8 Plate Model . . . . .	6.3-6
6.3-3 Applied Pressure History . . . . .	6.3-7
6.3-4 Displacements at Tip . . . . .	6.3-7
6.4-1 Disk and Mesh . . . . .	6.4-3
6.5-1 Dam/Water System and Mesh . . . . .	6.5-4
6.6-1 Three-Dimensional Frame and Model . . . . .	6.6-5
6.6-2 Spectral Density Function. . . . .	6.6-6
6.6-3 Three-Dimensional Frame – Mode 1 (Extensional). . . . .	6.6-7
6.6-4 Three-Dimensional Frame – Mode 2 (Bending). . . . .	6.6-8
6.6-5 Three-Dimensional Frame – Mode 3 (Torsional). . . . .	6.6-9
6.7-1 Capped Rubber Mount . . . . .	6.7-4
6.7-2 Displaced Mesh, Increment 1 . . . . .	6.7-5
6.7-3 von Mises Stress Distribution, Increment 1 . . . . .	6.7-6
6.7-4 Real Radial Stress 0.05 Cycle/Second . . . . .	6.7-7
6.7-5 Imaginary Radial Stress 0.05 Cycle/Second. . . . .	6.7-8
6.7-6 Real Radial Stress 0.5 Cycle/Second . . . . .	6.7-9
6.7-7 Imaginary Radial Stress 0.5 Cycle/Second. . . . .	6.7-10



<b>Figure</b>	<b>Page</b>
6.8-1 Tensile Harmonic Analysis Mesh. . . . .	6.8-3
6.9-1 Mesh of the Bar. . . . .	6.9-3
6.9-2 Time History of Displacements . . . . .	6.9-4
6.9-3 Time History of Velocity . . . . .	6.9-5
6.9-4 Time History of the Reaction . . . . .	6.9-6
6.10-1 Alternator Mount Model. . . . .	6.10-5
6.10-2 First Mode. . . . .	6.10-6
6.10-3 Second Mode . . . . .	6.10-7
6.10-4 Third Mode . . . . .	6.10-8
6.11-1 Mesh of a Wing Structure. . . . .	6.11-3
6.13-1 Mesh with Initial Velocity . . . . .	6.13-3
6.13-2 Small Displacement Analysis. . . . .	6.13-4
6.13-3 Small Displacement Analysis. . . . .	6.13-5
6.13-4 Small Displacement Analysis. . . . .	6.13-6
6.13-5 Includes Geometric Nonlinearity . . . . .	6.13-7
6.13-6 Includes Geometric Nonlinearity . . . . .	6.13-8
6.13-7 Includes Geometric Nonlinearity . . . . .	6.13-9
6.14-1 Dynamically Loaded Center-Cracked Rectangular Plate Problem. . . . .	6.14-4
6.14-2 Dynamic Crack Problem Mesh. . . . .	6.14-5
6.14-3 Crack Tip Region . . . . .	6.14-6
6.14-4 Normalized Dynamic Stress Intensity Factors . . . . .	6.14-7
6.15-1 Mesh . . . . .	6.15-3
6.15-2 First Mode Shape of Cantilevered Plate . . . . .	6.15-4
6.15-3 Third Mode Shape of Cantilevered Plate . . . . .	6.15-5
6.16-1 Impactor and Rigid Wall. . . . .	6.16-5
6.16-2 Impactor Geometry . . . . .	6.16-6
6.16-3 Deformation at Initial Contact . . . . .	6.16-7
6.16-4 Final Deformation. . . . .	6.16-8
6.16-5 (A) Displacement History (Newmark-Beta Method) . . . . .	6.16-9
6.16-5 (B) Displacement History (Central Difference Method) . . . . .	6.16-10



<b>Figure</b>	<b>Page</b>
6.16-6 (A) Velocity History (Newmark-Beta Method) . . . . .	6.16-11
6.16-6 (B) Velocity History (Central Difference Method) . . . . .	6.16-12
6.16-7 (A) Reaction/Impact Force History (Newmark-Beta Method). . . . .	6.16-13
6.16-7 (B) Reaction/Impact Force History (Central Difference Method) . . . . .	6.16-14
6.17-1 Impactor and Deformable Barrier. . . . .	6.17-4
6.17-2 Geometries . . . . .	6.17-5
6.17-3 Final Deformation. . . . .	6.17-6
6.17-4 (A) Displacement Histories (Newmark-beta Method) . . . . .	6.17-7
6.17-4 (B) Displacement History (Central Difference Method) . . . . .	6.17-8
6.17-5 (A) Velocity History (Newmark-beta Method) . . . . .	6.17-9
6.17-5 (B) Velocity History (Central Difference Method) . . . . .	6.17-10
6.18-1 Cantilever Pipe and its Cross Section. . . . .	6.18-3
6.19-1 Finite Element Mesh of Two Bars . . . . .	6.19-3
6.19-2 Displacement History of Selected Nodes . . . . .	6.19-4
6.19-3 Velocity History of Selected Nodes . . . . .	6.19-5
6.19-4 Acceleration History of Selected Node . . . . .	6.19-6
6.19-5 Reaction Force at Wall . . . . .	6.19-7
6.20-1 Beam Partially Submerged in Fluid . . . . .	6.20-4
6.21-1 Mesh of Box . . . . .	6.21-3
6.21-2 Seventh Eigenmode . . . . .	6.21-4
6.21-3 Ninth Eigenmode . . . . .	6.21-5



## **6** *Dynamics List of Figures*

---



---

 **6**

## *Dynamics List of Tables*



<b>Table</b>	<b>Page</b>
6.1 Dynamic Analysis Demonstration Problems . . . . .	6-2
6.2-1 Beam Frequencies (cps) . . . . .	6.2-2
6.3-1 Comparison of Frequencies in Cycles/Seconds . . . . .	6.3-3
6.4-1 Frequencies of the Disk (cps) . . . . .	6.4-2
6.5-1 Natural Frequencies of Dam/Water System ( $f = \text{cps}$ ) . . . . .	6.5-2
6.6-1 Eigenvalues (cps). . . . .	6.6-2
6.6-2 Spectrum Response at Node 2 . . . . .	6.6-3
6.8-1 Summary of Results: Real and Imaginary Displacements of Node 19 . . . . .	6.8-2
6.10-1 Geometric Properties of Beams Sections. . . . .	6.10-2
6.14-1 Normalized Dynamic Stress Intensity Factors . . . . .	6.14-2
6.15-1 Frequencies in Hertz . . . . .	6.15-2
6.18-1 Spectral Accelerations [m/sec <sup>2</sup> ] . . . . .	6.18-1
6.18-2 Displacements [m] in x and y Direction . . . . .	6.18-2
6.18-3 Eigenvalues [Hz] . . . . .	6.18-2
6.20-1 Displacements of the Beam (m) . . . . .	6.20-2



---

 **6**

## *Dynamics*



MARC K.7 contains both the modal superposition and direct integration capabilities for the analysis of dynamic problems. A discussion on the use of these capabilities can be found in *MARC Volume A: Theory and User Information* and a summary of the feature is given below.

Modal Analysis (inverse power sweep or Lanczos)

Direct Integration

- Newmark-beta operator
- Houbolt operator
- Central difference operator
- Modal superposition

Consistent and lumped mass matrices

Damping

- Modal damping
- Stiffness and/or mass damping
- Numerical damping

Initial conditions

- Nodal displacement
- Nodal velocity

Boundary conditions

- Nodal displacement history
- Nodal velocity history
- Nodal acceleration history

Nonlinear effects

- Material nonlinearity (plasticity)
- Geometric nonlinearity (large displacement)
- Boundary nonlinearity (gap-friction)

Variable time steps

- Newmark-beta operator

Compiled in this chapter are a number of solved problems. These problems illustrate the use of dynamic analysis options in MARC. Table 6.1 shows the MARC elements and options used in these demonstration problems.

**Table 6.1** Dynamic Analysis Demonstration Problems

Problem Number	Element Type	Parameters	Model Definition	History Definition	User Subroutines	Problem Description
6.1	5 45	DYNAMIC	CONTROL PRINT CHOICE	DYNAMIC CHANGE DIST LOADS	—	Dynamic response of a simply supported beam subjected to a uniformly distributed load.
6.2	45	DYNAMIC	—	MODAL SHAPE RECOVER	—	Frequencies and modal shapes of a Timoshenko beam.
6.3	4 8	DYNAMIC	CONTROL UFXORD FXORD INITIAL CONDITIONS	MODAL SHAPE DYNAMIC CHANGE DIST LOADS	UFXORD	Dynamic analysis of a cantilever plate using the modal procedure. Both inverse power sweep and Lanczos method.
6.4	10	DYNAMIC LARGE DISP FOLLOW FOR	ROTATION A CONTROL	MODAL SHAPE DIST LOADS	—	Frequencies of a rotating disk (centrifugal loading effect).
6.5	27 41	DYNAMIC FLU LOAD	FLUID SOLID	MODAL SHAPE	—	Frequencies of fluid-solid coupled (dam/water) system.
6.6	9	LARGE DISP DYNAMIC RESPONSE	RESPONSE SPECTRUM	MODAL SHAPE SPECTRUM	—	Evaluate eigenvalues for a space frame and perform spectrum response calculation.
6.7	28 33	LARGE DISP HARMONIC	TYING PHI-COEFI MOONEY	HARMONIC DISP CHANGE	—	Evaluate the response of a rubber mount subjected to several frequencies.
6.8	35	LARGE DISP HARMONIC	PHI-COEFI MOONEY	HARMONIC DISP CHANGE	—	Evaluate the response of a rubber block subjected to several frequencies at different amounts of deformation.
6.9	9	PRINT DAMPING LUMP DYNAMIC	POST INITIAL VEL DAMPING MASSES GAP DATA	DYNAMIC CHANGE	—	Elastic impact of a bar.

**Table 6.1** Dynamic Analysis Demonstration Problems (Continued)

Problem Number	Element Type	Parameters	Model Definition	History Definition	User Subroutines	Problem Description
6.10	52	DYNAMIC	POST TYING MASSES	MODAL SHAPE RECOVER	—	Frequencies of an alternator mount.
6.11	30	DYNAMIC LINEAR	POINT LOADS	MODAL SHAPE	—	Modal analysis of a wing caisson.
6.12	9	DYNAMIC UPDATE LARGE DISP	POINT LOADS	PROPORTIONAL MODAL SHAPE	—	Vibration of a cable.
6.13	16	DYNAMIC LARGE DISP	INITIAL VELOCITY RESTART	AUTO TIME	—	Elastic-perfectly plastic beam explosively loaded.
6.14	27	DYNAMIC	DEFINE LORENZI	DYNAMIC CHANGE DIST LOADS	—	Impact loading of a center cracked rectangular plate. DeLorenzi method used to evaluate K.
6.15	7	LUMP DYNAMIC PRINT, 3	FIXED DISP	MODAL SHAPE RECOVER	—	Modal shape calculations using assumed strain element.
6.16	7	PRINT, 5 LARGE DISP DYNAMIC LUMP	INITIAL VELOCITY FIXED DISP DAMPING CONTACT	DYNAMIC CHANGE	—	Dynamic impact between deformable body and a rigid surface.
6.17	7	PRINT, 5 DYNAMIC LUMP LARGE DISP	DAMPING FIXED DISP INITIAL VELOCITY CONTACT	DYNAMIC CHANGE	—	Dynamic contact between two deformable bodies.
6.18	52	DYNAMIC RESPONSE	CONN GENER NODE FILL	MODAL SHAPE RECOVER SPECTRUM	—	Spectral response of a pipe.
6.19	11	DYNAMIC LUMP	INITIAL VELOCITY CONTACT CONTACT TABLE	DYNAMIC CHANGE	—	Dynamic impact using explicit dynamics.
6.20	98	DYNAMIC	DIST LOADS FLUID DRAG	DYNAMIC CHANGE	—	Beam subjected to fluid loads.
6.21	72	DYNAMIC FOLLOW FOR LARGE DISP	DIST LOADS	DIST LOADS DISP CHANGE MODAL SHAPE RECOVER	—	Eigenvalues of structure with rigid body modes.



## **6** *Dynamics*

---

## 6.1 Dynamic Analysis of a Beam with Small Displacement Response

The dynamic response of a simply supported rectangular beam is analyzed. The beam is subjected to a uniformly distributed load over its length. Three different methods of analysis are employed and their results are compared. These methods are the Newmark-beta and the Houbolt method of direct integration and the method of modal extraction and superposition. This problem is modeled using the three techniques summarized below.

Data Set	Element Type(s)	Number of Elements	Number of Nodes	Differentiating Features
e6x1a	5	3	4	Houbolt
e6x1b	45	3	7	Newmark-beta
e6x1c	45	3	7	Newmark-beta, AUTO TIME

### Element

Element type 5 is a simple, two-dimensional, rectangular section beam-column. It has three degrees of freedom per node:  $u$ ,  $v$ , and right-handed rotation.

### Model

The intent of the example is to illustrate the comparable accuracies of different dynamic operators. Therefore, a very simple model is used. Only half the beam is modeled and only the symmetrical response is sought. It is modeled with three type 5 elements. Because this example involves the small displacement and pure bending of a beam, this type of element is adequate. It should be noted that any beam type element in MARC could be chosen for this problem and would produce the same results.

### Geometry

The beam is as shown in Figure 6.1-1 with height 23.13 in. (EGEOM1), cross-sectional area of 14.70 sq.in. and length of 144.0 inches.

### Material Properties

The material properties input are Young's modulus of  $30 \times 10^6$  psi, Poisson's ratio of 0.3, and mass density of  $7.6754 \times 10^{-4}$  lb-sec<sup>2</sup>/in<sup>4</sup>.



### Loading

The beam is loaded with the ramp pressure forcing function shown in Figure 6.1-2. The pressure load is ramped in the first increment to -655.65 psi and then brought down with constant slope to zero at time of .01 second. It remains at zero from then on as the beam's displacement oscillates around zero. Two different time steps are used for comparison with the implicit integration schemes, .001 second and .00025 second. For comparison, the natural frequencies are shown below:

Mode	Frequency (cycles per sec)
1	$.100 \times 10^3$
2	$.904 \times 10^3$
3	$.257 \times 10^4$
4	$.540 \times 10^4$
5	$.100 \times 10^5$

### Boundary Conditions

The boundary conditions specify that all four nodes are constrained from movement in the  $u$  direction, the cantilevered end (node 1) is also fixed in the  $v$  direction and the midpoint (node 4) is constrained from any right-hand rotation.

### Dynamic

The options are chosen on the DYNAMIC parameter by IDYN = 1 for modal extraction, IDYN = 2 for Newmark-beta, IDYN = 3 for Houbolt direct integration, and IDYN = 4 for the central difference operator. For the modal extraction scheme, the MODAL SHAPE option must be used. Although the beam response has six modes, only the first five modes are extracted in the solution. The assumption is made that the highest mode makes little contribution to the total response.

### Results

The results are summarized in the two plots (see Figure 6.1-3 and Figure 6.1-4) of the beam's midpoint (node 4) displacement,  $v$ , versus time for time steps of .001 and .0025 seconds. We know that for any sine, cosine, or constant ramping with time forcing function, the modal solution gives an exact integration independent of time step size based on the modes extracted [1]. Since we have assumed that the highest mode made no significant contribution to the response, we can also assume that our modal solution defines an exact solution for the beam's response.



The plot of the larger time step = .001 second (Figure 6.1-3) illustrates the inherent errors introduced by the implicit integration schemes. The Newmark operator introduces some periodicity error and so its response is slightly out of phase with the exact modal solution. The Houbolt operator shows larger differences both in the amplitude and the period of the response. This larger phase error is due to the artificial damping introduced by the Houbolt operator. Although this damping causes inaccuracies for this large time step, small displacement problem, it is sometimes a useful feature in large nonlinear dynamic analyses. There it serves to damp out any high-frequency responses which may cause instabilities in the solution [2].

The plot of the small time step = .00025 second (Figure 6.1-4) shows good agreement between the Newmark-beta and the Houbolt direct integration operator solutions and the exact or modal solution.

The central difference operator proves to be unsuitable for this problem. The stability limit for the time increment of this explicit integration operator is  $.172 \times 10^{-4}$ , which is far too small to show enough of the beam's response in a reasonable number of increments.

When the problem was run with beam element type 45, the curved Timoshenko beam in a plane, the comparative results between the methods were the same. Again, the Newmark operator introduced some error in both the period and amplitude of the response as shown by the exact modal solution (see Figure 6.1-5).

The Timoshenko beam element is a 3-node planar beam element which allows transverse shear. It has three nodes per element with three degrees of freedom per node. As shown in Figure 6.1-5, the greater flexibility of the Timoshenko beam model gives its displacement function a greater amplitude and a slightly longer period than the response of the type 5 element model.

## References

1. Dunham, R. S., Nickell, R. E., Stickler, D. S., "Integration Operators for Transient Structural Response", *Computers and Structures*, Vol. 2, pp. 1-15 (Pergamon Press, 1972).
2. Marcal, P. V., McNamara, J., "Incremental Stiffness Method for Finite Element Analysis of Nonlinear Dynamic Problem," *Numerical & Computer Methods in Structural Mechanics*, Symposium, Urbana, Illinois, September, 1971.



### Parameters, Options, and Subroutines Summary

Example e6x1a.dat:

<b>Parameters</b>	<b>Model Definition Options</b>	<b>History Definition Options</b>
DIST LOADS	CONNECTIVITY	CONTINUE
DYNAMIC	CONTROL	DIST LOADS
ELEMENT	COORDINATES	DYNAMIC CHANGE
END	END OPTION	
SIZING	FIXED DISP	
TITLE	GEOMETRY	
	ISOTROPIC	
	POST	
	PRINT CHOICE	

Example e6x1b.dat:

<b>Parameters</b>	<b>Model Definition Options</b>	<b>History Definition Options</b>
DIST LOADS	CONNECTIVITY	CONTINUE
DYNAMIC	CONTROL	DIST LOADS
ELEMENT	COORDINATE	DYNAMIC CHANGE
END	END OPTION	
SIZING	FIXED DISP	
TITLE	GEOMETRY	
	ISOTROPIC	
	PRINT CHOICE	

Example e6x1c.dat:

<b>Parameters</b>	<b>Model Definition Options</b>	<b>History Definition Options</b>
DIST LOADS	CONNECTIVITY	AUTO TIME
DYNAMIC	CONTROL	CONTINUE
ELEMENT	COORDINATE	DIST LOADS
END	END OPTION	DYNAMIC CHANGE
SIZING	FIXED DISP	PROPORTIONAL INCREMENT
TITLE	GEOMETRY	
	ISOTROPIC	
	PRINT CHOICE	

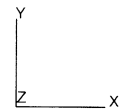
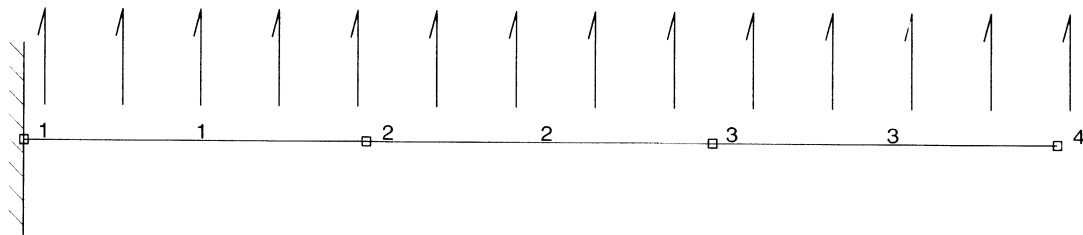


**Figure 6.1-1** Element Type 5 Beam-Column Model

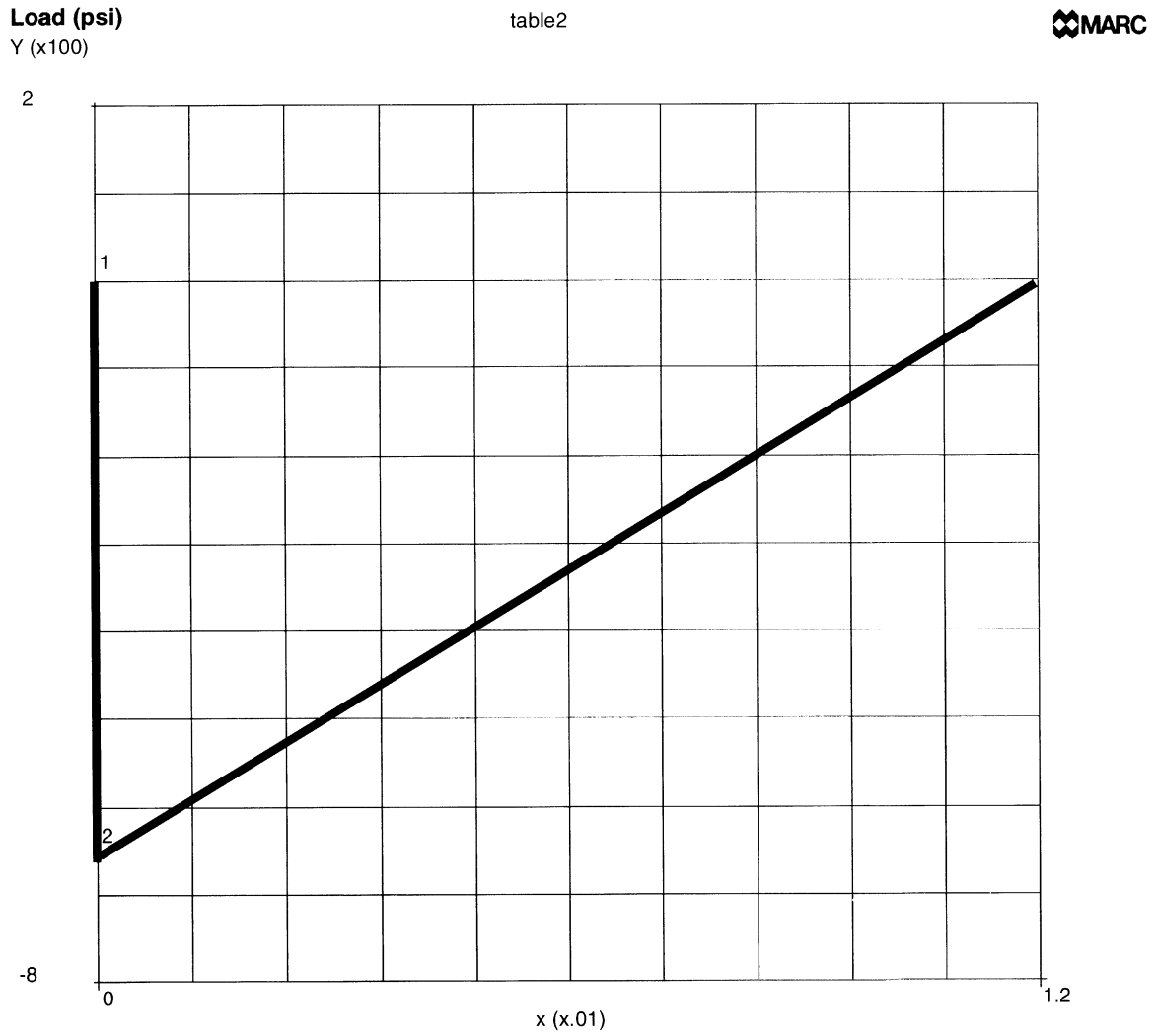


**Figure 6.1-2** Ramp Pressure Forcing Function

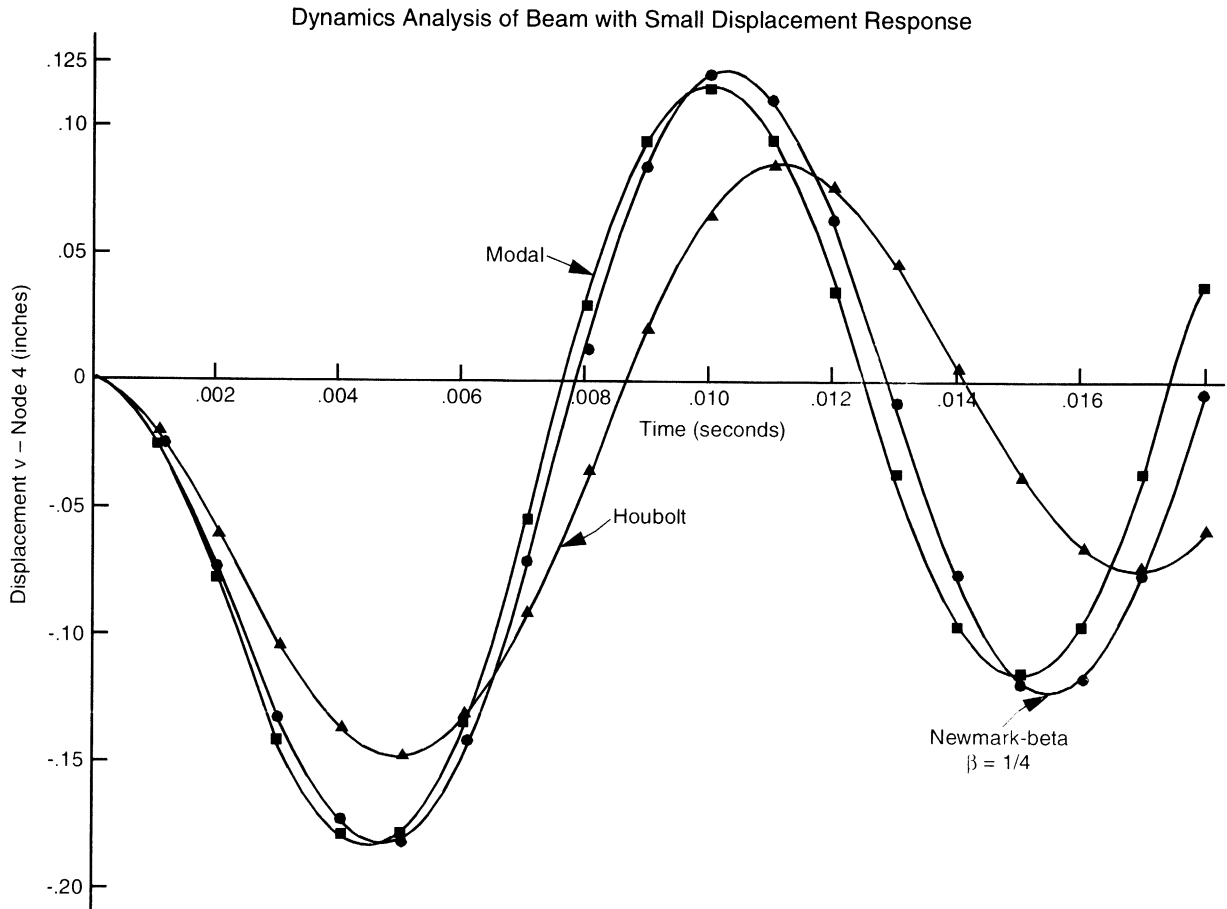


Figure 6.1-3 Time Step = .001 Second

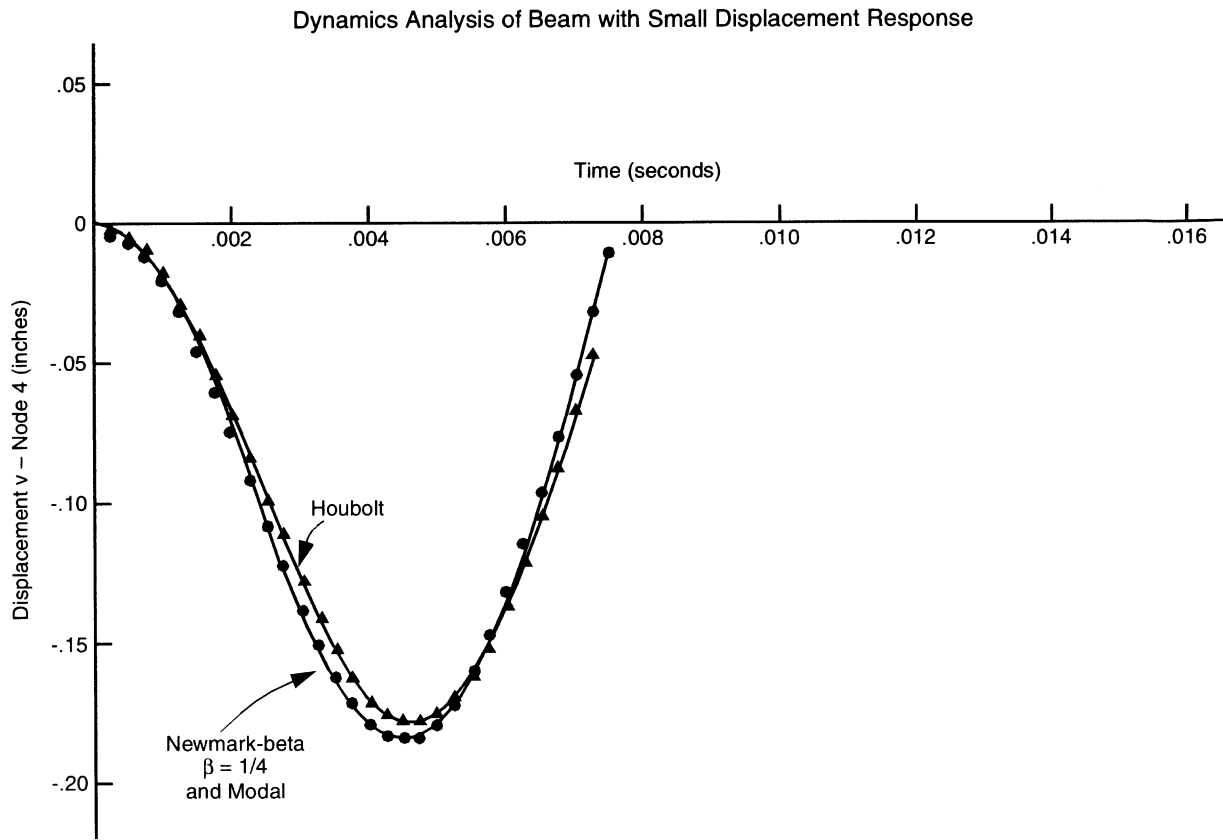


Figure 6.1-4 Time Step = .00025 Second

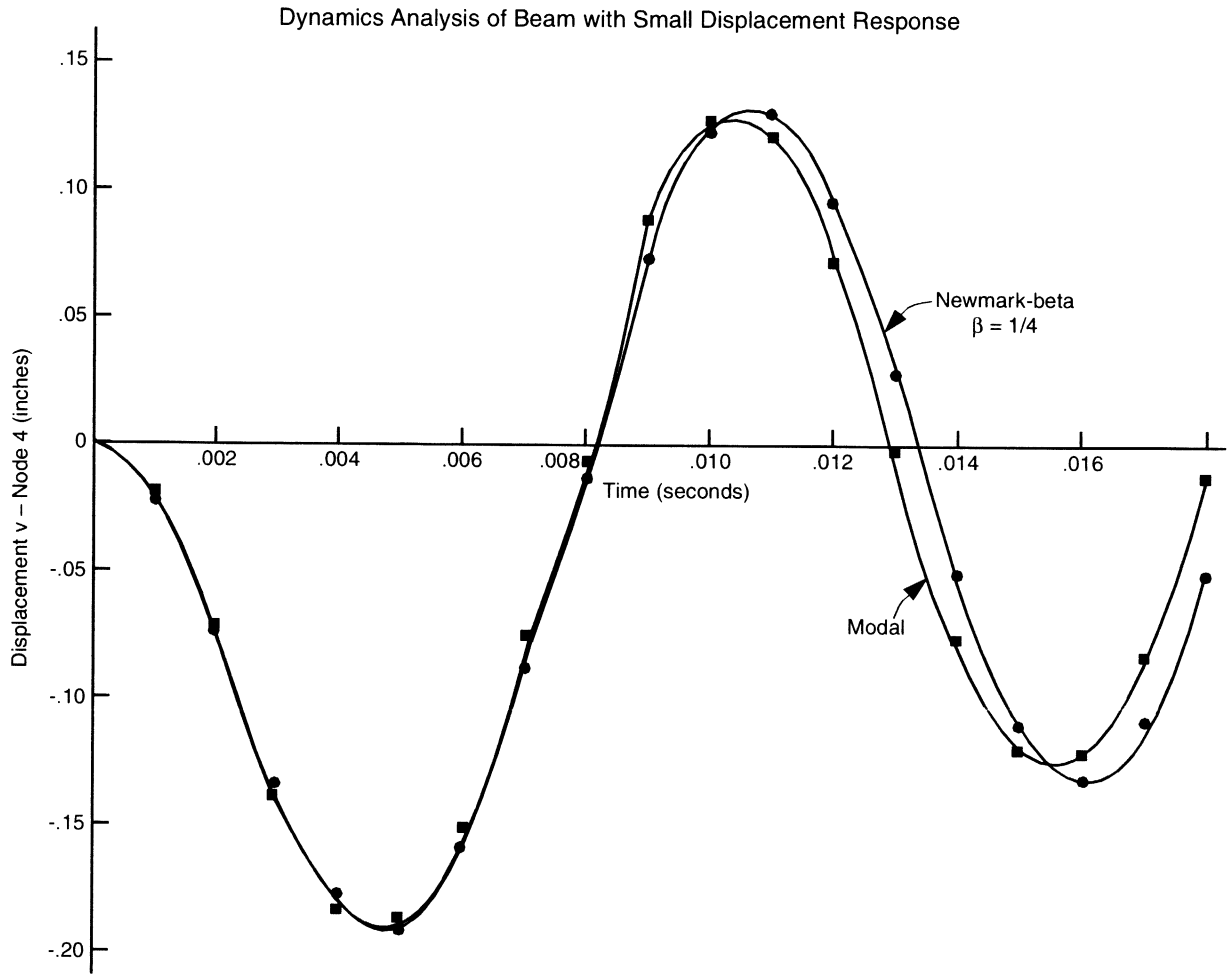


Figure 6.1-5 Timoshenko Beam, Time Step = .001 Second



## **6 Dynamics**

*Dynamic Analysis of a Beam with Small Displacement Response*

---



## 6.2 Beam Modes and Frequencies

This problem is an illustration of the use of the Timoshenko beam element. The first three modes of a square-section, cantilever beam are extracted.

### Element

Element type 45 is a two-dimensional Timoshenko beam with three nodes. Each node has two displacements and one rotational degree of freedom. The element uses a three-point Gaussian integration for mass and a two-point integration for stiffness. This is a consistently derived Timoshenko beam element.

Such elements are most commonly used in dynamic problems, because of the importance of shear and rotatory inertia effects in high-frequency beam response. The particular example is chosen because an exact Timoshenko beam solution is available.

### Model

The geometry and dimensions are shown in Figure 6.2-1.

### Material Properties

MARC only allows input of Poisson's ratio and Young's modulus as elastic material properties. The shear modulus is calculated from these. The Young's modulus is  $30 \times 10^6$  psi and the Poisson's ratio is  $1/3$ . The density is  $7.25257 \times 10^{-4}$  lb-sec<sup>2</sup>/in<sup>4</sup>.

### Loading

No load is imposed, since only modes and frequencies are calculated.

### Boundary Conditions

One end of the beam is built-in. All displacements and rotations are fixed. Thus,  $u = v = \phi_a = 0$  for the built-in end node.

### Results

The results in Table 6.2-1 are obtained for the first three modes. This mesh has 16 active degrees of freedom; a more refined mesh would show the calculated values converging on the exact values.

The first three mode shapes are shown in Figure 6.2-2.



**Table 6.2-1** Beam Frequencies (cps)

Node	Exact*	Calculated
1	995.2	992.3
2	6065.0	6098.0
3	16469.0	16594.0

\*Huang, T. C., "The Effect of Rotary Inertia and Shear Deformation on the Frequency and Normal Modes of Uniform Beams with Simple End Conditions," *J. Applied Mechanics.*, Vol. 28, pp. 279-584 (December 1961).

### Parameters, Options, and Subroutines Summary

Example e6x2.dat:

#### Parameters

DYNAMIC  
ELEMENT  
END  
SIZING  
TITLE

#### Model Definition Options

CONNECTIVITY  
COORDINATE  
END OPTION  
FIXED DISP  
GEOMETRY  
ISOTROPIC

#### History Definition Options

CONTINUE  
MODAL SHAPE

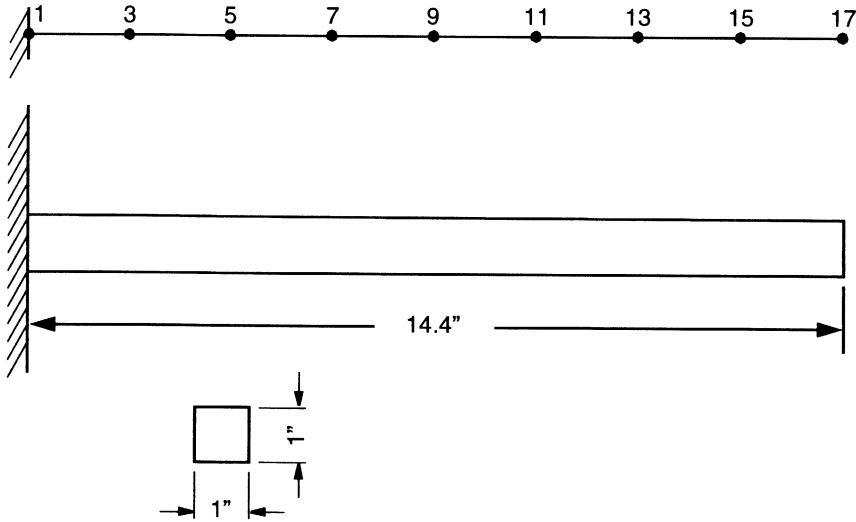
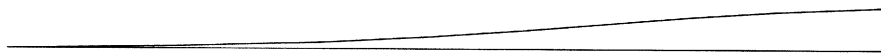
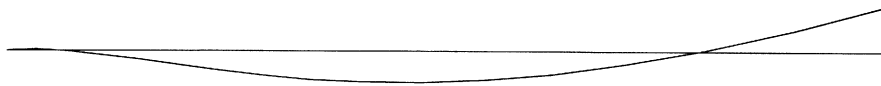


**Figure 6.2-1** Timoshenko Beam

Mode 1  
FREQ: 992



Mode 2  
FREQ: 6098



Mode 3  
FREQ: 16594



**Figure 6.2-2** Calculated Mode Shapes and Frequencies for a Timoshenko Cantilever Beam



### 6.3 Dynamic Analysis of a Plate with the Modal Procedure

The vibration analysis of a cantilevered plate is considered here. The use of the modal analysis procedure available in the program is demonstrated. The normal modes are subsequently used for a transient analysis of the same plate subjected to a suddenly applied pressure. This analysis is repeated four times for comparison of different techniques. The plate is modeled using element type 4 and element type 8. Each finite element model is analyzed once using the power sweep method (four modes are extracted), and again utilizing the Lanczos technique (20 modes are calculated).

This problem is modeled using the four techniques summarized below.

Data Set	Element Type(s)	Number of Elements	Number of Nodes	Differentiating Features
e6x3a	4	2	6	Inverse Power Sweep
e6x3b	8	4	6	Inverse Power Sweep
e6x3c	4	2	6	Lanczos
e6x3d	8	4	6	Lanczos

#### Elements

This problem illustrates the use of both element 4 and element 8, the doubly-curved quadrilateral and triangular shell elements.

#### Model

The mesh for the element 4 model is shown in Figure 6.3-1. It consists of 2 elements and 6 nodes with 66 degrees of freedom. The element 8 model is given in Figure 6.3-2 and consists of 4 elements, 6 nodes and 54 degrees of freedom.

For the element 4 model, use was made of the internal FXORD option for generation of the required 14 coordinates per node. The flat plate (type 5) option requires only the specification of two coordinates (global x and y) in this case.

The element 8 model makes use of the user subroutine UFXORD option and illustrates the ease with which various complex coordinate systems may be programmed by the user. This routine provides the 11 nodal coordinates required for element 8 at each of the nodes specified in the UFXORD option. The subroutine is written to allow for inclusion of various twist angles such as would be evident in a turbine blade for example.

**Geometry**

For both models the plate is assumed to have a uniform thickness of 0.1 in. and is specified as EGEOM1.

**Material Properties**

The following material data was assumed for both models: Young's modulus (E) is  $30.0 \times 10^6$  psi, Poisson's ratio ( $\nu$ ) is 0.3, weight density (w) is  $0.283 \text{ lb/in}^3$ , and mass density ( $\rho$ ) is  $7.324 \times 10^{-4} \text{ lb-sec}^2/\text{in}^4$ . The use of the default value for yield stress precludes any material nonlinear effects.

**Boundary Conditions**

In both cases, a clamped end condition is specified for nodes 1 and 2.

**Dynamics**

The modal method is selected by setting IDYN as 1 in the DYNAMIC parameter; the number of modes to be extracted (4 in this case) is also specified.

For input to E6.3A and E6.3B, the four designated modes and eigenvalues are extracted with the inverse power sweep method. This is accomplished by use of the MODAL SHAPE option immediately following the END OPTION option. A tolerance of 0.00001 was specified in this option as well as a limit on the number of sweeps of 40. MARC iterates until the change in eigenvalue is below the specified tolerance or the maximum number of iterations is reached.

Twenty modes are requested in E6.3C and E6.3D; and you request that the Lanczos technique of eigenvalue extraction be used.

**Loading**

The calculated modes and corresponding eigenvectors are then used to generate the transient solution induced by a suddenly applied uniform pressure transverse to the plate. The pressure time history is shown in Figure 6.3-3.

This loading is accomplished by use of a DYNAMIC CHANGE and DIST LOADS option. As can be seen in the input, the pressure (100 psi) is applied over a short time interval (0.00002 seconds) by the first of these options and removed by a second set with the same time interval but a reversed pressure loading. The final set of these options continues the transient analysis with the pressure held at zero for a total time of 0.001 seconds.

**Control**

The number of increments has been limited to six in the input decks; more complete output can be obtained by increasing the total number of increments allowed.

**Output**

The output provides first the increment zero results, which serve only to show the resulting initial accelerations. The output then provides four modal eigenvalues and eigenvectors as requested. This is followed by the transient analysis results.

**Results**

Referring to Table 6.3-1, the frequencies obtained for the first three modes compare quite well with the results found in Zienkiewicz, O. C., *The Finite Element Method in Engineering Science*, McGraw-Hill, 1971.

**Table 6.3-1** Comparison of Frequencies in Cycles/Seconds

Modes	Element 4		Element 8		
	Inverse Power Sweep	Lanczos	Inverse Power Sweep	Lanczos	Zienkiewicz
1	845	845	858	858	846
2	3,651	3,651	4,190	4,190	3,638
3	5,280	5,280	6,348	6,348	5,266
4	7,137	7,137	7,371	7,371	11,870
5		12,100		15,130	
6		17,830		19,370	
7		25,630		25,750	
8		26,000		29,190	
9		27,060		30,890	
10		28,150		35,200	
11		34,930		42,770	
12		49,980		64,360	
13		55,160		65,150	
14		60,540		75,480	
15		60,720		78,280	
16		74,830		81,830	
17		76,060		96,710	
18		90,760		107,000	

**Table 6.3-1** Comparison of Frequencies in Cycles/Seconds (Continued)

Element 4			Element 8		
Modes	Inverse Power Sweep	Lanczos	Inverse Power Sweep	Lanczos	Zienkiewicz
19		92,070		111,600	
20		97,170		119,500	

The element type 4 results show agreement in this case, although results at the higher modes do not agree with those found in Zienkiewicz for element type 8. The fifth mode calculated by MARC agrees with the fourth mode of the reference; therefore, it is presumed that the Zienkiewicz solution omitted the fourth mode.

The modes and eigenvalues are used to follow the transient solution for a suddenly applied pressure on the top face of the beam. Figure 6.3-4 shows the variation with time of the displacement of two nodes at the end of the cantilever. A maximum of 0.145 in. was reached during the first excursion. This displacement may be compared with the static displacement of 0.08 inches for the same beam and loading. The dominance of the first mode is indicated as the maximum displacement was reached at about half the longest period.

**Parameters, Options, and Subroutines Summary**

Examples e6x3a.dat, e6x3b.dat, e6x3c.dat, and e6x3d.dat:

<b>Parameters</b>	<b>Model Definition Options</b>	<b>History Definition Options</b>
DIST LOADS	CONNECTIVITY	DIST LOADS
DYNAMIC	CONTROL	DYNAMIC CHANGE
ELMENT	COORDINATES	CONTINUE
END	END OPTION	MODAL SHAPE
SIZING	FIXED DISP	
TITLE	GEOMETRY	
	ISOTROPIC	
	POST	

User subroutine in u6x3b.f and u6x3d.f:

UFXORD



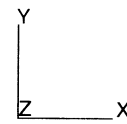
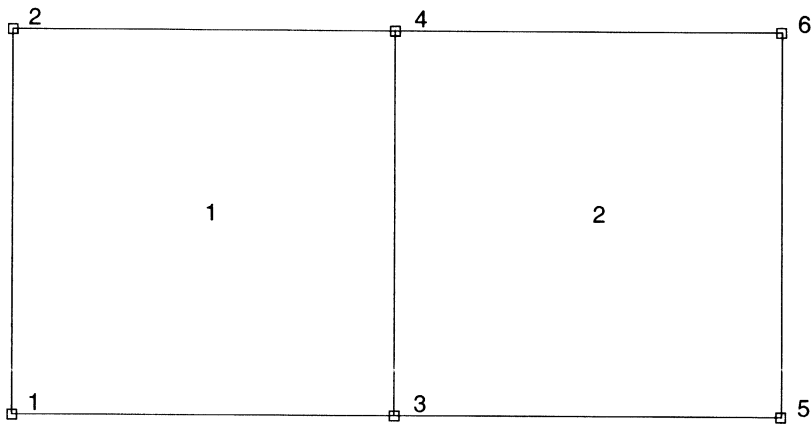


**Figure 6.3-1** Element 4 Plate Model

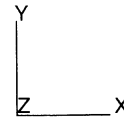
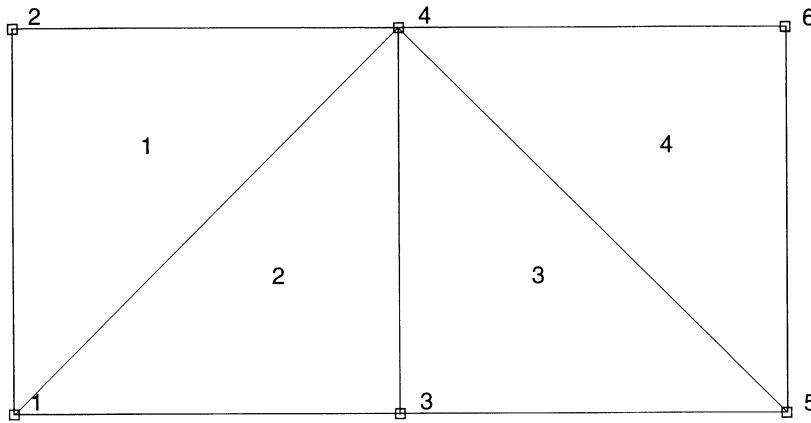


**Figure 6.3-2** Element 8 Plate Model

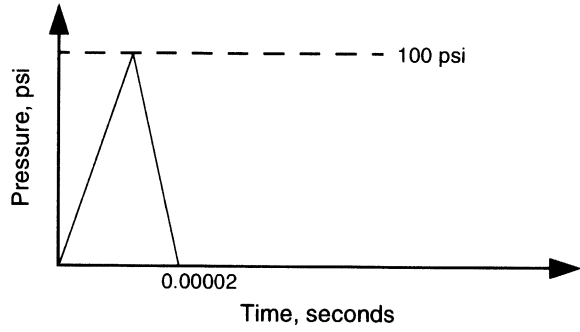


**Figure 6.3-3** Applied Pressure History

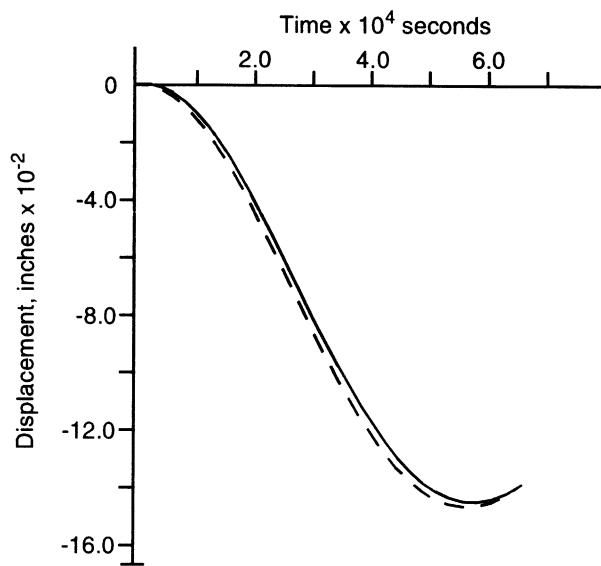


**Figure 6.3-4** Displacements at Tip





## 6.4 Frequencies of a Rotating Disk

This problem illustrates the use of the LARGE DISP and Centrifugal Loading options for the study of natural frequencies of a rotating disk.

### Model

Element type 10 is used in this analysis. There are 5 elements and 12 nodes. Disk dimensions and a finite element mesh are shown in Figure 6.4-1.

### Material Properties

The material properties of the disk are: Young's modulus is  $30 \times 10^6$  psi, and Poisson's ratio is 0.3. Mass density is  $7.338 \times 10^{-4}$  lb-sec/in<sup>4</sup>.

### Boundary Conditions

The z-displacements are constrained at the disk faces ( $z = 0$  and  $z = 0.5$ ). The radial-displacements are constrained at the line of symmetry ( $r = 0$ ).

### Centrifugal Loading

The input data for centrifugal loading is supplied by using the model definition option ROTATION A, the direction of the axis of rotation, and a point on that axis. The actual load is then invoked in the DIST LOADS option by specifying an IBODY load type = 100 and entering the quantity square of rotation speed in radians per time ( $\omega^2$ ), for the magnitude of the distributed load.

In the current problem the angular speed is:

$$\omega = 1000 \text{ rad/sec} = 500/\pi \text{ cycles/second}$$

and the axis of rotation is the symmetry axis.

### LARGE DISPLACEMENT Option

The load stiffness matrix is a large displacement effect; therefore, it is only formed after increment 0. To obtain the modes and frequencies including all the large displacement terms, the user inputs the centrifugal load in the DIST LOADS block in increment 0. Following increment 0, use one or two steps of zero increments of load. This will update the stiffness matrix so that the user can then invoke the MODAL SHAPE option in the next increment. The FOLLOW FOR option should also be invoked since centrifugal loading is a follower force effect.

**Results**

Natural frequencies of the disk with and without rotation are shown in Table 6.4-1. The effect of centrifugal force on natural frequencies of the disk is evident. A body which is in tension will have its natural frequencies increased due to the initial stress stiffness effects; the opposite will be true for a body in compression.

**Table 6.4-1** Frequencies of the Disk (cps)

<b>No Rotation: <math>\omega^2 = 0</math> (Small Displacement)</b>	<b><math>\omega^2 = 1.E8</math> (Large Displacement)</b>	<b>% Increase</b>
$\omega_1 = 1.593 \times 10^4$	$1.620 \times 10^4$	1.6
$\omega_2 = 4.172 \times 10^4$	$4.236 \times 10^4$	1.4
$\omega_3 = 6.978 \times 10^4$	$7.118 \times 10^4$	1.4
$\omega_4 = 1.008 \times 10^5$	$1.040 \times 10^5$	1.5

**Parameters, Options, and Subroutines Summary**

Example e6x4.dat:

<b>Parameters</b>	<b>Model Definition Options</b>	<b>History Definition Options</b>
DYNAMIC	CONNECTIVITY	CONTINUE
ELEMENT	CONTROL	DIST LOADS
END	COORDINATE	MODAL SHAPE
FOLLOW FOR	DIST LOADS	
LARGE DISP	END OPTION	
SIZING	FIXED DISP	
TITLE	ISOTROPIC	
	ROTATION AXIS	

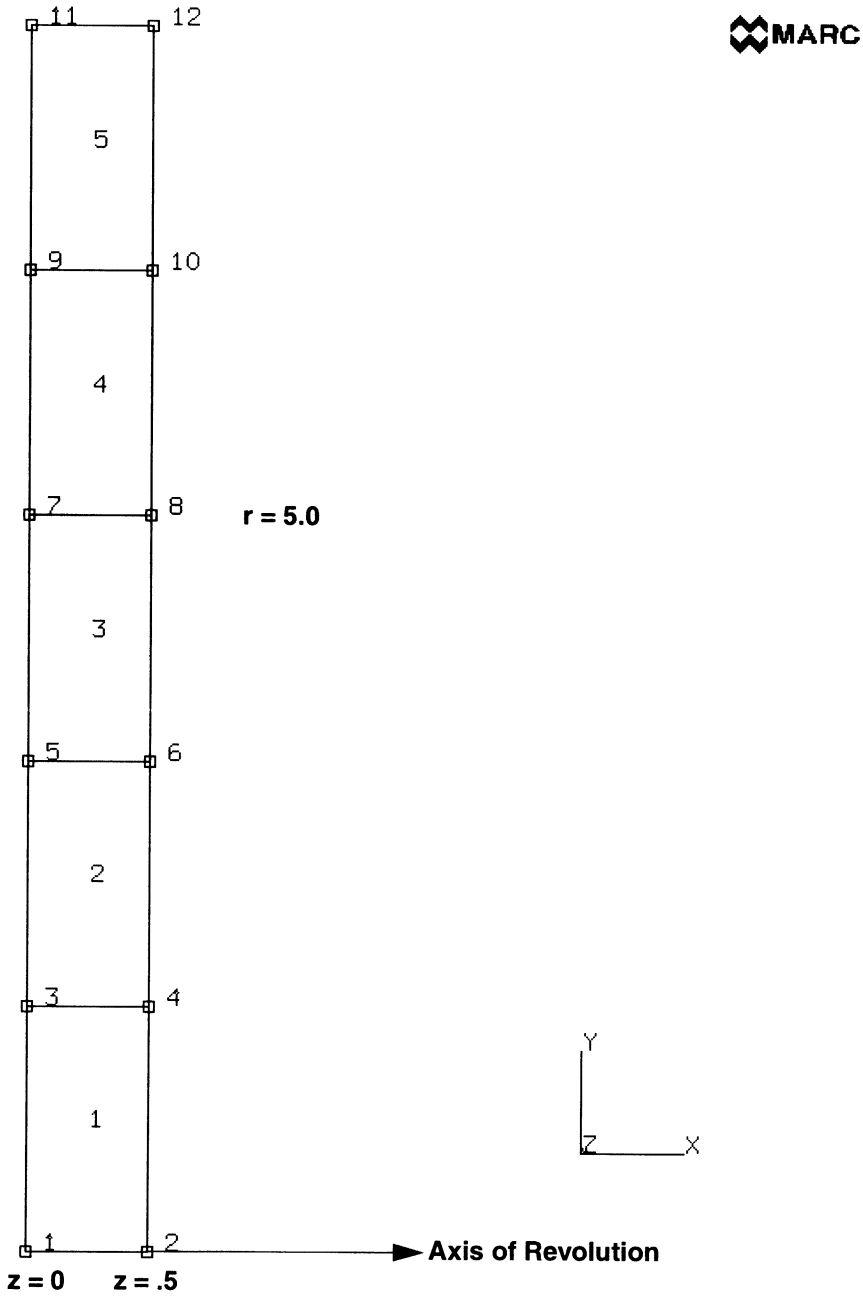


**Figure 6.4-1** Disk and Mesh





## 6.5 Frequencies of Fluid-solid Coupled System

Utilizing the low viscosity and incompressibility of water, a fluid-solid interaction model has been developed and included in MARC. This capability allows the study of natural frequencies of structures immersed in or containing a fluid which is assumed to be inviscid and incompressible. The fluid model allows infinitesimal vibrations only, so that a pressure potential description of the fluid is assumed. The model allows for the effect of pressure waves in the fluid. It is only relevant to dynamic analysis, since the only effect of the fluid is to augment the mass matrix of the structure.

The fluid is modeled with heat transfer elements (potential theory) and the structure modeled with normal stress-displacement elements. The element choice should ensure the interface between the structural and fluid models has compatible interpolation; that is, first order solid and fluid elements, or both second order. If necessary, the tying option can be used to achieve compatibility.

A dam vibration problem was solved using the solid/fluid interaction option. As shown in Figure 6.5-1, the problem consists of a concrete dam section with water on one side, all on a rigid foundation.

### Model

Number of elements = 6 (water: four element 41's; concrete: two element 27's)

Number of nodes = 31

Dimensions of the model and a finite element mesh are shown in Figure 6.5-1.

### Material Properties

For concrete elements:

$$E = 288 \times 10^6 \text{ psf}$$

$$\nu = 0$$

$$\rho = 4.66 \text{ lb-sec/ft}^4$$

For fluid (water) elements:

$$\rho = 1.94 \text{ lb-sec/ft}^4$$

### Boundary Conditions

$$u = 0 \text{ at nodes } 1, 6, 9, 14, 17$$

$$u = v = 0 \text{ at nodes } 23, 26, 31$$

**Fluid-Solid Interaction**

The inputs for this are:

On the parameter FLUID LOAD and the number of solid/fluid interface element surfaces (2) must be entered.

Using the model definition FLUID SOLID option, the element number and element face number for solid and fluid elements must be entered. The element numbers and face numbers are, respectively:

Solid Element Number	Solid Element Face Number	Fluid Element Number	Fluid Element Face Number
5	1	3	10
6	1	4	10

**Geometry**

The thickness of the dam/water system is 1.0 foot.

**Modal Shape**

Default control values are used for the eigenvalue extraction.

**Results**

Frequencies of the dam/water system are given in Table 6.5-1. As anticipated, the inclusion of the water increases the effective mass and reduces the natural frequency of the dam.

**Table 6.5-1** Natural Frequencies of Dam/Water System (f = cps)

Mode	Dam Without Water	Dam With Water
1	4.74	2.46
2	13.6	9.09



**Parameters, Options, and Subroutines Summary**

Example e6x5.dat:

**Parameters**

DYNAMIC  
ELEMENT  
END  
FLU LOAD  
SIZING  
TITLE

**Model Definition Options**

CONNECTIVITY  
COORDINATE  
END OPTION  
FIXED DISP  
FLUID SOLID  
GEOMETRY  
ISOTROPIC  
POST  
UDUMP

**History Definition Options**

CONTINUE  
MODAL SHAPE  
RECOVER

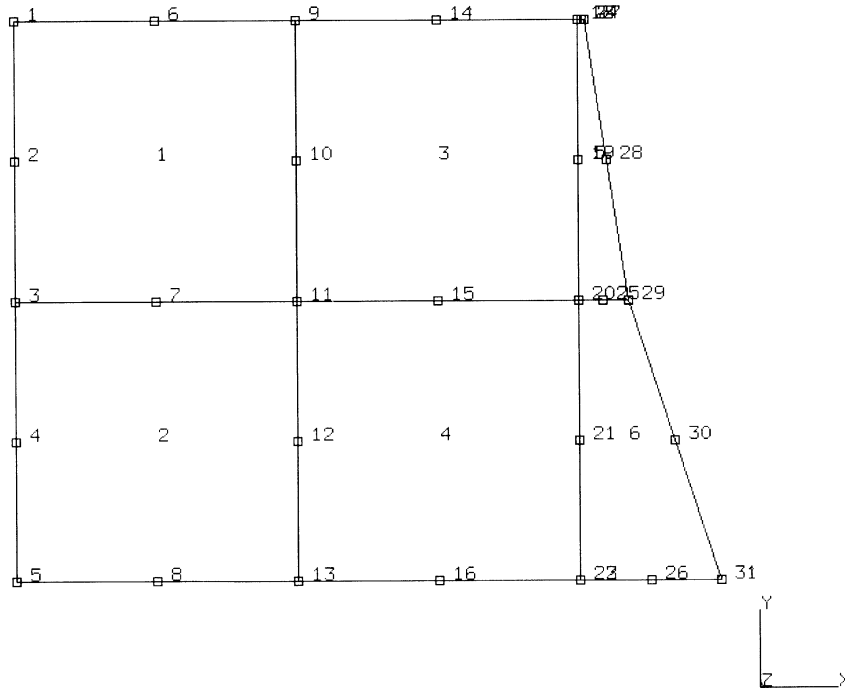
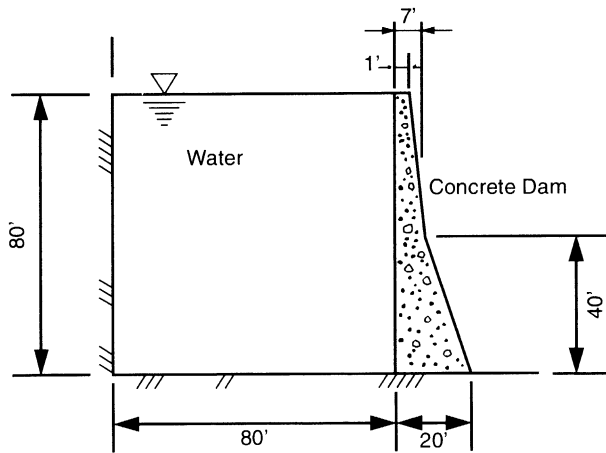


**Figure 6.5-1** Dam/Water System and Mesh



## 6.6 Spectrum Response of a Space Frame

This problem illustrates the spectrum response capabilities of the program to determine the behavior of a three-dimensional frame. In addition, the influence of a compressive load on the eigenvalues of the system is demonstrated. This in turn affects the spectrum response analysis.

This problem is modeled using the two techniques summarized below.

Data Set	Element Type(s)	Number of Elements	Number of Nodes	Differentiating Features
e6x6a	9	20	9	Include LARGE DISP
e6x6b	9	20	9	

### Model

The model is identical to that used in problem 2.24, consisting of 20 truss elements (type 9) and 9 nodes. The dimensions of the frame structure and a finite element model are shown in Figure 6.6-1.

### Material Properties

The Young's modulus is  $10 \times 10^6$  psi. The mass density is  $0.1 \text{ lb-sec}^2/\text{in}^4$ .

### Geometry

The primary members (elements 1-12) have a cross-sectional area of 1 square inch. The secondary members (elements 13-20) have a cross-sectional area of 0.25 square inch.

### Loads

A concentrated load at the apex (node 1) of 200,000 pounds is applied in the negative z-direction. This load is used to apply a compressive stress in the frame, as would be produced by guy wires.

### Boundary Conditions

The base (nodes 3, 5, 7, and 9) is assumed to be fixed in space.

### Displacement Spectral Density

A typical displacement spectral density function is entered. This could have optionally been specified through user subroutine USSD. The frequency is given in cycles per time unit (second). This function is shown in Figure 6.6-2.



**Eigenvalue Response**

This problem was run twice to observe the eigenvalue with and without the influence of the applied load. In the first case, the modal shape was placed immediately after the END OPTION; the stiffness matrix used includes only the elastic stiffness. In the second case, the modal shape was placed following a zero load step; the stiffness matrix also includes the initial stress stiffness contribution. In both problems, ten modes were extracted using the inverse power sweep method. The program performs a shift after the fifth mode. Table 6.6-1 gives the eigenvalues for the two cases. The “double modes” are clearly due to the symmetry with respect to the x,y axes.

**Table 6.6-1** Eigenvalues (cps)

	<b>No Initial Stress</b>	<b>With Initial Stress</b>
1	13.205*	12.520*
2	14.999	13.442
3	16.386	14.944
4	13.204*	18.867*
5	25.172*	12.520*
6	25.172*	18.745*
7	60.196	59.840
8	121.12*	120.29*
9	123.11	122.42
10	121.11*	120.29*

\*Indicates “double mode” pairs (closely-spaced modes).

As anticipated, the inclusion of the initial compressive stress resulted in a reduction in the magnitude of the eigenvalues. The mode shapes for the first, second, and third modes are shown in Figure 6.6-3 through Figure 6.6-5. It is important to ensure the body is in equilibrium before extracting mode if the initial stress stiffness is included.

**Spectrum Response**

After the eigenmodes were extracted, a spectrum response calculation was performed. This response was calculated using only the lowest eight modes. This was done in an arbitrary manner. It is also possible to give a range of frequencies for which the response is based. The program computes the root mean square of the displacement (RMS), velocity, and acceleration. Table 6.6-2 gives the response at node 2 of the structure.

**Table 6.6-2**     Spectrum Response at Node 2

	<b>No Initial Stress</b>	<b>With Initial Stress</b>
RMS – Displacement	0.405 in	0.47 in
RMS – Velocity	33.600 in/sec	37.00 in/sec
RMS – Acceleration	2793.000 in/sec <sup>2</sup>	2923.00 n/sec <sup>2</sup>

**Parameters, Options, and Subroutines Summary**

Example e6x6a.dat:

<b>Parameters</b>	<b>Model Definition Options</b>	<b>History Definition Options</b>
DYNAMIC	CONNECTIVITY	CONTINUE
ELEMENT	COORDINATE	MODAL SHAPE
END	END OPTION	PROPORTIONAL INCREMENT
LARGE DISP	FIXED DISP	SPECTRUM
MESH PLOT	GEOMETRY	
SIZING	ISOTROPIC	
TITLE	POINT LOAD	
	RESPONSE SPECTRUM	
	RESTART	



Example e6x6b.dat:

**Parameters**

DYNAMIC  
ELEMENT  
END  
MESH PLOT  
SIZING  
TITLE

**Model Definition Options**

CONNECTIVITY  
COORDINATE  
END OPTION  
FIXED DISP  
GEOMETRY  
ISOTROPIC  
POINT LOAD  
RESPONSE SPECTRUM  
RESTART

**History Definition Options**

CONTINUE  
MODAL SHAPE  
SPECTRUM



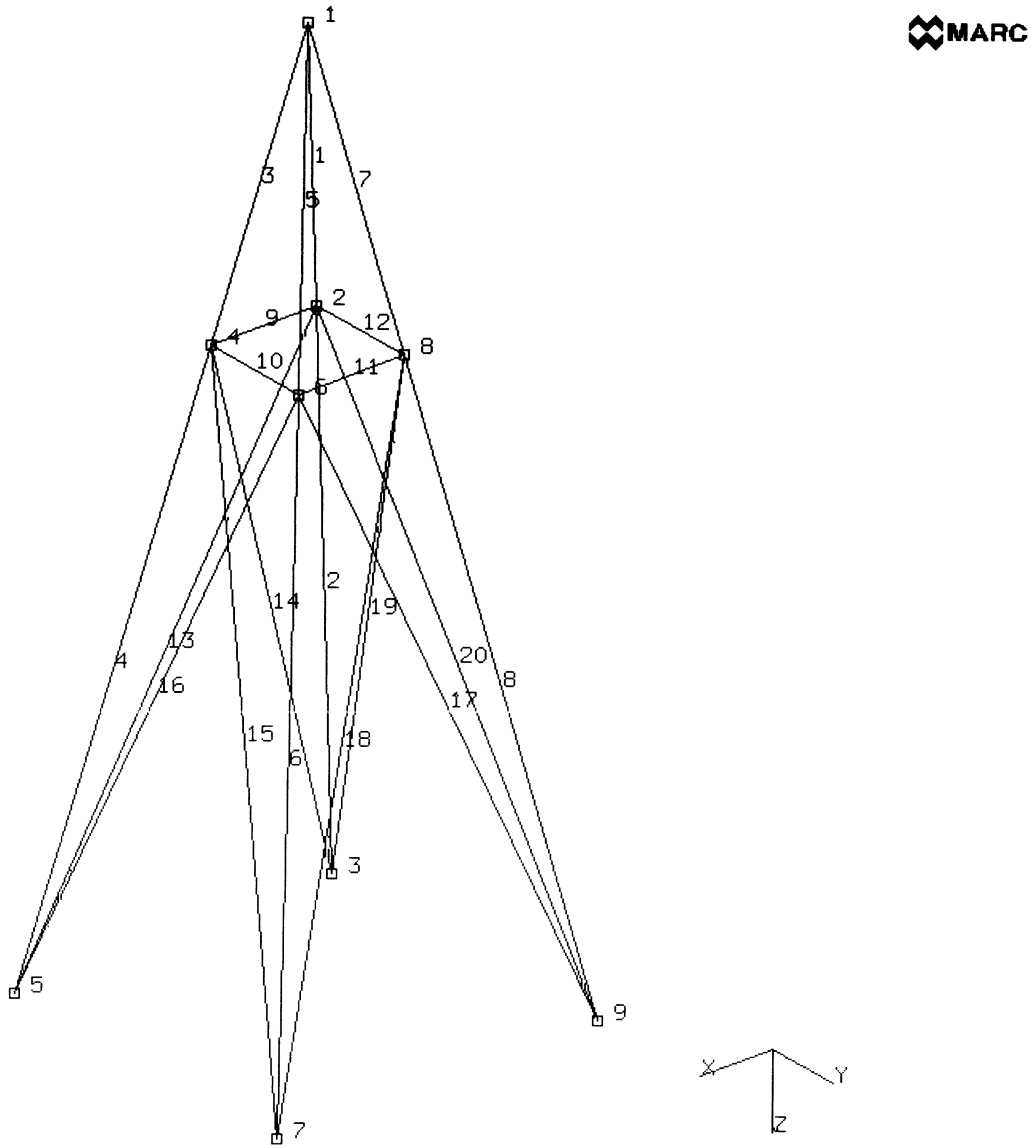
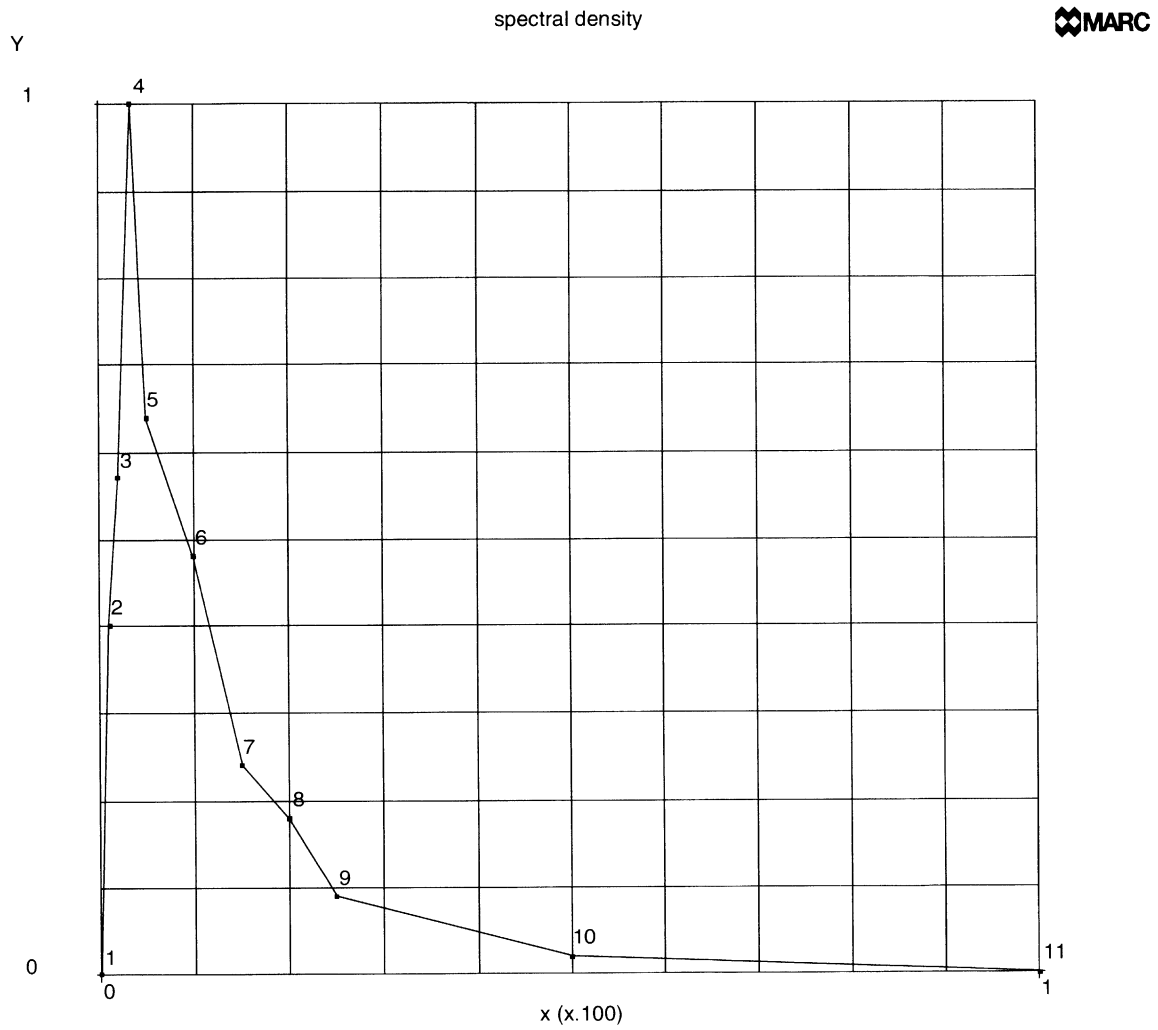
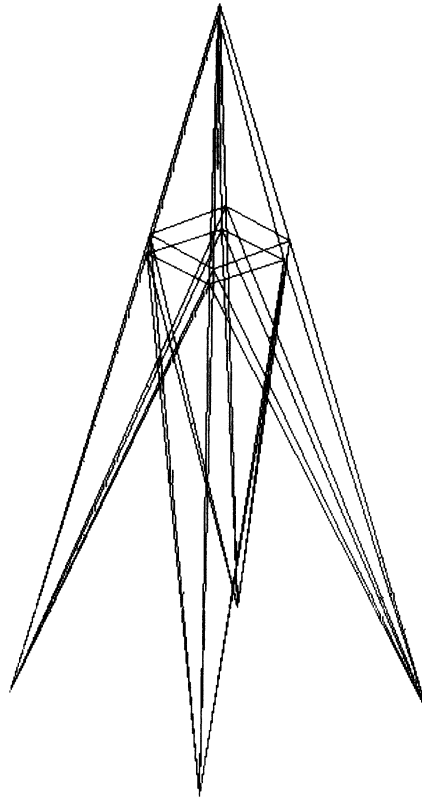


Figure 6.6-1 Three-Dimensional Frame and Model



**Figure 6.6-2** Spectral Density Function

INC : 1  
SUB : 1  
TIME : 0.000e+00  
FREQ : 7.867e+01



prob e6.6a2 spectrum response analysis  
Displacements x

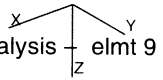
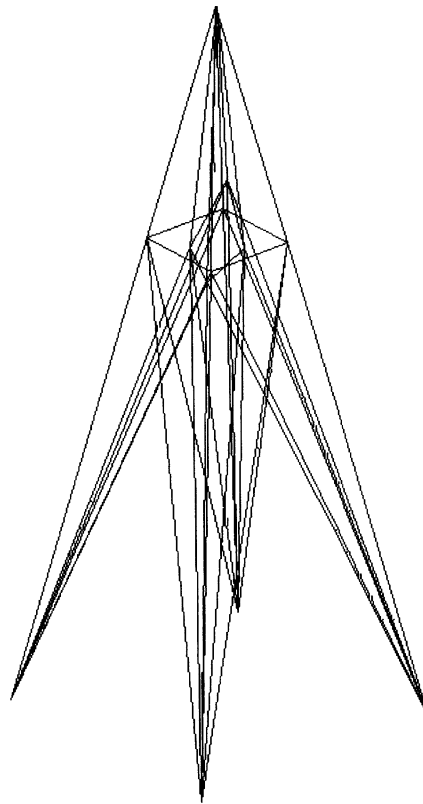


**Figure 6.6-3** Three-Dimensional Frame – Mode 1 (Extensional)

INC : 1  
SUB : 2  
TIME : 0.000e+00  
FREQ : 8.446e+01



prob e6.6a2 spectrum response analysis + elmt 9  
Displacements x

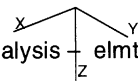
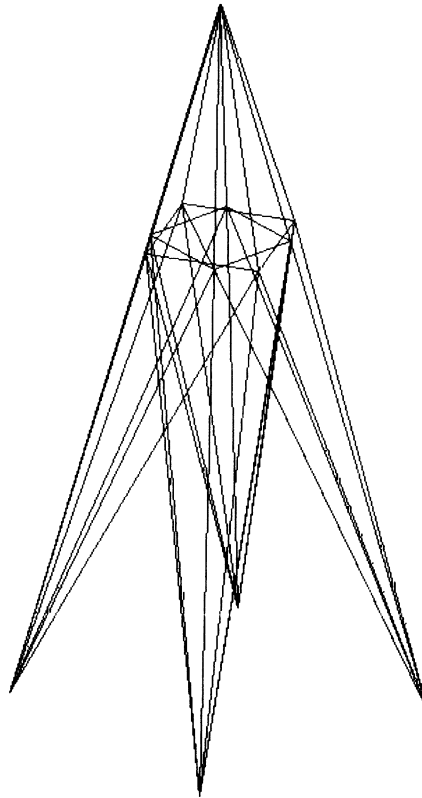


**Figure 6.6-4** Three-Dimensional Frame – Mode 2 (Bending)

INC : 1  
SUB : 3  
TIME : 0.000e+00  
FREQ : 9.390e+01



prob e6.6a2 spectrum response analysis  
Displacements x



**Figure 6.6-5** Three-Dimensional Frame – Mode 3 (Torsional)



## 6.7 Harmonic Analysis of a Capped Mount

A cylindrical rubber mount is bonded to two metal end caps and compressed to an in-service configuration. This assembly is subsequently subjected to harmonic excitation and the resultant harmonic response computed. This example demonstrates the use of the HARMONIC option of MARC.

### Element

Only one-quarter of the mount assembly is represented due to symmetry. A total of 20 elements and 88 nodes define the mount model.

Two different element types are selected. Element type 28 models the metal behavior and element type 33 the rubber behavior. These are both 8-node axisymmetric quadrilateral elements. Element type 33 is the hybrid formulation equivalent of type 28. This finite element mesh is shown in Figure 6.7-1.

### Model

The cylindrical rubber insert has a radius of 0.55 inch and a length of 0.5 inch. The metal end plates are 0.187 inch thick. A Mooney material model is used to describe the rubber behavior.

### Geometry

No geometry inputs are required for element types 28 and 33.

### Material Properties

The material constants for the third order invariant form  $C_{10}$ ,  $C_{01}$ ,  $C_{11}$ ,  $C_{20}$ , and  $C_{30}$  are specified as 36.012, 6.061, 1.443, -1.504, and 1.690 psi, respectively. The mass density for the rubber is  $9.53 \times 10^{-5}$  lbm/in<sup>3</sup>.

The metal has a Young's modulus of  $3 \times 10^7$  psi and Poisson's ratio of 0.3. The von Mises yield point is specified as  $1 \times 10^{21}$  psi. The rubber data is input through the MOONEY option, while the steel data is entered through the ISOTROPIC option.

### Boundary Conditions

Symmetry conditions are specified on the interior surfaces of the model. An initial displacement is applied to the metal caps of 0.022 in. total (0.011 in. for each cap).

An excitation magnitude of 0.05 in. is specified in the history definition DISP CHANGE option. This harmonic excitation is applied to the end caps.

### PHI-COEFF

The real and imaginary components of the relaxation function coefficients for the rubber material are defined in this option as functions of frequency.

**Optimize**

The Cuthill-McKee bandwidth optimization algorithm is requested. This reduces the half-bandwidth for this problem to 27 from 68 in 19 iterations resulting in improved efficiency.

**Restart**

The RESTART option is included such that the analysis can be continued at some later time. This can be used to perform either additional quasi-static deformation, perform a harmonic response calculation at an additional frequency, or for postprocessing.

**Harmonic**

The HARMONIC history definition option defines an excitation frequency of 0.05 cycles/second for the first analysis, and 0.5 cycles/second during the second.

**Tying**

In this option, the cap/rubber interface is defined by tying the first two degrees of freedom of nodes representing the rubber material to corresponding metal cap model nodes. The third degree of freedom of corner nodes in this first layer of elements (4, 8, 12, 16) are tied. Here, the reduction of Herrmann variables in the interfacing elements improves the solution quality.

**Proportional Increment**

A proportional increment of 0.0 enforces equilibrium after the initial deformation. This was necessary because the total displacement was applied in the zeroth increment, where linear behavior is assumed. Thus, the subsequent harmonic analysis is performed on an equilibrated configuration of the mount model.

**Results**

The displacement after the initial displacement is shown in Figure 6.7-2. The von Mises stresses for this configuration are plotted in Figure 6.7-3. The real and imaginary stress components are plotted for excitation frequencies 0.05 cycles/second and 0.5 cycles/second in Figure 6.7-4 through Figure 6.7-7.





**Parameters, Options, and Subroutines Summary**

Example e6x7.dat:

**Parameters**

END  
HARMONICS  
LARGE DISP  
SIZING  
TITLE

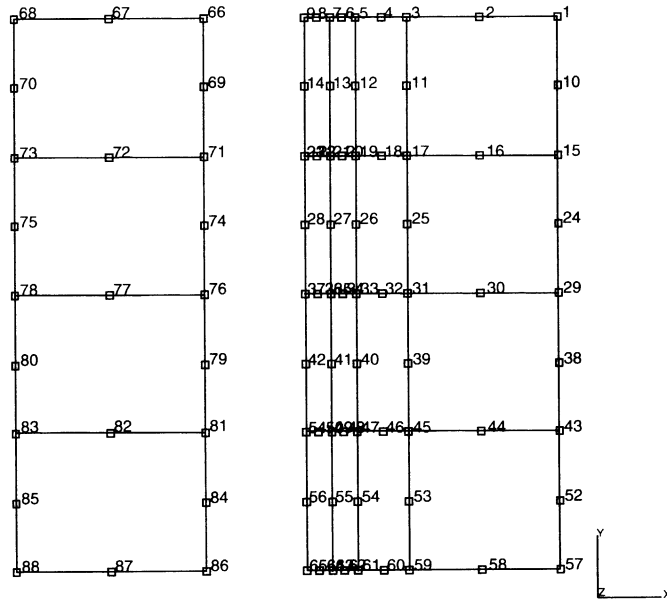
**Model Definition Options**

CONNECTIVITY  
CONTROL  
COORDINATE  
END OPTION  
FIXED DISP  
ISOTROPIC  
MOONEY  
PRINT CHOICE  
TYING

**History Definition Options**

CONTINUE  
DISP CHANGE  
HARMONIC  
PROPORTIONAL INCREMENT

MARC



MARC

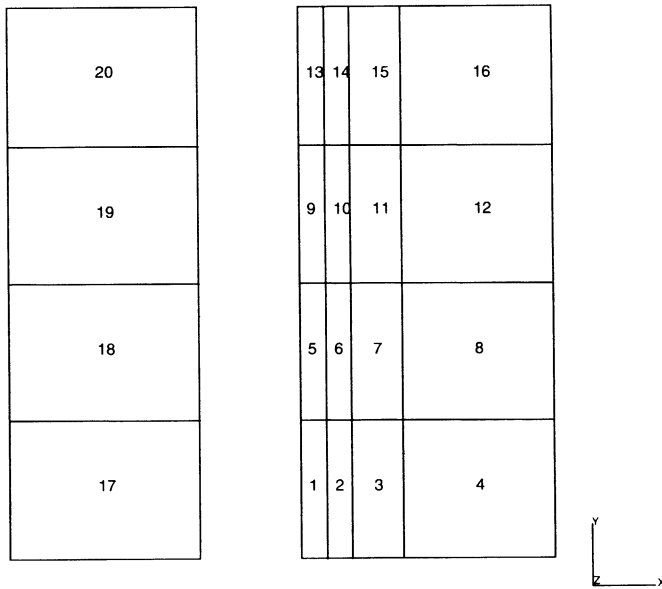
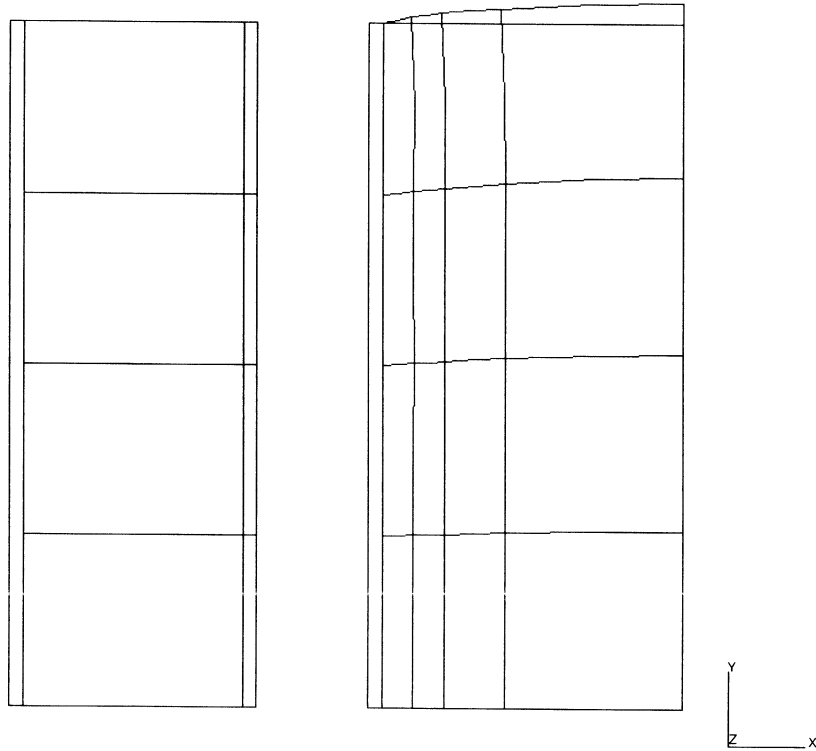


**Figure 6.7-1** Capped Rubber Mount

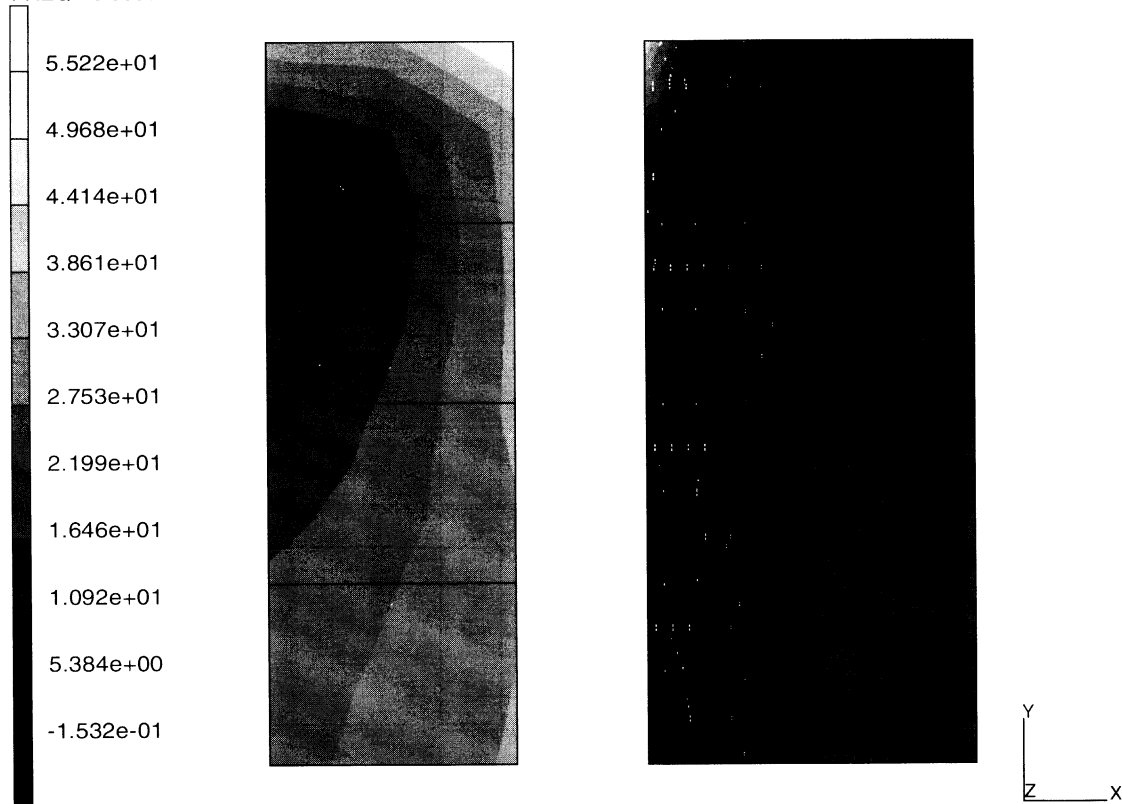
INC : 1  
SUB : 0  
TIME : 0.000e+00  
FREQ : 0.000e+00



prob 6.7 harmonic analysis  
Displacements x

**Figure 6.7-2** Displaced Mesh, Increment 1

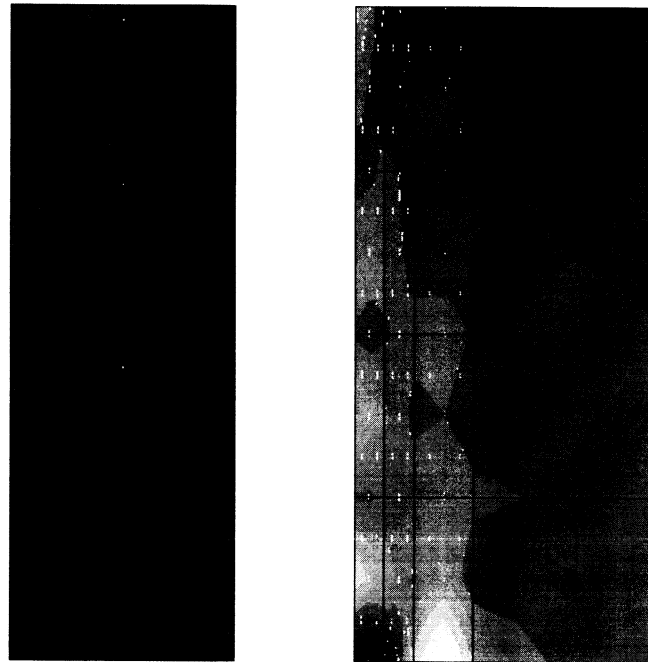
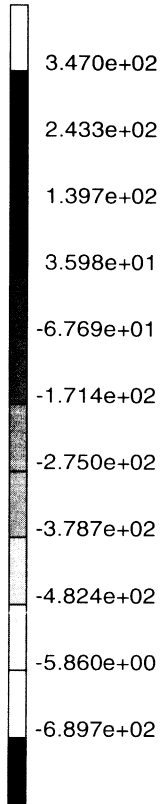
INC : 1  
SUB : 0  
TIME : 0.000e+00  
FREQ : 0.000e+00



prob 6.7 harmonic analysis  
Equivalent von Mises Stress

**Figure 6.7-3** von Mises Stress Distribution, Increment 1

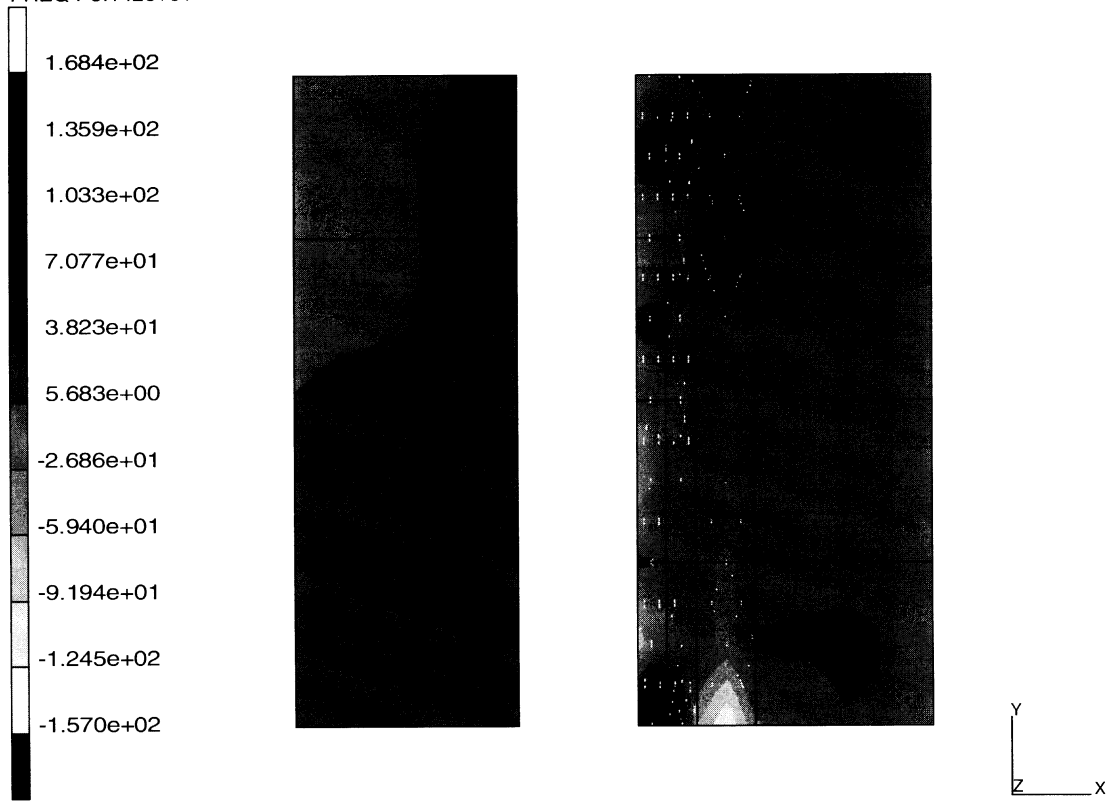
INC : 1  
SUB : 1  
TIME : 0.000e+00  
FREQ : 3.142e+01



prob 6.7 harmonic analysis  
2nd Real Comp of Harmonic Stress

**Figure 6.7-4** Real Radial Stress 0.05 Cycle/Second

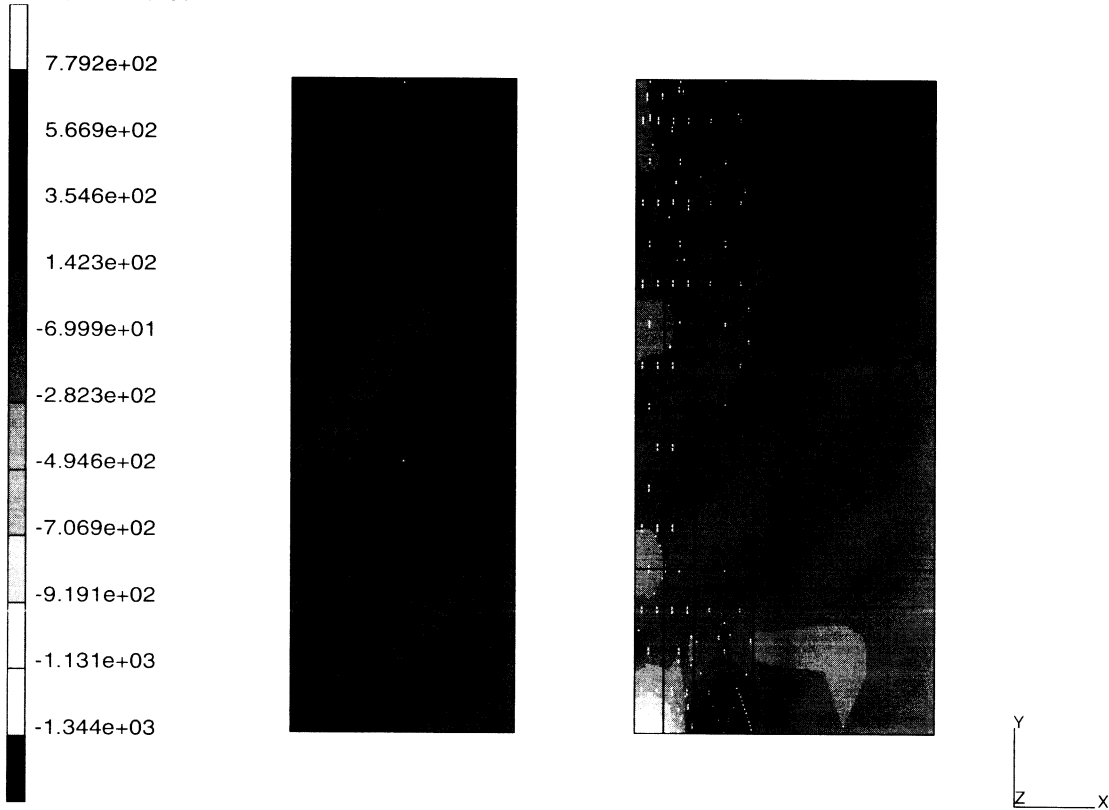
INC : 1  
SUB : 1  
TIME : 0.000e+00  
FREQ : 3.142e+01



prob 6.7 harmonic analysis  
2nd Imag Comp of Harmonic Stress

**Figure 6.7-5** Imaginary Radial Stress 0.05 Cycle/Second

INC : 1  
SUB : 2  
TIME : 0.000e+00  
FREQ : 3.142e+01

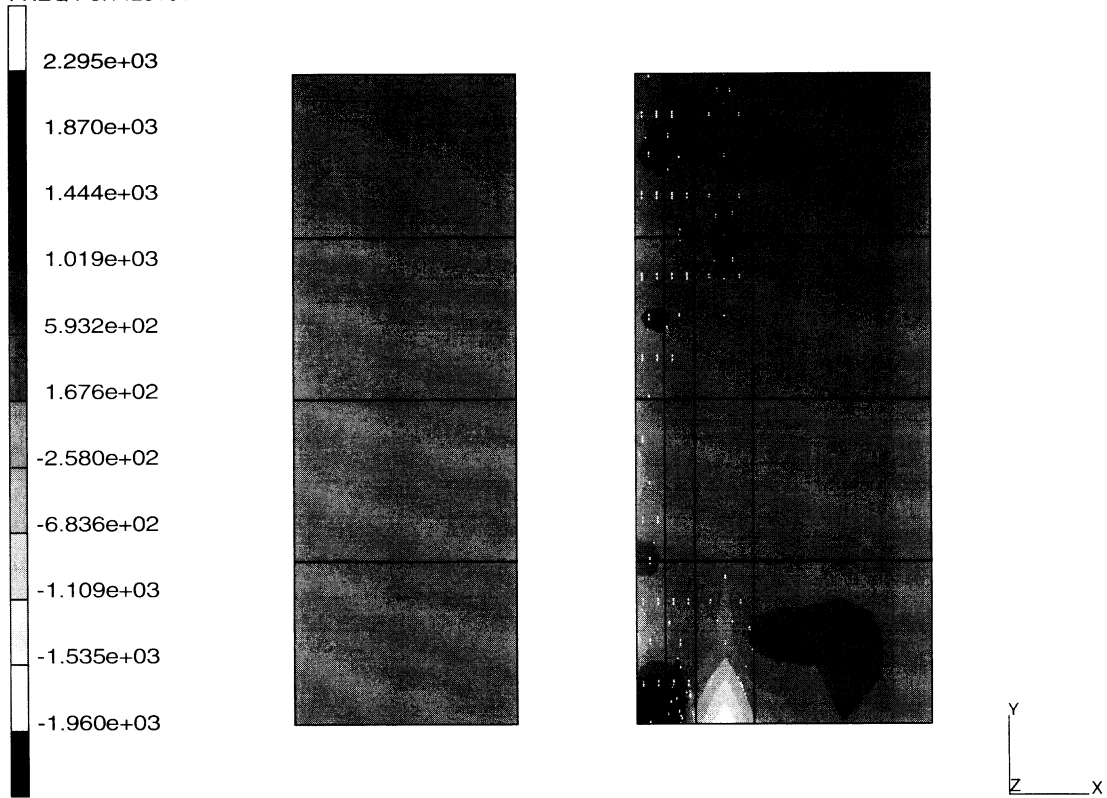


prob 6.7 harmonic analysis  
2nd Real Comp of Harmonic Stress

**Figure 6.7-6** Real Radial Stress 0.5 Cycle/Second



INC : 1  
SUB : 2  
TIME : 0.000e+00  
FREQ : 3.142e+01



prob 6.7 harmonic analysis  
2nd Imag Comp of Harmonic Stress

Figure 6.7-7 Imaginary Radial Stress 0.5 Cycle/Second



## 6.8 Harmonic Response of a Rubber Block

Using the HARMONIC option, the response of a solid block of elastometric material is calculated. The block is stretched in a quasi-static manner. The harmonic response of the block at three distinct frequencies are evaluated for three stretch ratios.

### Element

Element type 35 is used to model the block. This is a 20-node isoparametric brick element using the Herrmann formulation for Mooney or Ogden material models.

### Model

The finite element model of the block is shown in Figure 6.8-1. Only one element is used to model the block. Applying symmetry boundary conditions allows this single element to represent the whole block. The block dimensions are 50.8 x 9.754 x 9.754 inches.

### Geometry

No geometry is specified.

### Mooney

The material constants for the third order invariant form  $C_{10}$ ,  $C_{01}$ ,  $C_{11}$ ,  $C_{20}$ , and  $C_{30}$  are specified as 36.012, 6.061, 1.443, -1.504, and 1.690 psi, respectively. The mass density is given as  $9.53 \times 10^{-5}$  lbm/in<sup>3</sup>.

### Boundary Conditions

The base of the block is constrained axially. The  $x = 0$  and  $y = 0$  faces have symmetry conditions applied. Initially, the block is stretched 2.54 in. or 10% of the block height. Subsequently, the DISP CHANGE option increases the stretch to 4.791 inches, and then to 7.086 inches.

The DISP CHANGE option with a flag 1 in the second field of card 2 is used to specify the harmonic excitation magnitude of 1 inch.

### PHI-COEFF

The relaxation function coefficients are specified as a function of frequency in this option.

### Harmonic

Excitation frequencies of 0.1, 1.0 and 5.0 cycles/seconds are specified for each deformed configuration.

### Results

A summary of the harmonic displacements at node 19 for three stretch ratios are given in Table 6.8-1.

**Table 6.8-1** Summary of Results: Real and Imaginary Displacements of Node 19

Frequency (cycles/sec)		Stretch Ratios		
		1.2	1.338	1.558
0.1	U <sub>R</sub>	.4966	.4773	.4872
0.1	U <sub>I</sub>	.00028	.00040	.00339
1.0	U <sub>R</sub>	.4966	.4764	.4792
1.0	U <sub>I</sub>	.00022	.00025	.00145
5.0	U <sub>R</sub>	.4949	.4721	.4876
5.0	U <sub>I</sub>	.00015	.00012	.0004

**Parameters, Options, and Subroutines Summary**

Example e6x8.dat:

**Parameters**END  
HARMONICS  
LARGE DISP  
SIZING  
TITLE**Model Definition Options**CONNECTIVITY  
CONTROL  
COORDINATE  
END OPTION  
FIXED DISP  
MOONEY  
PRINT CHOICE  
RESTART**History Definition Options**CONTINUE  
DISP CHANGE  
HARMONIC  
PROPORTIONAL INCREMENT

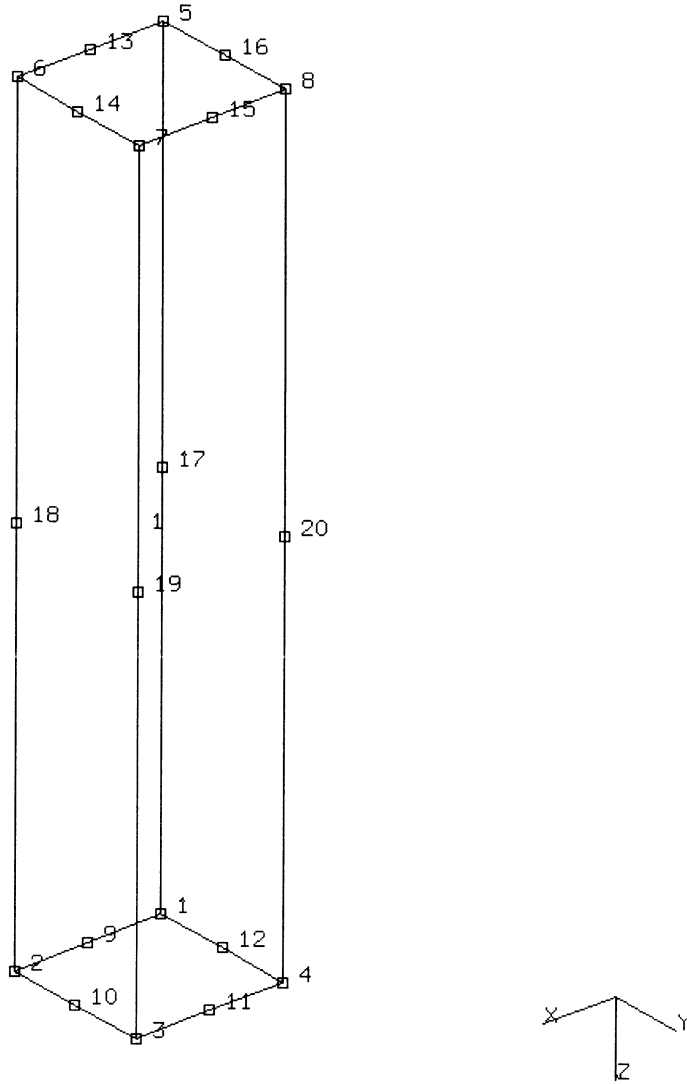


**Figure 6.8-1** Tensile Harmonic Analysis Mesh



## 6.9 Elastic Impact of a Bar

The dynamic impact of a bar hitting against a rigid wall has been computed using the Newmark-beta direct integration algorithm. The contact has been represented by a gap element. The material is assumed to remain elastic.

### Element

Element type 9, a simple linear straight truss with constant cross-section, has been used to represent the bar. It has three coordinates per node in the global  $x$ ,  $y$ ,  $z$  directions and uniaxial stress and strain. A gap element type 12 has been used to impose the contact condition.

### Model

A simple model is assumed to represent the problem of a bar hitting against a wall. The mesh consists of 15 elements of type 9 and 1 gap element – a total of 19 nodes. The mesh is more refined where the contact will occur.

### Geometry

The bar is shown in Figure 6.9-1. It is 100 mm long and has a uniform cross section of  $314.15 \text{ mm}^2$ .

### Material Properties

The material properties of the bar are:

Young's modulus is  $E = 1.96\text{E}+5 \text{ N/mm}^2$ ,  
Poisson's ratio is  $\nu = 3$ ,  
mass density is  $\rho = 7.85\text{E}-6 \text{ Kg/mm}^3$ , and  
yield point is  $\sigma_y = 235.2 \text{ N/mm}^2$ .

### Boundary Conditions

Only the axial displacements are free. The end node of the gap element associated with the wall has every degree of freedom constrained.

### Dynamics

The body has an initial velocity of 50 m/seconds.

The case has been studied for 200 seconds using 200 time-steps of 1 second in the DYNAMIC CHANGE option.



**Results**

The displacement of the last node is shown in Figure 6.9-2. The velocity is shown in Figure 6.9-3. The elastic wave is moving with a velocity:

$$c = \left[ \frac{E}{\rho} \right]^{1/2} = 5 \times 10^3 \text{ m/sec.}$$

The bar rebounds after a time:

$$t = \frac{2l}{c} = 40 \times 10^{-6} \text{ sec.}$$

In Figure 6.9-4, the reaction in the gap is equal to zero in the fourth increment, implying that separation has occurred.

**Parameters, Options, and Subroutines Summary**

Example e6x9.dat:

<b>Parameters</b>	<b>Model Definition Options</b>	<b>History Definition Options</b>
DAMPING	CONNECTIVITY	CONTINUE
DYNAMIC	CONTROL	DYNAMIC CHANGE
END	COORDINATE	
LUMP	DAMPING	
SIZING	END OPTION	
TITLE	FIXED DISP	
	GAP DATA	
	GEOMETRY	
	INITIAL VELOCITY	
	ISOTROPIC	
	MASSES	
	POST	
	PRINT CHOICE	

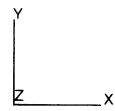
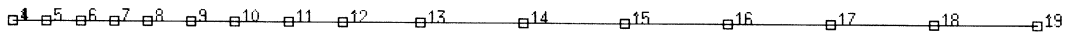


**Figure 6.9-1** Mesh of the Bar

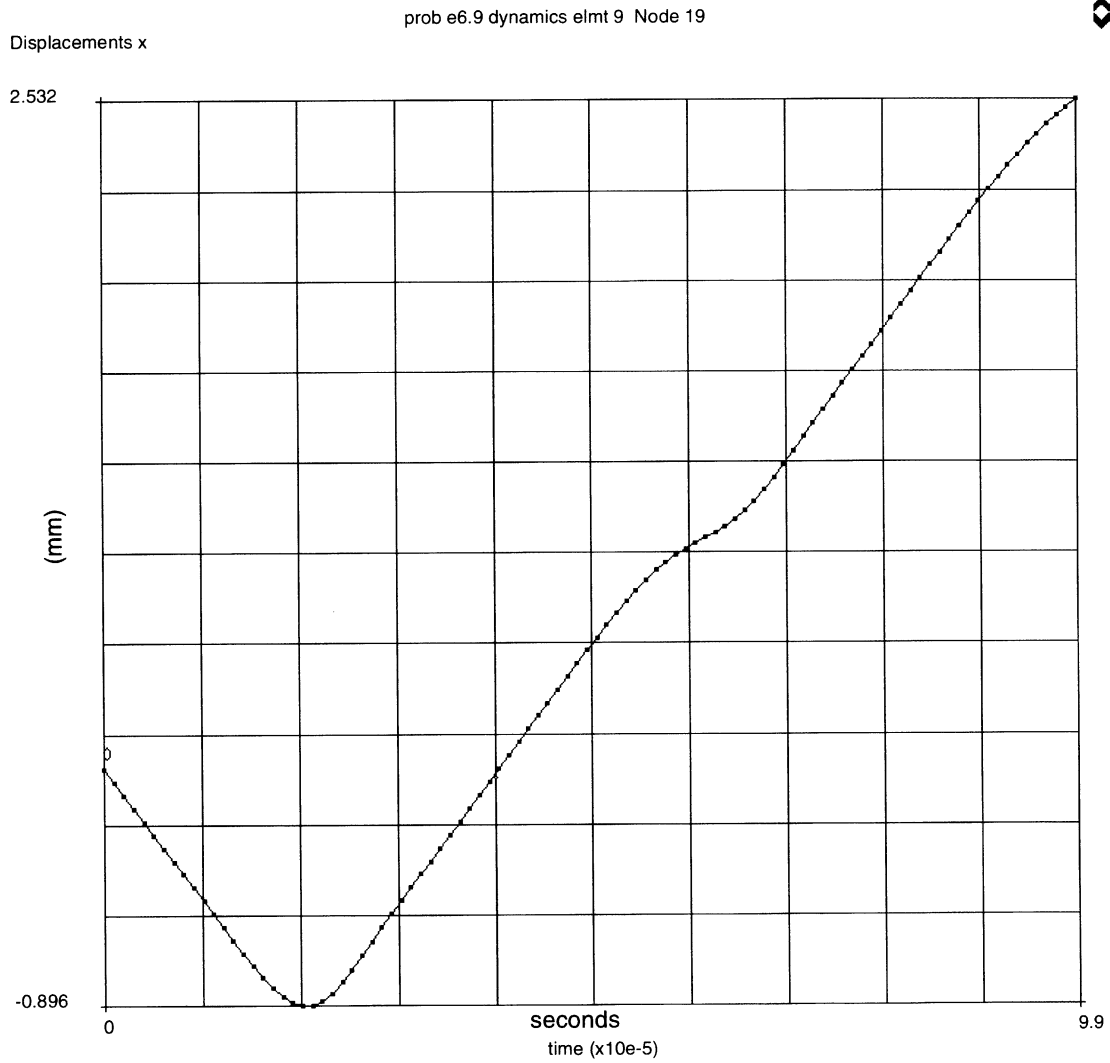


Figure 6.9-2 Time History of Displacements



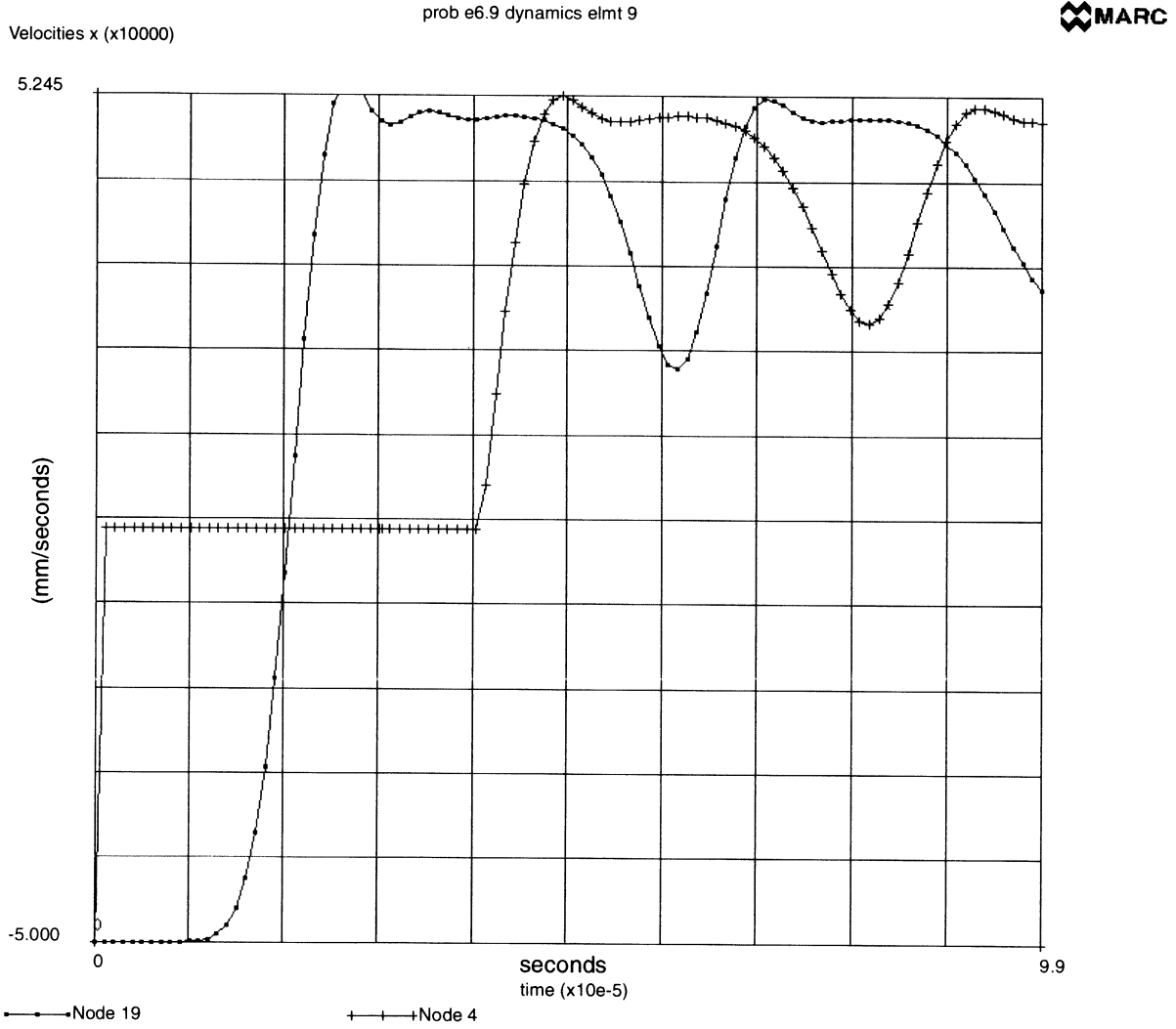


Figure 6.9-3 Time History of Velocity

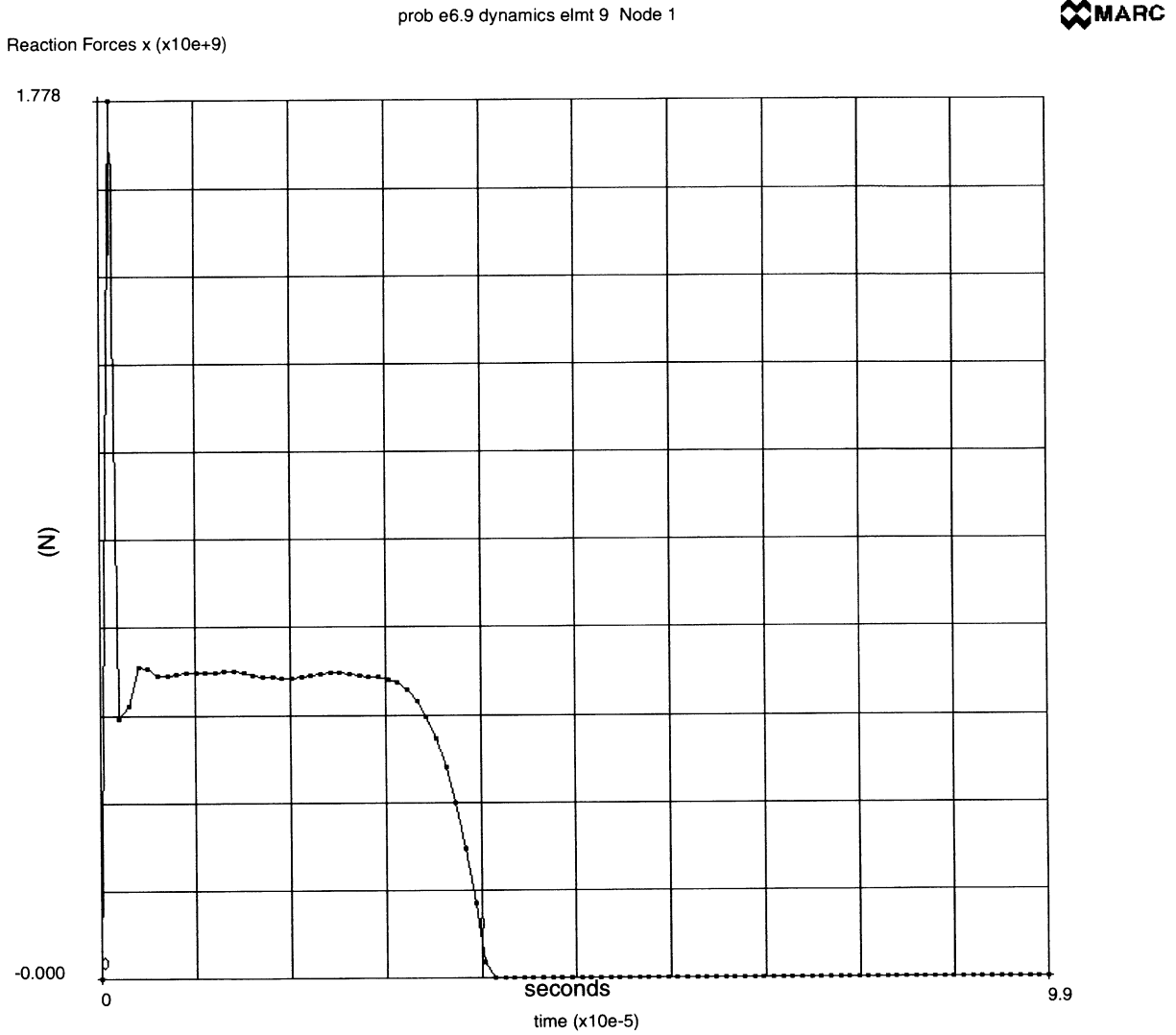


Figure 6.9-4 Time History of the Reaction



## 6.10 Frequencies of an Alternator Mount

The first six modal frequencies are computed for a spatial frame representing the support of an alternator. Two masses are lumped in the middle of two horizontal beams, at nodes 14 and 18 (Figure 6.10-1). The use of history definition option RECOVER for modal stress calculations is also demonstrated in this problem.

### Element

Element 52, a straight Euler-Bernoulli beam in space with linear elastic response, has been used. It has six coordinates per node: the first three are (x,y,z) global coordinates of the system, the other three are the global coordinates of a point in space which locates the local x-axis of the cross section.

### Model

The spatial frame has been modeled using 16 elements and 20 nodes. The columns are clamped at the base.

### Geometry

The columns are 250 cm high; the beams in the x-direction are 192.5 cm long and 157.5 cm in the z-direction. The geometric properties of the sections are given in Table 6.10-1.

The torsional stiffness for the rectangular section is as follows:

$$K_t = \frac{E}{2(1+\nu)} I_t$$

$$I_t = hb^3 \left[ \frac{1}{3} - \frac{3.35b}{16h} \left( 1 - \frac{b^4}{12h^4} \right) \right]$$

Element 52 computes the torsional stiffness of the section as:

$$K_t = \frac{E}{2(1+\nu)} (I_{xx} + I_{yy})$$

Then, in order to use the correct stiffness, an artificial Poisson's ratio  $\nu^*$  is chosen so that:

$$\frac{E}{2(1+\nu)} I_t = \frac{E}{2(1+\nu^*)} (I_{xx} + I_{yy})$$

$$\nu^* = \frac{(I_{xx} + I_{yy}) \cdot (1 + \nu)}{I_t} - 1$$

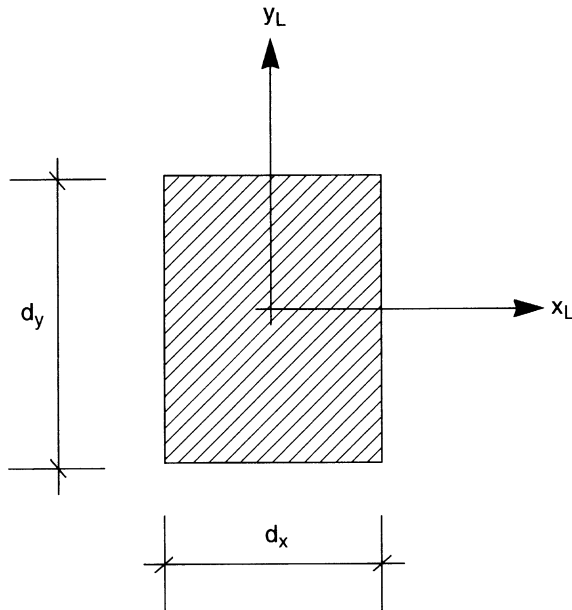


Table 6.10-1 Geometric Properties of Beams Sections

Set n	Elements n	d <sub>x</sub> [cm]	d <sub>y</sub> [cm]	A [cm <sup>2</sup> ]	J <sub>x</sub> [cm <sup>4</sup> ]	J <sub>y</sub> [cm <sup>4</sup> ]
1	1, 2, 7, 8	75	115	8,625	9,500,000	4,000,000
2	3, 4, 5, 6	85	115	10,925	12,000,000	8,200,000
3	9, 10, 13, 14	196	74	4,810	2,194,000	1,693,000
4	1, 12	196	74	14,504	6,618,000	46,430,000
5	15 16	133	74	9,842	4,491,000	14,500,000

**Material Properties**

The frame is made of reinforced concrete. Young's modulus is  $E = 2.5 \times 10^8 \text{ kg/cm sec}^2$  and the density is  $\rho = 2.55 \times 10^{-3} \text{ kg/cm}^3$ . Poisson's ratio is 0.3. The lumped masses are  $M = 19000 \text{ kg}$ .

**Analytical Solution**

An approximate analytical solution is used to compare analytic results with the MARC output. The volume of concrete, the total mass and the moment of inertia are as follows:

$$V = 30.923 \times 10^6 \text{ cm}^3$$

$$M = 1.09 \times 10^5 \text{ kg}$$

$$I = 5.4 \times 10^9 \text{ kg} \cdot \text{cm}^2$$

Let us write the following:

$$K_x \approx \frac{12 E \Sigma (J_y)_{col}}{h^3} = 5.86 \times 10^8 \text{ kg/sec}^2$$

$$K_y \approx \frac{12 E \Sigma (J_x)_{col}}{h^3} = 1.03 \times 10^9 \text{ kg/sec}^2$$

The first three modal frequencies are as follows

$$T_x = \frac{1}{2\pi} \quad \frac{K_x}{M} = 11.7 \text{ Hz}$$

$$T_z = \frac{1}{2\pi} \quad \frac{K_z}{M} = 15.5 \text{ Hz}$$

$$T_\theta = \frac{1}{2\pi} \quad \frac{K_\theta}{I} = 21.7 \text{ Hz}$$

**Recover**

The RECOVER option is used to first place the six eigenvectors on the post file.

The load incrementation option RECOVER is then used for the modal stress calculations for the first and second modes. The modal stresses are computed from the modal displacement vector  $\phi$  (eigenvector without normalization), and the nodal reactions are calculated from

$$F = K\phi - \omega^2 M\phi.$$

**Results**

The comparison between the approximate analytical solution and the numerical results is shown below:

<b>Eigenvalue</b>	<b>MARC Solution</b>	<b>Approximate Solution</b>	<b>Difference</b>
1	10.3 Hz	11.7 Hz	12%
2	14.0 Hz	15.5 Hz	10%
3	19.2 Hz	21.7 Hz	10%

It can be seen that the MARC solution is different from the analytical one by no more than 12%; the analytical solution is approximate. The three different modes are shown in Figure 6.10-2.

**Parameters, Options, and Subroutines Summary**

Example e6x10.dat:

<b>Parameters</b>	<b>Model Definition Options</b>	<b>History Definition Options</b>
DYNAMIC	CONNECTIVITY	CONTINUE
ELEMENT	COORDINATE	MODAL SHAPE
END	END OPTION	RECOVER
SIZING	FIXED DISP	
TITLE	GEOMETRY	
	ISOTROPIC	
	MASSES	
	POST	
	TYING	

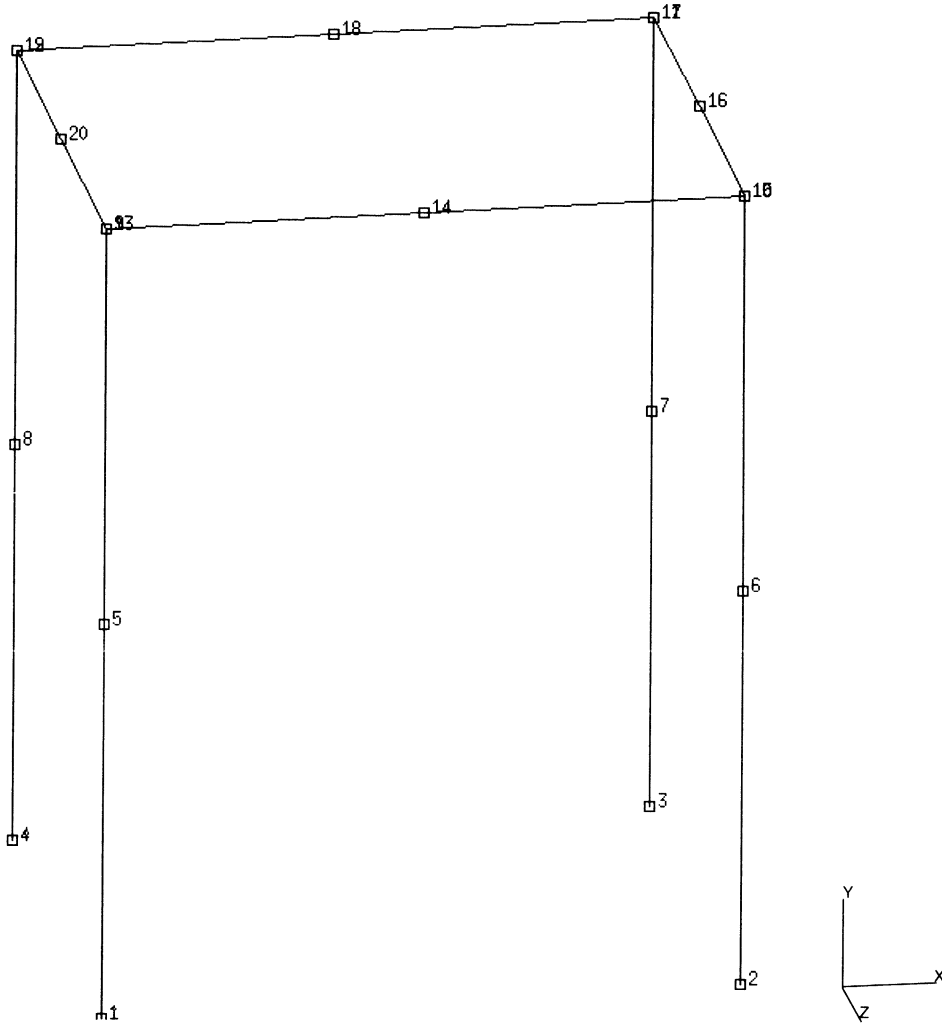
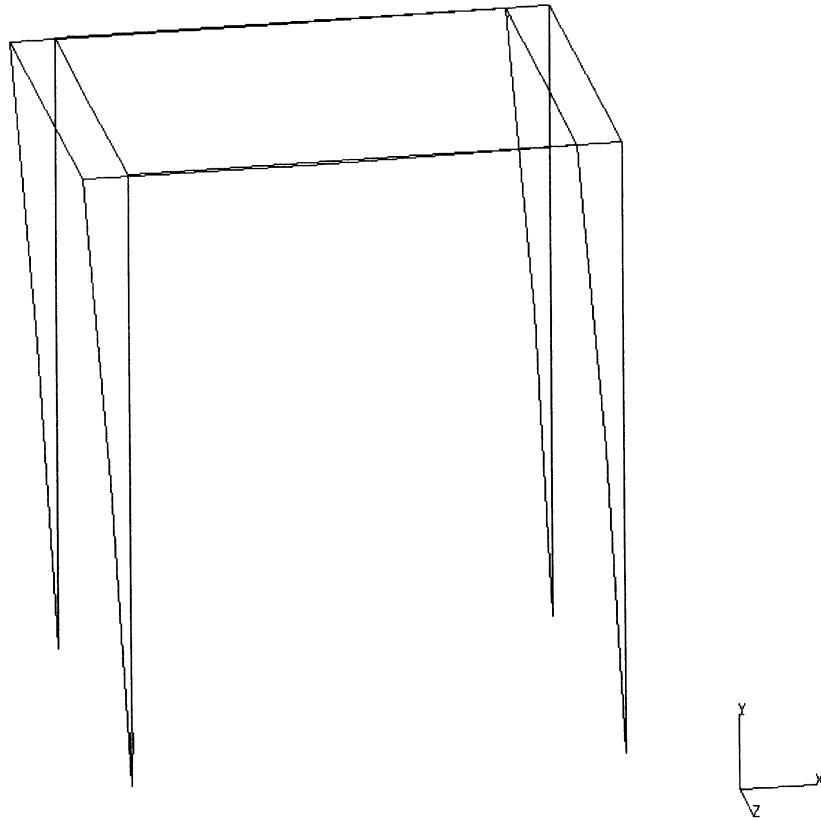


**Figure 6.10-1** Alternator Mount Model



INC : 0  
SUB : 1  
TIME : 0.000e+00  
FREQ : 6.450e+01

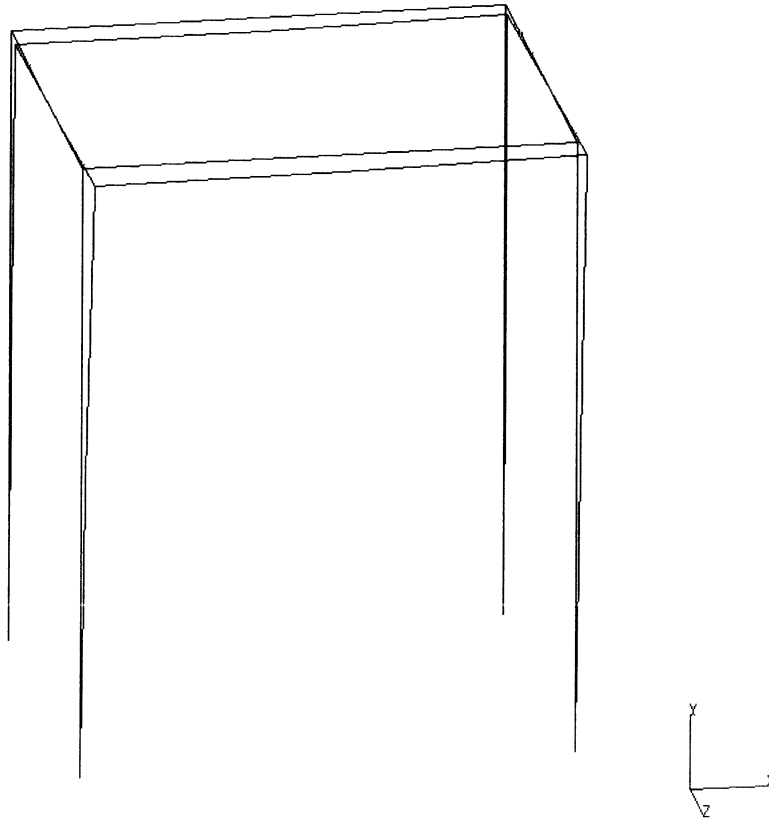


prob e6.10 dynamics elmt 52

Figure 6.10-2 First Mode



INC : 0  
SUB : 2  
TIME : 0.000e+00  
FREQ : 8.782e+01

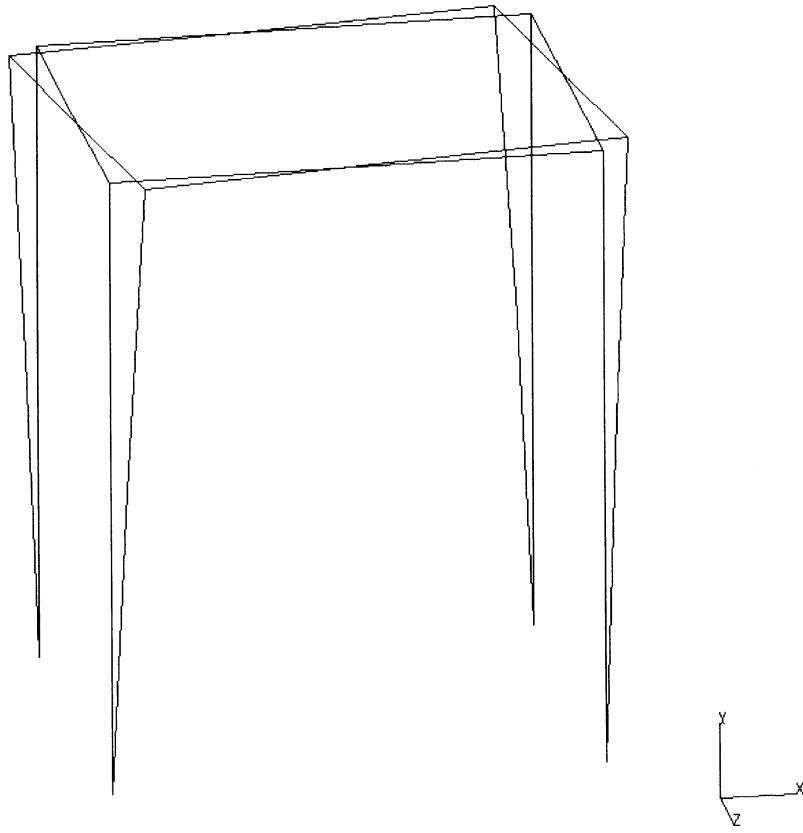


prob e6.10 dynamics elmt 52

**Figure 6.10-3** Second Mode



INC : 0  
SUB : 3  
TIME : 0.000e+00  
FREQ : 1.192e+01



prob e6.10 dynamics elmt 52

**Figure 6.10-4** Third Mode

## 6.11 Modal Analysis of a Wing Caisson

The modal analysis is performed of a thin-walled caisson in a wing structure. The problem is simplified by assuming the cross-section of the wing to remain constant.

In this case, the MARC results are compared with approximate analytical results.

### Element

Elements type 30 are used in the mesh. They are 8-node, second order isoparametric membrane elements, and have three global coordinates (x,y,z) at each node. The stress state of element 30 is that of a flat membrane.

### Model

The generated mesh is shown in Figure 6.11-1. It has 174 elements and 353 coordinates.

### Geometry

The caisson is 6000 mm long and the section is 1200 mm x 200 mm. The following geometric properties of the structure are computed, to be used in the analytical solution:

bending moment of inertia	$I_x = 2.6984 \times 10^7 \text{ mm}^4$
bending moment of inertia	$I_y = 4.6764 \times 10^8 \text{ mm}^4$
polar moment of inertia	$I_r = 4.9473 \times 10^8 \text{ mm}^4$

### Material Properties

The element properties are uniform; the material is elastic. Values for Young's modulus and Poisson's ratio are respectively  $E = 7750 \text{ kg/mm}^2$  and  $\nu = 0.3$ ; density is  $\rho = 2.75 \text{ kg/mm}^3$ .

### Boundary Conditions

The model is clamped in the first 22 nodes, along the edge at  $y = 0$ .

### Approximate Analytic Solution

The structure has been analyzed as a thin-walled closed section beam. The first two bending modes are:

$$\omega_n = K_n^2 \frac{\pi^2}{l^2} \sqrt{\frac{EI}{M}}$$

where  $K_1 = 0.597$  and  $K_2 = 1.49$ . Thus,

$$\begin{aligned}\omega_1 &= 46.3 \text{ rad/sec} \\ \omega_2 &= 169.2 \text{ rad/sec}\end{aligned}$$

The torsional frequency is:

$$\omega_4 = n \frac{\pi}{2l} \sqrt{\frac{GJ}{I_o}} = 353.29 \text{ rad/sec}$$

**Results**

The approximate solutions provided by beam theory are compared with the results from MARC as shown below. The largest difference among the first three modes is 6%.

Eigenvalue	MARC Output	Approximate Solution	Difference
1	43.3	46.3	6%
2	172.1	169.2	2%
3	342.3	353.3	3%

**Parameters, Options, and Subroutines Summary**

Example e6x11.dat:

Parameters	Model Definition Options	History Definition Options
DYNAMIC	CONNECTIVITY	CONTINUE
END	COORDINATE	MODAL SHAPE
LINEAR	END OPTION	
SIZING	FIXED DISP	
TITLE	ISOTROPIC	
	POINT LOAD	
	POST	

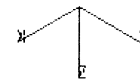
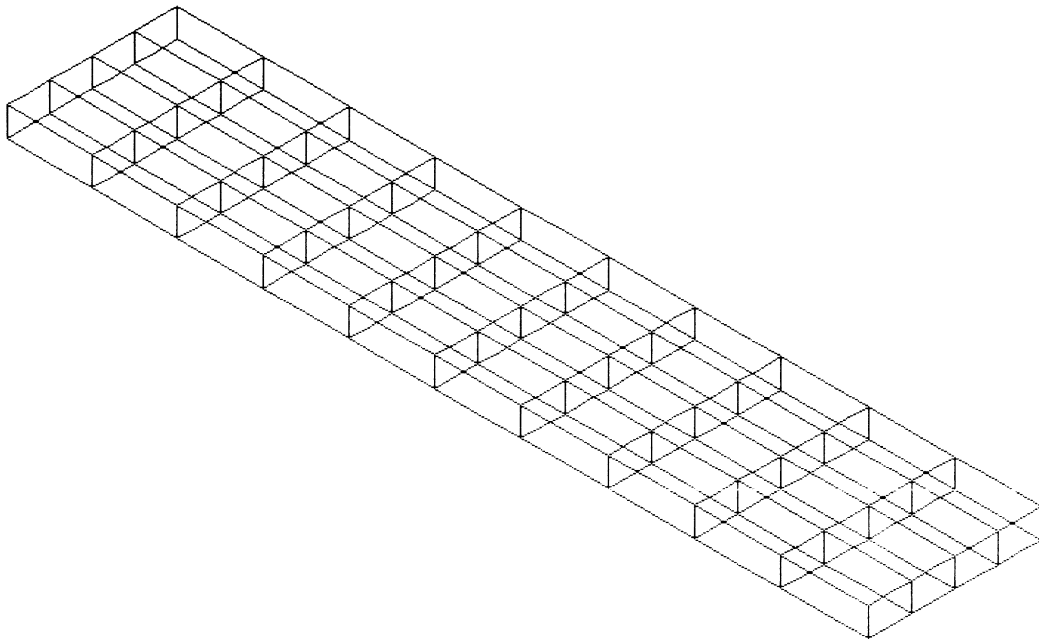


**Figure 6.11-1** Mesh of a Wing Structure



## 6.12 Vibrations of a Cable

The first two modal frequencies are computed for a straight flexible cable. The MARC results are checked against the analytical solution.

### Element

Element type 9, a three-dimensional two-node straight truss, is used. It has three coordinates per node in the global x, y, and z directions and an uniaxial state of stress.

### Model

The mesh is generated using the CONN GENER option. It has 11 elements and 12 nodes. One end is fixed; the other is free.

### Material Properties

The density is uniform throughout the cable and it is  $\rho = 84.969 \text{ t/m}^3$ . The Young's modulus varies along the length of the cable:

$$0 < L < 4.31 \text{ m} \quad E = 1.4715 \times 10^8 \text{ kN/m}^2$$

$$4.31 < L < 96.5 \text{ m} \quad E = 6.658 \times 10^6 \text{ kN/m}^2$$

### Geometry

The cable has length  $L = 96.5 \text{ m}$  and  $A = 2.54 \times 10^{-4} \text{ m}^2$ .

### Loading

A normal force is applied at the free end and its value is  $p = 49.05 \text{ kN}$ .

### Analytical Solution

The analytical formula for the modal frequencies of a prestressed cable is:

$$f_n = \frac{n}{2} \sqrt{\frac{p}{\rho A L^2}}$$

In this case, we obtain  $f_1 = 0.247 \text{ Hz}$  and  $f_2 = 0.494 \text{ Hz}$ .

### Results

The structure is not statically stable. Thus it has been necessary to use a nonlinear step of PROPORTIONAL INCREMENT, to apply the load before asking for the modes. This option forces the assembly of the incremental stiffness matrix.

The results are as follows:

<b>Eigenvalue</b>	<b>MARC Output</b>	<b>Analytical Solution</b>
1	0.2477 Hz	0.247 Hz
2	0.5010 Hz	0.494 Hz

It can be seen that the MARC results are very close to the analytical results. In fact, the larger difference is only 1.3%.

### **Parameters, Options, and Subroutines Summary**

Example e6x12.dat:

#### **Parameters**

DYNAMIC  
END  
LARGE DISP  
SIZING  
TITLE  
UPDATE

#### **Model Definition Options**

CONNECTIVITY  
COORDINATE  
END OPTION  
FIXED DISP  
GEOMETRY  
ISOTROPIC  
POINT LOAD  
POST

#### **History Definition Options**

CONTINUE  
MODAL SHAPE  
PROPORTIONAL INCREMENT



## 6.13 Perfectly Plastic Beam Explosively Loaded

This demonstration problem illustrates the use of the adaptive time-stepping procedure for the analysis of a beam subjected to an impulsive load. The beam is elastic, perfectly plastic. The analysis is performed twice, first with no geometric nonlinearities included, and then doing a finite strain plasticity, updated Lagrange analysis.

A simple beam with built-in ends is modeled using element type 16. Only one half of the beam is used because of symmetry. The model consists of five elements with six nodes. The beam is five inches long.

This problem is modeled using the two techniques summarized below.

Data Set	Element Type(s)	Number of Elements	Number of Nodes	Differentiating Features
e6x13	16	5	6	AUTO TIME
e6x13b	16	5	6	

### Geometry

The beam has a height of 0.125 inches and a depth of 1.2 inches.

### Material Properties

Young's modulus is  $10.4 \times 10^6$  psi, and Poisson's ratio is 0.3. The mass density is  $2.5 \times 10^{-4}$  lb/in<sup>3</sup>. The yield stress is 41,400 psi and there is no work hardening in the material.

### Boundary Conditions

The first node is given the boundary conditions of built in  $u = v = \frac{\partial v}{\partial s} = 0$ .

The last node is given the symmetry boundary conditions  $u = \frac{\partial v}{\partial s} = 0$ .

### Loading

The problem is driven by the initial conditions, which are a large initial velocity at the center of the beam. An initial condition of 5020 in/second is applied at nodes 5 and 6.

### Control

The AUTO TIME option is used to control the time step size. The procedure is such that if the residuals are large compared to the reactions, the time step is reduced. If the convergence is well satisfied, the time step is increased in the next increment. The initial time step is chosen as 5 x



$10^{-6}$  s. This time step was chosen such that  $[\Delta t \cdot V_o]$  was small compared to the other geometric dimensions. The total time to be modeled is  $1.5 \times 10^{-3}$ s. A maximum of 100 steps is allowed.

### Results

Figure 6.13-2 through Figure 6.13-4 show the displacements, velocities, and accelerations for the small displacement analysis. Figure 6.13-5 through Figure 6.13-7 show the results for the large displacement analysis. Each mark on the graph indicates a new increment; hence, you can observe the change in the time step. In the problem including geometric nonlinearities, many more time steps are used to remain in equilibrium. You can observe that there is a large acceleration initially, which reverses the sign for the center node and then begins to approach zero.

### Parameters, Options, and Subroutines Summary

Example e6x13.dat:

#### Parameters

DYNAMIC  
ELEMENT  
END  
SIZING  
TITLE

#### Model Definition Options

CONNECTIVITY  
CONTROL  
COORDINATE  
END OPTION  
FIXED DISP  
GEOMETRY  
INITIAL VELOCITY  
ISOTROPIC  
POST  
PRINT CHOICE  
RESTART

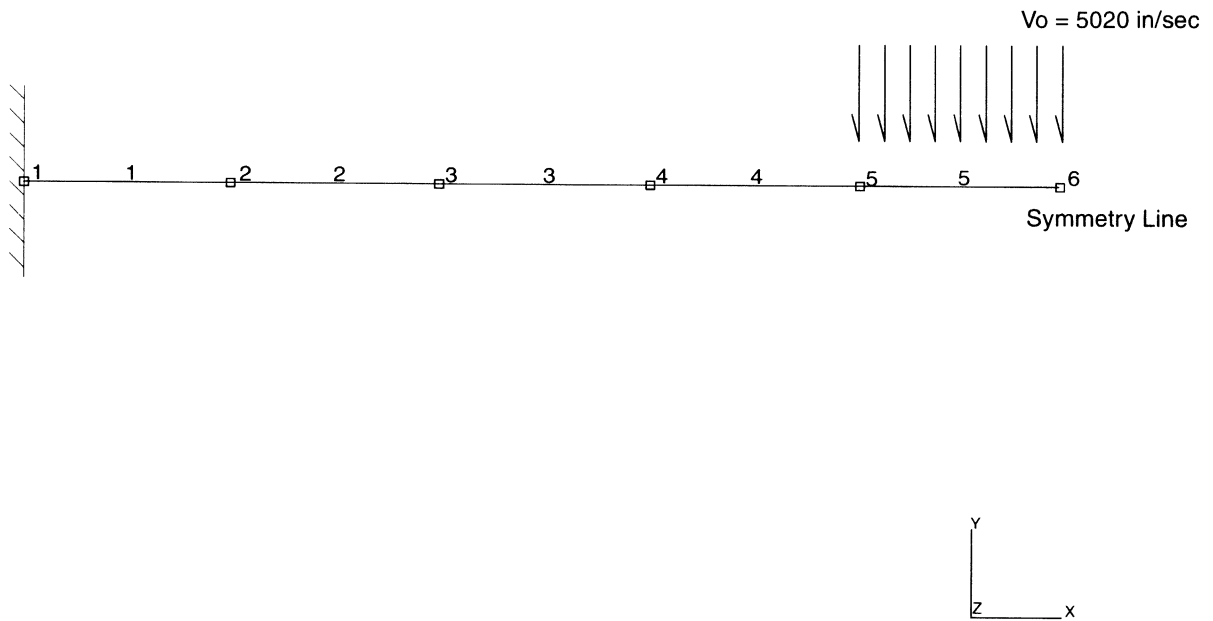


**Figure 6.13-1** Mesh with Initial Velocity

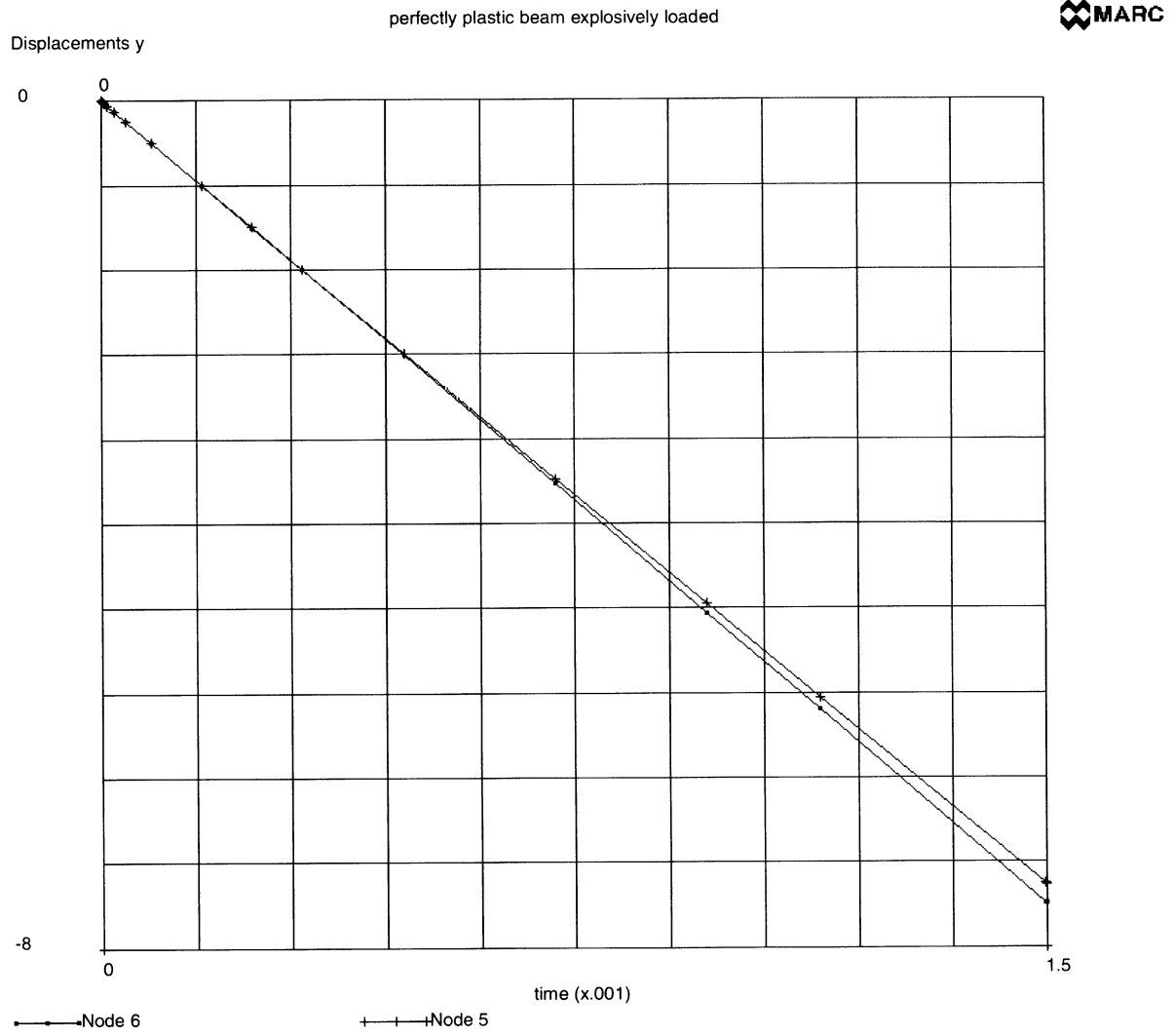


**Figure 6.13-2** Small Displacement Analysis

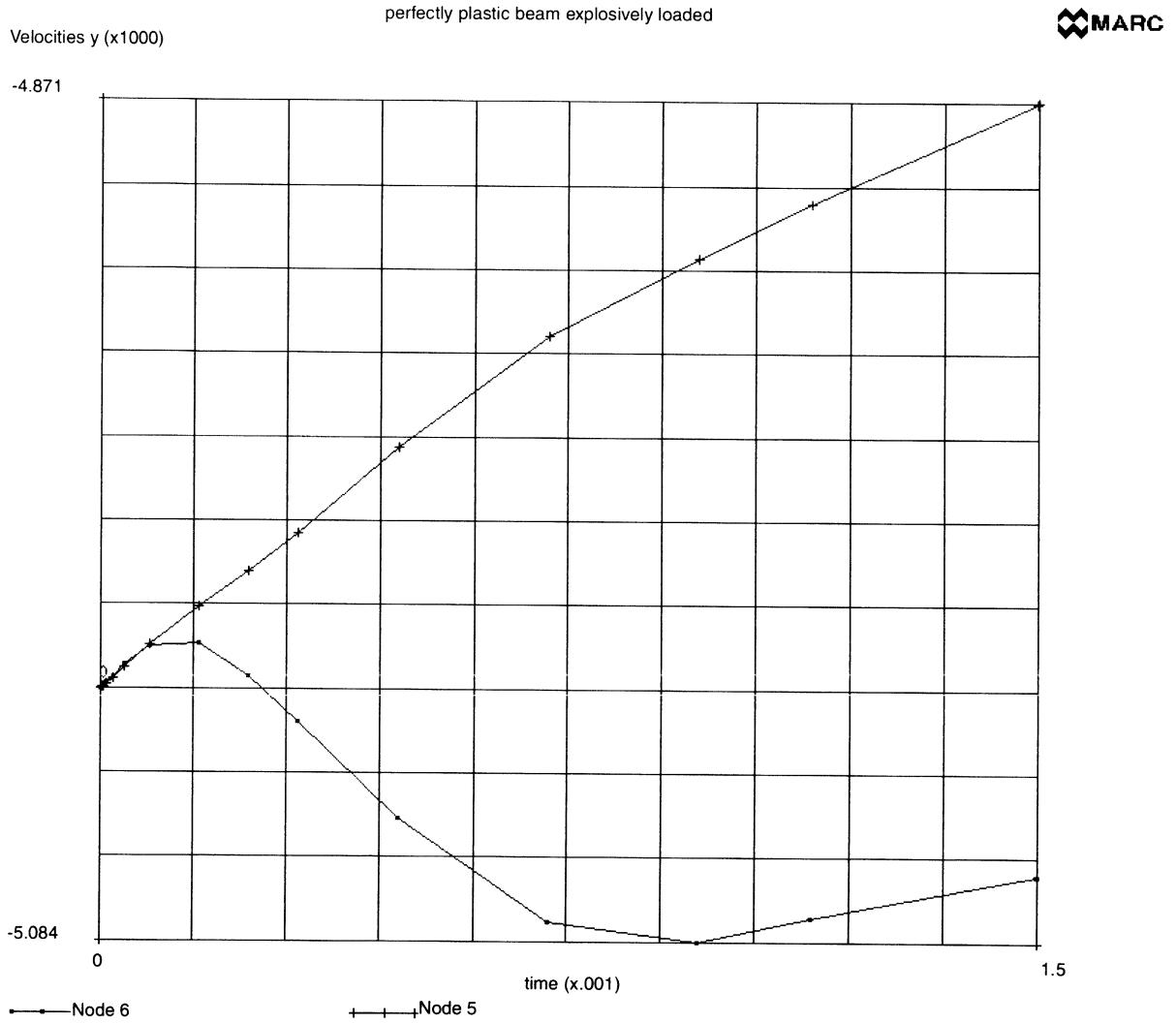
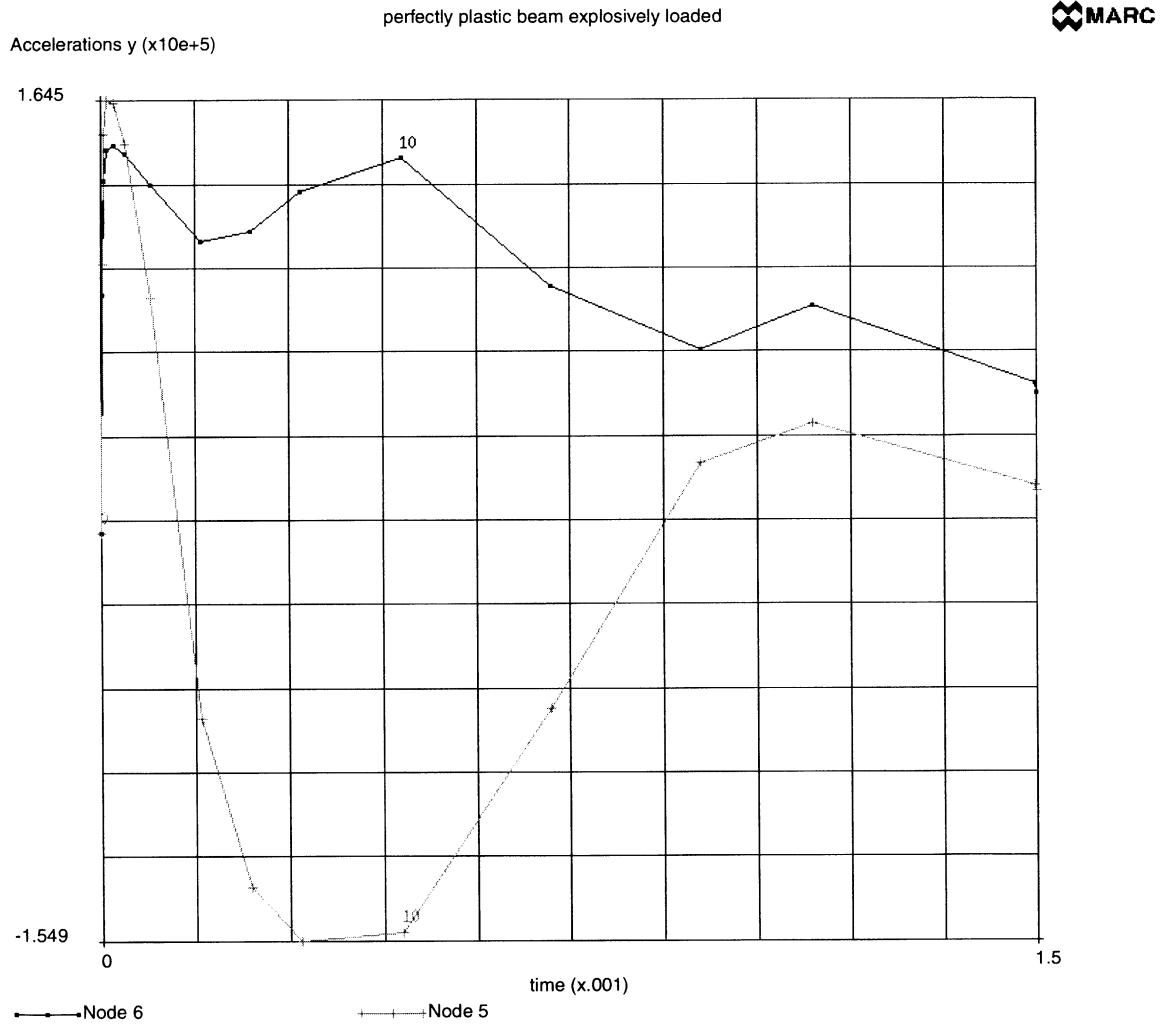
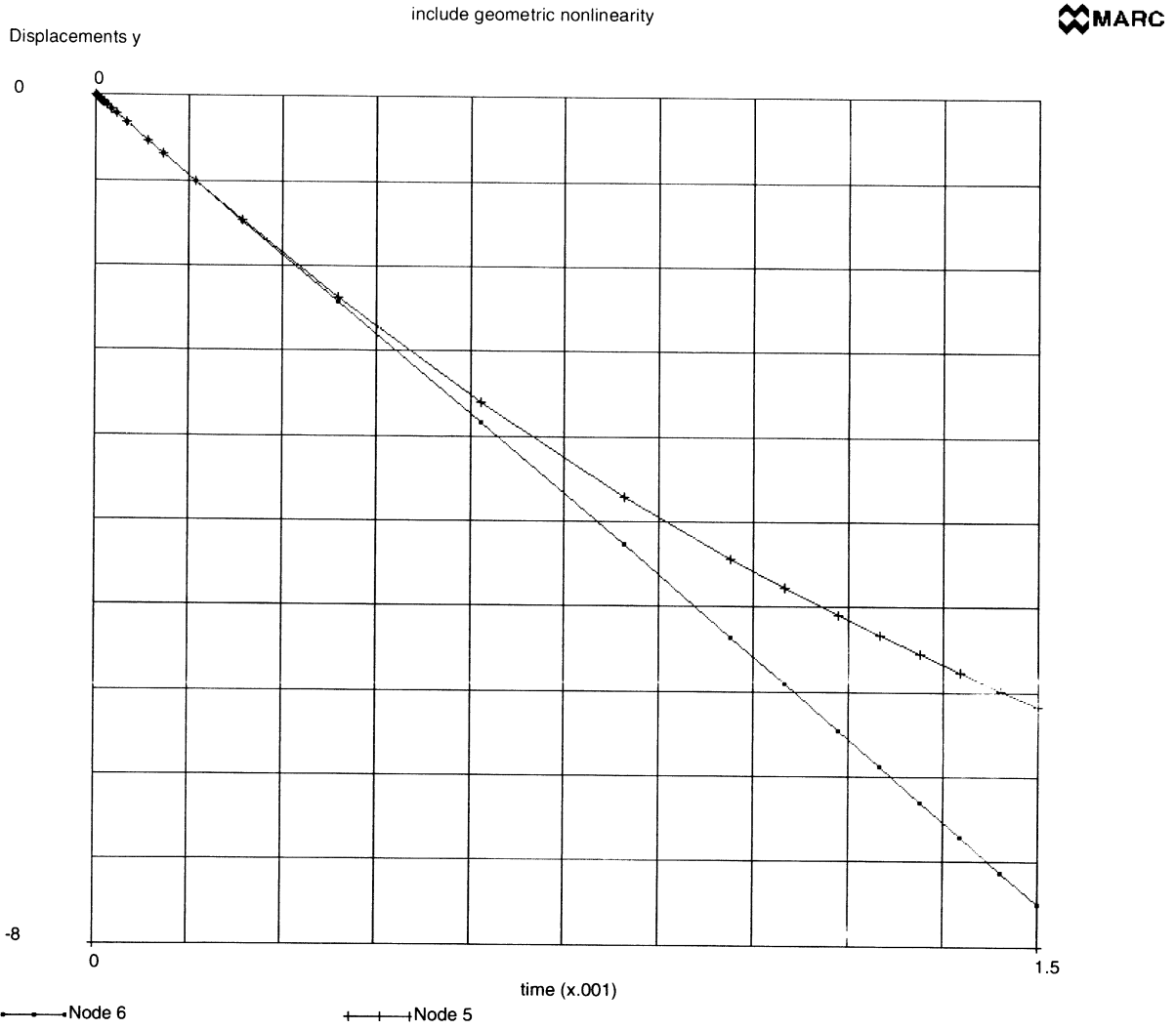


Figure 6.13-3 Small Displacement Analysis



**Figure 6.13-4** Small Displacement Analysis



**Figure 6.13-5** Includes Geometric Nonlinearity

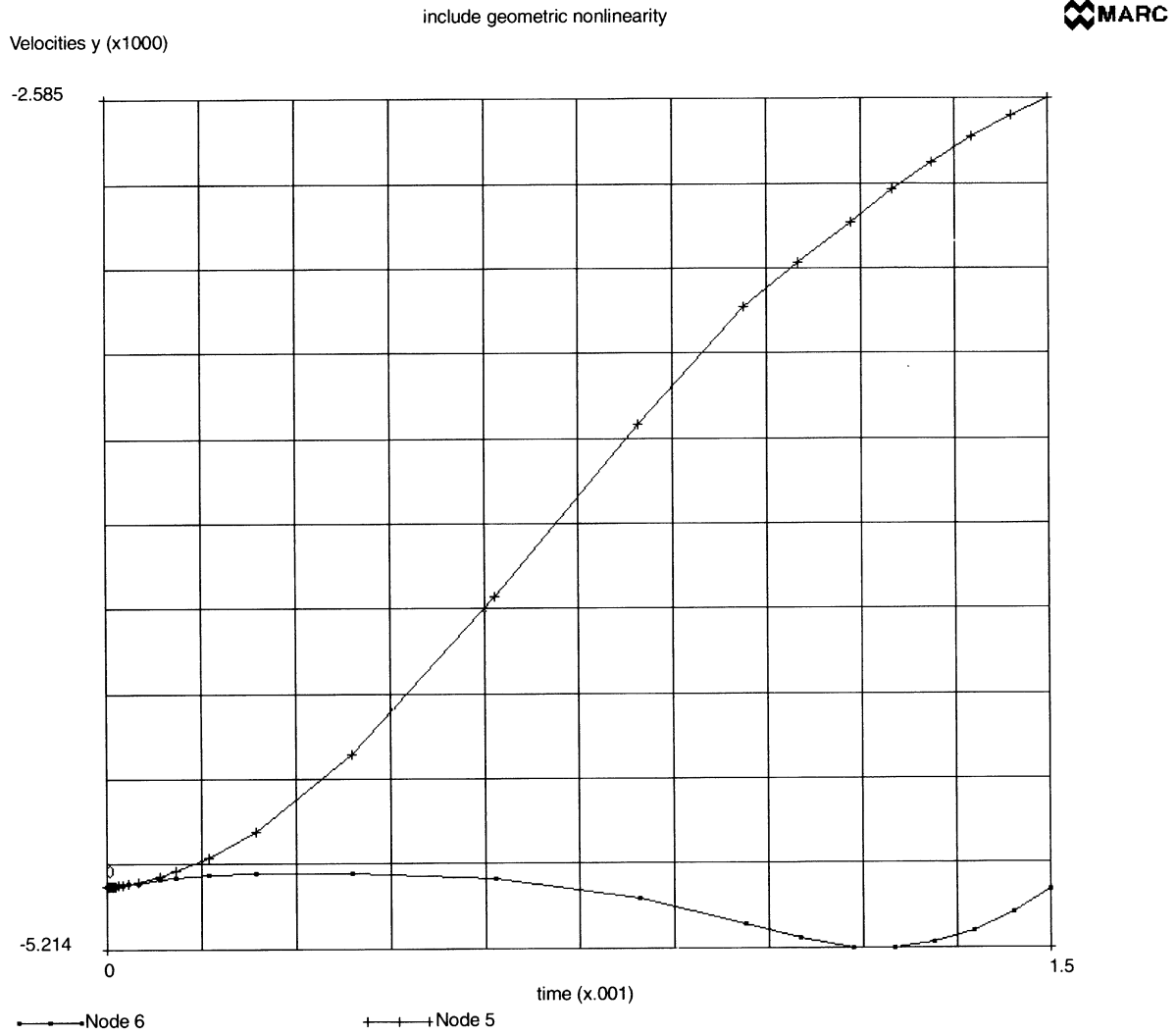


Figure 6.13-6 Includes Geometric Nonlinearity



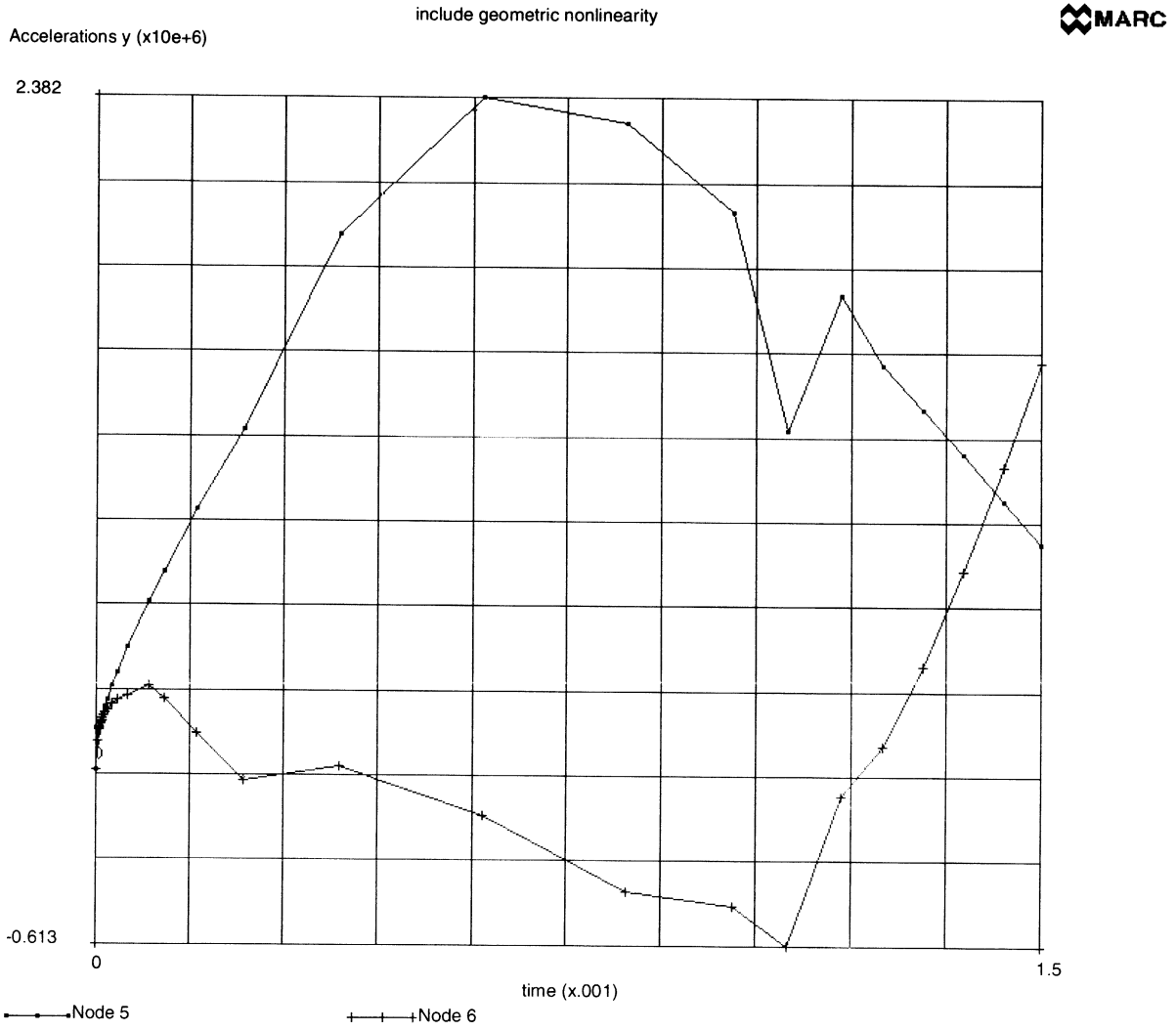


Figure 6.13-7 Includes Geometric Nonlinearity



## 6.14 Dynamic Fracture Mechanics

This example illustrates the use of the DeLorenzi method [1] to evaluate J-integral values in MARC for dynamically responding structures. The problem consists of a center-cracked plate which is initially at rest, and which is subjected to a uniform tensile load that is suddenly applied and then maintained for  $t > 0$ . This problem was originally analyzed by Chen [2] who used a finite difference method. Over the past years, it has become more or less a benchmark problem for demonstrating the applicability of various alternative procedures to calculate dynamic stress intensity factors. See Brickstad [3] and Jung [4].

Details on the dimensions, material properties, and loading conditions are given in Figure 6.14-1.

### Element

Element type 27 is an 8-noded plane strain quadrilateral.

### Model

Because of symmetry, only one quarter of the plate is modeled. A graded mesh subdivision is chosen, identical to the mesh used in [4]. No quarter-point elements are used. Figure 6.14-2 shows the finite element model.

### Geometry

No geometry is specified and thus a unit thickness is assumed by MARC.

### Material Properties

The Young's modulus is set to  $2000 \text{ N/cm}^2$  and Poisson's ratio is 0.3. The mass density amounts to  $5 \text{ g/cm}^3$ . In order to obtain consistent units, a value of  $5.0 \times 10^{-5}$  has to be entered in the mass density field of the ISOTROPIC block.

### Boundary Conditions

Because of symmetry conditions all nodal DOF's in the first coordinate direction are suppressed along  $x = 0$ . All nodal DOF's in the second coordinate direction are suppressed along the uncracked part of  $y = 0$ .

### Loading

The step function in the tensile load is specified as follows:

- increment 0 :  $\sigma = 0$
- increment 1 :  $\Delta\sigma = 40000 \text{ N/cm}^2$
- increment  $> 1$  :  $\Delta\sigma = 0$

The full tensile load is applied in a single short time step of  $1 \times 10^{-4}$   $\mu\text{sec}$ . The implicit Newmark-beta method with a constant time step of 0.15  $\mu\text{sec}$ . is employed for the direct time integration up to a time of 12  $\mu\text{sec}$ . The time step is chosen such that the longitudinal wave reaches the crack-plane in approximately 10 increments. Because of the linear nature of the problem the control value for residual checking has been set to a large value (that is, 10).

**Lorenzi**

A unit crack extension of 1 cm. has been specified for three different paths. The first J-value is based on a unit movement of the crack tip only. Elements 3 and 4 will be the only deforming elements. The second J-value is based on a rigid movement of the first ring of elements (3 and 4). The third J-value is based on a rigid movement of the first and second ring of elements. In order to incorporate all inertia effects, all movements of the nodes in the regions with “rigid” movements must be specified. Figure 6.14-3 shows the relevant element and node numbers in the crack-tip region.

**Results**

MARC provides for the output of the strain energy changes per crack movement for each increment. These values have to be normalized by the crack opening area to obtain the J-values. Because of symmetry, the actual strain energy that can be released at every crack tip is twice the value that is printed out. In addition, the J-values can be converted to  $K_I$  values using the relation:

$$K_I = \sqrt{\frac{E}{1-\nu^2}} J$$

Table 6.14-1 summarizes the J-values that are obtained for the first path as well as the normalized  $K_I$  values (that is,  $K_I/\sigma\sqrt{\pi a}$ ) for every 10th increment. More details about the results and a comparison with other numerical solutions can be found in [5]. Figure 6.14-4 shows the dynamic stress intensity factors normalized with respect to a static stress intensity factor of an infinite plate as a function of time for the complete analysis.

**Table 6.14-1** Normalized Dynamic Stress Intensity Factors

Increment Number	Time ( $\mu\text{sec}$ )	J/2	$K_{\text{dynamic}}/\sigma\sqrt{\pi a}$
11	1.5	0.103E-4	0.0061
21	3.0	29.92	1.0442
31	4.5	82.26	1.7313

**Table 6.14-1** Normalized Dynamic Stress Intensity Factors (Continued)

Increment Number	Time (μsec)	J/2	$K_{dynamic}/\sigma\sqrt{\pi a}$
41	6.0	171.50	2.4998
51	7.5	146.62	2.3114
61	9.0	45.58	1.2887
71	10.5	11.91	0.6588

**References**

1. DeLorenzi, H.G., "On the Energy Release Rate and the J-integral for 3D Crack Configurations", *Inst. J. Fracture*, Vol. 19, 1982, pp. 183-193.
2. Chen, Y.M., "Numerical Computation of Dynamic Stress Intensity Factors" by a Lagrangian Finite Difference Method (the HEMP Code)", *Eng. Fract. Mech.*, Vol. 7, 1975, pp. 653-660.
3. Brickstad, B., "A FEM Analysis of Crack Arrest Experiments", *Int. J. Fract.*, Vol. 21, 1983, pp. 177-194.
4. Jung, J., Ahmad, J., Kanninen, M.F. and Popelar, C.H., "Finite Element Analysis of Dynamic Crack Propagation", presented at the 1981 ASEM Failure Prevention and Reliability Conference, September 23-26, 1981, Hartford, Conn., U.S.A.
5. Peeters, F.J.H. and Koers, R.W.J., "Numerical Simulation of Dynamic Crack Propagation Phenomena by Means of the Finite Element Method", *Proceedings of the 6th European Conference on Fracture*, ECF6, Amsterdam, The Netherlands, June 15-20, 1986.

**Parameters, Options, and Subroutines Summary**

Example e6x14.dat:

Parameters	Model Definition Options	History Definition Options
DYNAMIC	CONNECTIVITY	CONTINUE
ELEMENT	CONTROL	DIST LOADS
END	COORDINATE	DYNAMIC CHANGE
SIZING	DIST LOADS	
TITLE	END OPTION	
	FIXED DISP	
	ISOTROPIC	
	LORENZI	
	NO PRINT	

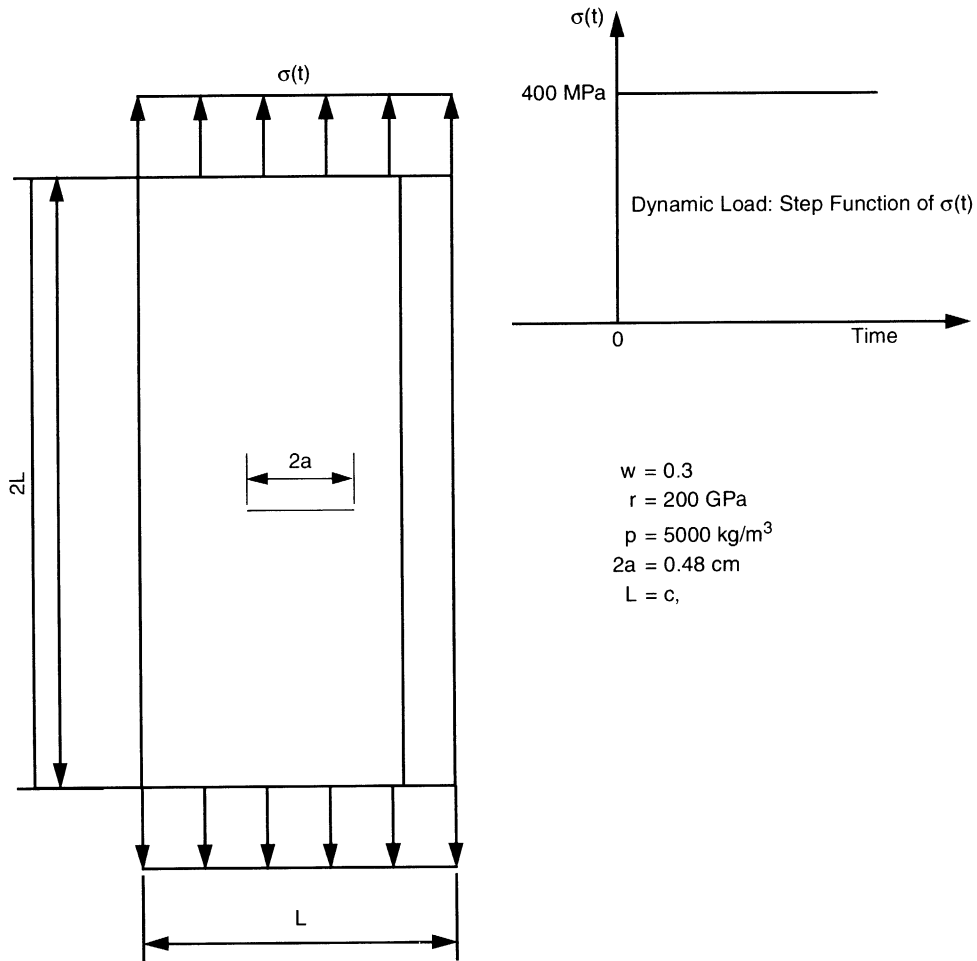
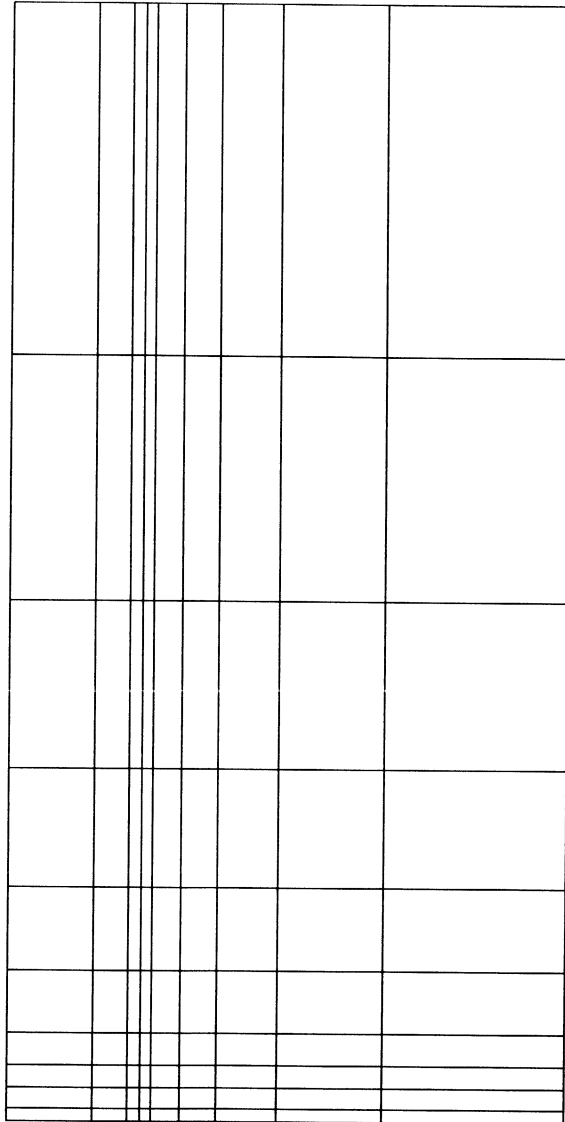
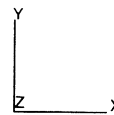


Figure 6.14-1 Dynamically Loaded Center-Cracked Rectangular Plate Problem



 MARC



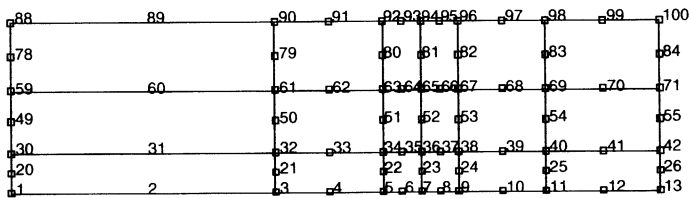
**Figure 6.14-2** Dynamic Crack Problem Mesh



19	20	21	22	23	24
10	11	12	13	14	15
1	2	3	4	5	6



Element Numbers



Node Numbers

**Figure 6.14-3** Crack Tip Region



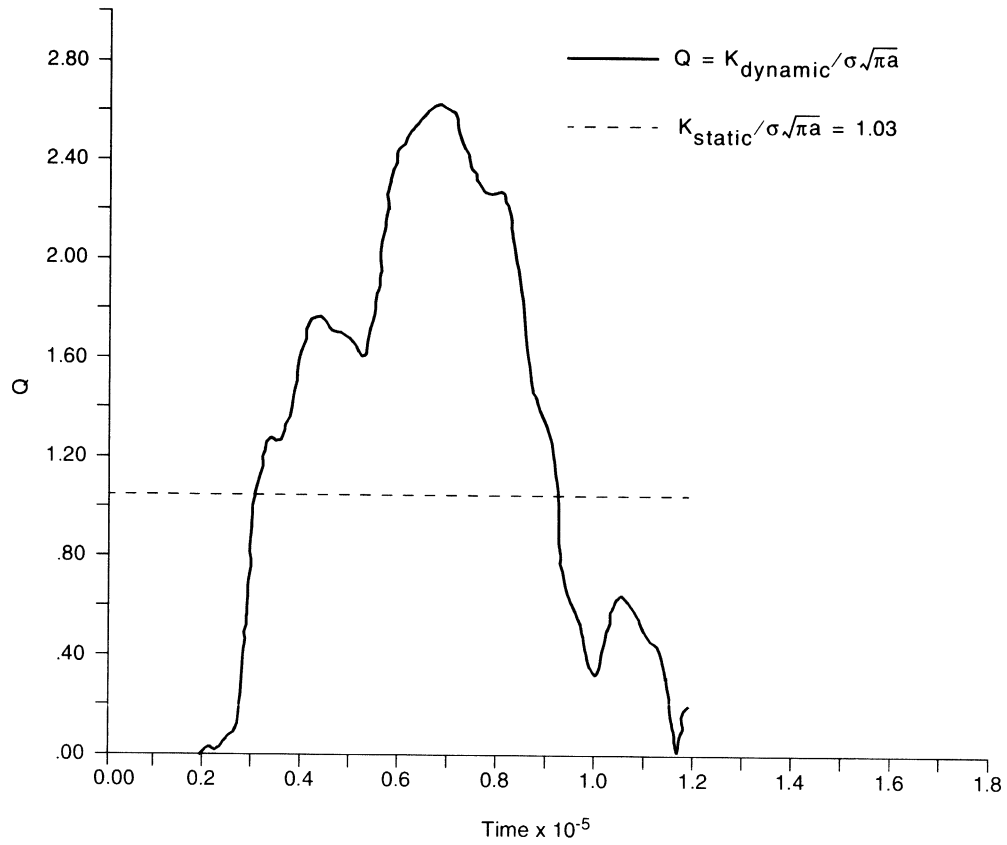


**Figure 6.14-4** Normalized Dynamic Stress Intensity Factors



## 6.15 Eigenmodes of a Plate

In this problem, the eigenvalues are calculated for a cantilevered, rectangular plate, using element type 7. In the first case, the assumed strain formulation is used. In the second case, the conventional isoparametric element is used. This eigenproblem illustrates the superiority of the assumed strain element over the conventional isoparametric element in the plate or shell analyses.

This problem is modeled using the two techniques summarized below.

Data Set	Element Type(s)	Number of Elements	Number of Nodes	Differentiating Features
e6x15	7	392	870	Assumed strain
e6x15b	7	392	870	Without assumed strain

### Model

The plate is of length 0.6 inch and width 0.25 inch and thickness of 0.003 inch. It is modeled using a 28x14 mesh of element type 7, eight-node brick as shown in Figure 6.15-1. Four eigenvalues are extracted using the inverse power sweep method. The lumped mass matrix is formed.

### Geometry

In the first case, a “1” is placed in the third field to indicate that the assumed strain formulation is to be used.

### Material Properties

The material has a Young’s modulus of  $26 \times 10^6$  psi, and a Poisson’s ratio of 0.32. The mass density is 0.000755 lb/in<sup>3</sup>.

### Boundary Conditions

The one end is completely constrained to represent the cantilevered boundary conditions. The other end is simply supported at its midpoint.

### Results

The frequencies calculated are summarized in Table 6.15-1. For comparison, the results using element 75 are also included.



**Table 6.15-1** Frequencies in Hertz

Mode	Assumed Strain Element	Conventional Isoparametric Element	Element 75
1	1140	1929	1140
2	1323	5024	1324
3	3551	8469	3553
4	4235	14713	4239

One observes that using the conventional elements, the frequencies are significantly higher and incorrect. This is because the element is too stiff in bending. The agreement between the assumed strain element and the shell element is very good.

Figure 6.15-2 and Figure 6.15-3 show the first and third mode shapes.

**Parameters, Options, and Subroutines Summary**

Example e6x15.dat:

Parameters	Model Definition Options	History Definition Options
DYNAMIC	CONNECTIVITY	CONTINUE
ELEMENT	COORDINATE	MODAL SHAPE
END	END OPTION	
LUMP	FIXED DISP	
PRINT	GEOMETRY	
SIZING	ISOTROPIC	
TITLE		

Example e6x15b.dat:

Parameters	Model Definition Options	History Definition Options
DYNAMIC	CONNECTIVITY	CONTINUE
ELEMENT	COORDINATE	MODAL SHAPE
END	END OPTION	
LUMP	FIXED DISP	
SIZING	GEOMETRY	
TITLE	ISOTROPIC	

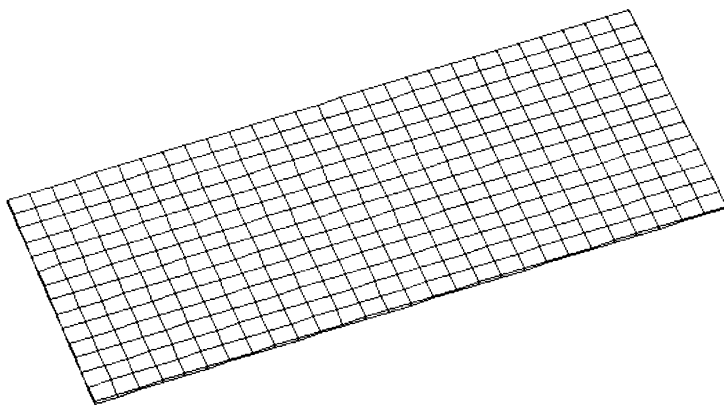
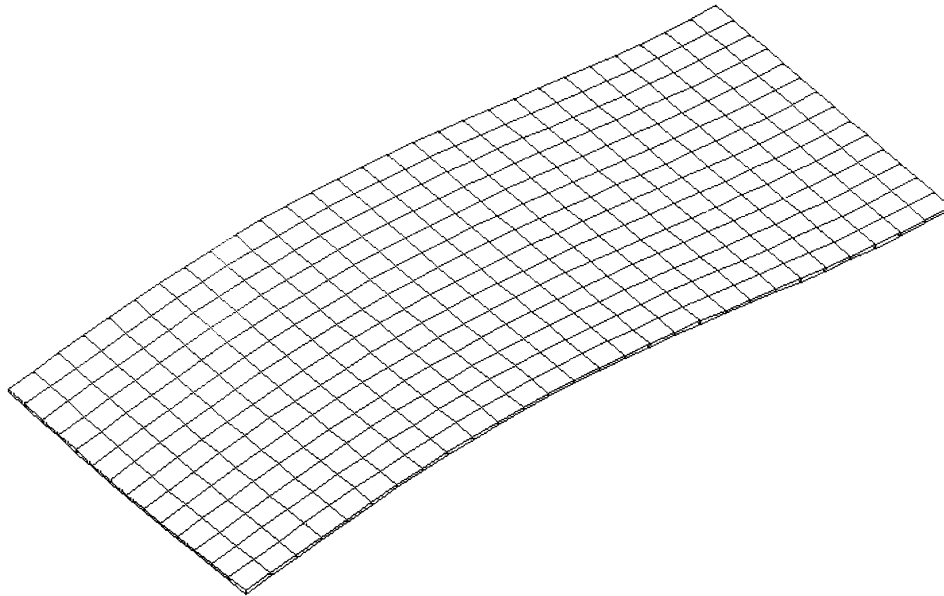


**Figure 6.15-1** Mesh

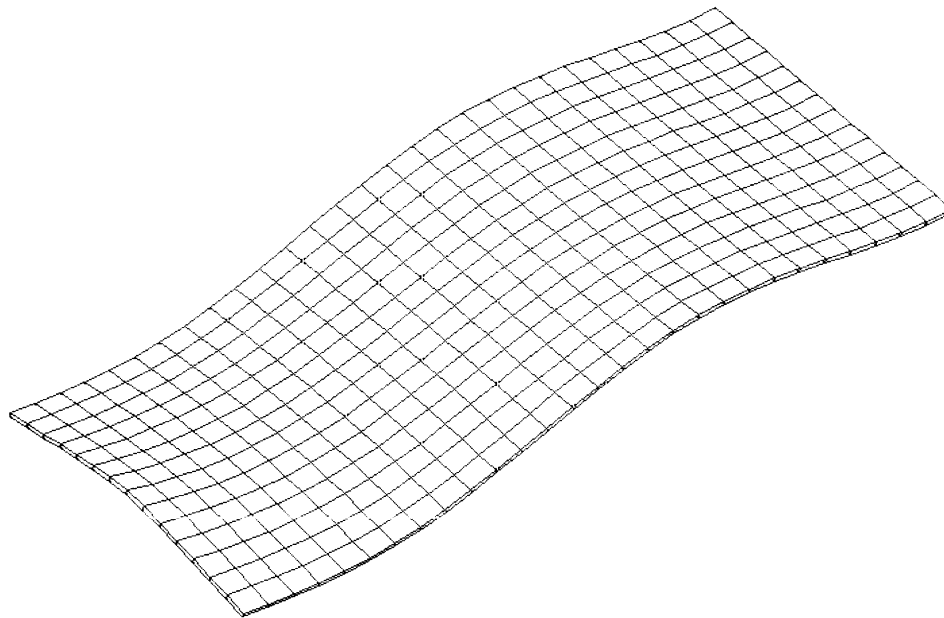
INC : 0  
SUB : 1  
TIME : 0.000e+00  
FREQ : 7.163e+03

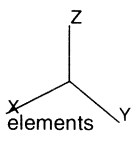


modal shape using assumed strain elements

**Figure 6.15-2** First Mode Shape of Cantilevered Plate

INC : 0  
SUB : 3  
TIME : 0.000e+00  
FREQ : 2.232e+04



modal shape using assumed strain elements 

**Figure 6.15-3** Third Mode Shape of Cantilevered Plate





## 6.16 Dynamic Contact Between a Projectile and a Rigid Barrier

This problem demonstrates the dynamic impact between a deformable body and a rigid surface. The problem is executed using both an implicit Newmark-beta operator and the explicit central difference operator.

This problem is modeled using the four techniques summarized below.

Data Set	Element Type(s)	Number of Elements	Number of Nodes	Differentiating Features
e6x16a	7	9	32	DYNAMIC,2 DEF-RIGID
e6x16b	7	9	32	DYNAMIC,4 DEF-RIGID
e6x16c	7	9	32	DYNAMIC,5 DEF-RIGID

### Model

A deformable projectile consists of nine element type 7, eight-node bricks as shown in Figure 6.16-1. As an alternative, the analysis is also performed with element type 120 which is the reduced integration formulation. The projectile is initially 0.1 units away from the rigid surface. The DYNAMIC parameter specifies which operator is to be chosen: a “2” indicates Newmark-beta and a “4” indicates central difference. The projectile may undergo large deformations, so a LARGE DISP parameter is included. The projectile is considered elastic and a total Lagrange analysis is performed.

### Material Properties

An artificial material was created, such that the stability limit for central difference was a large number. The Young’s modulus is 10,000 psi and the mass density is 0.1 lbf-sec<sup>2</sup>/in<sup>4</sup>. A lumped mass matrix is created based upon the LUMP parameter. The projectile is given a numerical damping of 0.4. Numerical dampening is preferred over stiffness damping, because the time step can change in contact analyses, resulting in stiffness damping overdamping the system.

Given the material parameters, the elastic wave speed is  $c = \sqrt{E/\rho} = 316 \text{ in./s}$ .

### Boundary Conditions

The nodes on the xz-plane have been constrained in the y-direction. The nodes on the xy-plane have been constrained in the z-direction. The projectile has an initial velocity of -100 in/second in the x-direction.

**Controls**

The maximum number of increments is 100 with the maximum number of iterations being three. Relative displacement error control is used with a tolerance value of 10%. Note that when using the explicit dynamic method, iteration does not occur. A formatted post file is written which contains only nodal information. The restart file is written at every increment.

**Contact**

There are two bodies in this analysis. The first is the deformable projectile. The second is the rigid barrier. There is no friction between these two surfaces.

The other parameters on the second block are upper bounds to the number of surface entities and surface nodes.

The contact tolerance is 0.03 inch which is small compared to an element dimension. A very large separation force is given which effectively ensures that the projectile sticks to the barrier.

The first body is the deformable one consisting of nine elements. The second body consists of one patch. The order of the numbering ensures the correct normal direction is associated with the rigid surface.

**Time Step**

The time step chosen is 0.0005 second which is below the stability limit of 0.002 second. In this period, the elastic wave travels 0.158 inch which is smaller than a typical element dimension. The total period is 0.01 second, so 20 increments are performed.

**Results**

Figure 6.16-3 and Figure 6.16-4 show the projectile at increment two after contact first occurs, and at increment 20 at the end of the analysis. Figure 6.16-5, Figure 6.16-6, and Figure 6.16-7 show the displacement, velocity, and reaction forces at selected nodes for the Newmark-beta analysis and central difference analysis. You can observe that the results are almost indistinguishable. Node 26 first comes into contact at increment 2, the displacement is .1 and remains fixed for the remainder of the analysis; velocity is zero. Node 25 comes into contact during increment 10 and remains fixed the remainder of the analysis. Nodes 31 and 32 simply decelerate during the analysis. The reactions show that spikes occur at the increments where contact occurs. The results using the reduced integration element are not substantially different.

The implicit Newmark-beta ran three times longer. This is an anomaly due to the fact that an artificial material was created such that the time steps in the two procedures were allowed to be the same.

**Parameters, Options, and Subroutines Summary**

Example e6x16a.dat:

<b>Parameters</b>	<b>Model Definition Options</b>	<b>History Definition Options</b>
DYNAMIC	CONNECTIVITY	CONTINUE
ELEMENT	CONTACT	DYNAMIC CHANGE
END	CONTROL	
LARGE DISP	COORDINATE	
LUMP	END OPTION	
PRINT	FIXED DISP	
SIZING	INITIAL VELOCITY	
TITLE	ISOTROPIC	
	POST	
	PRINT ELEM	
	RESTART	

Example e6x16b.dat:

<b>Parameters</b>	<b>Model Definition Options</b>	<b>History Definition Options</b>
DYNAMIC	CONNECTIVITY	CONTINUE
ELEMENT	CONTACT	DYNAMIC CHANGE
END	CONTROL	
LARGE DISP	COORDINATE	
LUMP	END OPTION	
PRINT	FIXED DISP	
SIZING	INITIAL VELOCITY	
TITLE	ISOTROPIC	
	POST	
	PRINT ELEM	
	RESTART	



Example e6x16c.dat:

**Parameters**

ALIAS  
DYNAMIC  
ELEMENT  
END  
LARGE DISP  
LUMP  
PRINT  
SIZING  
TITLE

**Model Definition Options**

CONNECTIVITY  
CONTACT  
CONTROL  
COORDINATE  
END OPTION  
FIXED DISP  
INITIAL VELOCITY  
ISOTROPIC  
POST  
RESTART

**History Definition Options**

CONTINUE  
DYNAMIC CHANGE

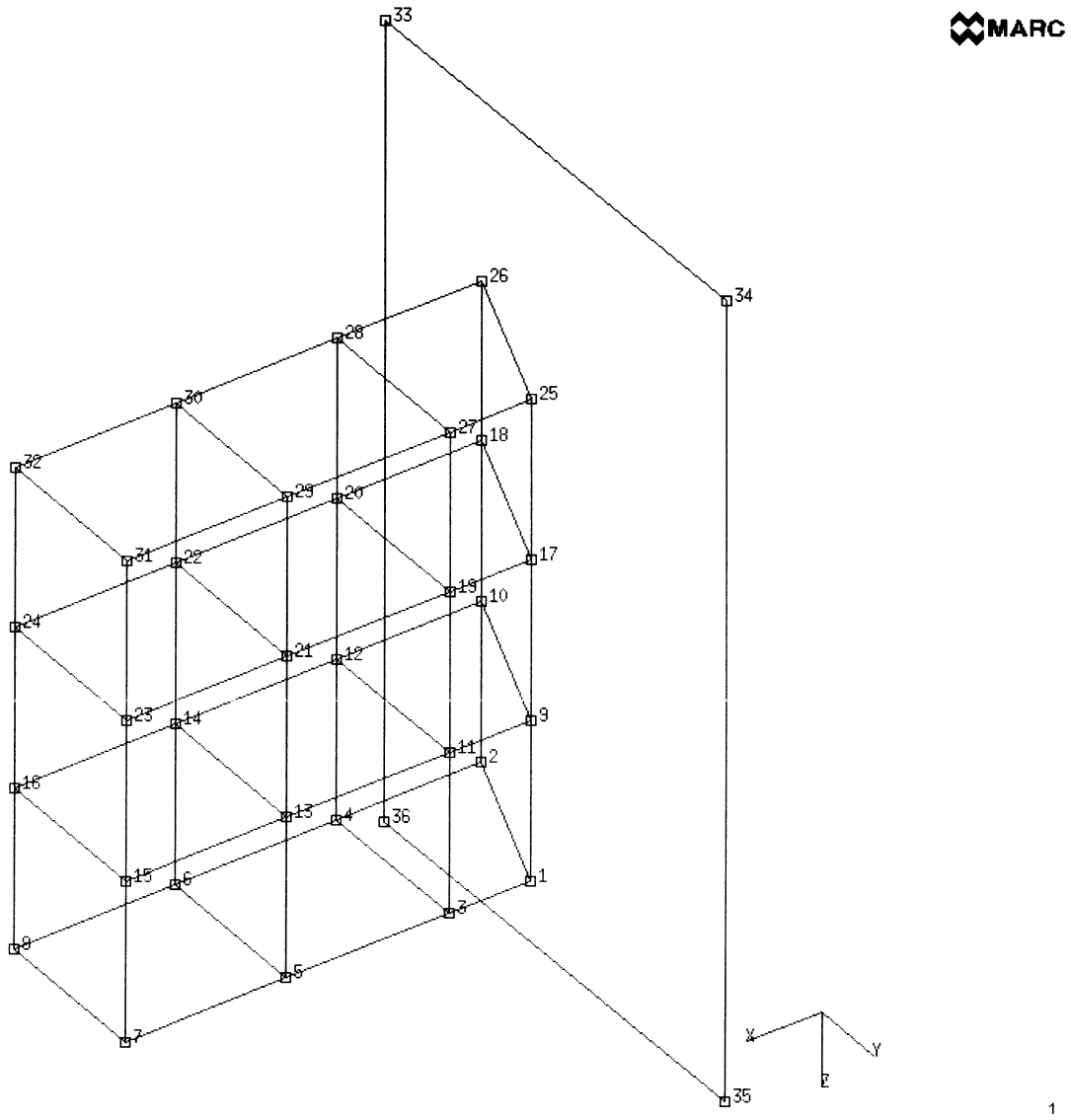


**Figure 6.16-1** Impactor and Rigid Wall

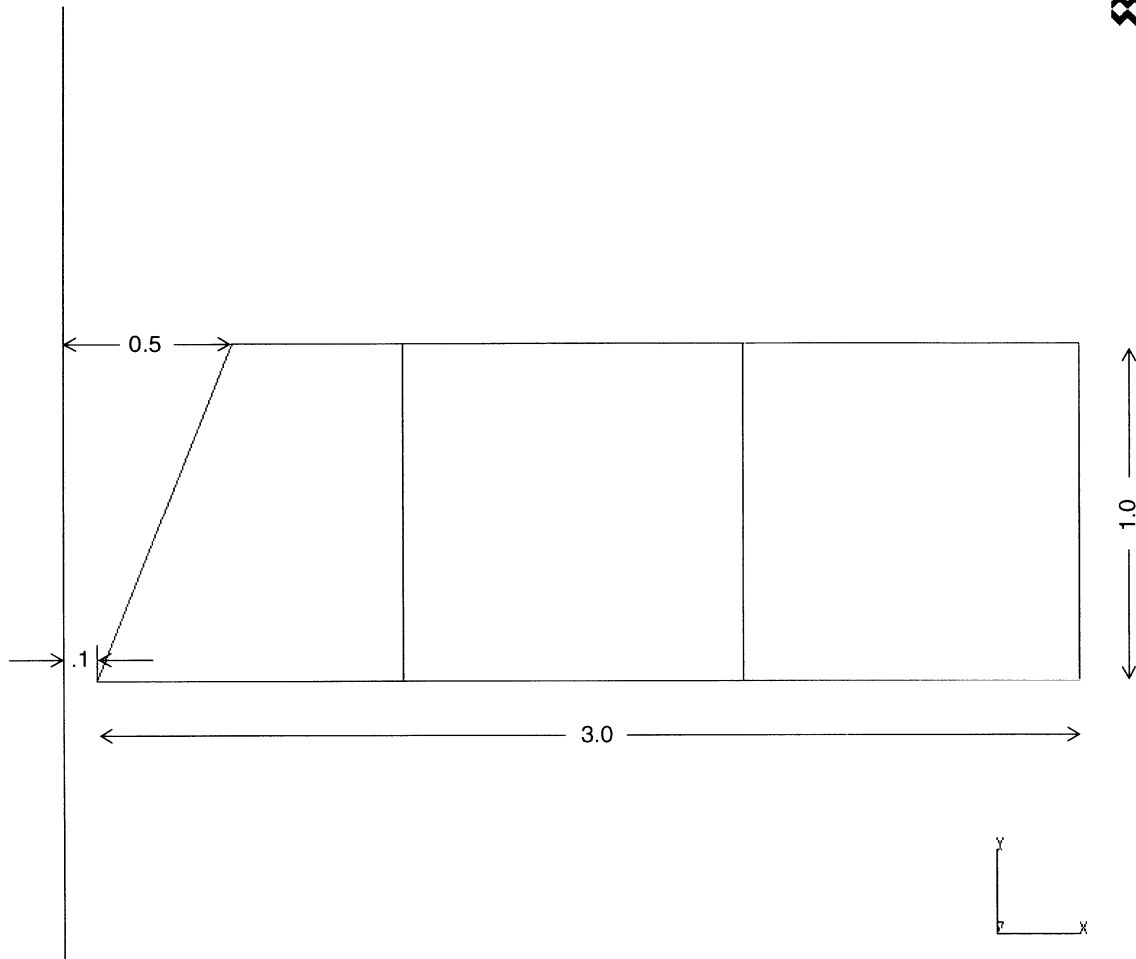


**Figure 6.16-2** Impactor Geometry

INC : 2  
SUB : 0  
TIME : 1.000e-03  
FREQ : 0.000e+00

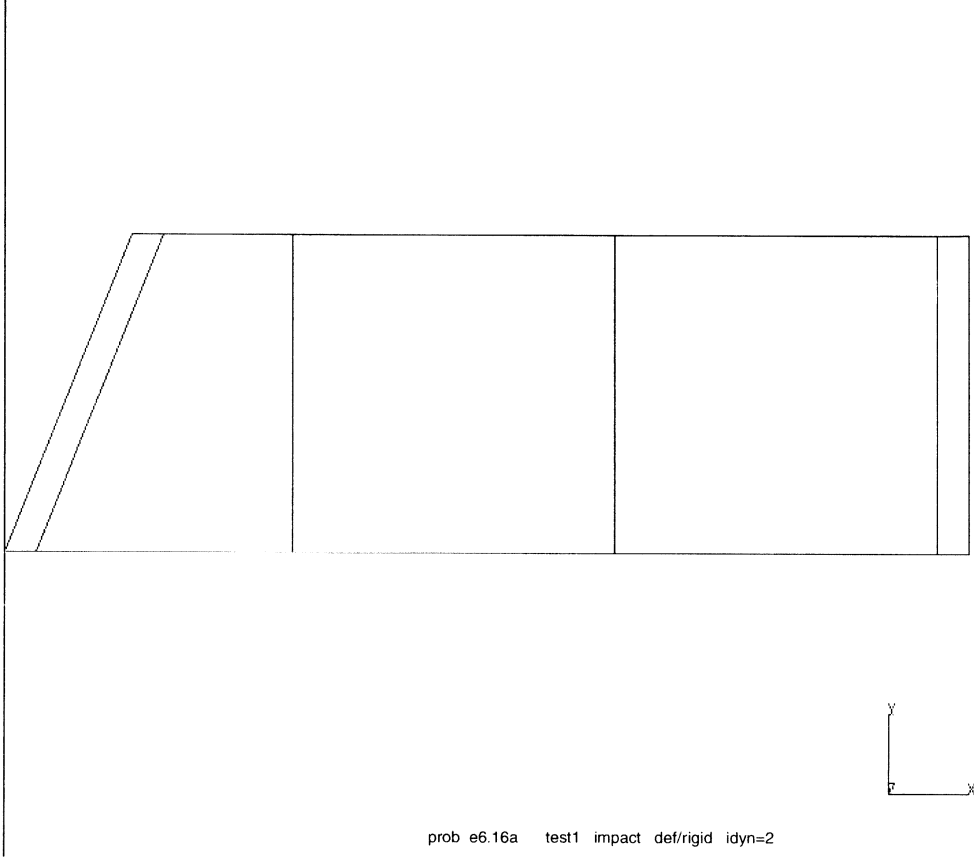


**Figure 6.16-3** Deformation at Initial Contact

INC : 20  
SUB : 0  
TIME : 1.000e-02  
FREQ: 0.000e+00

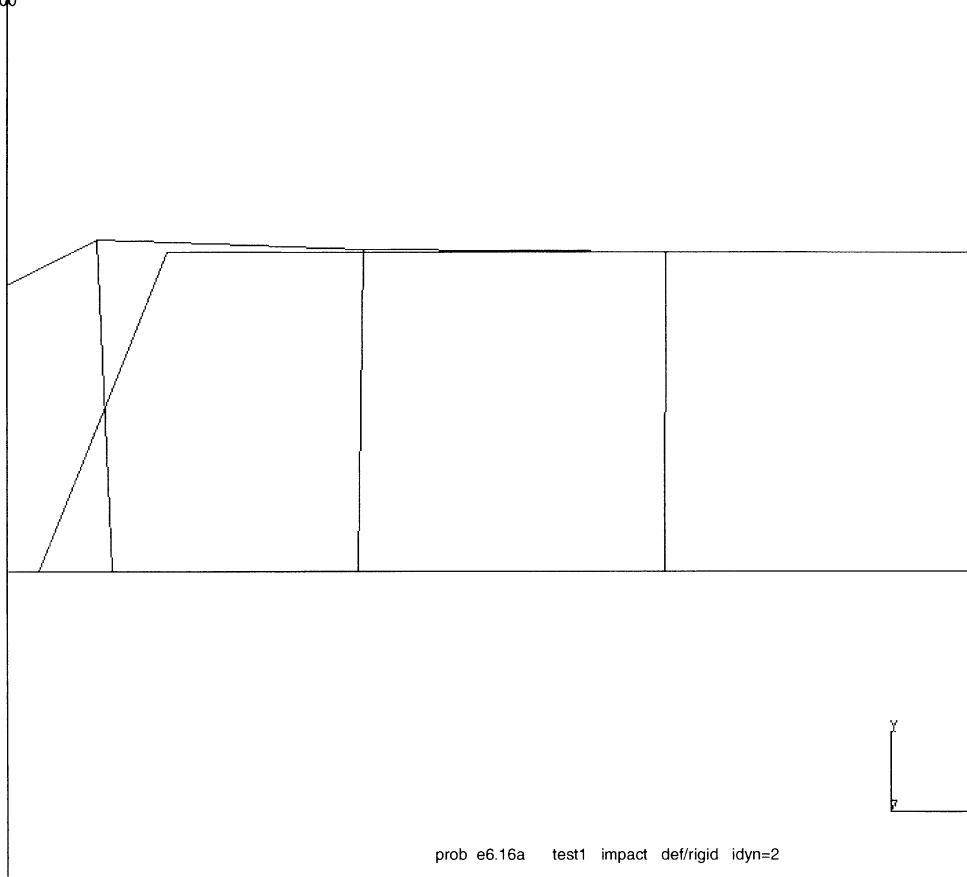


**Figure 6.16-4** Final Deformation



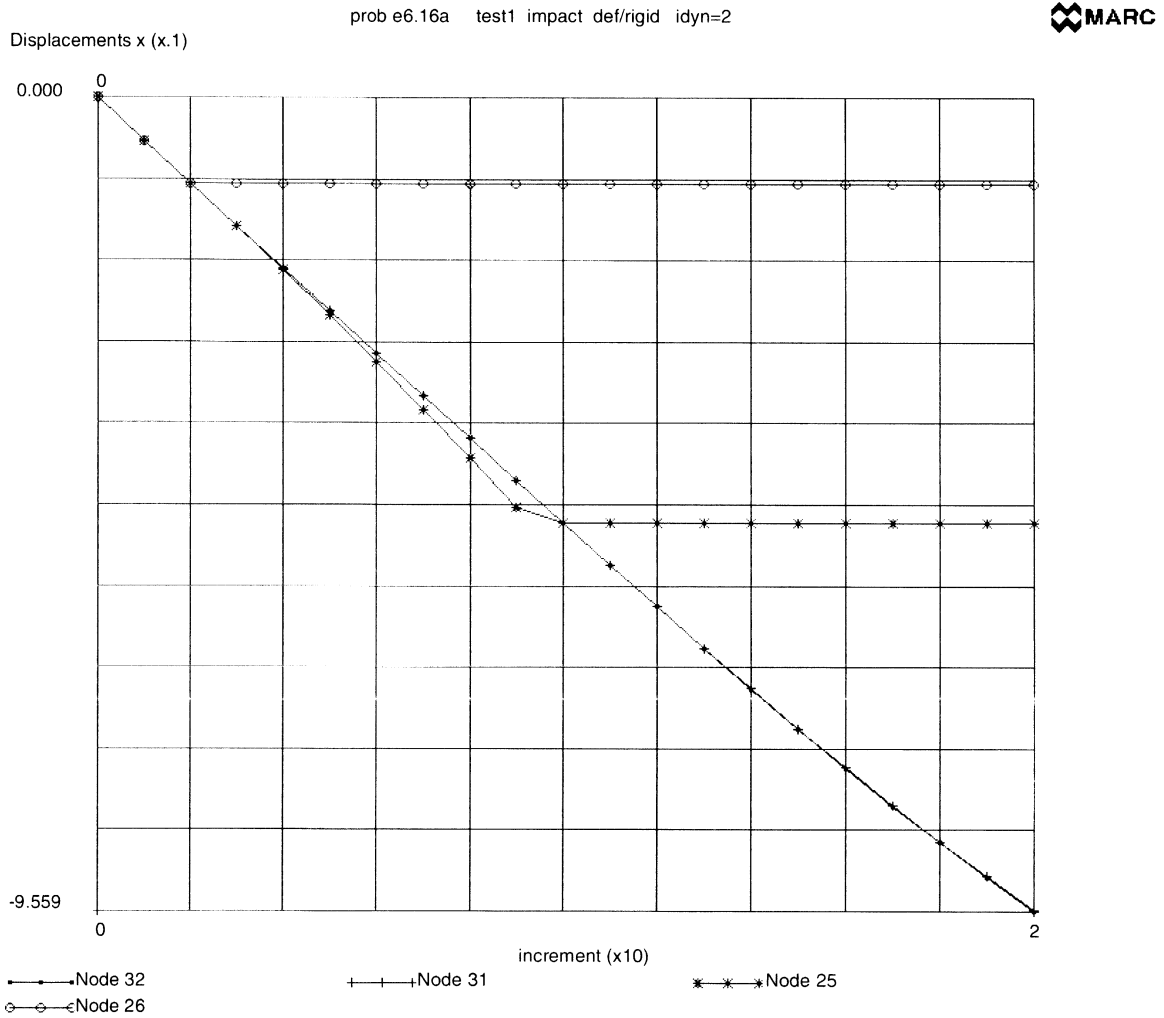


**Figure 6.16-5** (A) Displacement History (Newmark-Beta Method)

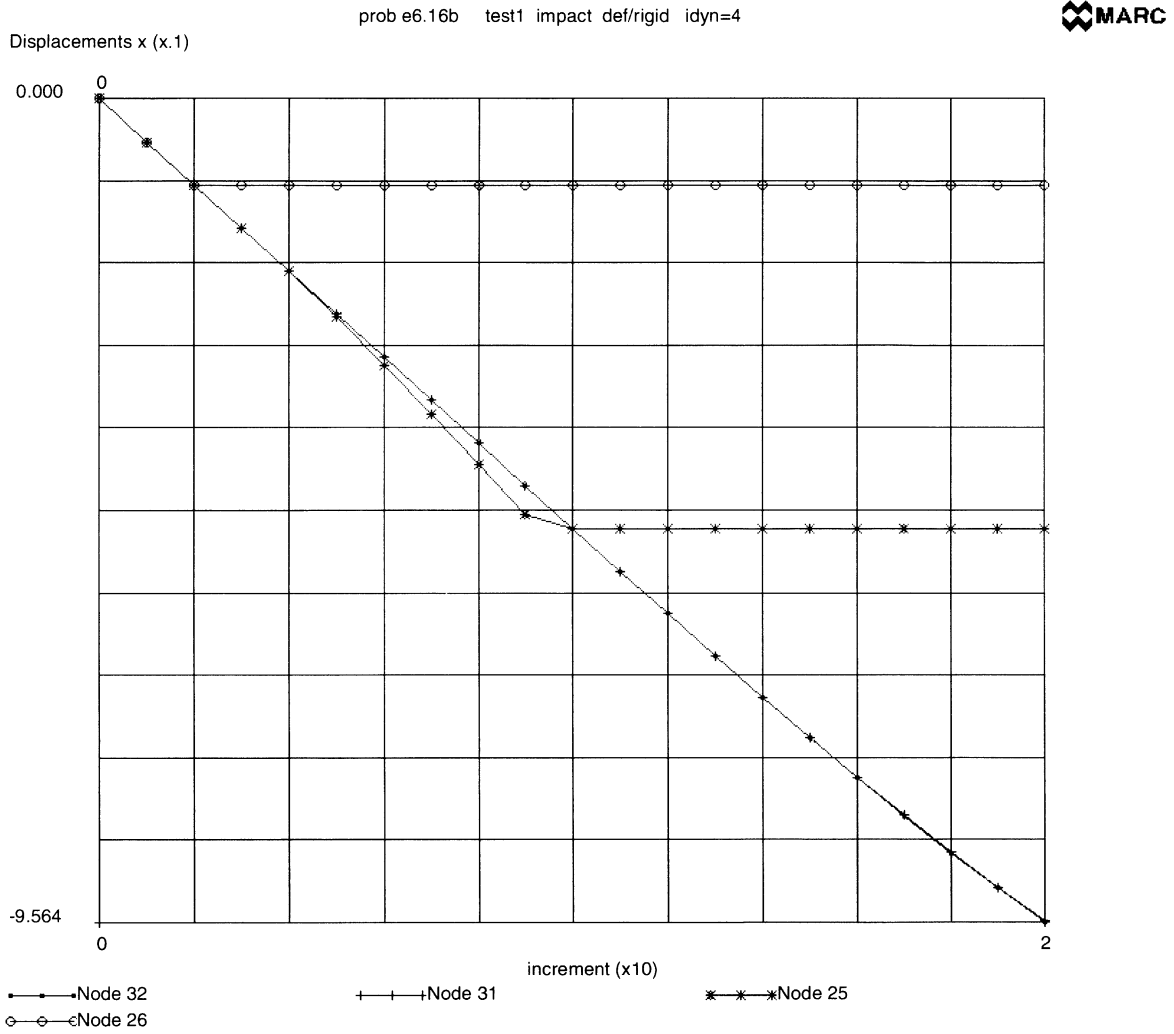


**Figure 6.16-5 (B) Displacement History (Central Difference Method)**

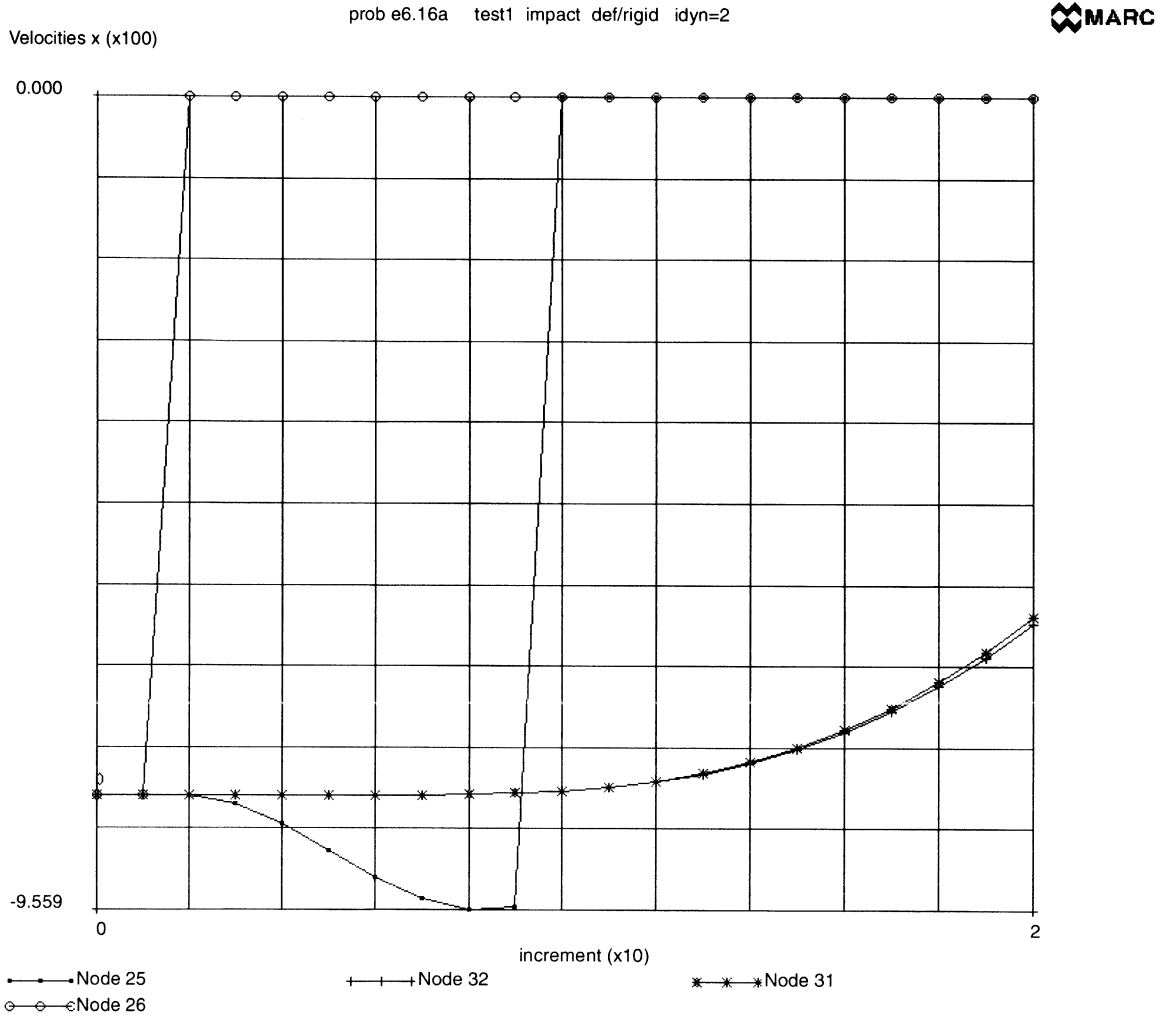


**Figure 6.16-6 (A) Velocity History (Newmark-Beta Method)**

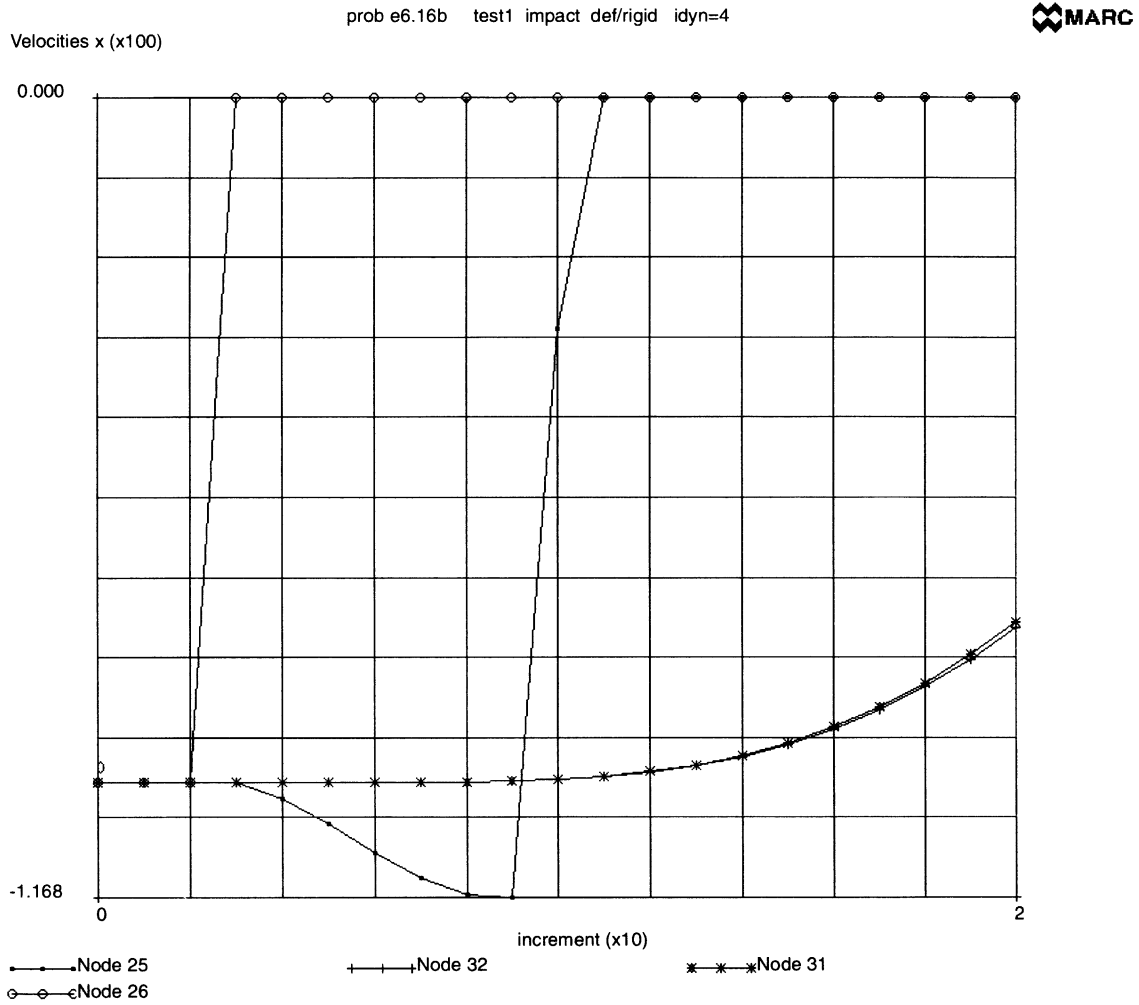


**Figure 6.16-6 (B) Velocity History (Central Difference Method)**

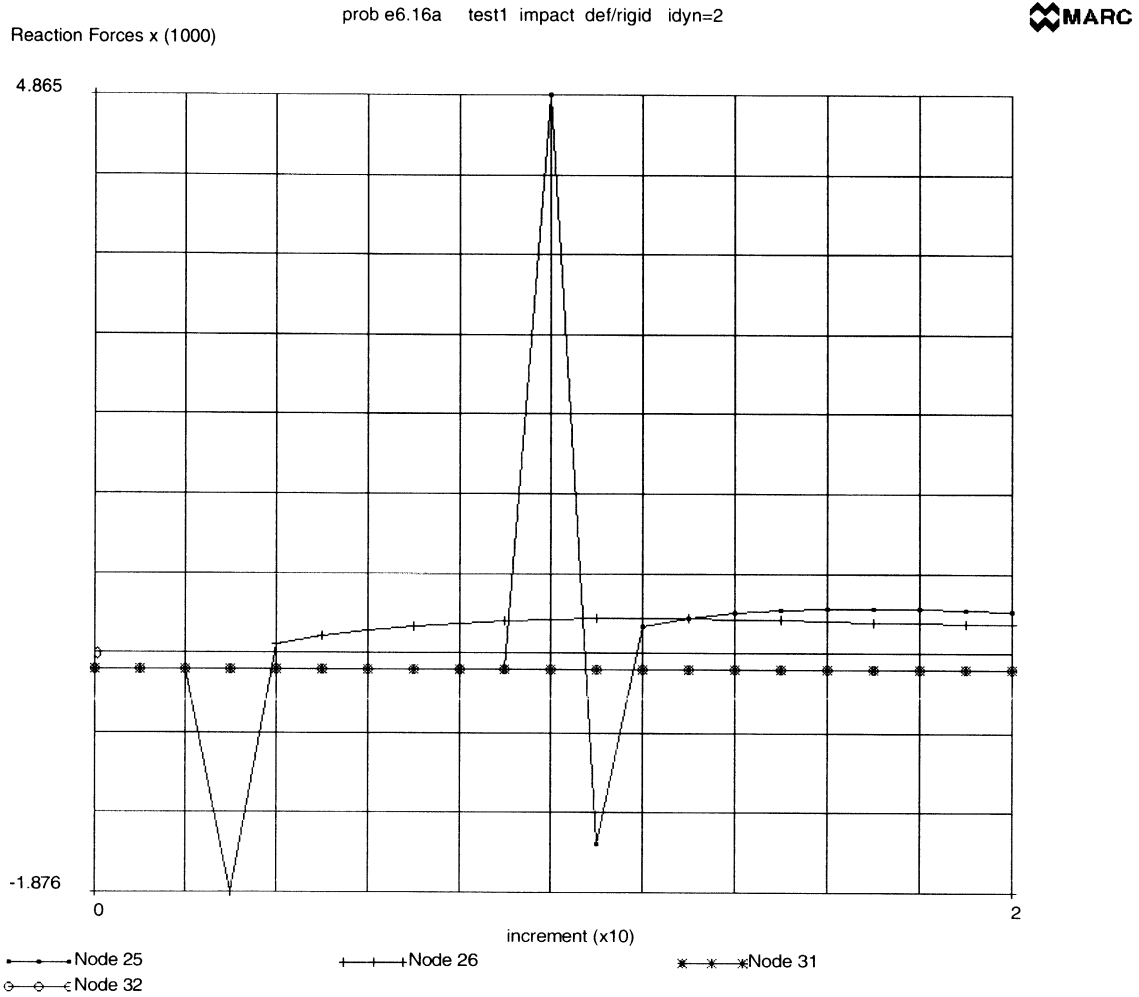


**Figure 6.16-7 (A) Reaction/Impact Force History (Newmark-Beta Method)**

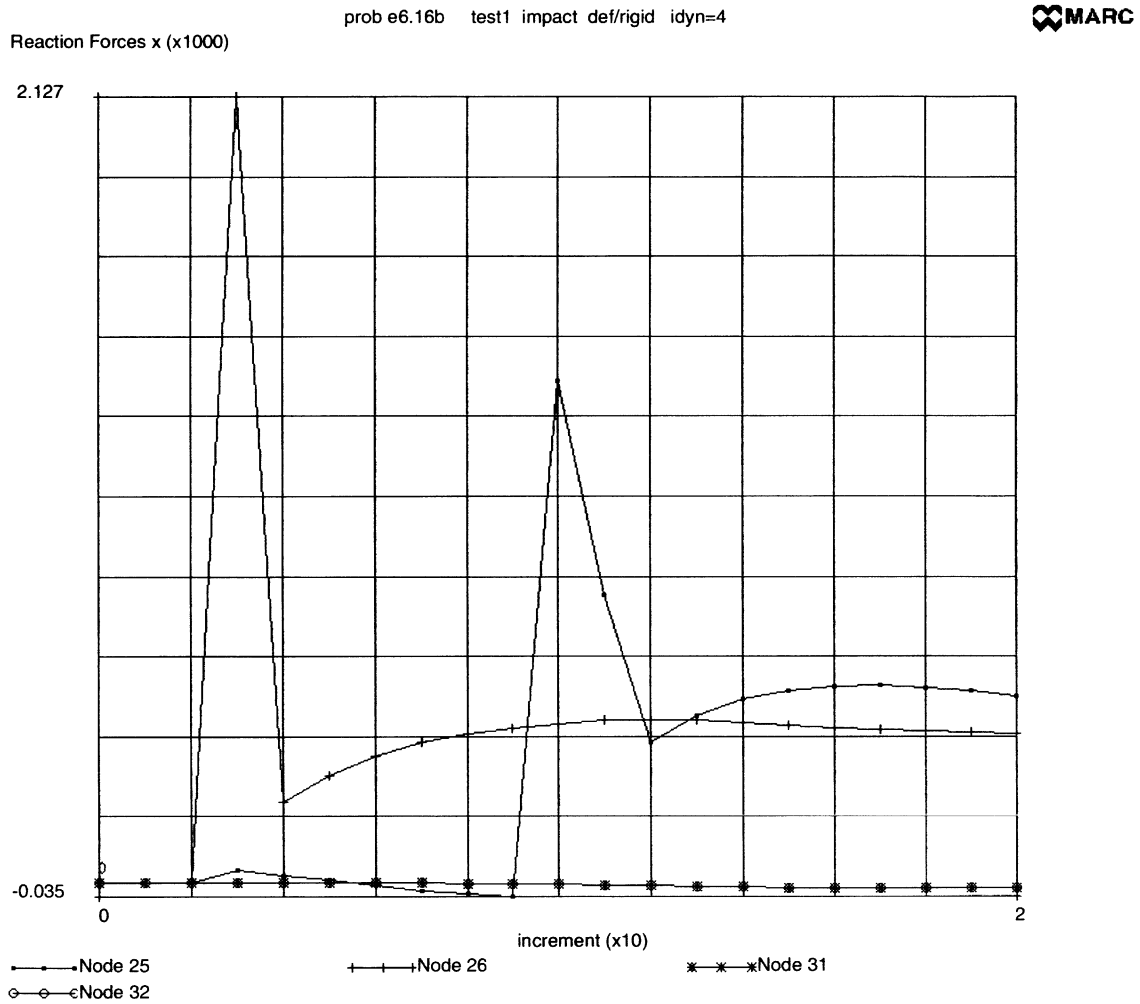


**Figure 6.16-7 (B) Reaction/Impact Force History (Central Difference Method)**

## 6.17 Dynamic Contact Between Two Deformable Bodies

This problem demonstrates the dynamic impact between two deformable bodies. It is very similar to problem 6.16, except the rigid barrier has been replaced by a deformable, yet stiff, body. Both the implicit Newmark-beta and explicit central difference procedures are demonstrated.

This problem is modeled using the two techniques summarized below.

Data Set	Element Type(s)	Number of Elements	Number of Nodes	Differentiating Features
e6x17a	7	49	122	DYNAMIC,2 Newmark-beta
e6x17b	7	49	122	DYNAMIC,4 Central Difference

### Model

The model is shown in Figure 6.17-1 and Figure 6.17-2. The project is made up of 9 brick elements type 7, where the barrier is composed of 40 brick elements. The DYNAMIC parameter specifies which operator is to be chosen: a “2” indicates Newmark-beta and a “4” indicates central difference. The projectile may undergo elastic deformation, so the LARGE DISP parameter is included.

### Material Properties

An artificial material was created, such that the stability limit for central difference was a large number. For the projectile (elements 1 – 9), the Young’s modulus is 10,000 psi and the mass density is 0.1 lbf-sec<sup>2</sup>/in<sup>4</sup>. The barrier is ten times stiffer with a Young’s modulus of 100,000 psi. A lumped mass matrix is created based upon the LUMP parameter. The model is given a numerical damping of 0.4. Given the material parameters, the elastic wave speed in the projectile is  $c = \sqrt{E/\rho} = 316$  in/sec. In the barrier, it is 1000 in/second.

### Boundary Conditions

The nodes on the xz-plane have been constrained in the y-direction. The nodes on the xy-plane have been constrained in the z-direction for the projectile. The projectile has an initial velocity of -100 in/second in the x-direction.

### Controls

The maximum number of increments is 100 with the maximum number of iterations as 25. Relative displacement error control is used with a tolerance value of 10%. A formatted post file is written which contains only nodal information. Both the restart and post file are written every increment.

**Contact**

There are two bodies in this analysis. The first is the deformable projectile. The second is the deformable barrier. There is no friction between these two surfaces.

The other parameters on the second block are upper bounds to the number of surface entities and surface nodes.

The contact tolerance is 0.032 inch which is small compared to an element dimension. A very large separation force is given which effectively ensures that the projectile sticks to the barrier.

**Time Step**

The time step chosen is 0.0005 second which is below the stability limit of 0.0012 second. The stability limit is smaller in this problem than in 6.16 because of the stiff barrier. The total period is 0.01 second, so 20 increments are performed.

**Results**

Figure 6.17-3 shows the deformation at increment 20. The barrier is significantly stiffer and undergoes very little deformation. The projectile is originally 0.2 inches from the barrier. You can observe in Figure 6.17-4 that node 26 contacts the barrier in increment 3 using the implicit procedure, and increment 4 in the explicit procedure. This is due to the nature of these two different methods. There is more deformation of the barrier using the implicit procedure.

Figure 6.17-5 shows the velocity histories using the new methods. The basic correlation is good. The Newmark-beta method shows some oscillations at later increments. This could be eliminated by using more damping or decreasing the time step.

**Parameters, Options, and Subroutines Summary**

Example e6x17a.dat:

<b>Parameters</b>	<b>Model Definition Options</b>	<b>History Definition Options</b>
DYNAMIC	CONNECTIVITY	CONTINUE
ELEMENT	CONTACT	DYNAMIC CHANGE
END	CONTROL	
LARGE DISP	COORDINATE	
LUMP	END OPTION	
PRINT	FIXED DISP	
SIZING	INITIAL VELOCITY	
TITLE	ISOTROPIC	
	POST	
	PRINT ELEM	
	RESTART	





Example e6x17b.dat:

**Parameters**

DYNAMIC  
ELEMENT  
END  
LARGE DISP  
LUMP  
PRINT  
SIZING  
TITLE

**Model Definition Options**

CONNECTIVITY  
CONTACT  
CONTROL  
COORDINATE  
END OPTION  
FIXED DISP  
INITIAL VELOCITY  
ISOTROPIC  
POST  
PRINT ELEM  
RESTART

**History Definition Options**

CONTINUE  
DYNAMIC CHANGE

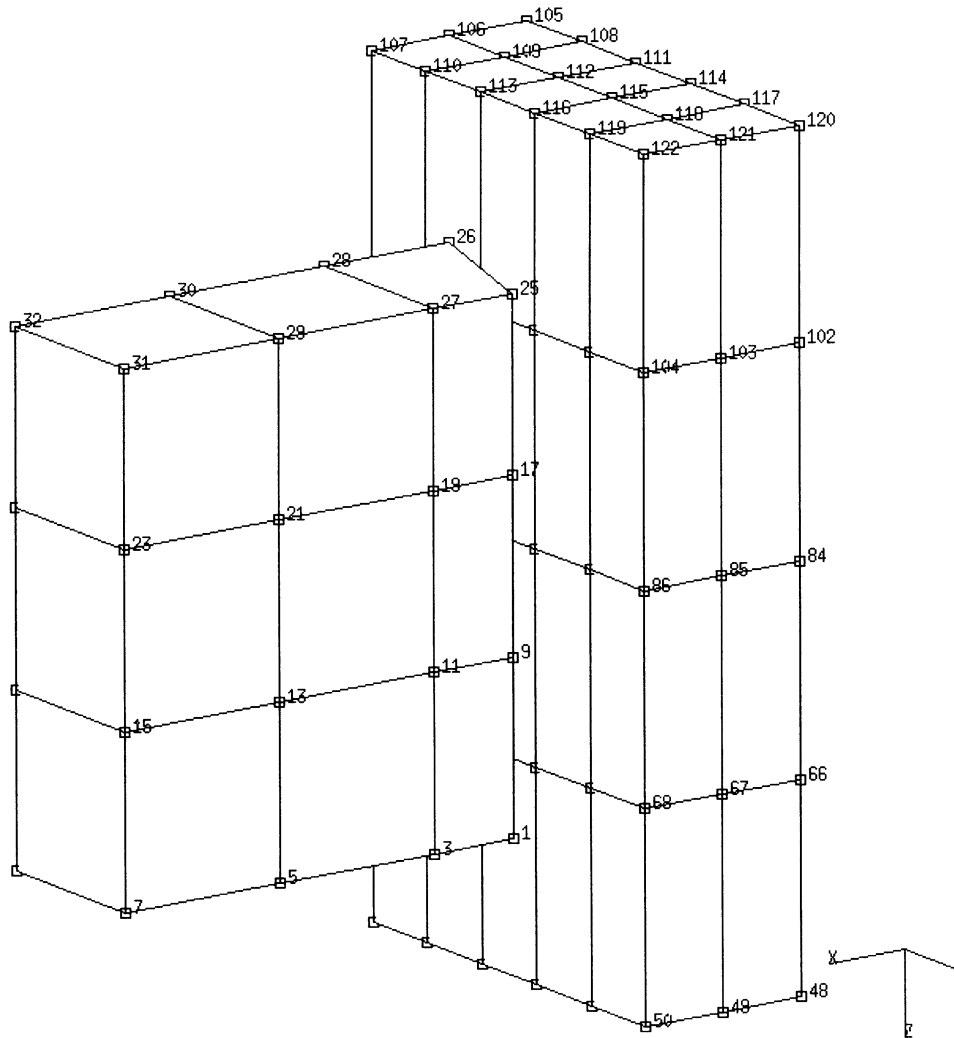


**Figure 6.17-1** Impactor and Deformable Barrier

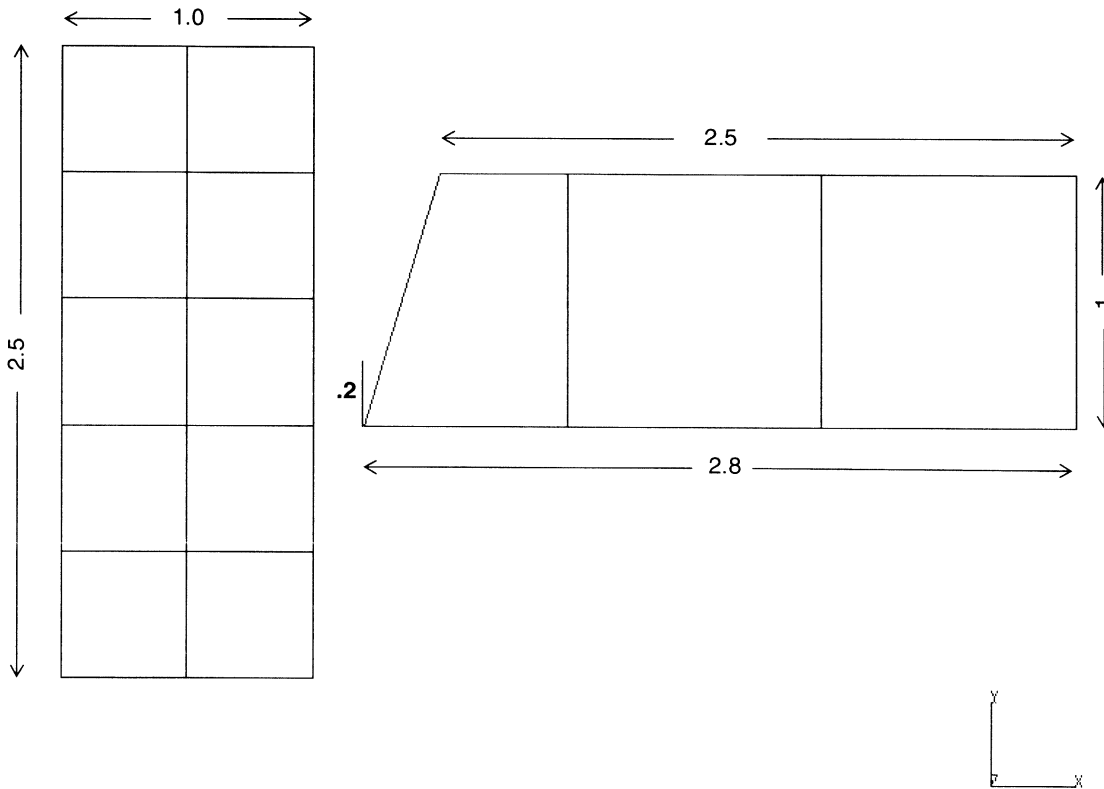


**Figure 6.17-2** Geometries

INC : 20  
SUB : 0  
TIME : 1.000e-02  
FREQ : 0.000e+00

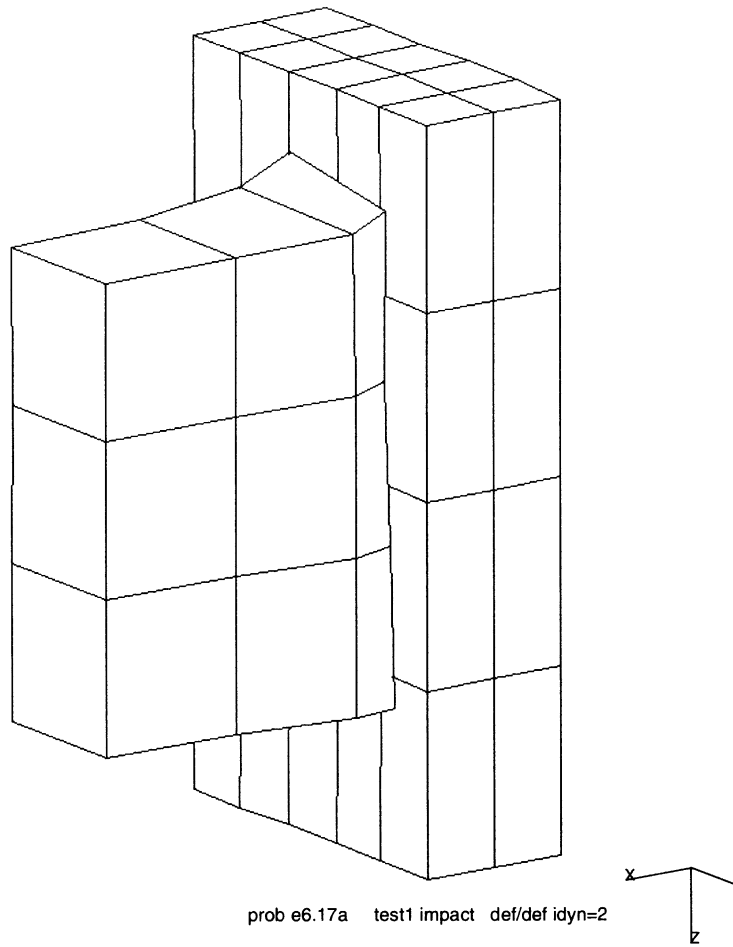


**Figure 6.17-3** Final Deformation

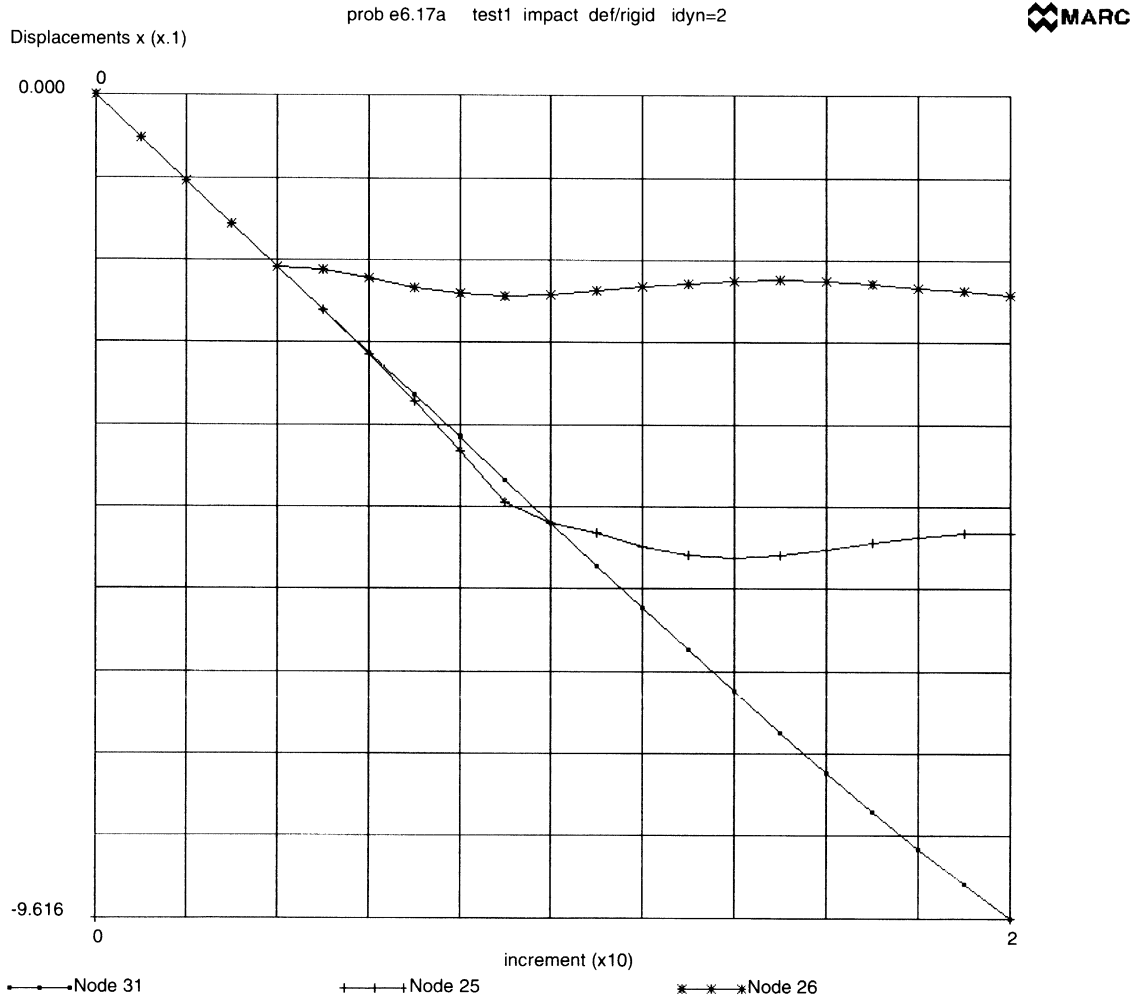


**Figure 6.17-4** (A) Displacement Histories (Newmark-beta Method)

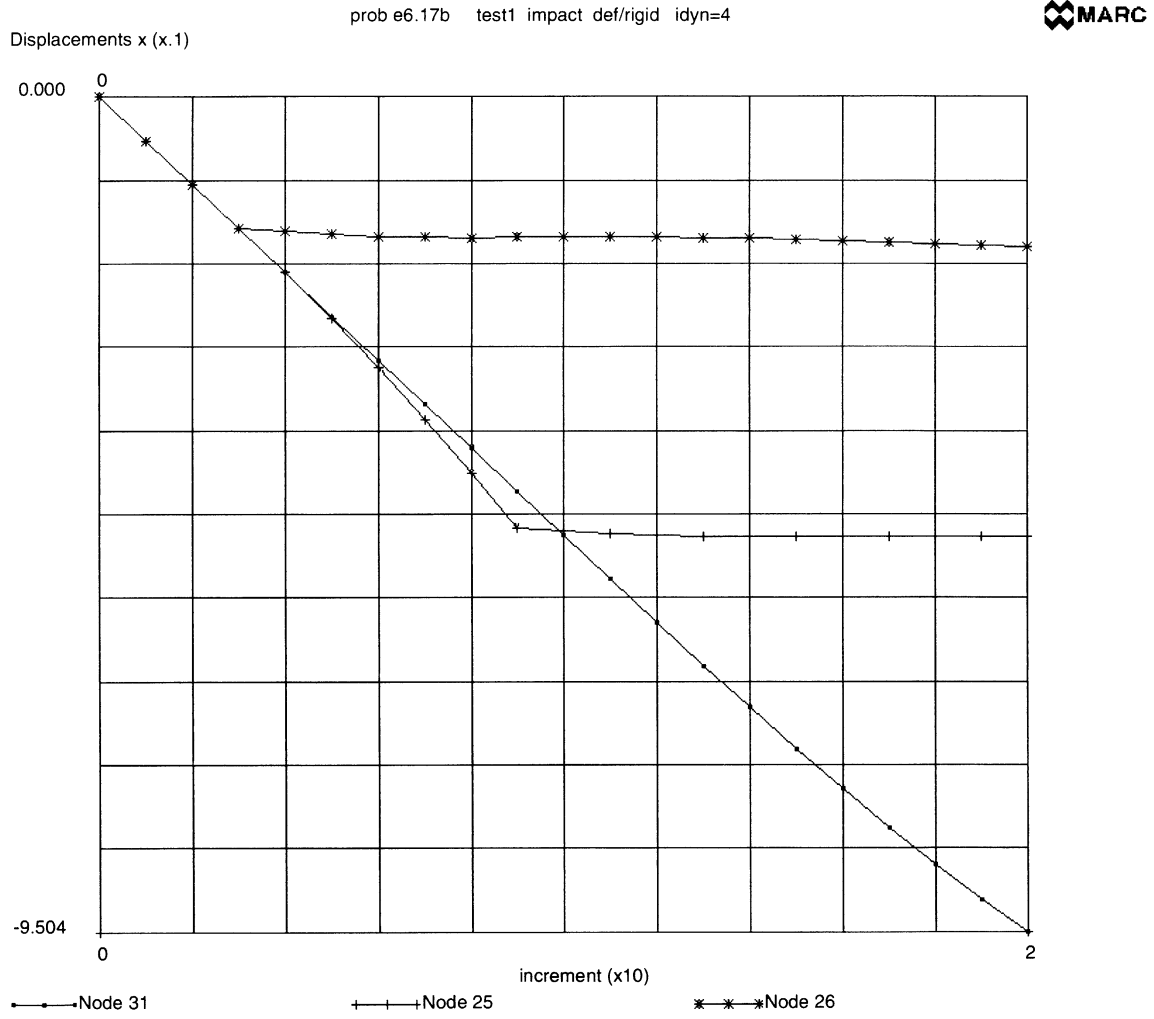


**Figure 6.17-4 (B) Displacement History (Central Difference Method)**



## 6.18 Spectral Response of a Pipe

This problem illustrates the spectrum response capabilities of MARC. The spectral displacements of a cantilever are computed and compared with analytical results.

### Model

The structure is shown in Figure 6.18-1. The mesh consists of 21 type 52 elements and 22 nodes.

### Geometry

The pipe has a cross-sectional area of  $5.34 \text{ E-}3$  square meters. The moments of inertia of the section are  $1.936 \text{ E-}5 \text{ m}^4$  about the local x-axis and  $1.936 \text{ E-}5 \text{ m}^4$  about the local y-axis.

### Boundary Conditions

The pipe is clamped at the left end. Node 1 is assumed to be fixed.

### Material Properties

Young's modulus is  $1.58 \text{ E}11$  Newton/m<sup>2</sup>. The mass density is  $21138 \text{ kg/m}^3$ .

### Displacement Spectral Density

A displacement spectral density function is entered through user subroutine USSD and is assigned in both the x- and y-directions. The spectral values are obtained from the spectral accelerations shown in Table 6.18-1 via linear interpolation in a semilogarithmic plane.

### Spectral Response

Four eigenvalues and the related eigenmodes were extracted using the inverse power sweep method. The response was calculated based on the extracted modes. The spectral displacements, both analytical and computed by MARC, are given in Table 6.18-2. The eigenvalues are given in Table 6.18-3.

Notice that the analytical values do not include the rotational inertia effects.

**Table 6.18-1** Spectral Accelerations [m/sec<sup>2</sup>]

Frequencies (Hz)	Accelerations (g)
0.0001	0.03
0.1	0.03
0.85	0.98
1.15	0.98
3.21	0.35
3.83	0.44
5.18	0.44
13.	0.24
1000.	0.24

**Table 6.18-2** Displacements [m] in x and y Direction

<b>z</b>	<b>Analytical</b>	<b>MARC</b>
0.8	3.77 E-4	3.78 E-4
1.2	8.08 E-4	8.10 E-4
1.8	1.68 E-3	1.69 E-3
2.2	2.39 E-3	2.39 E-3
2.8	3.56 E-3	3.56 E-3
3.4	4.81 E-3	4.82 E-3
4.0	6.10 E-3	6.11 E-3
4.265	6.67 E-3	6.68 E-3

**Table 6.18-3** Eigenvalues [Hz]

<b>N</b>	<b>Analytical</b>	<b>MARC</b>
1	5.066	5.059
2	5.066	5.059
3	31.986	31.61
4	31.986	31.61

**Parameters, Options, and Subroutines Summary**

Example e6x18.dat:

**Parameters**

DYNAMIC  
ELEMENTS  
END  
RESPONSE  
SIZING  
TITLE

**Model Definition Options**

CON GENER  
CONNECTIVITY  
COORDINATE  
END OPTION  
FIXED DISP  
GEOMETRY  
ISOTROPIC  
NODE FILL  
POST

**History Definition Options**

CONTINUE  
MODAL SHAPE  
RECOVER  
SPECTRUM



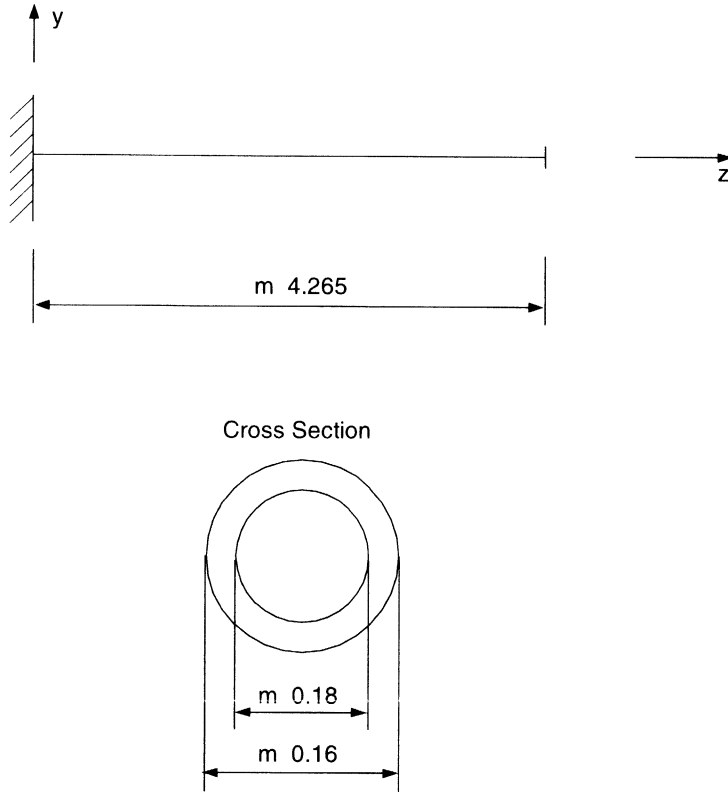


Figure 6.18-1 Cantilever Pipe and its Cross Section





## 6.19 Dynamic Impact of Two Bars

This problem demonstrates the dynamic impact of a bar hitting against another bar fixed in space using the explicit method. The DYNAMIC, 5 option is used in this example.

### Element

Element type 11 is a plane-strain element used to model both bars. Both bars are 10 cm x 1 cm and are modeled by 10 beam elements, respectively. There is a 0.5 cm gap between the two bars as shown in Figure 6.19-1.

### Model

The structure is shown in Figure 6.19-1. The mesh consists of 20 type 10 elements and 44 nodes.

### Material Properties

The material properties of both bars are:

$$\text{Young's modulus is } E = 1000.0 \text{ N/cm}^2$$

$$\text{Poisson's ratio is } \nu = 0.0$$

$$\text{Mass density is } \rho = 1.0 \text{ kg/cm}^3$$

### Boundary Conditions

Only the displacement along x-direction is free. The bar at the right is fixed at the right end.

### Dynamics

The body has an initial velocity of 1.0 cm/second. The case has been studied for 12.0 seconds using a time step of 0.04 second through the DYNAMIC CHANGE option.

### Results

Figure 6.19-2 illustrates contact occurring at increment 13 and separation occurring approximately at increment 125. Figure 6.19-3 and Figure 6.19-4 show the velocity and acceleration histories. The reaction force at the wall is shown in Figure 6.19-5.



**Parameters, Options, and Subroutines Summary**

Example 6x19.dat:

**Parameters**

SIZING  
ELEMENTS  
DYNAMIC  
PRINT  
LUMP

**Model Definition Options**

CONNECTIVITY  
OPTIMIZE  
COORDINATES  
ISOTROPIC  
INITIAL VELOCITY  
CONTACT  
CONTACT TABLE  
FIXED DISPLACEMENT  
POST  
PRINT ELEMENT  
PRINT NODE  
END OPTION

**History Definition Options**

DYNAMIC CHANGE  
CONTINUE

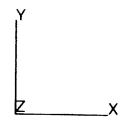
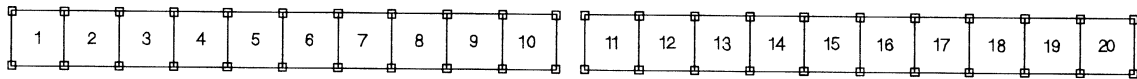


**Figure 6.19-1** Finite Element Mesh of Two Bars



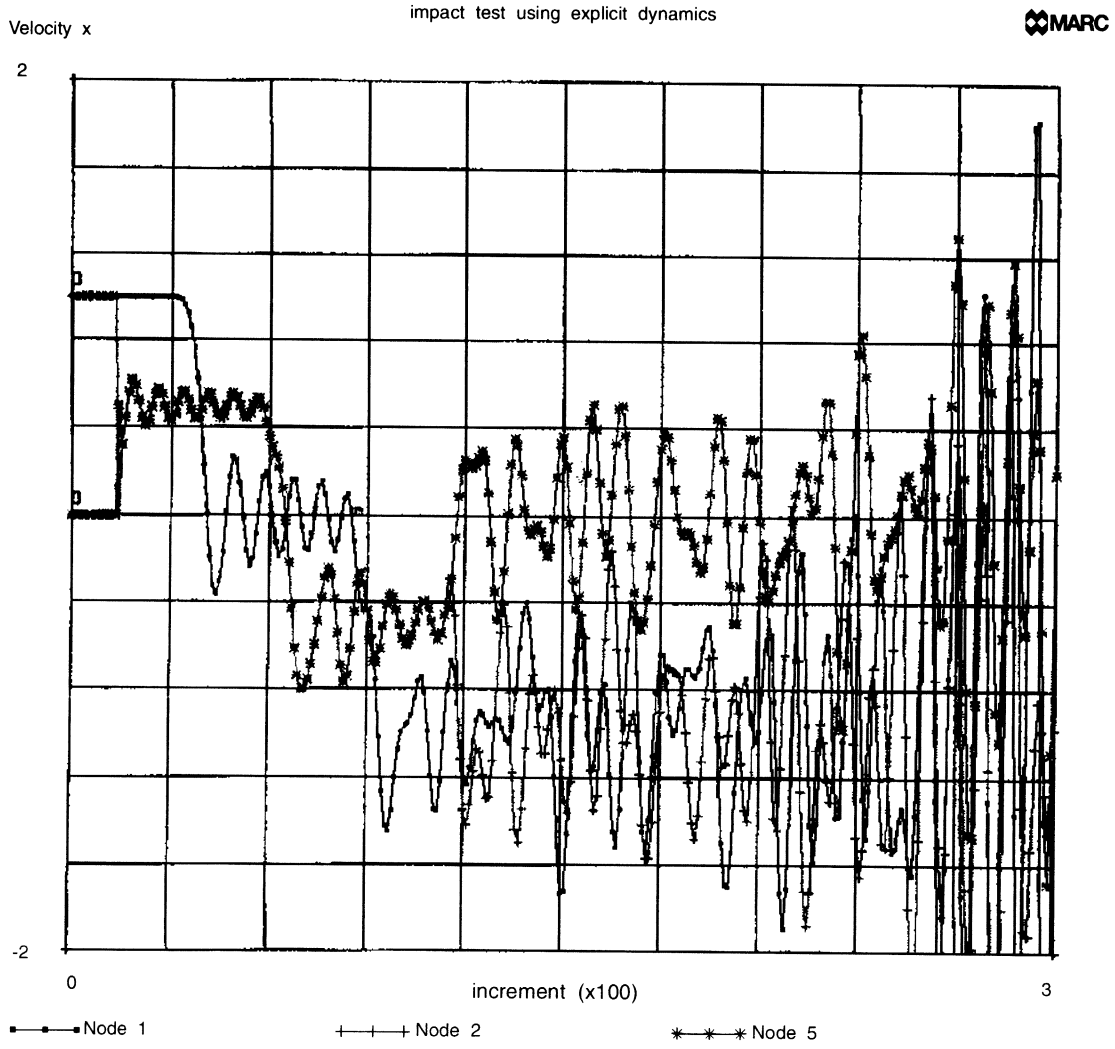


Figure 6.19-3 Velocity History of Selected Nodes

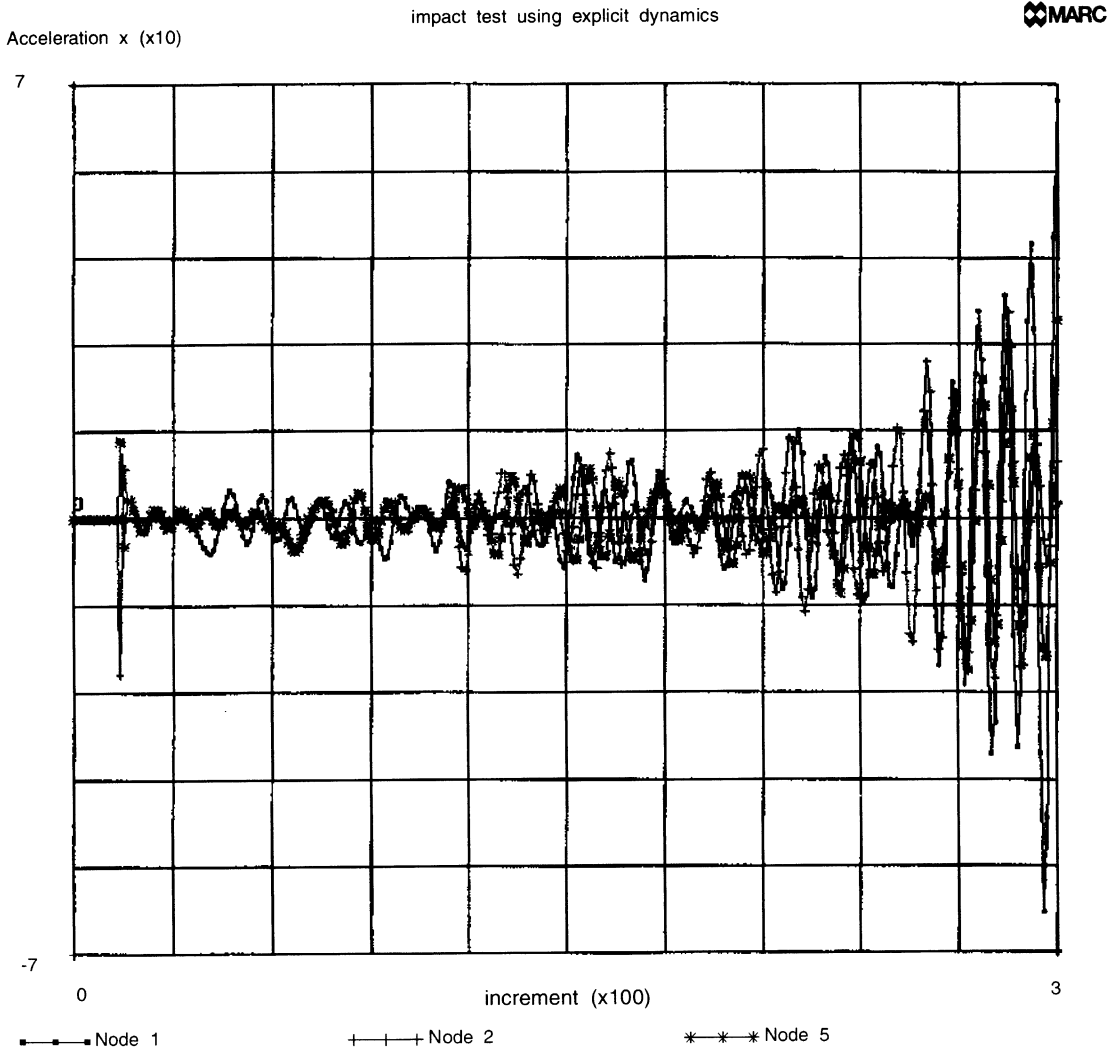
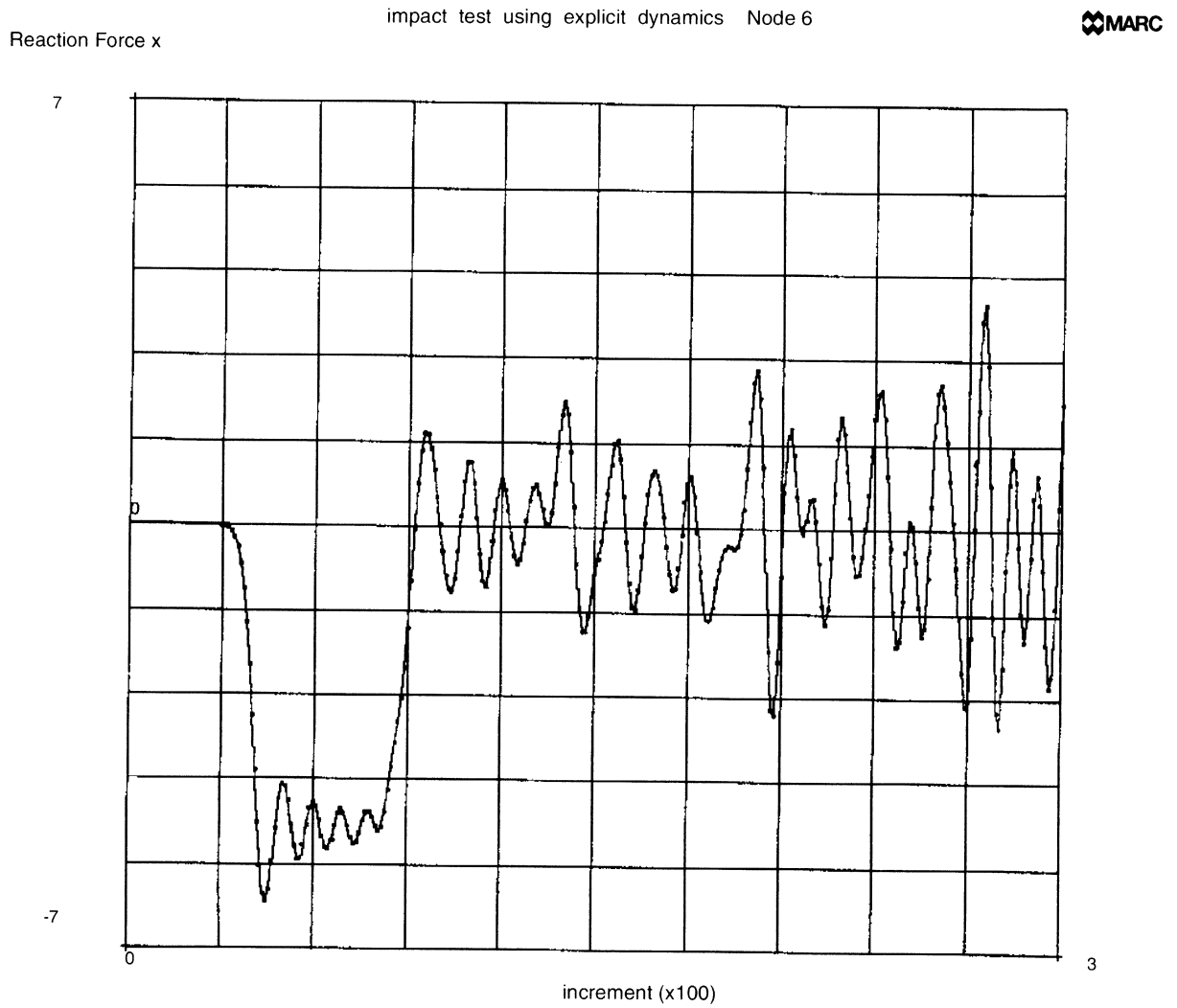


Figure 6.19-4 Acceleration History of Selected Node





**Figure 6.19-5** Reaction Force at Wall



## 6.20 Elastic Beam Subjected to Fluid-Drag Loading

This problem demonstrates an elastic beam partially submerged under a flowing fluid being analyzed for static analysis. In addition, a dynamic analysis is performed in which wave loading is also considered.

This problem is modeled using the two techniques summarized below.

Data Set	Element Type(s)	Number of Elements	Number of Nodes	Differentiating Features
e6x20a	98	10	11	Fluid Drag - Static
e6x20b	98	10	11	Fluid Drag - Dynamic

### Element

Element type 98 is a 2-node straight elastic beam with the transverse shear effect in its formulation.

### Model

An elastic beam of length 115.47 m which lies at an angle of 60° is partially submerged under some fluid (Figure 6.20-1). The depth of the fluid is 50 m. The beam is modeled using 10 elements and 11 nodes.

### Geometry

The GEOMETRY block is used for inputting beam section properties. The beam has a cross-section area of 0.1935 m<sup>2</sup> and moments of inertia ( $I_{xx}$  and  $I_{yy}$ ) equaling 0.00321 m<sup>4</sup>.

### Material Properties

The material of the beam is assumed to have a Young's modulus of 2.6e+07 N/m<sup>2</sup> and a Poisson's ratio of 0.3. The beam has a mass density of 8.0e+4 Kg/m<sup>3</sup>.

### Loading

Elements 1 to 5 are subjected to fluid drag loading. The mass density of the fluid inside the pipe is assumed to be 0.8 Kg/m<sup>3</sup> and the fluid outside of the pipe is assumed to be 1 Kg/m<sup>3</sup>. The gravity constant is assumed to be 10 m/sec<sup>2</sup>. The drag coefficient is assumed to be 0.05, and the inertia coefficient is assumed to be 0.05. The fluid outside of the pipe is flowing with a velocity of 1 m/sec in the x-direction. It has a velocity gradient of 0.04 per second. For the dynamic analysis case, the beam is subjected to wave loading in addition to the fluid-drag loading. The wave height is assumed to be 2 and the wave period is assumed to be 5. The wave phase is taken to be 0. The wave front is assumed to be moving in the x-direction.

**Boundary Conditions**

Nodes 1 and 11 are assumed to be hinged ( $u_x = u_y = u_z = \theta_x = \theta_z = 0$ ).

**Results**

The displacements of the beam due to fluid drag loading are given in Table 6.20-1.

**Table 6.20-1** Displacements of the Beam (m)

<b>Node</b>	<b><math>u_x</math> (m)</b>	<b><math>u_z</math> (m)</b>	<b><math>\theta_y</math> (rad)</b>
1	0	0	$-7.96 \times 10^{-2}$
2	-0.767	0.443	$-7.40 \times 10^{-2}$
3	-1.432	0.827	$-5.89 \times 10^{-2}$
4	-1.916	1.106	$-3.78 \times 10^{-2}$
5	-2.176	1.256	$-1.41 \times 10^{-2}$
6	-2.204	1.272	$8.60 \times 10^{-3}$
7	-2.021	1.167	$2.79 \times 10^{-2}$
8	-1.666	0.962	$4.3 \times 10^{-2}$
9	-1.183	0.683	$5.37 \times 10^{-2}$
10	-0.613	0.354	$6.02 \times 10^{-2}$
11	0	0	$6.23 \times 10^{-2}$



**Parameters, Options, and Subroutines Summary**

Example 6x20a.dat:

<b>Parameters</b>	<b>Model Definition Options</b>	<b>History Definition Options</b>
ALIAS	CONTINUE	DYNAMIC CHANGE
ELEMENT	CONNECTIVITY	CONTINUE
END	COORDINATES	
SIZING	DIST LOADS	
TITLE	END OPTIONS	
	FIXED DISP	
	FLUID DRAG	
	GEOMETRY	
	ISOTROPIC	

Example 6x20b.dat:

<b>Parameters</b>	<b>Model Definition Options</b>	<b>History Definition Options</b>
ALIAS	CONNECTIVITY	CONTINUE
DYNAMIC	COORDINATES	DIST LOADS
ELEMENT	DIST LOADS	DYNAMIC CHANGE
END	END OPTION	
SIZING	FIXED DISP	
TITLE	FLUID DRAG	
	GEOMETRY	
	ISOTROPIC	

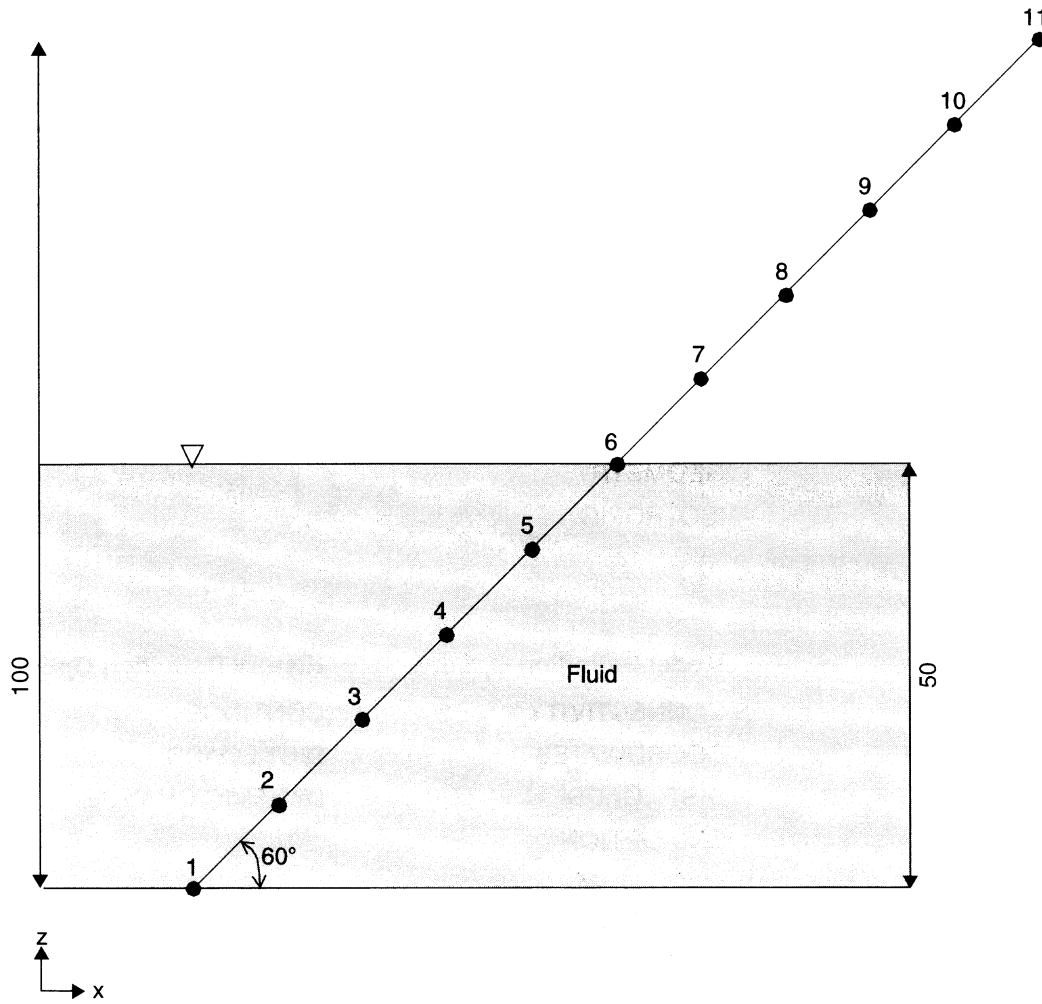


**Figure 6.20-1** Beam Partially Submerged in Fluid



## 6.21 Eigenvalue Analysis of a Box

This example demonstrates the use of follower force stiffness for the eigenvalue analysis of a preloaded box.

### Element

Library element type 72 is a thin shell used for this analysis. There are 96 elements and 290 nodes in the model as shown in Figure 6.21-1. The box, 10 cm x 10 cm x 10 cm, is fixed in space to prevent rigid body motion and preloaded with uniform pressure of 10.0 N/cm<sup>2</sup>. The rigid body constraint is then released and the eigenvalue analysis is performed. The FOLLOW FOR option is used to insure that the load is applied on the deformed geometry.

### Material Properties

The material is elastic and its properties are:

Young's modulus is  $E = 10000.0 \text{ N/cm}^2$

Poisson's ratio is  $\nu = 0.45$

Mass density is  $\rho = 7.0\text{e-}5 \text{ kg/cm}^3$

### Geometry

The thickness of the shell is 0.5 cm.

### Boundary Conditions

The model is fixed at three corners of the box. The constraints are then released to demonstrate the extraction of rigid body modes.

### Control

The full Newton-Raphson iterative method is used with a convergence tolerance of 0.0001% on residuals requested.

### Results

The modal shapes are shown in Figure 6.21-2 and Figure 6.21-2. The six eigenvalues for rigid body are:

Eigenvalue	With Follower Force Stiffness (Cycles/s)	Without Follower Force Stiffness (Cycles/s)
1	1.29857e-4	3.38527e-6
2	9.55539e-6	5.83730e-6
3	1.75523e-5	1.94645e-4



Eigenvalue	With Follower Force Stiffness (Cycles/s)	Without Follower Force Stiffness (Cycles/s)
4	5.2039e+0	30.1477e+0
5	5.20390e+0	30.1573e+0
6	5.20390e+0	30.1478e+0

You can observe that the inclusion of the follower force stiffness results in a more accurate representation.

### Parameters, Options, and Subroutines Summary

Example e6x21.dat:

#### Parameters

ELEMENT  
DYNAMIC  
FOLLOW FOR  
END  
LARGE DISP  
SIZING  
TITLE

#### Model Definition Options

CONNECTIVITY  
CONTROL  
COORDINATES  
GEOMETRYTIME STEP  
ISOTROPIC  
FIXED DISP  
DEFINE  
DIST LOADS  
END OPTION  
OPTIMIZE  
POST

#### History Definition Options

DIST LOADS  
AUTO LOAD  
CONTINUE  
DISP CHANGE  
MODAL SHAPE  
RECOVER



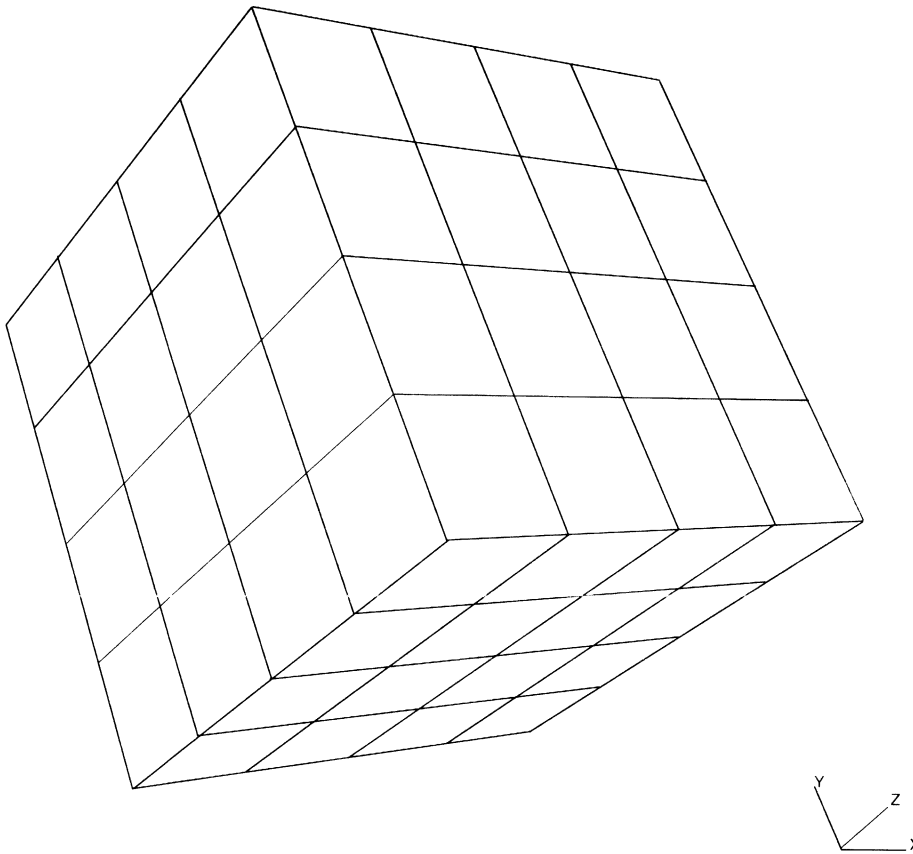


**Figure 6.21-1** Mesh of Box

